



The University of
Nottingham

UNITED KINGDOM • CHINA • MALAYSIA

Division of Drug Delivery and Tissue Engineering

School of Pharmacy

**Novel Amphiphilic Block Co-
polymers from Renewable
Feedstocks: “Synthesis,
Characterisation and
Applications”**

Kuldeep Kumar Bansal

Thesis submitted to the University of Nottingham
for the degree of Doctor of Philosophy

JUNE 2015

Abstract

Development of novel biodegradable polymers from renewable resources has attracted attention due to the limitations associated with polymers obtained from petroleum resources. The objective of the work presented in this thesis was to develop various novel biodegradable amphiphilic block copolymers from commercially available sustainable feedstocks for drug delivery applications. Synthesis was performed using a reported method under mild reaction conditions.

Renewable δ -decalactone was chosen as a key monomer to synthesise novel amphiphilic block copolymers *via* ROP using PEG as initiator. A diblock (i.e. mPEG-b-PDL) and a triblock (i.e. PDL-b-PEG-b-PDL) copolymer of poly(decalactone) (PDL) was synthesised and purified successfully. Additionally, a novel triblock copolymer (i.e. mPEG-b-PDL-b-PPDL) was synthesised using ω -pentadecalactone as monomer and mPEG-b-PDL as initiator *via* ROP to generate a copolymer with different physical properties. Further, a di-block copolymer of ϵ -caprolactone (i.e. mPEG-b-PCL) was synthesised for comparative studies with novel block copolymers. Micelles of synthesised block copolymers were fabricated using a reported nanoprecipitation method. Micelles fabricated from these novel

block copolymers were of sizes <200nm and possessed low critical micelle concentration (CMC) values.

Curcumin and Amphotericin B were successfully encapsulated in the novel block copolymer micelles *via* nanoprecipitation method. The results obtained from curcumin loading and release studies suggested that these novel PDL block copolymers could perform in similar fashion when compared with poly(caprolactone) (PCL) block copolymer micelles. However, in subsequent study micelle of mPEG-b-PDL gave high loading content compared to mPEG-b-PCL micelles when amphotericin B was used as a drug. Further, a preliminary *in vitro* degradation study of mPEG-b-PDL micelles was performed and the results proposed that the ester linkage of PDL chain were susceptible to hydrolytic degradation in physiological condition. Additionally, *in vitro* cytotoxicity studies performed on HCT-116 human colon cancer cells revealed that the novel mPEG-b-PDL micelles have similar toxicity profiles when compared to the well-established mPEG-b-PCL micelles.

Ligand mediated targeting efficiency of novel diblock copolymer micelles was also studied for potential future applications in cancer therapy. Amphiphilic block copolymers using PEG and PDL were synthesised via click chemistry to

generate functionalised block copolymers. Folic acid and rhodamine B were used as targeting ligand and tracker dye respectively. Mixed micelles fabricated from functionalised block copolymers (i.e. FA-PEG-b-PDL, RhB-PEG-b-PDL and mPEG-b-PDL) were tested on folate receptor positive (MCF-7 FR+ve) and folate receptor negative (A549 FR-ve) human cancer cell lines for receptor mediated endocytosis. The acquired confocal images demonstrated the nonspecific uptake of the PEG-b-PDL micelles formulations (targeted and non-targeted) in both cell lines selected in current study.

The results obtained from this thesis study suggested that the synthesised novel PDL block copolymer micelles have potential to act as a novel drug delivery system. However, further studies have been proposed to explore the possible applications of these renewable block copolymers.

Table of Contents

Abstract	i
List of Figures	viii
List of Tables	xvii
List of Schemes	xviii
Acknowledgement	xx
Abbreviation List	xxi
Chapter 1 Introduction	1
1.1 Introduction to Biodegradable Polymers in Drug Delivery	2
1.2 Classification of Biodegradable Polymers.....	3
1.2.1 Biodegradable Polymers from Natural Origin.....	3
1.2.2 Biodegradable Polymers from Synthetic Origin	5
1.3 Classification of Synthetic Poly(esters).....	13
1.3.1 Poly(esters) Synthesised from Non-Renewable Monomers ...	13
1.3.2 Poly(esters) Synthesised from Renewable Monomers.....	17
1.4 Polymeric Micelles in Drug Delivery and Cancer Therapy	35
1.5 Summary.....	54
1.6 Aim and Objectives	55
1.7 References.....	57
Chapter 2 Materials and Methods	68
2.1 Materials.....	69
2.2 Instruments and Methods	70
2.3 References.....	78

Chapter 3 Synthesis and Characterisation of Homopolymers and Block Copolymers based on δ-Decalactone	79
3.1 Introduction	80
3.2 General Synthesis Method for δ -Decalactone Polymers	86
3.2.1 Synthesis of δ -Decalactone Homopolymers	86
3.2.2 Synthesis of Block Copolymers of δ -Decalactone	89
3.2.3 Synthesis of Block Copolymer of ϵ -Caprolactone	91
3.2.4 Copolymer Synthesis of ω -Pentadecalactone with mPEG-b-PDL (ABC Type).....	92
3.3 Results	93
3.3.1 Synthesis and Characterisation of Homopolymers of δ -Decalactone.....	93
3.3.2 Synthesis and Characterisation of Block Copolymers of δ -Decalactone.....	103
3.3.3 Synthesis and Characterisation of block Copolymer of ϵ -Caprolactone	110
3.3.4 Synthesis and Characterisation of block Copolymer of ω -Pentadecalactone	113
3.4 Discussion.....	116
3.5 Conclusion	123
3.6 References.....	125
Chapter 4 Evaluation of Surfactant Properties of Novel Amphiphilic Block Copolymers of Poly(Decalactone).....	128
4.1 Introduction	129
4.2 Methods	135
4.2.1 Determination of CMC of Poly(decalactone) and Poly(caprolactone) Block Copolymers Micelles	135

4.2.2 Empty and Dye/Drug Loaded Micelles Preparation from PDL and PCL Block Copolymers.....	135
4.2.3 Preparation of Nano-emulsion from homopolymer of Poly(decylactone).....	137
4.2.4 Characterisation of micelles for size, zeta potential and surface morphology	138
4.2.5 Determination of Drug Content, Curcumin Stability and <i>in vitro</i> Release behaviour from Micelles.....	139
4.3 Results	142
4.3.1 Determination of CMC of Poly(decylactone) and Poly(caprolactone) Block Copolymer Micelles	142
4.3.2 Preparation and Characterisation of Empty Micelles.	146
4.3.3 Characterisation of Drug/Dye loaded Micelles.	154
4.3.4 Curcumin Stability Study and <i>In vitro</i> Release Behaviour from Block Copolymers Micelles	165
4.4 Discussions	169
4.5 Conclusion	178
4.6 References.....	181
Chapter 5 Novel Poly(Decylactone) Micelles for Solubilisation and Controlled Delivery of Amphotericin B	186
5.1 Introduction	187
5.2 Methods	191
5.2.1 Preparation and Characterisation of Blank and Amphotericin B loaded Micelles.....	191
5.2.2 <i>In vitro</i> Release Study of Amphotericin B from Block Copolymers Micelles	192

5.2.3 <i>In vitro</i> Degradation Study of mPEG-b-PDL Micelles.....	194
5.2.4 <i>In vitro</i> Cytotoxicity Study of mPEG-b-PDL and mPEG-b-PCL Micelles	195
5.3 Results	196
5.3.1 Preparation and Characterisation of Blank and Amphotericin B loaded Micelles.....	196
5.3.2 <i>In Vitro</i> Release Study of AmpB from Block Copolymer Micelles	203
5.3.3 <i>In Vitro</i> Degradation Study of mPEG-b-PDL Micelles	204
5.3.4 Effect of Micelles on Cells Metabolic Activity by Alamar Blue Assay.....	207
5.4 Discussion.....	208
5.5 Conclusion	212
5.6 References.....	214
Chapter 6 Synthesis and Characterisation of Folate tipped Poly(decylactone) Micelles for Receptor Mediated Tumor Targeting.....	217
6.1 Introduction	218
6.2 Methods	224
6.2.1 Synthesis of Azide Terminated Poly(ethylene glycol) methyl ether	224
6.2.2 Synthesis of Folate Conjugated Poly(ethylene glycol).....	226
6.2.3 Synthesis of Rhodamine B Conjugated Poly(ethylene glycol)	229
6.2.4 Synthesis of Propargyl-PDL	230
6.2.5 Synthesis of Block Copolymers via Click Chemistry	230

6.2.6 Preparation and Characterisation of Mixed Micelles	234
6.2.7 Cellular Uptake Studies	235
6.3 Results	236
6.3.1 Synthesis and Characterisation of Block Copolymers.....	236
6.3.2 Preparation and Characterisation of Block Copolymer Micelles	252
6.3.3 Cellular Uptake Study of Block Copolymer Micelles	258
6.4 Discussion.....	265
6.5 Conclusion	270
6.6 References.....	272
Chapter 7 Conclusions and Future Work.....	276
7.1 Conclusion	277
7.1.1 Synthesis, Characterisation and Evaluation of Polymers and Block Copolymers generated from Renewable δ -Decalactone	277
7.1.2 Synthesis, Characterisation and Evaluation of Ligand Mediated Targeting Efficiency of Amphiphilic Block Copolymers generated from Poly(decalactone)	281
7.2 Future Work.....	283

List of Figures

Figure 1-1 Schematic representation of hydrolytic degradable functional groups with their degraded products.	6
Figure 1-2 Graphical representation of polycondensation and ring opening polymerisation reaction	7
Figure 1-3 Structures made from PCL.	15
Figure 1-4 Two-stage synthesis method for copolymerization of ω -pentadecalactone, diethyl succinate, and 1,4-butanediol and confocal microscopic images of Lewis lung carcinoma cells after 2 h incubation.	22
Figure 1-5 Picture of poly(1,8-octanediol-co-citrate) (POC) scaffold, non-porous, sponge and porous and SEM image of the porous POC scaffold cross section.	23
Figure 1-6 SEM pictures of microsphere, nanofibers and TEM pictures of nanoparticles, micelles prepared from PLGA	27
Figure 1-7 Hydrolytic degradation of PM and its copolymer in PBS at 37°C.	29
Figure 1-8 SEM image of DOX-loaded nanoparticles prepared from poly(PDL-co-DO) copolymers and change in number-average molecular weight with respect to time for blank poly(PDL-co-DO) nanoparticles.	31
Figure 1-9 Structures of macrolactones synthesized from ricinoleic acid.	32
Figure 1-10 Pictorial presentation of self-assembly of an amphiphilic block copolymer into micelles when dispersed in water.	36
Figure 1-11 Schematic presentation of NK911, NK012, NC-6004 and Genexol-PM micelle formulation.	39

Figure 1-12 Pictorial presentation of methods used for micelle preparation and drug encapsulation	40
Figure 1-13 Schematic presentation of targeted therapy to tumors with the aid of nanoparticles (micelles).	43
Figure 1-14 Differences between normal and tumor tissues, which explains the passive targeting of nanocarriers by the EPR effect. ...	45
Figure 1-15 Receptor mediated endocytosis mechanism of a ligand after being attached to the specific receptor	49
Figure 1-16 CLSM images of human MCF-7, SGC-7901, and SKOV3 cells incubated with Tfm-RhB or M-RhB.	51
Figure 1-17 CLSM images of HeLa, KB, A549 and MCF7/ADR cells, after incubation with different DOX formulations for 3 h.	52
Figure 1-18 Tumor volume growth for various formulations of free DOX, DOX micelles, and DOX/FOL micelles as a function of time. .	53
Figure 1-19 Pictorial representation of general overview of proposed work	56
Figure 2-1 Pyrene fluorescence spectra in solvents with different polarity and in different concentration of amphiphilic block copolymer in water	76
Figure 3-1 ¹ HNMR of δ-decalactone acquired in chloroform-d.	95
Figure 3-2 ¹ HNMR spectra of propargyl PDL before and after purification of polymer.	95
Figure 3-3 ¹ HNMR spectra of propargyl-PDL, BZD-PDL and Gly-PDL acquired in CDCl ₃	96
Figure 3-4 DSC plot of propargyl PDL.....	97

Figure 3-5 ^{13}C Carbon NMR of BZD-PDL, propargyl-PDL and Gly-PDL acquired in CDCl_3	98
Figure 3-6 SEC traces of BZD-PDL, propargyl-PDL and Gly-PDL ..	100
Figure 3-7 SEC traces of BZD-PDL and propargyl-PDL using THF as eluent.	101
Figure 3-8 ^1H NMR spectrum and SEC trace of mPEG-b-PDL (during kinetic study).....	104
Figure 3-9 Reaction kinetics for ROP of δ -decalactone using mPEG as initiator and TBD (5 mole%) as catalyst.	105
Figure 3-10 Overlapped FTIR spectra of mPEG, δ -decalactone and mPEG-b-PDL copolymer.	105
Figure 3-11 ^1H NMR of mPEG-b-PDL and PDL-b-PEG-b-PDL copolymer acquired in CDCl_3	106
Figure 3-12 Carbon 13 NMR of mPEG-b-PDL and PDL-b-PEG-b-PDL copolymer acquired in CDCl_3	107
Figure 3-13 SEC traces of initiators and different block copolymers of δ -decalactone.....	108
Figure 3-14 DSC plot of mPEG-b-PDL and PDL-b-PEG-b-PDL.	109
Figure 3-15 SEC trace of mPEG-b-PCL obtained using chloroform as eluent and polystyrene as internal standard.....	111
Figure 3-16 ^1H NMR and ^{13}C NMR of mPEG-b-PCL in chloroform-d.	112
Figure 3-17 ^1H NMR and ^{13}C NMR spectra of mPEG-b-PDL-b-PPDL acquired in chloroform-d	114
Figure 3-18 DSC plot of mPEG-b-PDL-b-PPDL	115
Figure 3-19 ^1H NMR spectra of at 0 hr and after conversion of the reaction mixture obtained during the attempt of ROP of ω -	

pentadecalactone using TBD as catalyst and mPEG-b-PDL as initiator.....	121
Figure 4-1 Proposed assembly of low molecular weight surfactant and amphiphilic block polymer after dispersion in water.	130
Figure 4-2 Pictorial representation of preparation, purification and characterisation of curcumin loaded micelles.....	137
Figure 4-3 Standard calibration curve of Nile red.	139
Figure 4-4 Fluorescence emission spectra of curcumin at different concentration in acetone and standard calibration curve of curcumin.....	140
Figure 4-5 CMC plot for mPEG-b-PDL, PDL-b-PEG-b-PDL, mPEG-b-PDL-b-PPDL and mPEG-b-PCL obtained by pyrene 1:3 peak ratio method.	144
Figure 4-6 Comparison of 95% confidence interval (IC50) of the CMC values of synthesised copolymers.....	144
Figure 4-7 Size distributions by intensity and by volume of blank micelles determine by DLS method in water.	148
Figure 4-8 Physical appearance of purified blank micelles in water obtained from different copolymers.	148
Figure 4-9 TEM images and size distribution histogram of empty mPEG-b-PDL, PDL-b-PEG-b-PDL, mPEG-b-PDL-b-PPDL and mPEG-b-PCL micelles.	149
Figure 4-10 TEM images of empty mPEG-b-PDL, PDL-b-PEG-b-PDL, mPEG-b-PDL-b-PPDL and mPEG-b-PCL micelles.....	150
Figure 4-11 Size distribution spectrum of propargyl-PDL nano emulsion..	152

Figure 4-12 Zeta potential spectrum of propargyl-PDL nano emulsion measured in 10mM HEPES (pH-7.4) buffer.....	153
Figure 4-13 Zeta potential curve of mPEG-b-PDL, PDL-b-PEG-b-PDL, mPEG-b-PCL and mPEG-b-PDL-b-PPDL micelles.....	153
Figure 4-14 UV-Visible absorbance spectra of Nile red in acetone and micelles..	154
Figure 4-15 Appearance of micellar solutions and control (formulation without polymer) after Nile red loading and Nile Red content in different polymeric micelles	156
Figure 4-16 Size distribution curve by volume of mPEG-b-PDL, PDL-b-PEG-b-PDL, mPEG-b-PDL-b-PPDL and by intensity of PDL-b-PEG-b-PDL copolymer micelles in water after Nile Red loading.	157
Figure 4-17 Polymer micelles after curcumin loading and curcumin content in polymeric micelles..	159
Figure 4-18 Size distribution by volume of the micelles in water after loading of Curcumin.	160
Figure 4-19 TEM images of curcumin loaded micelles of mPEG-b-PDL and mPEG-b-PCL copolymer.	161
Figure 4-20 TEM images of curcumin loaded micelles of PDL-b-PEG-b-PDL and mPEG-b-PDL-b-PPDL copolymer.....	162
Figure 4-21 Percent encapsulation efficiency (EE%) observed for curcumin in different polymeric micelles	164
Figure 4-22 Plot representing the percentage of curcumin remains with respect to time of free curcumin and curcumin loaded in micelles incubated in PBS (pH-7.4) at 37°C.	166
Figure 4-23 <i>In-vitro</i> release pattern of curcumin from different block copolymer micelles	167

Figure 4-24 Proposed assembly of synthesized di-block and tri-block copolymer in water and the formation of cluster from triblock copolymer micelles.	170
Figure 4-25 Physical appearance of mPEG-b-PDL and mPEG-b-PDL-b-PPDL copolymer in 5mL acetone.....	173
Figure 4-26 Proposed encapsulation of curcumin in mPEG-b-PDL-b-PPDL copolymer micelles..	177
Figure 5-1 Physical appearance of solution of mPEG-b-PDL and mPEG-b-PCL copolymer after being dissolved in 5mL of methanol.	192
Figure 5-2 Standard calibration curve of Amphotericin B.	193
Figure 5-3 Sample distribution for release study.....	194
Figure 5-4 Physical appearance of micellar suspension (obtained <i>via</i> nanoprecipitation method) in water before and after filtration through 0.22 μm syringe filter.	197
Figure 5-5 Size distribution curve by intensity of Blank mPEG-b-PDL, AmpB loaded mPEG-b-PDL, Blank mPEG-b-PCL and AmpB loaded mPEG-b-PCL micelles.	198
Figure 5-6 Size distribution curve by volume of Blank mPEG-b-PDL, AmpB loaded mPEG-b-PDL, Blank mPEG-b-PCL and AmpB loaded mPEG-b-PCL micelles.	198
Figure 5-7 TEM image of blank mPEG-b-PDL and AmpB loaded mPEG-b-PDL micelles.....	199
Figure 5-8 TEM image of blank mPEG-b-PCL and AmpB loaded mPEG-b-PCL micelles.....	200

Figure 5-9 Graph represents Amphotericin B content (weight % to polymer) and encapsulation efficiency (EE%) observed in micelles	202
Figure 5-10 Cumulative release (%) of AmpB from different test formulations in water containing Tween 80 (1% v/v) at 37°C.....	203
Figure 5-11 SEC trace of mPEG-b-PDL after 120 days of storage at pH 7.4 (temperature – 37°C)..	206
Figure 5-12 Loss in molecular weight (M_n) of mPEG-b-PDL micelles with time at two different pH as determined by SEC.	206
Figure 5-13 <i>In vitro</i> cytotoxicity of empty micelles formulations.	207
Figure 5-14 Pictorial presentation of control “B” showing the AmpB equilibration from Tween 80 micelles to mPEG-b-PDL micelles and diffusion of AmpB in release media from dialysis membrane.	210
Figure 6-1 Standard calibration curve of folic acid and rhodamine B isothiocyanate.....	228
Figure 6-2 ^1H NMR spectra of mPEG-OTs and mPEG- N_3 acquired in chloroform-d.....	238
Figure 6-3 Overlapped FTIR spectra of mPEG $_{5000}$ -OH before and after azide conversion of hydroxyl group.	239
Figure 6-4 ^1H NMR of FA-PEG- N_3 in DMSO- d_6 that contained few drops of D_2O	240
Figure 6-5 ^1H NMR of RhB-PEG- N_3 conjugate acquired in chloroform-d and DMSO- d_6	241
Figure 6-6 Overlapped MALDI-TOF MASS spectra of folic acid (FA), rhodamine B (RhB) conjugated PEG and non-conjugated PEG. ...	243
Figure 6-7 SEC trace of PEG conjugates and commercial PEG-azide.	244

Figure 6-8 Picture of separated copper at bottom of eppendorf after centrifugation at 15000 rpm for 2 minutes.....	245
Figure 6-9 Overlapped FTIR spectra of mPEG-azide and mPEG-b-PDL synthesised by click reaction.	247
Figure 6-10 ¹ HNMR spectra of mPEG-b-PDL synthesised by click reaction and overlapped ¹ HNMR spectra of mPEG-N ₃ , mPEG-b-PDL,FA-PEG-N ₃ and FA-PEG-b-PDL.	248
Figure 6-11 ¹ HNMR spectra of FA-PEG-b-PDL acquired in chloroform-d and DMSO-d ₆	249
Figure 6-12 ¹ HNMR spectra of RhB-PEG-b-PDL acquired in chloroform-d and DMSO-d ₆	250
Figure 6-13 Overlapped SEC traces of various PEG-b-PDL copolymers.....	251
Figure 6-14 Pictorial presentation of different micelle formulations prepared in this study..	252
Figure 6-15 Size distribution by Intensity and volume of PDL and PDLFA micelles dispersed in PBS at room temperature.	253
Figure 6-16 Size distribution by intensity of the micelles dispersed in RPMI media at room temperature.....	254
Figure 6-17 Zeta potential distribution of PDL and PDLFA micelles in HEPES buffer (10mM, pH-7.4).....	255
Figure 6-18 TEM image of PDL and PDLFA micelles.	256
Figure 6-19 UV-Visible spectra of PDL and PDLFA micelles acquired using PBS as solvent.....	257
Figure 6-20 Confocal microscopy images of the A549 (FR-ve) cells treated with PDL micelles without and with added free folic acid present in the culture medium.	259

Figure 6-21 Confocal microscopy images of the A549 (FR-ve) cells treated with PDLFA micelles (folate conjugated) without and with added free folic acid present in the culture medium	260
Figure 6-22 Confocal microscopy images of the MCF-7 (FR+ve) cells treated with PDL micelles without and with added free folic acid present in the culture medium	261
Figure 6-23 Confocal microscopy images of the MCF-7 (FR+ve) cells treated with PDLFA micelles (folate conjugated) without and with added free folic acid present in the culture medium	262
Figure 6-24 Confocal microscopy images of the A549 (FR-ve) cells treated with PDL and PDLFA (folate conjugated) micelles at 4°C for 2.5 hrs in the absence of folic acid in the culture medium.....	263
Figure 6-25 Confocal microscopy images of the MCF-7 (FR+ve) cells treated with PDL and PDLFA (folate conjugated) micelles at 4°C for 2.5 hrs in the absence of folic acid in the culture medium.....	264

List of Tables

Table 1-1 Glass transition temperature and degradation time of PLA, PGA and PLGA polymers.....	26
Table 1-2 Examples of micelles formulations, which demonstrated enhanced tumor uptake by EPR effect. (mPEG- monomethoxyl PEG)	47
Table 3-1 Summary of experimental details and molecular weight obtained after ROP of δ -decalactone, ϵ -caprolactone and ω -pentadecalactone..	102
Table 3-2 Data obtained from the kinetic study of mPEG-b-PDL synthesis.....	104
Table 4-1 Intensity ratio of peak 1 and 3 of pyrene fluorescence spectrum acquired using different concentration of polymer in water.	143
Table 4-2 Characterization data of polymeric micelles prepared from block copolymers of Poly(decalactone) and Poly(caprolactone)...	145
Table 4-3 Average size by intensity and volume of PDL-b-PEG-b-PDL micelles in bimodal size distribution curve.	147
Table 5-1 Characterisation data of micelles prepared by nanoprecipitation method using methanol as an organic solvent..	197
Table 6-1 M_n of synthesised copolymers determined by ^1H NMR and by SEC.....	247
Table 6-2 Mean size and zeta potential of PDL and PDLFA micelles..	253

List of Schemes

Scheme 1-1 Mechanism of acid catalysed Fischer esterification reaction.	8
Scheme 1-2 Mechanism of acid catalysed trans-esterification reaction.	9
Scheme 1-3 Mechanism of Steglich esterification reaction	10
Scheme 1-4 Anionic mechanism for ROP of lactone (I) acyl-oxygen scission (II) alkyl-oxygen scission.....	12
Scheme 1-5 Coordination-insertion mechanism for ROP of lactones	12
Scheme 1-6 Cationic mechanism for ROP of lactones	13
Scheme 1-7 Synthesis scheme of the 20,20-polyester by polycondensation	19
Scheme 1-8 Synthesis scheme of functional monomers by thiol-ene chemistry using renewable methyl 10-undecenoate	20
Scheme 1-9 Synthesis scheme of Poly(glycerol-sebacate)	24
Scheme 1-10 Synthesis scheme of poly(MBL-co-CL) <i>via</i> ring opening polymerisation.	30
Scheme 1-11 Synthesis scheme of D-glucose carbonate monomer and its copolymerisation with polyphosphoester to make amphiphilic copolymers.....	34
Scheme 3-1 Ring opening polymerization of δ -decalactone catalysed by TBD using different initiators.	94
Scheme 3-2 Ring opening polymerization of ϵ -caprolactone using TBD as catalyst	110

Scheme 3-3 Ring opening polymerization of ω -pentadecalactone using lipase as catalyst	113
Scheme 3-4 Ring opening mechanism of TBD suggested by Pratt <i>et. al.</i>	118
Scheme 4-1 Degradation products of curcumin observed after its hydrolysis in 0.1 M phosphate buffer, (pH 7.2) at 37°C.	165
Scheme 6-1 Synthesis scheme of PEG-azide, FA-PEG-azide and RhB-PEG-azide.....	237
Scheme 6-2 Synthesis scheme of block copolymers of δ -decalactone via click chemistry	246

Acknowledgement

I am exceptionally grateful to Prof. Cameron Alexander, for giving me the opportunity to carry out research in his lab and freedom for doing innovative work during my PhD tenure. I am especially indebted to my co-supervisors Prof. Steve Howdle, Prof. Derek Irvin and Dr. Giuseppe Mantovani, who offered their continuous advice and encouragement throughout.

This thesis would not have been possible without the help of Dr. Laura Purdie and Lee Moir, who have performed the cell studies for me. I also owe my sincere thanks to all senior scientists (Post-Docs) for been always there to listen and give advice.

I would like to thank members of the administrative staff for their support and patience with the administrative and instrumental matters. I must give special thanks to all former and present students in B-15 lab and my other friends for their help and for providing a warm, friendly atmosphere throughout my stay in Nottingham.

The financial aid provided by Government of India is duly acknowledged. Finally, I would like to show my appreciation to my family members for their continuous moral support, without which this work would not have been possible.

Abbreviation List

^{13}C NMR	Carbon ¹³ nuclear magnetic resonance spectroscopy
^1H NMR	Proton nuclear magnetic resonance spectroscopy
AmpB	Amphotericin B
ANOVA	Analysis of variance
ATCC	American Type Culture Collection
CMC	Critical micelle concentrations
CO ₂	Carbon dioxide
DC	Drug content
DCC	<i>N,N'</i> -Dicyclohexylcarbodiimide
DCM	Dichloromethane
DDSA	Dodecenylsuccinic anhydride
DLS	Dynamic light scattering
DMac	Dimethyl acetamide
DMAP	4-(Dimethylamino) pyridine
DMSO	Dimethyl sulfoxide
DSC	Differential scanning calorimetry
EE	Encapsulation Efficiency
FA	Folic acid
FBS	Fetal bovine serum
FDA	Food and drug administration
FTIR	Fourier Transform Infrared Spectroscopy
HEPES	<i>N</i> -(2-hydroxyethyl) piperazine- <i>N'</i> -(2-ethanesulphonic acid)
IND	Indomethacin
KDa	Kilo dalton = 10 ³ g/mol
MALDI-TOF	Matrix-assisted laser desorption/ionization time-of-flight
MASS	mass spectroscopy
M_n	Number average molecular weight
MWCO	Molecular weight cut off
NHS	<i>N</i> -hydroxysuccinimide
nm/ d.nm	Nanometer/ diameter in nanometer
NMR	Nuclear Magnetic Resonance

NR	Nile red
PBS	Phosphate Buffer Saline (10 milimolar, pH- 7.4)
PCL	Poly (caprolactone)
PD/PDI	Polydispersity / Polydispersity Index
PDL	Poly(decalactone)
PEG / mPEG	Poly(ethylene glycol)/ methoxy poly(ethylene glycol)
PLA	Poly(lactide)
PLGA	Poly (lactide-co-glycolide)
PPDL	Poly(pentadecalactone)
RhB	Rhodamine B
ROP	Ring opening polymerization
ROP	Ring-Opening Polymerisation
RT	Room Temperature
SEC	Size exclusion chromatography
TEG	Tetraethylene glycol
TEM	Transmission Electron Microscope
T_g	Glass Transition Temperature
TGA	Thermogravimetry Analysis
THF	tetrahydrofuran
UV-Vis	Ultraviolet-visible
wt%	Weight %
μg	Micrograms

Chapter 1 Introduction

1.1 Introduction to Biodegradable Polymers in Drug Delivery

Development of novel formulations is paramount to improve the bioavailability of active pharmaceutical ingredients (API). Improved bioavailability of an API may eventually lead to an increase in the pharmacological response, lower the dose size and therefore minimise the side effects of API. Bioavailability of a drug can be increased by enhancing its aqueous solubility, stabilising the drug *in vivo*, providing controlled release of drug over prolonged time and by the change of route of administration^{1, 2}. With the aid of polymeric carriers, one or all of the above factors can be altered to improve bioavailability. Therefore, polymers play a vital role in the development of several novel drug-delivery systems. Specifically, biodegradable polymers have attracted special attention in drug delivery because they do not accumulate in the body^{3, 4}.

Biodegradable polymers are the materials, which can be broken down and excreted from the human body after they have served their function. These materials are typically excreted from the body by renal clearance after degradation into small molecules^{4, 5}. Polymer degradation can take place mainly through the chain scission, which is stimulated by oxidation, thermal activation, radiolysis, photolysis, hydrolysis

and enzymes. However, degradation by hydrolysis and/or enzymes is of utmost importance because these mechanisms mostly involve degradation of polymers in the human body³⁻⁵.

1.2 Classification of Biodegradable Polymers

Biodegradable polymers have been divided into two classes based on the source of origin *i.e.* Natural and Synthetic. Naturally occurring polymers generally undergo enzymatic degradation whereas synthetic polymers can be degraded hydrolytically as well as enzymatically⁵. Enzymatically degradable polymers can be further defined as materials, which possess hydrolytically cleavable bonds but require catalyst to undergo significant degradation under physiological conditions. Normally the degradation rate of enzymatically degradable polymers is much lower due to the presence of either ether or amide bonds^{4, 5}.

1.2.1 Biodegradable Polymers from Natural Origin

Polymers obtained from natural origin are available in ample quantity and fulfil most of the properties generally required for a biomaterial, to be used clinically. Natural polymers possess numerous inherent benefits such as natural remodeling, bioactivity, susceptibility to cell-triggered proteolytic degradation and the ability to present receptor-binding ligands to cells⁴. Several naturally occurring polymers have been

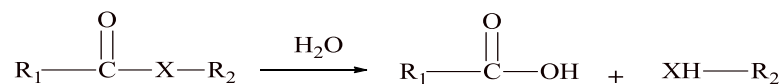
reported for drug delivery and tissue engineering applications. For instance, micro/nano-particles prepared from chitosan⁶, a modified natural carbohydrate polymer has been successfully used for the delivery of Insulin⁷, Cyclosporine A⁸, Doxorubicin⁹ etc. Similarly, collagen and its derivatives have been widely used to produce the scaffolds for bone tissue engineering¹⁰. Since, natural polymers mimic the extracellular matrix (ECM), they have therefore been extensively utilised for tissue engineering applications^{11, 12}. Several other polymers obtained from natural resources have been reported for various biomedical applications and were reviewed recently^{1, 4, 13-15}.

Despite their several advantages as biomaterial for drug and/or macromolecules delivery and tissue engineering, some restrictions are associated with the natural polymers. For instance, the rate of *in vivo* degradation of such polymers varies considerably with the site of implantation. Additionally, chemical modification can also affect their degradation rate⁴. Furthermore, the undesirable immunological response, difficulty in purification and processing, risk of transmitting pathogens (origin related) and batch-to-batch variability limits their applications^{4, 11, 16}.

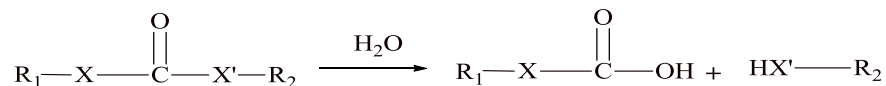
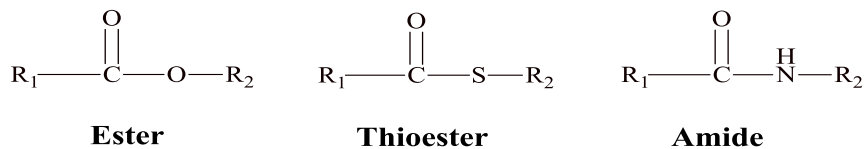
1.2.2 Biodegradable Polymers from Synthetic Origin

Synthetic biodegradable polymers used for biomedical applications are able to offer certain advantages over naturally occurring polymers^{17, 18}. These polymers provide the opportunity to synthesise tailor made material with desired properties. Furthermore, with synthetic polymers, it is possible to obtain material reproducibly with better quality control. Polymers with a desired property can be prepared by blending or copolymerising two or more different polymers^{4, 18, 19}. In view of the above advantages, it can be concluded that synthetic polymers can possibly overcome the various disadvantages associated with natural polymers.

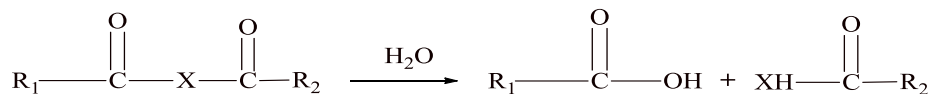
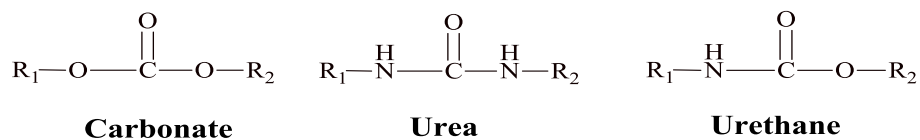
Synthetic biodegradable polymer generally contain a hydrolytically cleavable bond such as esters, thioesters, amides, carbonates, ureas, urethanes, imides, anhydrides, acetals, phosphonates etc. (figure 1-1). However, poly(esters) are the earliest and most studied class of biodegradable polymers due to their easy method of synthesis from commercially available monomers^{5, 20}. Therefore, in the current study, the literature review is limited to poly(ester) polymers.



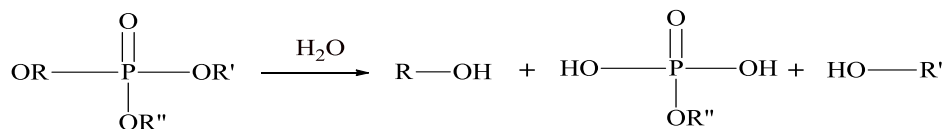
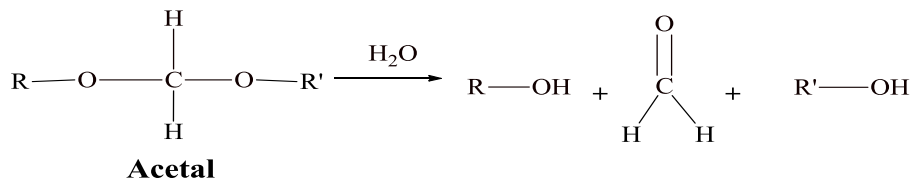
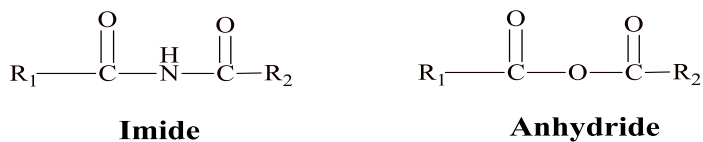
Where X= O, N-H, S



Where X and X'= O, N-H, S



Where X = O, N-H, S



Phosphonate

Figure 1-1 Schematic representation of hydrolytic degradable functional groups with their degraded products.

The two general routes used to synthesise poly (esters) polymers are step growth polymerisation (*i.e.* polycondensation) and chain growth polymerisation, which includes ring opening polymerisation (figure 1-2).

Polycondensation Reaction

Homo-polymerisation of a single monomer having two different end groups (for example: lactic acid) or copolymerisation of two monomers (for example: succinic acid and 1,4 butanediol) yield a polymer via polycondensation reaction. When two functional groups (acid and alcohol) join together during polyester synthesis, a small molecule (condensate) most often water is generally liberated as a by-product ²¹.

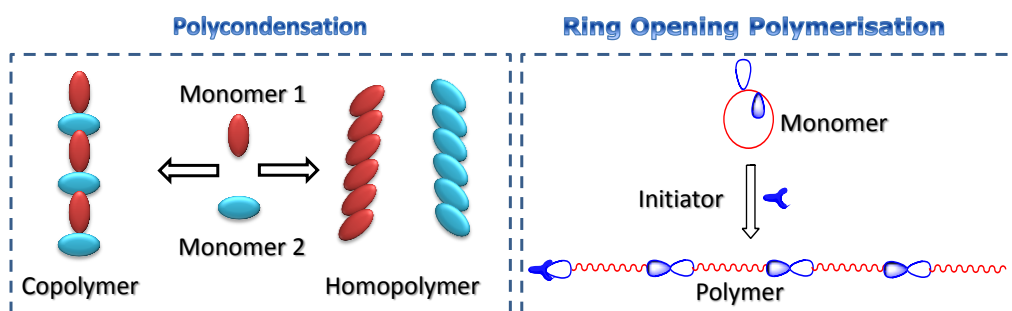
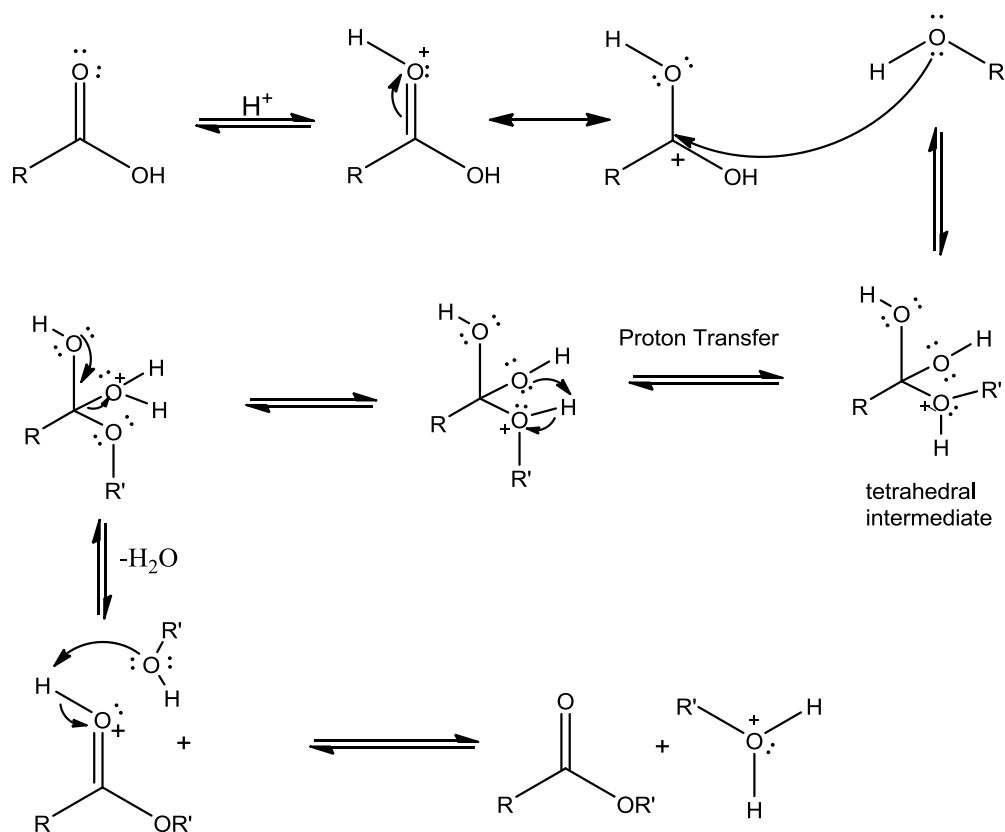


Figure 1-2 Graphical representation of polycondensation and ring opening polymerisation reaction

Mechanism involved in Polycondensation Reaction:

Fischer Esterification

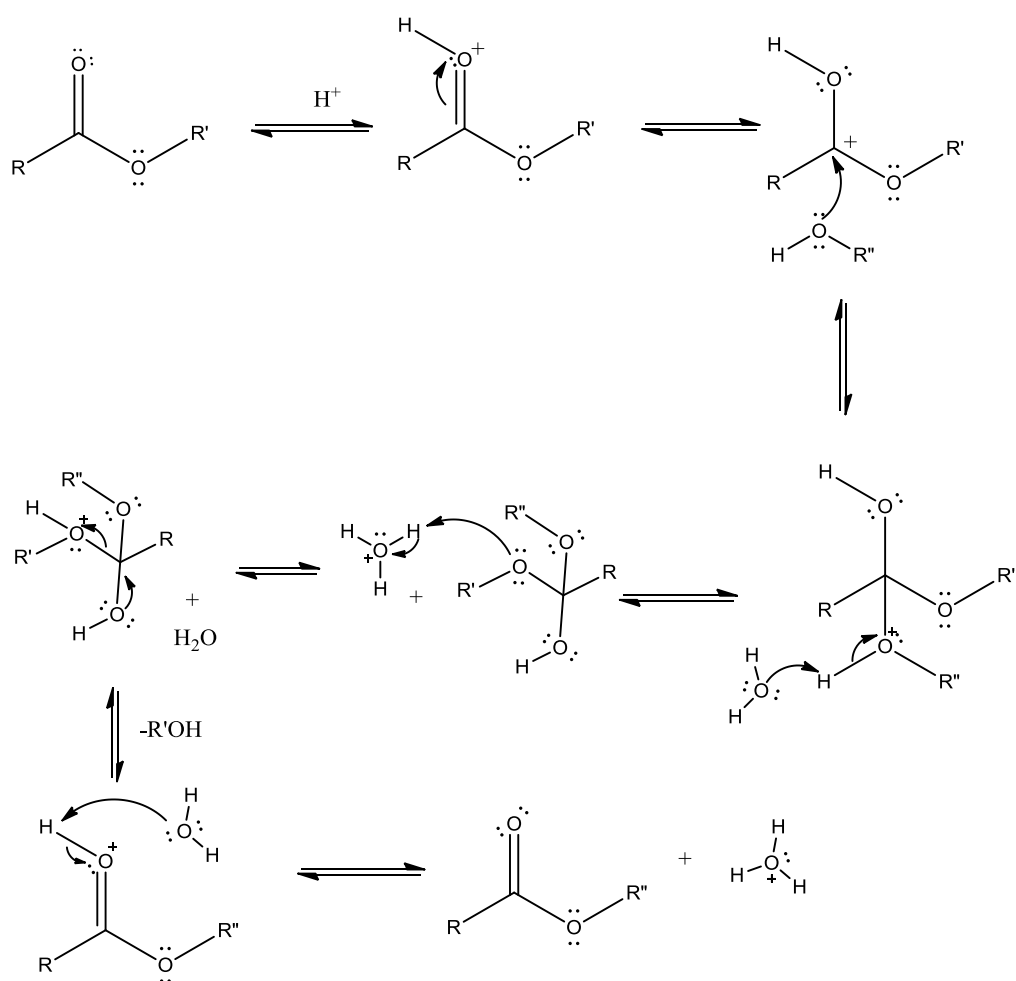
In Fischer esterification a carboxylic acid reacts with alcohol in the presence of Lewis or Bronsted acid to give esters by releasing a molecule of water²². The products and reactants are in equilibrium in this reaction (scheme 1-1). So, to drive equilibrium for the effective conversion of monomers to polymer, water is often removed continuously from the reaction medium.



Scheme 1-1 Mechanism of acid catalysed Fischer esterification reaction.²³

Trans-esterification Reaction

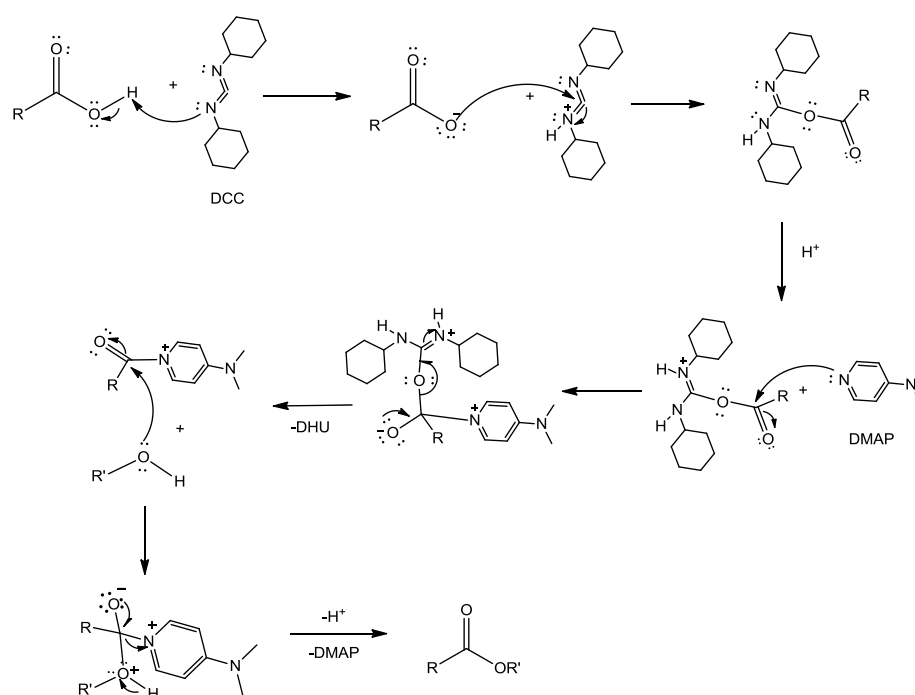
It is a route where an ester is converted into another ester by reacting with an alcohol in the presence of acid/base catalyst²⁴. To drive the equilibrium (to get the efficient conversion), either excess of reacting alcohol was used or the by-product (alcohol) was removed continuously from the reaction mixture (scheme 1-2).



Scheme 1-2 Mechanism of acid catalysed trans-esterification reaction.²⁴

These reactions are reversible and therefore high conversion cannot be achieved without the removal of condensate

molecule. Additionally, in Fischer esterification reactions, high temperature is often required to generate the polyesters in acceptable yield. Therefore, a mild approach was developed in 1978 by Wolfgang Steglich to synthesise esters²⁵. Dicyclohexylcarbodiimide was used as a coupling reagent and 4-dimethylaminopyridine acted as a catalyst. Dicyclohexylurea (DHU) is the by-product during the reaction, which can be removed easily by filtration (scheme 1-3).



Scheme 1-3 Mechanism of Steglich esterification reaction²⁵

Ring Opening Polymerisation

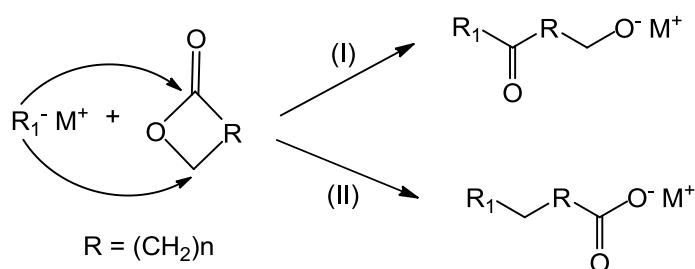
Ring opening polymerisation (ROP) is a widely investigated synthetic route to develop poly(esters). In this method, cyclic esters were used to synthesise long chain polyesters (figure 1-1). The target molecular weight can be predefined, based on

the quantity of monomer used. ROP is advantageous over polycondensation route to synthesise polyesters in terms of reaction condition and time, absence of by-product and control over the molecular weight. ROP is a form of chain-growth polymerisation, where the terminal ends of the chain have a reactive functional group, which repeatedly reacts with cyclic monomer, opening the next available ring until all monomers are consumed. However, an initiator is always required to open the first ring of cyclic monomer^{26, 27}. The three general mechanisms involved in ROP are cationic, anionic, and coordination-insertion. However, it has been reported that the high molecular weight polyesters can only be obtained by either anionic or coordination-insertion mechanism²⁶.

Anionic Mechanism of ROP

In an anionic ROP, the reaction is started by the nucleophilic attack of negatively charged initiator on the carbonyl carbon or on the carbon atom present beside the acyl oxygen of the lactone ring, yielding polyester (scheme 1-4). The commonly used initiators for an anionic ROP are alkali metals, alkali metal oxides etc. The propagating species in this mechanism is negatively charged which can attack the next available ring²⁶. In 4-membered rings such as β -butyrolactone, β -propiolactone, either alkyl or acyl-oxygen cleavage has been

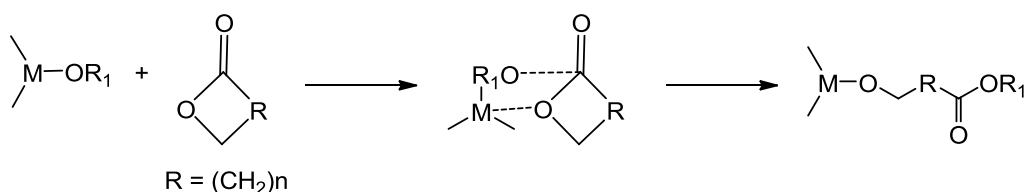
reported giving a carboxylate or alkoxide respectively²⁸. However, in bigger size ring such as lactide, only acyl-oxygen scission has been involved giving an alkoxide as the propagating species²⁶.



Scheme 1-4 Anionic mechanism for ROP of lactone (I) acyl-oxygen scission (II) alkyl-oxygen scission²⁶

Coordination-Insertion Mechanism of ROP

The coordination-insertion mechanism for ROP of lactones is shown in scheme 1-5.



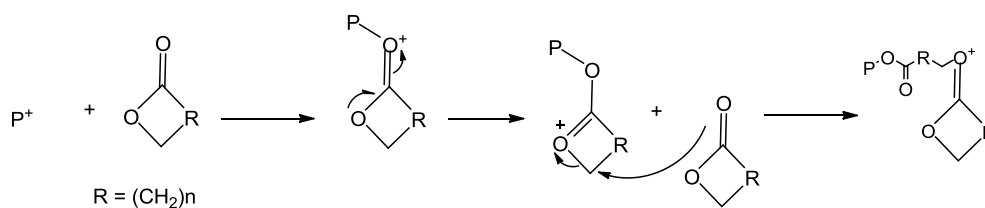
Scheme 1-5 Coordination-insertion mechanism for ROP of lactones²⁶

The initiators which open the lactone ring via this mechanism are aluminium and tin alkoxides and carboxylates²⁶. These initiators with vacant "d" orbitals react as coordination initiators and not as anionic initiators. Cleavage of the acyl oxygen bond leads to ring opening of the lactone. The propagation continues by coordination of the monomer to the active species and then insertion of the monomer into the

metal-oxygen bond. The coordination of metal with the exocyclic oxygen makes the carbonyl carbon more susceptible for nucleophilic attack (scheme 1-5). However, in this mechanism long reaction time or high temperature leads to both inter and intramolecular transesterification reactions²⁶.

Cationic Mechanism of ROP

In this mechanism, a positively charged species of monomer is generated after reacting with a cationic catalyst. The subsequent attack by another monomer leads to ring opening *via* S_N2 reaction (scheme 1-6)^{27, 29, 30}.



Scheme 1-6 Cationic mechanism for ROP of lactones³⁰

1.3 Classification of Synthetic Poly(esters):

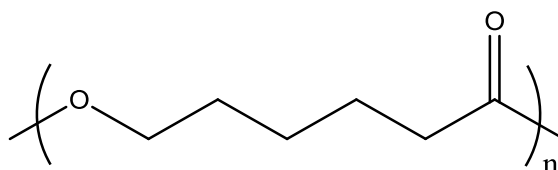
Synthetic biodegradable poly(esters) can be further classified into two classes:

1.3.1 Poly(esters) Synthesised from Non-Renewable Monomers

Non-renewable monomers are those monomers whose supply is limited. These monomers are procured directly from fossil fuels, which exist within the earth. Fossil fuels are extracted

from organic matter; which are the remains of once living material. As generation of organic matters takes millions of years, the available fossil fuels are going to be finished in the near future³¹. Several polymers, synthesised from monomers derived from fossil fuels are currently in use for biomedical applications^{3, 32}. However, the objective of the current study is to make biodegradable poly(esters) from renewable monomers and hence this section has not been exhaustively reviewed. Some brief examples of such polymers with cleavable bonds (esters) are given below:

Poly(caprolactone):



Poly(caprolactone) (PCL) synthesised by ROP of ϵ -caprolactone, is one of the most extensively studied biodegradable polymers. The key precursor used for the preparation of caprolactone is cyclohexanone whose starting material is benzene. The use of PCL in the drug delivery and tissue engineering applications has been reported by several researchers and reviewed recently (figure 1-3)^{3, 13, 33, 34}. The complete hydrolytic degradation of PCL generally takes 2–3 years³³.

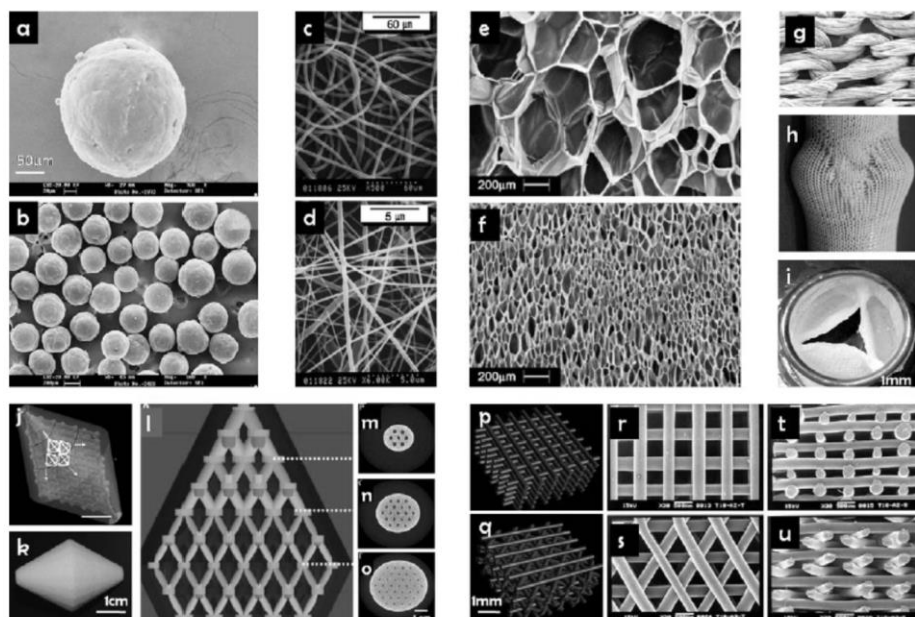
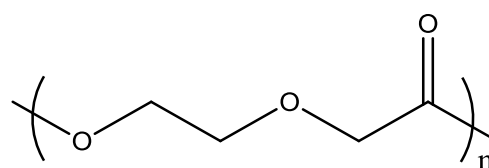


Figure 1-3 Structures made from PCL: Nanospheres (a,b). Nanofibres (c,d). Foams (e,f). Knitted textiles (g,h,i). Selective laser sintered scaffold (j-o). Fused deposition modeled scaffolds (p-u)³³.

“Capronor” is the regulatory approved formulation of PCL used for the sustained subdermal delivery of contraceptive steroids (levonorgestrel)^{33, 35}.

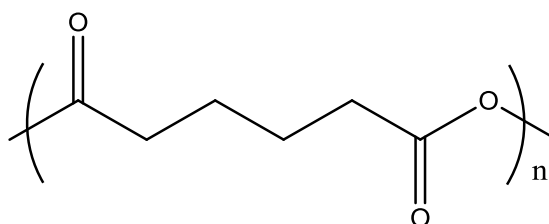
Poly(p-dioxanone):



Poly(p-dioxanone) (PPDO) has been synthesised by ring opening polymerisation of p-dioxanone (PDO). PDO was prepared by oxidative dehydrogenation of diethylene glycol over Cu(O) catalyst supported on silica particles³⁶. Diethylene glycol is generally produced by the hydrolysis of ethylene oxide, an oxidised ethylene (hydrocarbon). PPDO has been

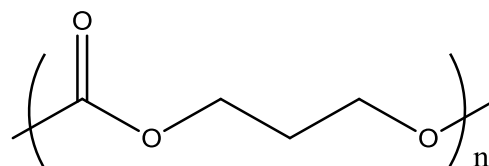
used for the preparation of sutures (FDA approved)³⁷, in tissue engineering³⁶ and its copolymers have also been studied for drug delivery applications³⁸.

Poly(anhydrides):



For a long time, poly (anhydrides) have been used for the controlled release drug delivery applications³⁹. For instance, microspheres of poly(adipic anhydride), synthesised by ROP of oxepan-2,7-dione has been used for ocular drug (Timolol maleate) delivery in controlled fashion⁴⁰. The key monomer for the synthesis of oxepan-2,7-dione is adipic acid, which is prepared using cyclohexane (hydrocarbon), as starting material⁴¹.

Poly(trimethylene carbonate)



Poly (trimethylene carbonate) (PTMC) has been used in biomedical field because it degrades into biocompatible 1,3-propanediol and carbonic acid⁴². PTMC is generally synthesised

by the ROP of trimethylene carbonate (TMC) which is commercially available. TMC is usually prepared from 1,3-propanediol and ethyl chloroformate or from oxetane and carbon dioxide⁴³. Nanoparticles⁴⁴, microparticles⁴⁵ and gels⁴⁶ have been prepared from PTMC but more often it has been copolymerised with PLA⁴⁷ or PCL⁴⁸ to improve its drug delivery potential.

1.3.2 Poly(esters) Synthesised from Renewable Monomers

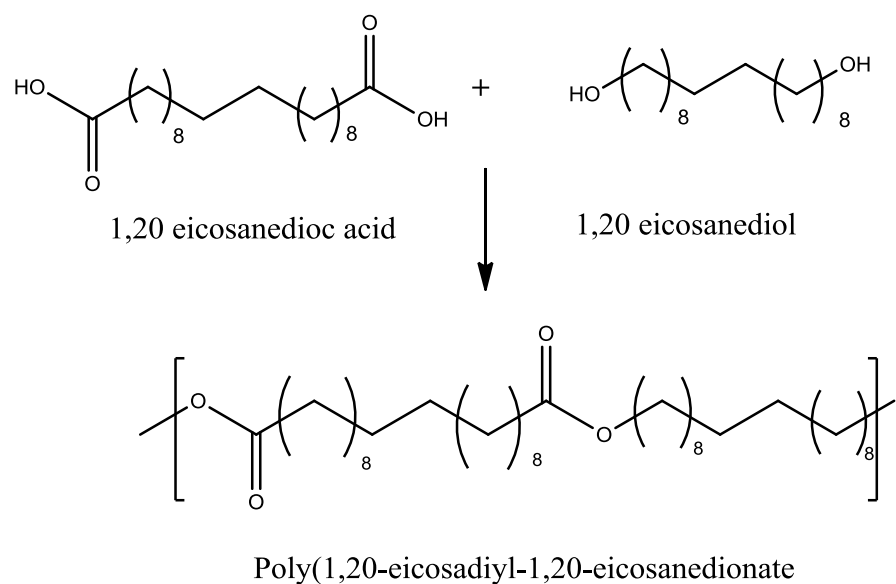
Renewable resources can be defined as “any animal or vegetable species which is exploited without endangering its survival and which is renewed by biological (short term) instead of geochemical (very long term) activities”⁴⁹. They are the most attractive feedstock to synthesise polymers of choice. Based on the concept “acting responsibly to meet the needs of the present without compromising the ability of future generations to meet their own needs”⁵⁰, several renewable feedstocks have been discovered, which are obtained from either plant or animal source. A biodegradable polymer obtained solely from renewable resources can be described as a “green” polymeric material⁵¹. A polymer synthesised using monomers obtained from natural resources might be a good alternative for natural and synthetic polymers

(non-renewables). Some examples of biodegradable polymers having ester bonds, synthesised from the natural monomers are described below:

In the first section, renewable poly(esters) synthesised by polycondensation reaction have been reviewed, while in the second section, polyesters synthesised by ROP have been reported.

(I) Renewable Poly (esters) via Polycondensation Reaction

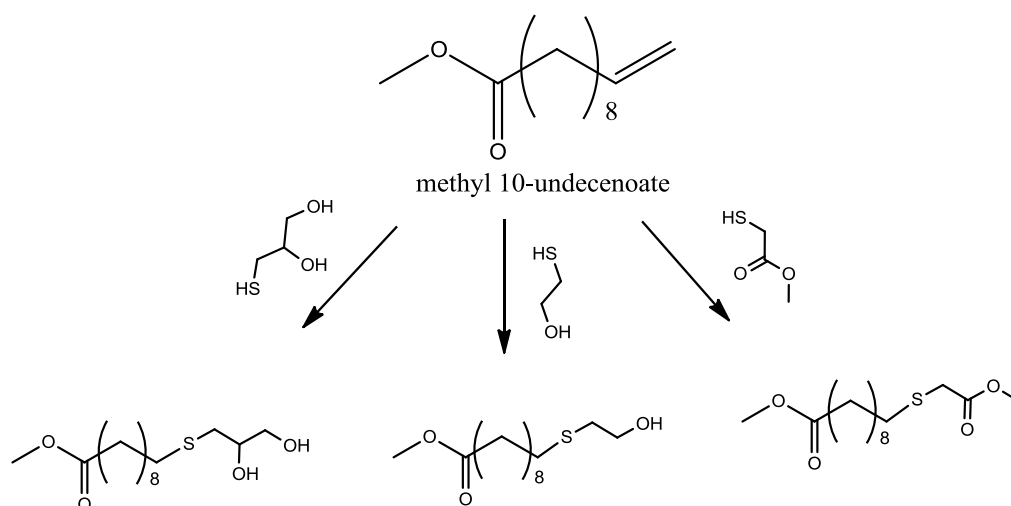
Ricinoleic acid (RA) (12-hydroxy-9-cis-octadecenoic acid) obtained from castor oil is the most important fatty acid based monomer, due to its bifunctionality⁵⁰. RA is a C18 fatty acid containing a hydroxyl group in the chain. RA can be used to synthesise γ -Decalactone and ϵ -decalactone⁵². Undecenoic acid produced from ricinoleic acid was utilised to synthesise 1,20-eicosanedioic acid and eicosane-1,20-diol. Polycondensation reactions between the diacid and the diol, produced a high molecular weight polymer named "polyester 20,20" (T_m -108°C)(scheme 1-7)⁵³.



Scheme 1-7 Synthesis scheme of the 20,20-polyester by polycondensation⁵³

Ricinoleic acid has been also incorporated in different ratios into anhydride end-capped poly(sebacic acid) by transesterification reactions. Release of cisplatin from these degradable polymers was studied, which suggested that increases in the RA content decreased the release rate⁵⁴. Similarly, RA has been copolymerised with lactic acid to decrease the degradation rate of resultant polymer and to slow down the release of incorporated drugs⁵⁵.

In another study, methyl 10-undecenoate, a castor oil derived product, was functionalised by thiol-ene chemistry to prepare renewable monomers (scheme 1-8). Aliphatic polyesters have been synthesized from the prepared monomer in the form of hyperbranched, dendritic, and linear chains⁵⁶.



Scheme 1-8 Synthesis scheme of functional monomers by thiol-ene chemistry using renewable methyl 10-undecenoate⁵⁶

18-Hydroxy-9,10- epoxyoctadecanoic acid, 15-hydroxy-hexadecanoic, 9(10),16-dihydroxyhexadecanoic acid are other examples of fatty acid-based monomers used in the preparation of polyesters^{50, 57, 58}.

Some other examples of renewable monomers used to generate polyesters are succinic acid, fumaric acid, citric acid, sebacic acid, suberic acid, itaconic acid and 2,5-furandicarboxylic acid. Bio-based alcohols used for polyester synthesis include 1,3-propanediol, 1,4-butanediol, isosorbide and glycerol⁵⁰.

For instance, Goerz *et. al.* reported the synthesis of a series of polyesters using isosorbide, itaconic acid and succinic acid under microwave irradiation. The polyesters demonstrated glass transition temperature (T_g) values between 57°C to 65°C and possessed one-way shape memory effect⁵⁹. In

another work, synthesis of poly(propylene sebacate) has been reported using 1,3-propanediol, sebacic acid, and itaconic acid. Biodegradable poly(propylene sebacate) (PPS) was found to be non-toxic when tested on NIH3T3 cell lines. Additionally, it was also demonstrated that the shape memory behaviour of PPS was tunable by introducing diethylene glycol⁶⁰. Copolymers of sebacic acid or fumaric acid with poly(ethylene glycol) (PEG) have also been prepared for the controlled drug delivery applications⁶¹.

Poly(butylene succinate) (PBSu) synthesised by polycondensation reaction between succinic acid and 1,4-butanediol is a commercially available polymer. However, PBSu has been less explored for drug delivery applications because of the poor degradability and functionality^{3, 62, 63}. To address these problems, copolymers of PBSu are most often prepared to obtain the polymer with suitable properties. For instance, novel aliphatic poly(butylene succinate-co-cyclic carbonate) bearing various functionalisable carbonate building blocks have been reported⁶³. In another study, a copolymer of PBSu with ω -pentadecalactone *i.e.* poly(ω -pentadecalactone-co-butylene -co-succinate) (PPDL-co-PBSu) has been synthesised in two steps for the effective delivery of Camptothecin (CPT). The PPDL-co-PBSu nanoparticles loaded

with CPT demonstrated high cellular uptake compared to free CPT against Lewis lung carcinoma cell lines *in vitro* (figure 1-4)⁶⁴.

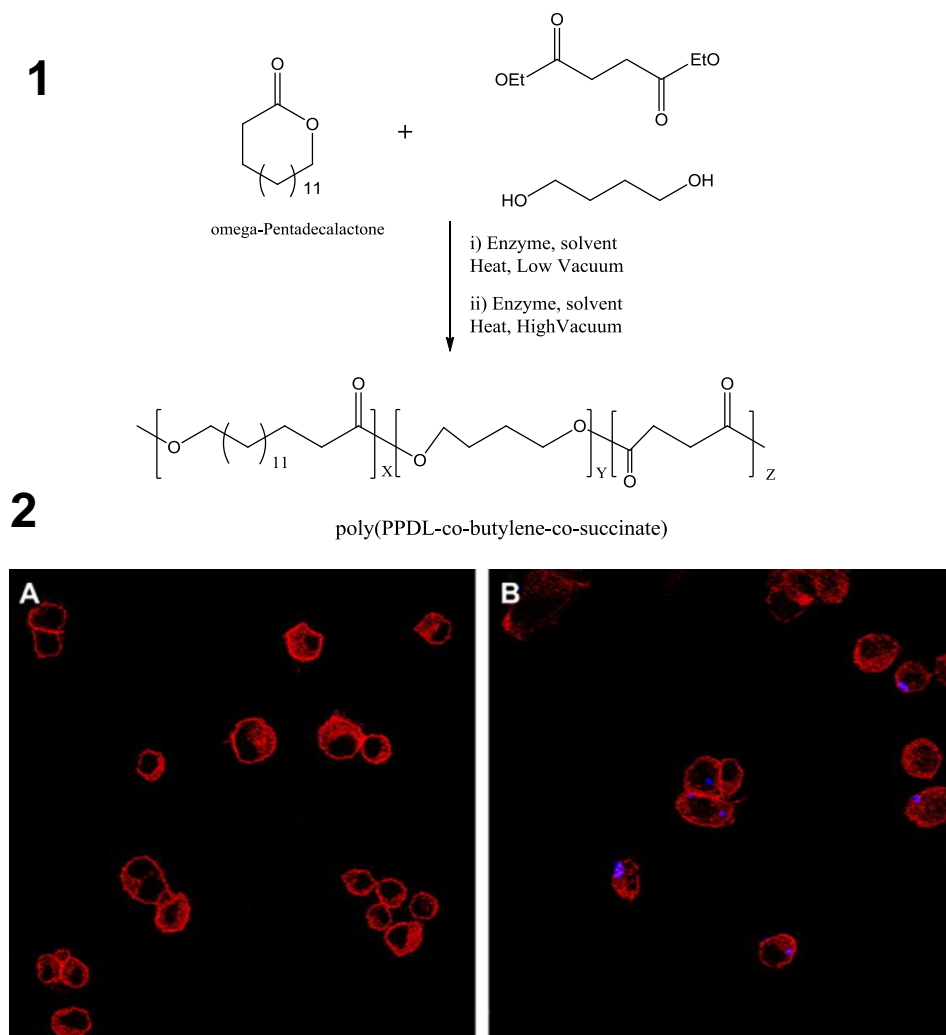


Figure 1-4 (1) Two-stage synthesis method for copolymerization of ω -pentadecalactone, diethyl succinate, and 1,4-butanediol. (2) Confocal microscopic images of Lewis lung carcinoma cells after 2 h incubation with (A) free CPT and (B) CPT-loaded PPDL-co-PBSu nanoparticles. Cells and CPT are visualized in the red and blue channels, respectively⁶⁴.

Citric acid, due to its branched structure is generally used to prepare hyperbranched polyesters and dendrimers. For instance, Namazi *et.al.* reported the successful synthesis of a citric acid dendrimer using PEG as the core molecule. The

aqueous solubility of 5-amino salicylic acid, pyridine, mefenamic acid, and diclofenac have been improved using this water soluble dendrimer⁶⁵. Recently synthesis of a hyperbranched polymer of citric acid and glycerol *via* a polycondensation route has been reported. This polymer has been used for the improved delivery of the cytotoxic drug, cisplatin⁶⁶. In another study, a series of poly(diols citrates) has been synthesised by reacting citric acid with various diols via a polycondensation reaction.

These novel poly(diols citrates) were tunable in terms of mechanical properties, degradation and surface characteristics by varying the diols and by manipulating the cross-link density. The synthesised poly(diols citrate)s were fabricated into various type of soft scaffold for tissue engineering applications (figure 1-5)^{67, 68}.

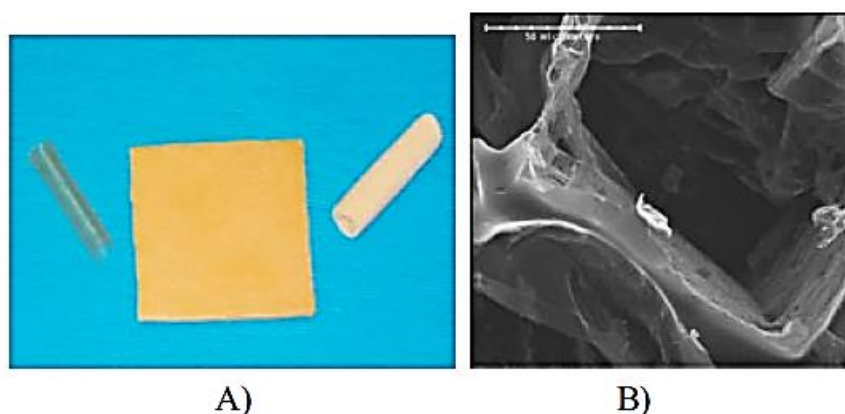
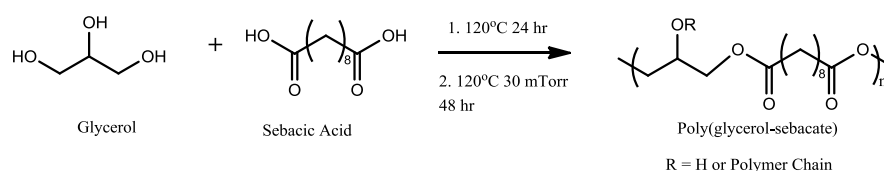


Figure 1-5 (A) Picture of poly(1,8-octanediol-co-citrate) (POC) scaffold, non-porous (left), sponge (middle) and porous (right). (B) SEM image of the porous POC scaffold cross section. Scale bar 50 μm ⁶⁷

Glycerol, a renewable monomer has attracted special attention to prepare polyesters due to its large amount of production as a by-product during biodiesel production. Recently, Dow announced the production of propylene glycol from glycerol⁵⁷. Glycerol can also be converted into 1,3-propanediol using biotechnological methods⁶⁹. Several useful monomers and polymers have been derived from glycerol including poly(esters) for various applications and were reviewed recently^{70, 71}.

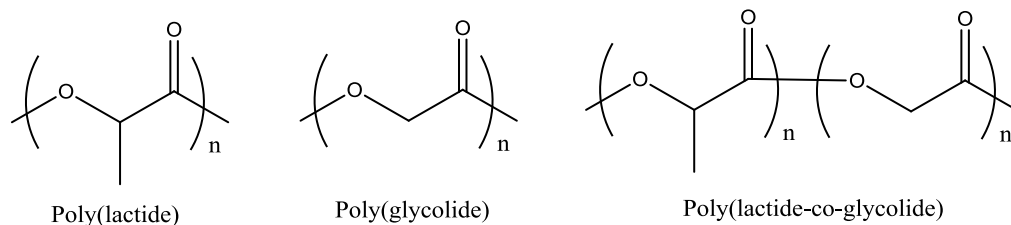


Scheme 1-9 Synthesis scheme of Poly(glycerol-sebacate)⁷²

Langer and co-workers synthesised poly(glycerol sebacate) (PGS), a tough biodegradable elastomer using glycerol and sebacic acid for various tissue engineering applications (scheme 1-9)^{72, 73}. The *in vitro* degradation of this elastomer was compared with poly(DL-lactide-co-glycolide) (PLGA) and it was found that unlike PLGA, PGS gave a linear degradation profile⁷⁴. Biodegradable PGS implants loaded with 5-fluorouracil (5-FU) showed control release of 5-FU for 7 days with superior antitumour activity *in vitro*⁷⁵. Degradable polyesters of glycerol with adipic acid, citric acid, 1,18-cis-9-octanedecenedioic acid have also been reported⁷⁶.

(II) Renewable Poly(esters) via Ring Opening Polymerisation

Poly(esters) of Lactide and Glycolide



Poly(lactide) (PLA) and poly(glycolide) (PGA) are generally prepared by ring opening polymerisation of renewable lactide and glycolide respectively. Although PLA and PGA can also be synthesise by polycondensation of lactic acid and glycolic acid, but due to the better control over molecular weight during ROP, cyclic monomers (lactide and glycolide) are generally preferred. Lactic acid is commercially produced by the fermentation of glucose and sucrose (from corn or sugar) by lactic acid bacteria. The lactic acid is then converted into its cyclic dimer, lactide with the help of an acid catalyst at high temperature. Similarly, glycolic acid can be isolated from natural sources, such as sugarcane, sugar beets, pineapple and unripe grapes and then converted into glycolide³². Several reviews have been published recently, summarising their potential for various biomedical applications^{5, 15, 19, 77-79}.

Polymer	Glass Transition Temperature (T_g) (°C)	Degradation time (months)
PGA	36	2-4
PLA	60-67	18-24
PDLLA	57-59	12-16
50: 50 Poly(DLLA-co-GA)	46.1	2
85: 15 Poly(DLLA-co-GA)	45	5

Table 1-1 Glass transition temperature and degradation time of PLA, PGA and PLGA polymers⁸⁰

However, due to the high crystallinity, rapid degradation and poor solubility of PGA (in many common organic solvents), the use of PGA in drug delivery has been limited. On the other hand, PLA, specifically poly(L-lactic acid) (PLLA), poly(DL-lactic acid) (PDLLA), has been widely investigated for drug delivery applications. PLLA is a semicrystalline polymer whereas PDLLA is an amorphous polymer due to the random positions of methyl groups in the polymer chain. The presence of methyl groups in PLA increased its hydrophobicity and hence reduced the degradation time^{5, 79}. Therefore, copolymers of PLA and PGA have been synthesised to alter the degradation time of final polymer (table 1-1).

Poly(lactide-co-glycolide) (PLGA), a random copolymer of PLA and PGA is the most investigated degradable polymer for biomedical applications. It has been used to prepare drug

delivery carriers, sutures, and tissue engineering scaffolds^{77, 79}. Due to the difference in the properties of PLA and PGA, it is possible to make PLGA of choice by careful selection of copolymer composition for intended applications (table 1-1).

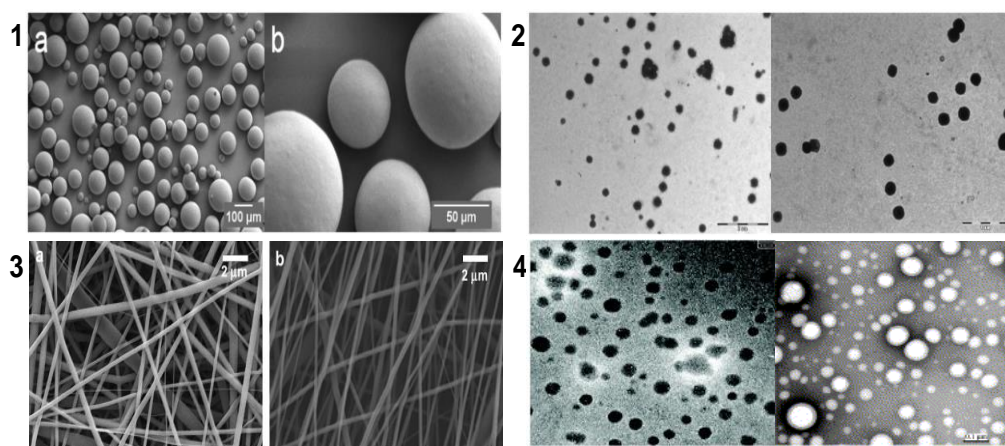
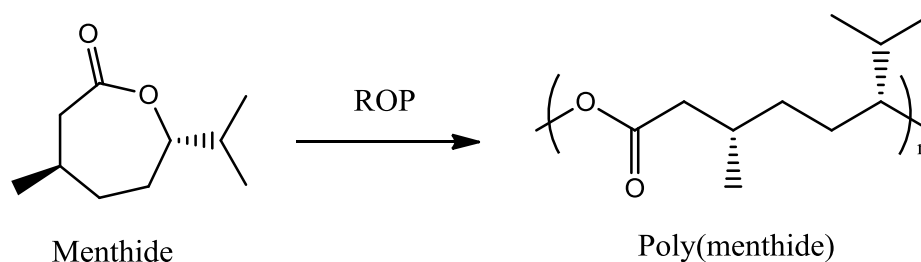


Figure 1-6 SEM pictures of (1) microsphere⁸¹, (3) nanofibers⁸² and TEM pictures of (2) nanoparticles⁸³, (4) micelles⁸⁴ prepared from PLGA

PLGA has been fabricated into microspheres^{81, 85}, nanoparticles⁸⁶, nanofibers^{82, 87}, micelles⁸⁸ (figure 1-6), for controlled and improved delivery of vaccines⁸⁹ cytotoxic drugs⁹⁰, proteins⁹¹, antibiotics⁹², siRNA⁹³ etc. PLGA and PLA have already been approved by the "United States Food and Drug Administration" (US-FDA) and "European Medicine Agency" (EMA) for human use.

Poly(esters) Synthesised from Renewable Lactone Monomers



The synthesis of high molecular weight (90 kg/mol) poly(menthide) (PM), an amorphous polymer ($T_g \approx -25^\circ\text{C}$) via the ROP of menthide has been reported recently⁹⁴. Menthide, a seven-membered lactone monomer was prepared by the simple Baeyer-Villiger oxidation reaction of menthone. Menthol, a natural product extracted from the plant *Mentha Arvensis*, (in ton scale) is the starting material to prepare menthone⁹⁴. Later PM was used as initiator to synthesise a triblock copolymer of PLA. The obtained triblock copolymer (PLA-PM-PLA) possessed the properties similar to styrene based systems. Further, *in vitro* degradation of PLA-PM-PLA copolymers was assessed in phosphate buffer solution (pH 7.4) at 37 °C. It was observed that the rate of degradation of triblock copolymers was in between that of PLA and PM homopolymers (figure 1-7). These copolymers maintained their mechanical properties for approximately 21 weeks, which was claimed to be better than any previously reported PLA-containing block copolymers^{95, 96}.

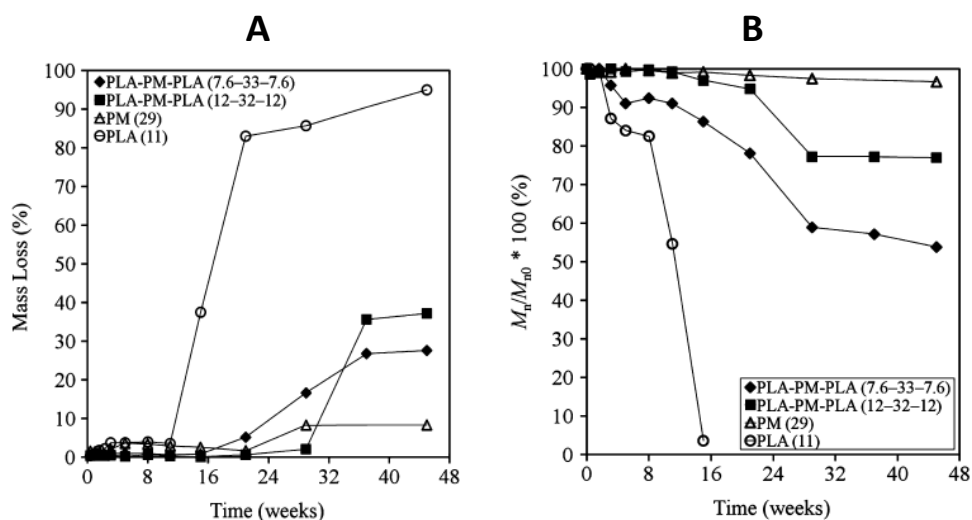
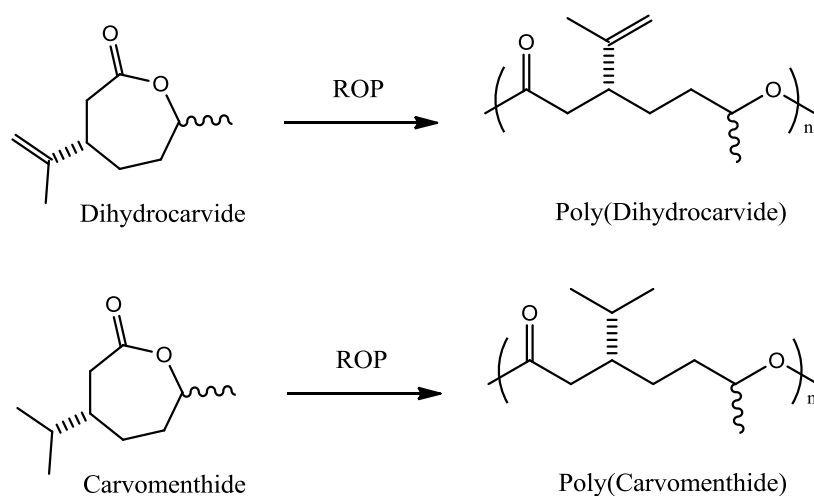
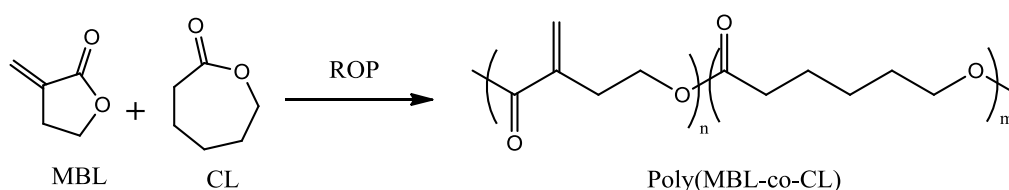


Figure 1-7 Hydrolytic degradation of PM and its copolymer in PBS at 37°C. (A) mass loss with time and (B) molecular weight loss (determined by SEC) with time⁹⁵

Carvone is another monomer investigated to prepare renewable lactone rings. Carvone is a natural product found in spearmint (*Mentha spicata*) and caraway oils (*Carum carvi*). Hydrogenation of carvone produced dihydrocarvone and carvomenthone, which can be easily converted into respective lactone *i.e.* dihydrocarvide and carvomenthide by Baeyer-Villiger oxidation⁹⁷.



In another study, the ROP of renewable δ -decalactone using an organic catalyst 1,5,7-triazabicyclo[4.4.0]dec-5-ene (TBD) has been published to synthesise amorphous poly(δ -decalactone)⁹⁸. The synthesis of high molecular weight triblock copolymer *i.e.* poly (lactide)-b-poly(δ -decalactone)-b-poly(lactide) was also reported by sequential addition of monomers⁹⁸. A very similar study was done with renewable ϵ -decalactone monomer to prepare a tough and thermo-resistant copolymer⁹⁹.



Scheme 1-10 Synthesis scheme of poly(MBL-co-CL) *via* ring opening polymerisation.¹⁰⁰

Recently Tulipaline A or α -methylene- γ -butyrolactone (MBL), a natural product isolated from tulips has been explored to make polyester by ROP using lanthanide based catalysts¹⁰⁰. It has been known that due to the high thermodynamic stability (or low strain energy) of five membered rings, the ROP of MBL is difficult²⁶. Due to this reason, a copolymer with caprolactone (high strain energy) was prepared (scheme 1-10)¹⁰⁰. The resultant unsaturated copolymer can be of great interest due to the presence of allyl functional group for post functionalization¹⁰¹. However, to date, no application has been

reported. Based on this approach, other renewable lactones with high ring strain might also be used to make copolymer with MBL in order to obtain a complete renewable polymer¹⁰².

Macrolactones obtained from naturally occurring macrocyclic musks such as ω -pentadecalactone and Globalide (GI), have been also explored for the synthesis of poly(ester) by ROP using enzyme as catalyst^{103, 104}.

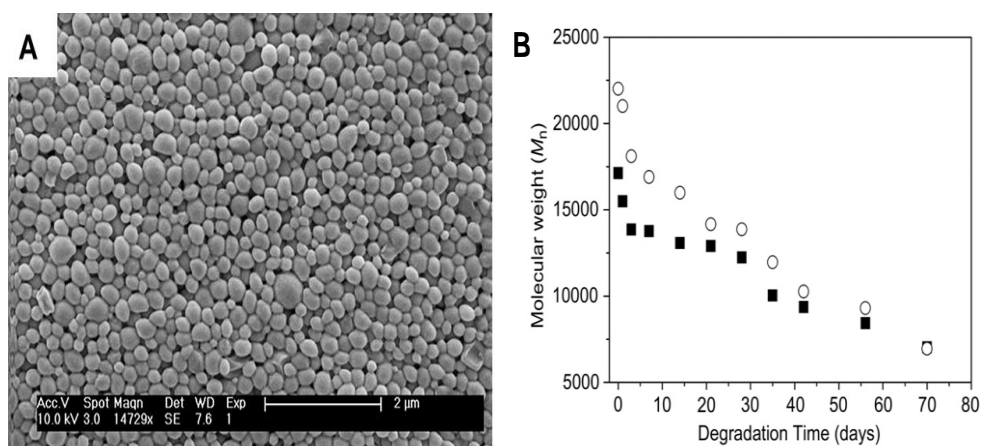


Figure 1-8 (A) SEM image of DOX-loaded nanoparticles prepared from poly(PDL-co-DO) copolymers and (B) change in number-average molecular weight with respect to time for blank poly(PDL-co-DO) nanoparticles having different concentration of PDL incubated in PBS solution (pH - 7.4) at 37°C¹⁰⁵.

The poly(ω -pentadecalactone) synthesised from ω -pentadecalactone was found to be nontoxic as determined by MTT (3-(4,5-dimethylthiazol-2-yl)-2,5-diphenyltetrazolium bromide) assay on 3T3 mouse fibroblast cell line. However, due to high crystallinity and highly hydrophobic nature of the polymer, no hydrolytic or enzymatic degradation was observed¹⁰⁴. To address this problem, a copolymer with p-

dioxanone (DO) has been synthesised named poly(ω -pentadecalactone-co-p-dioxanone) (poly(PPDL-co-DO)) using different ratios of ω -pentadecalactone and DO. The nanoparticles fabricated using poly(PPDL-co-DO) showed hydrolytic degradation at 37 °C (figure 1-8).

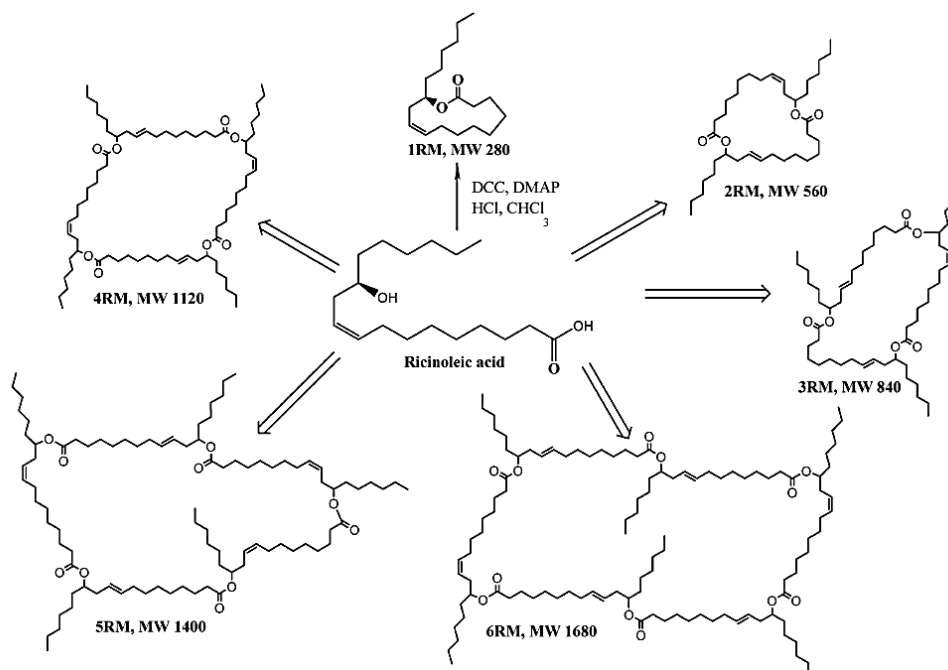
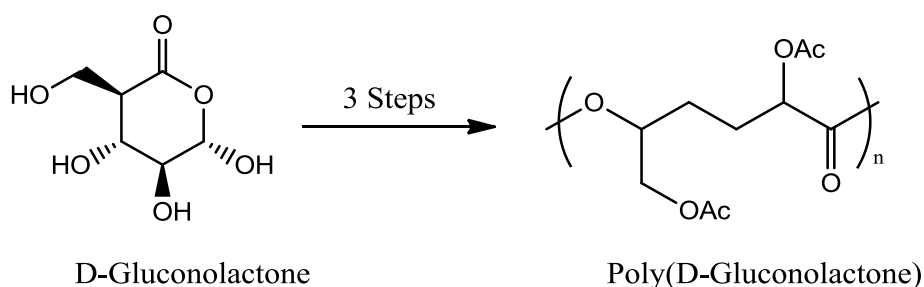


Figure 1-9 Structures of macrolactones synthesized from ricinoleic acid. Abbreviations for cyclic macrolactones: 1RM, monolactone; 2RM, dilactone, 3RM, trilactone; 4RM, tetralactone; 5RM, pentalactone; 6RM, hexalactone.¹⁰⁶

Doxorubicin (DOX) and siRNA were successfully encapsulated in the poly(PPDL-co-DO) nanoparticles with the maximum encapsulation efficiency of 42 and 33 % respectively. The loaded poly(PPDL-co-DO) nanoparticles demonstrated the controlled release of encapsulated molecules for up to 60 days¹⁰⁵.

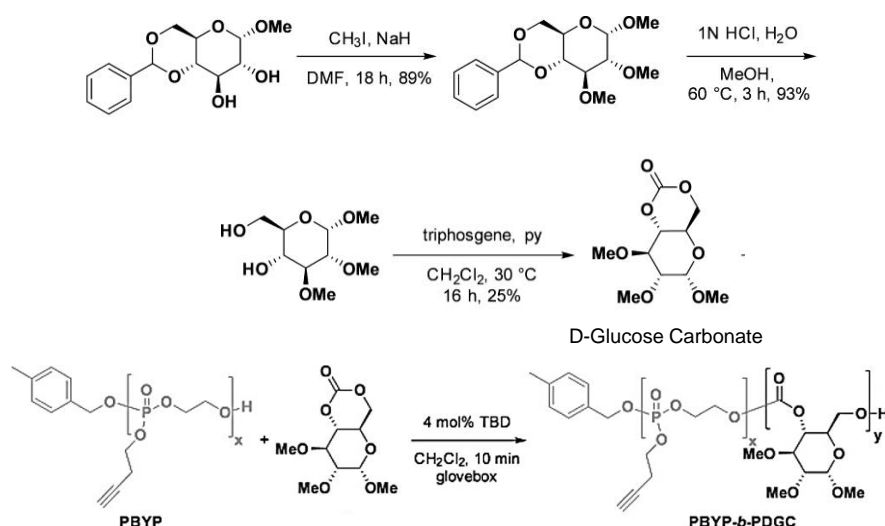
In an interesting study, Domb *et al.* reported the synthesis of macrolactones using ricinoleic acid (figure 1-9). Several catalysts were explored to make the polyesters using these lactone rings by ROP but only low molecular weight homopolymers were obtained. The low reactivity towards ROP of these lactone monomers was suggested to be due to the low ring strain and steric hindrance of the ester bond by the fatty acid side chain¹⁰⁶. However, TBD has been proven to be an efficient catalyst for the ROP of hindered lactones and might be helpful to synthesise high molecular weight polyesters using these lactones^{98, 107}.



In another study, a poly(ester) synthesised by the ROP of a *D*-gluconolactone, a commercially available (and cheap) carbohydrate lactone has been reported¹⁰⁸. Gluconic acid is the starting material to synthesis *D*-Gluconolactone and the former is generally produced from glucose. In a similar study, a renewable lactone monomer was prepared from a reduced galactose, *D*-dulcitol and copolymerised with caprolactone to generate high molecular weight polyester¹⁰⁹.

Poly(carbonate) from Renewable Monomers

A carbonate monomer was recently reported via a multistep synthesis beginning with a commercially available glucose derivative, methyl 4,6-O-benzylidene- α -D-glucopyranoside. The monomer was successfully copolymerized using a water soluble polyphosphoester (PBYP) as initiator to prepare PBYP-*b*-PDGC block copolymer (scheme 1-11)¹¹⁰. The PDGC is an amorphous polymer with T_g of 106–123°C¹¹¹.



Scheme 1-11 Synthesis scheme of D-glucose carbonate monomer and its copolymerisation with polyphosphoester to make amphiphilic copolymers¹¹⁰

The preparation of spherical micelles was also reported using synthesised block copolymer after post functionalization which suggested its potential to be used as biomaterial¹¹⁰. Renewable poly(carbonate)s can also be prepared from glycerol^{70, 112}, levulinic or itaconic acids¹¹³ as starting material.

However, despite the unique properties of the above mentioned polyesters and their copolymers, very few of them has been investigated for drug delivery applications. Therefore, more research is required in this field to identify the potential renewable polymers for such applications.

1.4 Polymeric Micelles in Drug Delivery and Cancer Therapy

A surfactant is a molecule, which comprises both a water soluble and insoluble portion. Surfactants can form micelles after being dispersed in aqueous solutions by self-assembly above their critical micelle concentrations (CMC). The CMC is defined as the concentration of surfactant molecules above which they start forming micelles. However, small surfactant molecules such as sodium lauryl sulphate, polysorbates etc. usually have a very high CMC value thus can dissociate upon dilution in the bloodstream or other biological fluids *in vivo*. Due to this limitation, the use of these surfactants as drug delivery vehicles have been limited and therefore alternative amphiphilic block copolymers surfactants have been developed to address this problem¹¹⁴. Polymeric micelles prepared from amphiphilic block copolymers have recently attracted more attention due to their unique structure with low CMC values.

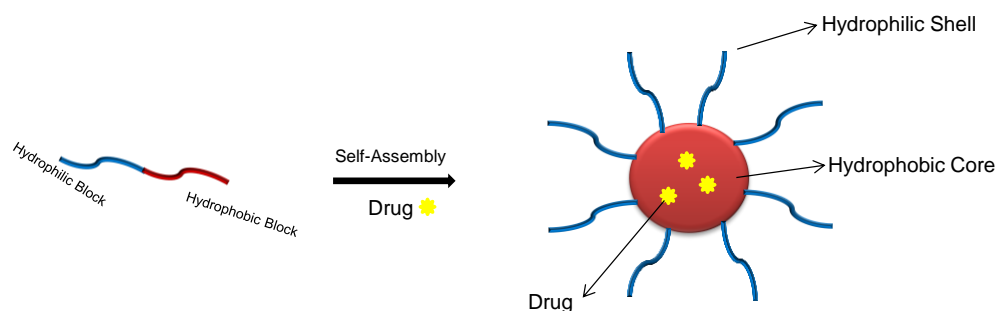


Figure 1-10 Pictorial presentation of self-assembly of an amphiphilic block copolymer into micelles when dispersed in water.

Amphiphilic block copolymers can form micelles in aqueous solvent with a hydrophobic core sterically stabilized by a hydrophilic shell (figure 1-10). The hydrophobic core serves as a reservoir for drugs with low aqueous solubility while the hydrophilic shell prevents the adsorption of opsonins on the surface. Additionally the nano-scope sized polymeric micelles (10 – 200 nm in diameter) are sufficiently large to avoid renal excretion (>50 kDa) as well as small enough to bypass the filtration of inter-endothelial cells in the spleen. All these factors contribute towards the longer blood circulation time of micelles, which leads to improved accumulation at tissue sites with vascular abnormalities¹¹⁵⁻¹¹⁸. PEG is the polymer of choice to be used as the hydrophilic block whereas the hydrophobic block can be chosen based on the required application¹¹⁵⁻¹¹⁸.

Some of the reasons, which makes PEG consistently a polymer of choice for fabricating amphiphilic block copolymers are: it is an inexpensive, non-toxic, and FDA approved polymer for the

use in drug products¹¹⁶. Additionally, in micelles structure, PEG forms a dense, brush-like shell which imparts steric stability to the formulation¹¹⁷. Further, PEG is known to increase the circulatory time of carriers by impeding their uptake by the cells of the Reticuloendothelial System (RES)¹¹⁹. Moreover, PEG can be easily functionalised to attach the targeting ligands for targeted drug delivery applications¹²⁰. Polymeric micelles have been widely utilised as solubilising tool for hydrophobic drugs¹¹⁶. The micelle structures are known to have an anisotropic distribution of water and therefore the core of the micelles is usually water free¹²¹. During the drug loading procedure, the hydrophobic drugs migrate towards the hydrophobic block (core) due to the hydrophobic interaction.

Hydrophobic interaction is defined as the interaction between the non-polar substances in water. This interaction brings the non-polar (hydrophobic) molecules together in order to have minimal contact with water. This is a spontaneous process and is reasonably stronger than other weak intermolecular forces such as hydrogen bonding¹²². Therefore, during drug encapsulation procedure, hydrophobic core and drug come together to obtain drug loaded micelles. Furthermore, hydrophilic block provides the steric stability to micelles due to

which they remain well dispersed in aqueous solution without aggregation^{115, 117, 123}. In terms of thermodynamics, the drug solubilisation in micelles core can be considered as a partitioning of the drug between polar and non-polar phases¹²¹. In addition to the solubilisation tool, micelles have also known to increase the bioavailability, reduce the toxicity and offer the control release of loaded drugs leading to patient compliance^{117, 124}.

As shown in figure 1-10 and figure 1-11, drug molecules are generally localised within the hydrophobic core separated from the outside environment by hydrophilic shell. This unique feature prevents the direct interaction of encapsulated drugs with the physiological environment such as cells or body fluids. This in turn, prevents any undesirable pharmacodynamics and pharmacokinetics reactions, which leads in improved bioavailability and reduction in toxicity of a drug.

Using polymeric micelles as a drug delivery carrier is certainly beneficial because of various advantages it holds over other carrier systems like easier preparation method with tunable property, good loading capacity and better formulation stability^{116-118, 121, 124, 129-131}. All these advantages are due to the unique structure (core-shell) of polymeric micelles as

discussed above. A number of micelles formulations are already in the clinical trials such as NK012, SP1049C, NC-6004, NK911 etc., (figure 1-11) while FDA has approved Genexol-PM for the treatment of breast cancer^{116, 132}.

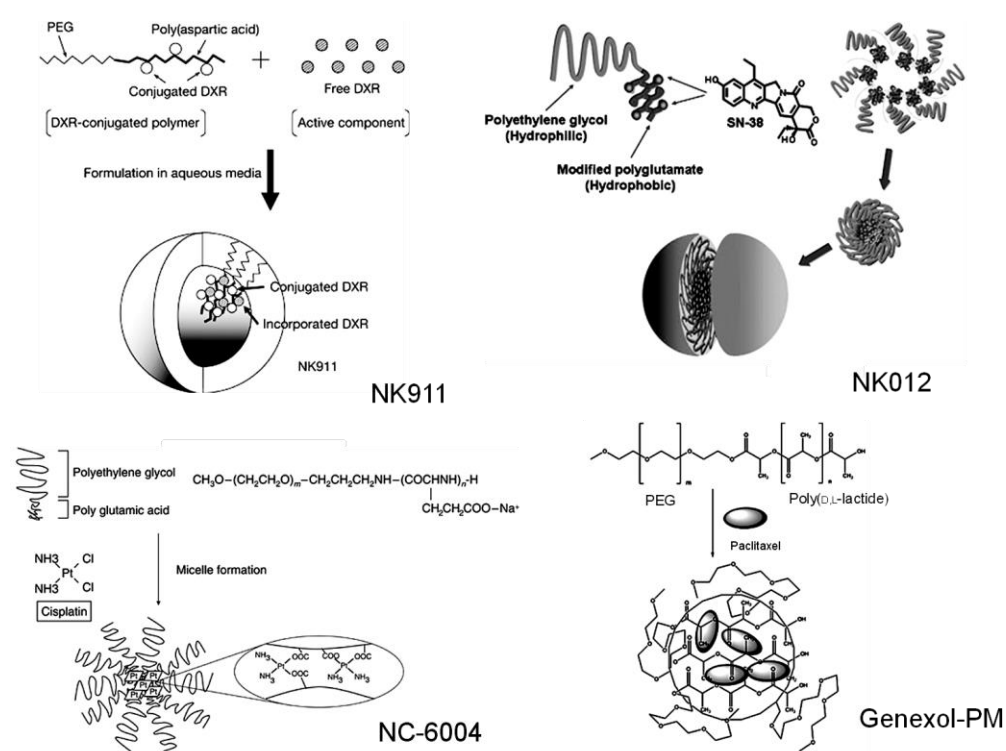


Figure 1-11 Schematic presentation of NK911¹²⁵, NK012¹²⁶, NC-6004¹²⁷ and Genexol-PM¹²⁸ micelle formulation.

1.4.1 Methods of Fabrication of Drug Loaded Polymeric Micelles

The four frequently used methods for the preparation of micelles and drug encapsulation are described below:

Dialysis Method

In this method, block copolymer and drug are dissolved in a water miscible non-volatile organic solvent (such as dimethyl sulfoxide and *N,N*-dimethyl formamide) followed by dialysis of the obtained solution against water (figure 1-12A).

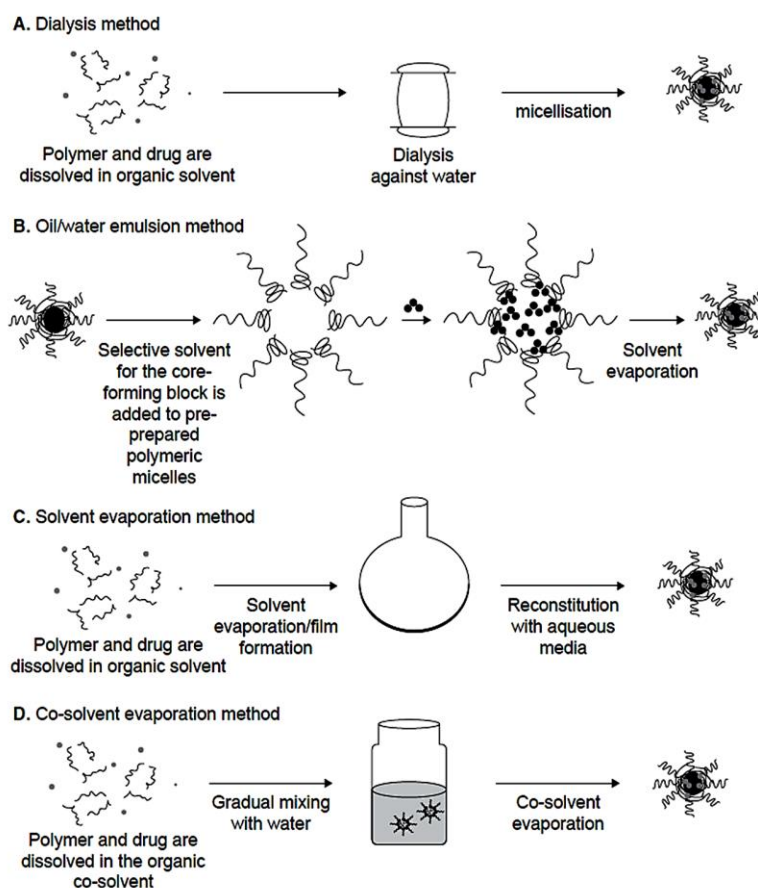


Figure 1-12 Pictorial presentation of methods used for micelle preparation and drug encapsulation¹³³

During dialysis, water will gradually replace the organic solvent from the dialysis bag leading to the self-assembly of amphiphilic polymer in micelles with encapsulated hydrophobic drug. It was suggested that during dialysis any unencapsulated drug will be removed from micellar solution leaving behind the drug loaded micelles only¹³³. However, it should be noted that the replacement of organic solvent with water is a slow process. Hence, diffusion of some amount of drug into external media (water) might be possible before self-assembly. To avoid this problem Allen *et al.* prepared the drug loaded micelles by adding the water directly to the drug-polymer solution (in DMSO) followed by dialysis in order to remove the solvent¹³⁴.

Oil-in-Water Emulsion Method

In this method, block copolymer and drug are dissolved in a water immiscible volatile organic solvent such as chloroform ethyl acetate and methylene chloride. The solution is then slowly added to the aqueous phase under stirring to make an oil-in-water emulsion (figure 1-12B). In some cases, additional surfactants are also used to make a stable emulsion. The organic solvent is then evaporated at room temperature to yield the drug loaded micelles^{131, 133}.

Solvent Evaporation/Film Method

In this method, block copolymer and drug are dissolved in a suitable volatile organic solvent and then the solvent is evaporated to make a thin polymer-drug film on the wall of a flask. The film is then reconstituted with the aid of aqueous solvent by vigorous shaking to produce the drug loaded polymeric micelles (figure 1-12C)^{131, 135}. Large scale production is possible with the solvent evaporation method. However, the use of this method is not preferred to make micelles from block copolymers with high hydrophobic to hydrophilic ratio. Due to the high hydrophobicity, the complete reconstitution of such polymers by simple mixing is difficult¹³³.

Co-solvent evaporation/Nanoprecipitation Method

In this method, block copolymer and drug are dissolved in a water miscible volatile organic solvent and then added drop wise to water under stirring. The diffusion of solvent in water with simultaneous evaporation triggered the self-assembly of copolymer, yielding the drug loaded polymeric micelles (figure 1-12D)^{133, 136}.

1.4.2 Polymeric Micelles in Cancer Therapy

Cancer therapy (chemotherapy) needs targeted delivery of cytotoxic drugs to tumours to avoid unwanted side-effects,

which are attributed to the distribution of drugs in normal tissues. Targeted delivery of drugs to the tumors (cancer cells) can be achieved with the aid of suitable drug delivery carriers based on active and passive targeting strategies (figure 1-13)¹³⁷⁻¹⁴⁰.

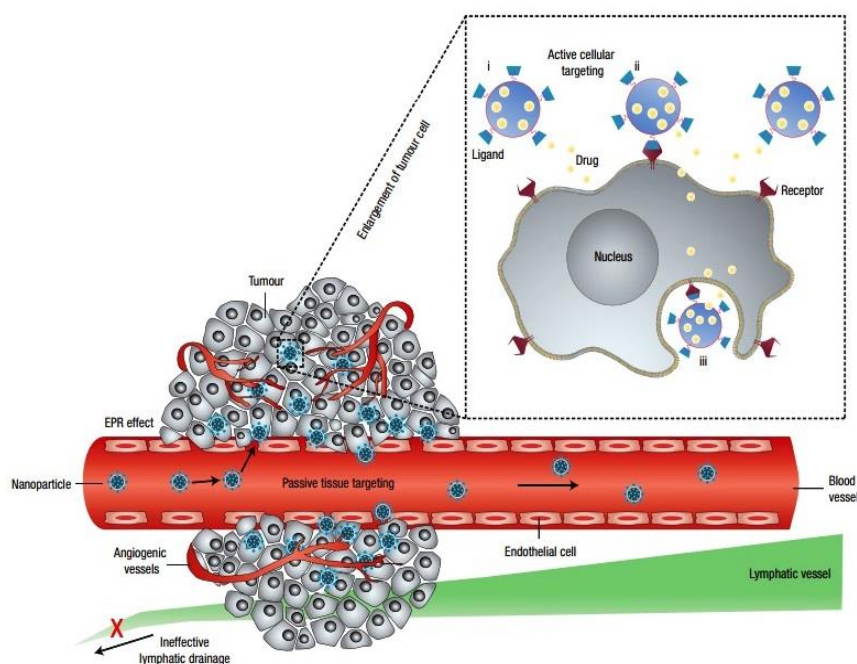


Figure 1-13 Schematic presentation of targeted therapy to tumors with the aid of nanoparticles (micelles) by active and passive mechanism¹⁴⁰.

Indeed, polymeric micelles as a drug delivery carrier for cytotoxic drugs offer numerous advantages in chemotherapy^{123, 130-132}. For instance, the incorporation of cytotoxic drugs into micelles has been reported to increase the half-life of drug by circumventing its elimination by the liver and/or kidneys thus increasing the bioavailability¹³². Additionally, small size micelles have been reported to

passively target the tumors by the Enhanced Permeability and Retention (EPR) effect^{141, 142}. Moreover, many anticancer drugs are hydrophobic in nature and hence encapsulating them within polymeric micelles can enhance their aqueous solubility (thus they can be more easily administrable in the body) and consequently bioavailability¹³⁰⁻¹³². Furthermore, the controlled release of bio-actives for a longer duration at a tumor site can also increase the effectiveness of treatment¹³⁰⁻¹³². In addition to that, the shell of polymeric micelles can be modified for active targeting by attaching specific ligands. This modification enhanced the selectivity of polymeric micelles for tumor cells and consequently improved the intracellular drug delivery (figure 1-13)^{120, 132}. Thus, the use of micelles for cancer therapy can be beneficial in order to improve the bioavailability and to reduce the side effects of anticancer drugs^{141, 142}.

Passively targeted micelles for Cancer Therapy

Targeting solid tumors using long circulatory drug delivery carriers *via* the Enhanced Permeability and Retention (EPR) effect is considered as passive targeting. The EPR effect was first described by Maeda and co-worker¹⁴³. Physiological and pathological studies of solid tumours suggested that the tumor vasculature possessed some unique characteristics such as

incomplete architecture and immature lymphatic capillaries. Tumor vasculature generally has poorly aligned and defective endothelial cells with broad fenestrations (up to 4 μm) and lacking smooth muscle layer (or innervations and functional lymphatics). Additionally, impaired receptor function for vasoactive mediators especially angiotensin II in tumor vascular has been observed (Figure 1-13 and 1-14)^{137, 139}.

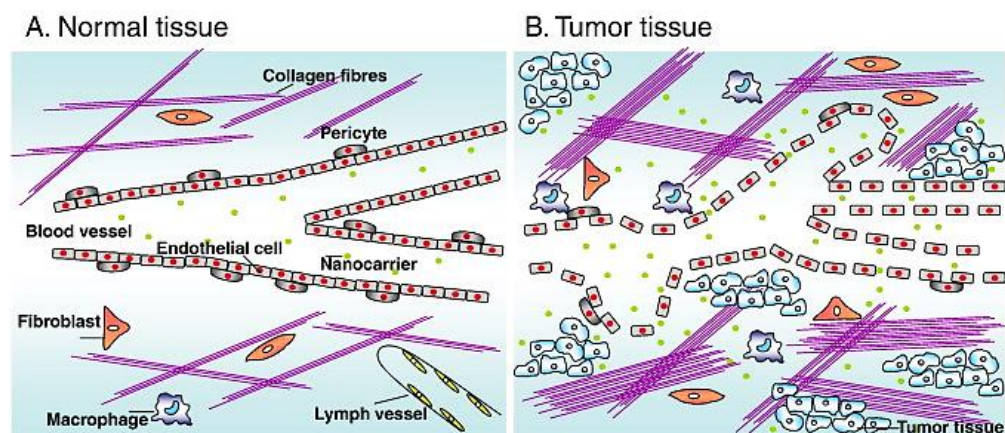


Figure 1-14 Differences between normal and tumor tissues, which explains the passive targeting of nanocarriers by the EPR effect. (A) normal tissues contain linear blood vessels maintained by pericytes. (B) tumor tissues with defective blood vessels with many sac-like formations and fenestrations. The extracellular matrix contains extra collagen fibres, fibroblasts and macrophages compared to normal tissue. Lymph vessels are absent¹³⁹.

The excessive production of vascular mediators, such as vascular endothelial growth factor (VEGF), bradykinin, fibroblast growth factor (bFGF), nitric oxide, peroxynitrite, prostaglandins, and matrix metalloproteinases, are responsible for the hyper-permeability in tumor tissues^{144, 145}. VEGF, a protein excessively secreted by tumors, plays an important

role in the angiogenesis process which includes degradation of vascular basement membrane and surrounding extracellular matrix, as well as vascular endothelial cell division and migration¹¹⁸. This enhanced vascular permeability ensures the adequate supply of oxygen and nutrients for rapid growth of tumor tissues^{145, 146}. Recently, reduction in vascular permeability in colon carcinomas when treated with anti-VEGF antibody confirmed the role of VEGF in enhanced permeability of tumor vasculature¹⁴⁷.

Furthermore, due to the defective lymphatic function in tumors, continuous draining and renewal of interstitial fluid is minimal¹⁴⁸. As a result, high retention time of a macromolecule has been observed in tumor tissues compared to normal tissues^{140,149}. These two factors (*i.e.* Enhanced Permeation and Retention) comprise the EPR effect, due to which selective extravasation and accumulation of macromolecules in tumor tissues were observed^{142, 143, 145}.

Indeed several polymeric micelle formulations have been reported which accumulate at the tumor sites *via* the EPR effect¹⁴². For instance, PEG-poly(*g*-benzyl L-glutamate) block copolymer micelles loaded with cisplatin, demonstrated high accumulation in solid tumor in Lewis lung carcinoma bearing mice, compared to free drug. The high accumulation at the

tumor site was suggested to occur *via* the EPR effect due to the prolonged blood circulation and small size (approx. 30 nm in diameter) of micelles¹⁵⁰. This formulation is now in Phase II clinical trials with the trade name "NC-6004"¹²⁷.

Polymer	Drug	Size of micelles
PEG2000-PE/Vitamin E ¹⁵²	Paclitaxel, Curcumin	15-20 nm
Pluronic [®] L61 and F127 (SP1049C) ¹⁵³	Doxorubicin	30 nm
mPEG-b-poly(D,L-lactide) ¹⁵⁴	Docetaxel	16.62±0.31 nm
mPEG-b-poly(D,L-lactide) (Genexol-PM) ¹⁵⁵	Paclitaxel	<50 nm

Table 1-2 Examples of micelles formulations, which demonstrated enhanced tumor uptake by EPR effect. (mPEG- monomethoxyl PEG)

NK105, PEG-poly(aspartic acid) micelles loaded with paclitaxel is another formulation which is in clinical trials. Approximately 50% of carboxylic acid groups of poly(aspartic acid) have been modified with 4-phenyl-1-butanol in the NK105 formulation, which increased the hydrophobicity of polymer and eventually paclitaxel loading (23% w/w approx.). The average size of 85 nm was observed with this formulation after redispersion in aqueous solvent. Approximately, 90-fold increase in the plasma area under curve (AUC), 25-fold increase in tumor AUC in Colon-26 tumors bearing CDF1 mice was observed, when compared with free drug. This high tumor uptake efficiency was attributed to the EPR effect of long circulatory

NK105 micelles. Phase II clinical trials of NK105 were conducted in Japan, which was successfully completed in 2010 with positive results. Phase III Studies are on-going on patients with breast cancer and due to end by September 2016¹⁵¹. Some more examples of polymeric micelles studied for tumor targeting via EPR effect are listed in table 1-2.

Actively Targeted Micelles for Cancer Therapy

Tumor targeting potential of polymeric micelles can be further enhanced by attaching the targeting ligands on to the micelle surface (actively targeted micelles). The concept of active targeting is based on the ligand–receptor interactions at the target site i. e. tumor. After reaching the target site, ligand decorated micelles should interact with certain specific receptors present on the tumor cell and then be internalised by receptor-mediated endocytosis (figure 1-13 and 1-15)^{120, 131, 132, 139, 140}.

Increase in the cellular concentration of anticancer agents via receptor mediated endocytosis leads to superior therapeutic efficacy of the drugs. This in turn reduces the dose size and side effects of cytotoxic drugs¹⁵⁶. The selection of ligands is usually based on any receptor, which is overexpressed by tumor cells or tumor vasculature but have minimal or no expression by normal cells.

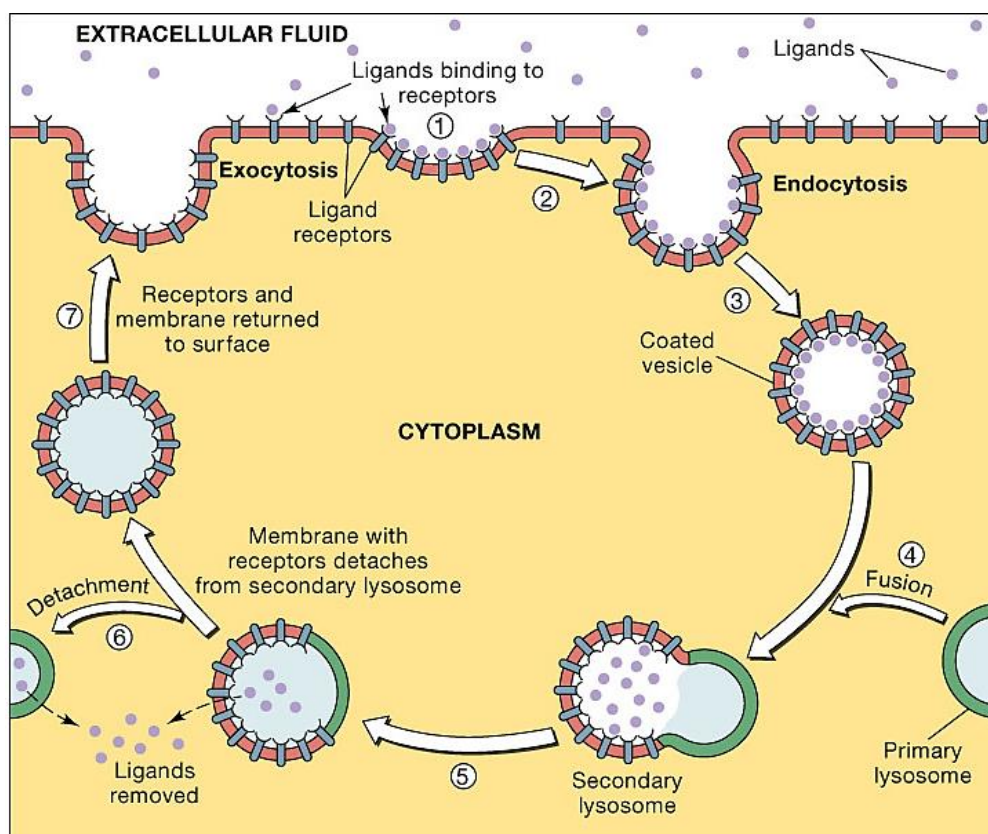


Figure 1-15 Receptor mediated endocytosis mechanism of a ligand after being attached to the specific receptor (source - <http://droualb.faculty.mjc.edu>).

Commonly used targeting ligands include antibodies, peptides, proteins, carbohydrates, small organic molecules and aptamers. The attachment of a ligand on to the surface of micelles is generally achieved either by the post-modification of a block copolymer with bifunctional spacer molecules or by the direct synthesis of hetero-bifunctional blocks¹¹⁵. Several polymeric micellar formulations based on ligand mediated targeting have been reported in literatures and were reviewed recently^{120, 131, 132, 157}.

For instance, monoclonal antinucleosomal antibody (2C5) conjugated poly(ethylene glycol)-block-phosphatidyl ethanolamine (PEG-b-PE) micelles loaded with Doxorubicin (DOX) have been tested in a DOX-resistant ovarian cancer cell spheroid model. The 2C5 conjugated micelles demonstrated higher uptake (two fold) and penetration with greater cell death in spheroids compared to free DOX and non-targeted DOX micelles. The mean size observed for PEG-PE targeted micelles was 15 nm¹⁵⁸. In another study Herceptin conjugated to d- α -tocopheryl polyethylene glycol succinate (vitamin E TPGS) micelles have been developed for targeted co-delivery of docetaxel and siRNA¹⁵⁹. Antibodies are very popular as targeting ligands, but only limited conjugation of these moieties on micelle surface is possible due to their large size (~150 kDa). Furthermore, rapid clearance of antibody conjugated micelles might be observed due to their potential immunogenicity¹⁶⁰.

Transferrin (Tf) (protein) conjugation is another widely studied approach to fabricate targeted carriers for the specific delivery of cytotoxic drugs to the cancer cells¹⁶¹. For instance, Yue *et. al.* developed the transferrin conjugated mPEG-b-PLA polymeric micelles for their enhanced uptake in cancer cells¹⁶². The size range of the micelles was between 85-110 nm. They

were tested on three human cell lines, SGC-7901 (gastric carcinoma), SKOV-3 (ovarian carcinoma), and MCF-7 (breast carcinoma) for uptake studies. Higher uptake of Tf-conjugated micelles (TfM-RhB) was evident by confocal laser scanning microscopy (CLSM) (using Rhodamine as marker) on MCF-7 and SGC-7901 cell lines compared to Tf-free micelles (M-RhB). SKOV-3 cells expressed a low level of transferrin and hence little difference in uptake was observed between TfM-RhB and M-RhB (figure 1-16). This study suggested that the high uptake was due to transferrin receptor mediated endocytosis¹⁶².

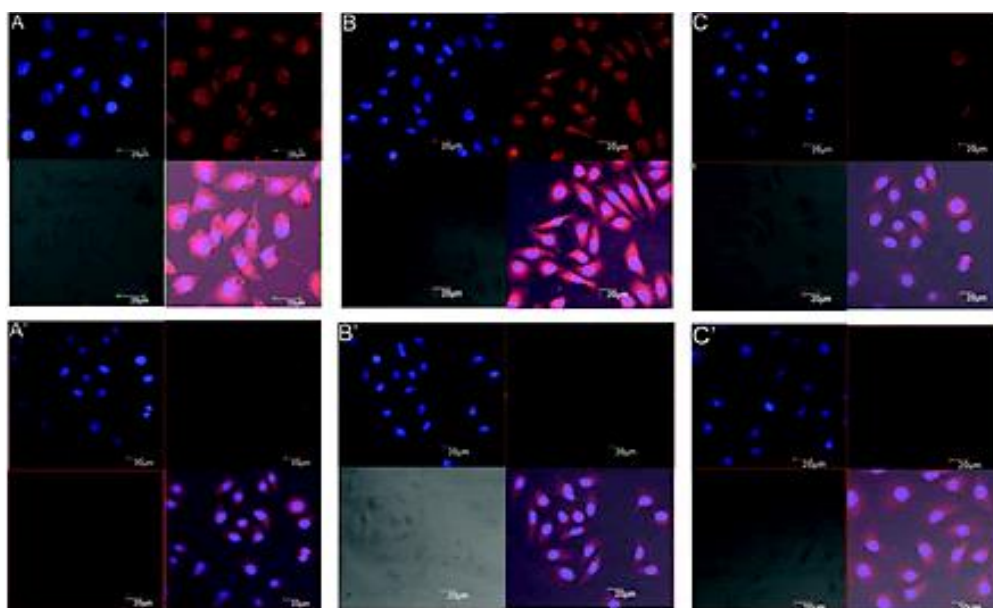


Figure 1-16 CLSM images of human MCF-7 (A and A'), SGC-7901 (B and B'), and SKOV3 (C and C') cells incubated with TfM-RhB (A, B, and C) or M-RhB (A', B', and C')¹⁶².

High cellular uptake and effective tumor growth inhibition have been also demonstrated by using arginylglycylaspartic

acid (RGD) (peptide)¹⁶³, lactose¹⁶⁴ and galactose¹⁶⁵ (carbohydrates) and A10-aptamer¹⁶⁶ as targeting ligand.

Due to the higher expression level of folate receptors in tumors (100 to 300 times) compared to normal tissue, folic acid as targeting ligand has been widely studied for cancer chemotherapy^{167, 168}. Folic acid is a commercially available small molecule that can be easily conjugated on to micelles surfaces^{168, 169}.

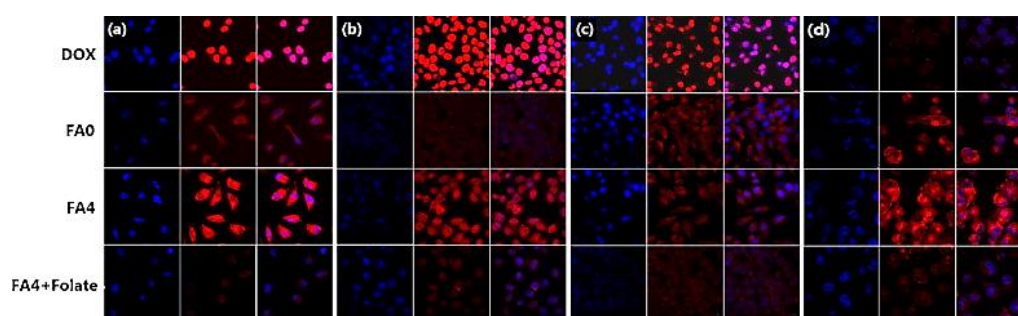


Figure 1-17 CLSM images of HeLa (a), KB (b), A549 (c) and MCF7/ADR cells (d), after incubation with different DOX formulations for 3 h. For each images, the columns from left to right correspond to Hoechst, DOX and merge, respectively¹⁷⁰

Recently, Qiu *et. al.* reported the fabrication of targeted micelles using folate-modified poly (2-ethyl-2-oxazoline)-b-poly (ϵ -caprolactone) (FA-PEOz-PCL) block copolymer¹⁷⁰. DOX loaded FA-PEOz-PCL micelles with the size range of 157-191 nm were tested for cellular uptake using folate receptor positive (FR+) Human HeLa cervical carcinoma cell lines (HeLa), human KB nasopharyngeal epidermal carcinoma cell lines (KB), Multidrug-resistant human breast cancer MCF-

7/ADR cell lines and folate receptor negative (FR-) human A549 lung adenocarcinoma cell lines.

As shown in figure 1-17, higher cellular uptake of folate conjugated micelles (FA4) was observed with FR+ cell lines compared to non-folate micelles (FA0) and DOX. Further, folate receptor mediated endocytosis was confirmed by addition of free folic acid in cell culture media (FA4 + Folate). Addition of free folic acid competes with folate receptors for binding and thus reduced uptake of FA4 as evident by CLSM images (figure 1-17). Moreover FA4 demonstrated lower IC_{50} values in FR+ cell lines compared to FA0¹⁷⁰.

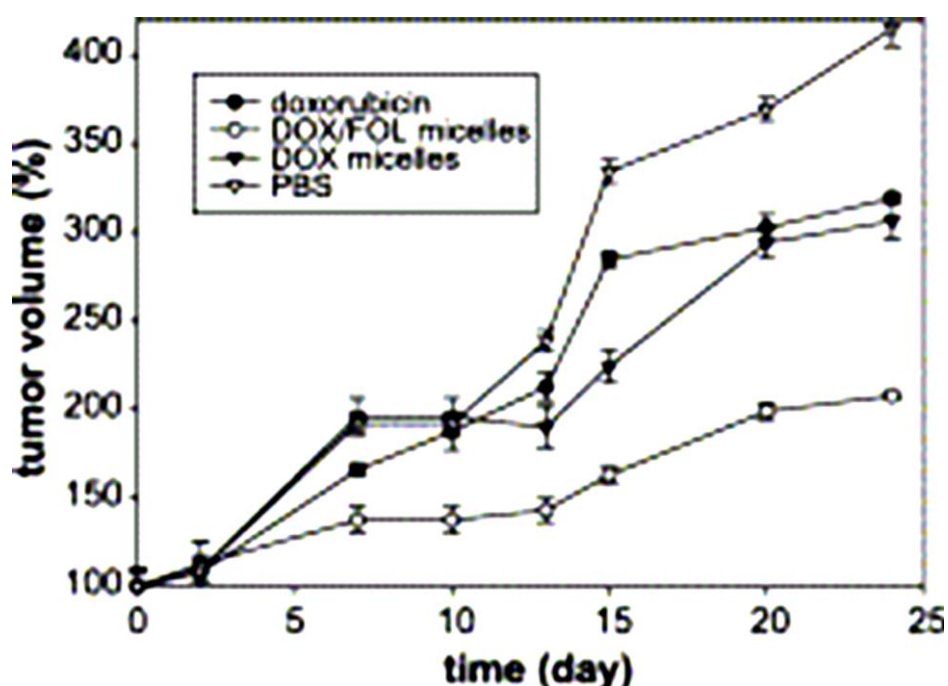


Figure 1-18 Tumor volume growth for various formulations of free DOX, DOX micelles, and DOX/FOL micelles as a function of time¹⁷².

Kim *et.al.* demonstrated the effectiveness of folate mediated targeting in multi-drug resistant (MDR) tumors using PLLA-b-PEG-folate micelles¹⁷¹. In another study, a significant reduction in tumor size was observed using PLGA-b-PEG-FA micelles containing DOX as cytotoxic agent (DOX/FOL micelles) compared to free drug (doxorubicin) and non-folate micelles (DOX micelles) (figure 1-18)¹⁷².

1.5 Summary

Polymeric drug-delivery systems have been investigated to address the problems associated with drugs such as poor aqueous solubility, stability and significant side effects. Indeed, polymeric micelles as a drug delivery carrier have demonstrated their potential to address some of the above mentioned problems as discussed earlier. Polymeric micelles can be easily prepared by conjugating a hydrophilic and hydrophobic polymer followed by its dispersion in aqueous solvent. Further, the unique core-corona structure of polymeric micelles provides satisfactory stability to this formulation. Due to these advantages, several polymeric micelles have been studied for the effective treatment of cancer and some of them are in clinical trials.

Apparently, biodegradable polymers because of their low toxicity and biodegradability are the polymers of choice to

fabricate micelles for *in vivo* applications. Undoubtedly, polyesters are the front-runner biodegradable polymers used to generate the micelles. Polyesters derived from renewable feedstocks recently have attracted more attention due to the depletion of fossil fuel reserves and their increased prices. As discussed earlier, several new polyesters, which have been derived from renewable feedstocks are in a development stage. However, new sustainable materials are produced frequently; their applications in drug delivery have been rather less investigated.

1.6 Aim and Objectives

Based on the published research, the aim of this project has been designed. By considering the advantages of polymeric micelles and polyesters, it was decided to fabricate micelles using polyesters synthesised from renewable feedstock. Further, the investigation of prepared micelles in drug delivery applications was proposed. To synthesise amphiphilic block copolymer, PEG as a hydrophilic polymer was chosen due to its extensive use in pharmaceutical formulations (see section 1.4). Synthesis of hydrophobic polyester polymer was proposed *via* ROP route because of its advantages over polycondensation reaction (see section 1.2.2). Lactone monomer obtained from renewable resources (*i.e.* δ -

decalactone and ω -pentadecalactone) were chosen to synthesise polymers using mild reaction conditions. Additionally, the preparation of ligand tethered polymeric micelles for tumor targeted delivery was also suggested. Folic acid was selected as the targeting ligand due to its extensive reported use (see section 1.4.2).

All materials were picked on the basis of their commercial availability and a cheap price in order to reduce the cost of formulation. A general overview of proposed work is shown in figure 1-19.

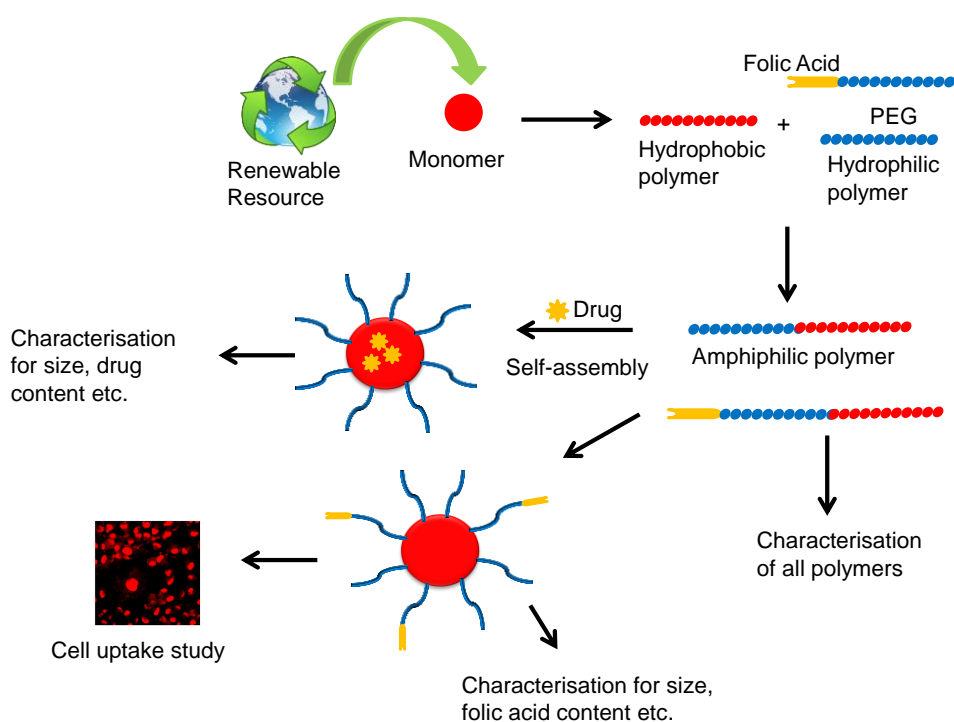


Figure 1-19 Pictorial representation of general overview of proposed work

1.7 References

1. Vilar, G.; Tulla-Puche, J.; Albericio, F., *Current Drug Delivery* 2012, 9 (4), 367-394.
2. Davis, S. S.; Illum, L.; Stolnik, S., *Current Opinion in Colloid & Interface Science* 1996, 1 (5), 660-666.
3. Ikada, Y.; Tsuji, H., *Macromolecular Rapid Communications* 2000, 21 (3), 117-132.
4. Nair, L. S.; Laurencin, C. T., *Progress in Polymer Science* 2007, 32 (8-9), 762-798.
5. Ulery, B. D.; Nair, L. S.; Laurencin, C. T., *Journal of Polymer Science Part B-Polymer Physics* 2011, 49 (12), 832-864.
6. Agnihotri, S. A.; Mallikarjuna, N. N.; Aminabhavi, T. M., *Journal of Controlled Release* 2004, 100 (1), 5-28.
7. Sarmento, B.; Ribeiro, A.; Veiga, F.; Sampaio, P.; Neufeld, R.; Ferreira, D., *Pharmaceutical Research* 2007, 24 (12), 2198-2206.
8. De Campos, A. M.; Sanchez, A.; Alonso, M. J., *International Journal of Pharmaceutics* 2001, 224 (1-2), 159-168.
9. Janes, K. A.; Fresneau, M. P.; Marazuela, A.; Fabra, A.; Alonso, M. J., *Journal of Controlled Release* 2001, 73 (2-3), 255-267.
10. Hubbell, J. A., *Bio-Technology* 1995, 13 (6), 565-576; Hutmacher, D. W., *Biomaterials* 2000, 21 (24), 2529-2543.
11. Malafaya, P. B.; Silva, G. A.; Reis, R. L., *Advanced Drug Delivery Reviews* 2007, 59 (4-5), 207-233.
12. Mano, J. F.; Silva, G. A.; Azevedo, H. S.; Malafaya, P. B.; Sousa, R. A.; Silva, S. S.; Boesel, L. F.; Oliveira, J. M.; Santos, T. C.; Marques, A. P.; Neves, N. M.; Reis, R. L., *Journal of the Royal Society Interface* 2007, 4 (17), 999-1030.
13. Kumari, A.; Yadav, S. K.; Yadav, S. C., *Colloids and Surfaces B-Biointerfaces* 2010, 75 (1), 1-18.
14. Kaul, G.; Amiji, M., *Pharmaceutical Research* 2005, 22 (6), 951-961.
15. Gombotz, W. R.; Pettit, D. K., *Bioconjugate Chemistry* 1995, 6 (4), 332-351.
16. Lee, S.-H.; Shin, H., *Advanced Drug Delivery Reviews* 2007, 59 (4-5), 339-359.
17. Tian, H.; Tang, Z.; Zhuang, X.; Chen, X.; Jing, X., *Progress in Polymer Science* 2012, 37 (2), 237-280.

18. Middleton, J. C.; Tipton, A. J., *Biomaterials* 2000, 21 (23), 2335-2346.
19. Gunatillake, P.; Mayadunne, R.; Adhikari, R., *Biotechnology Annual Review, Vol 12* 2006, 12, 301-347.
20. Okada, M., *Progress in Polymer Science* 2002, 27 (1), 87-133.
21. Jikei, M.; Kakimoto, M., *Progress in Polymer Science* 2001, 26 (8), 1233-1285; Kuchanov, S.; Slot, H.; Stroeks, A., *Progress in Polymer Science* 2004, 29 (6), 563-633.
22. Forbes, D. C.; Weaver, K. J., *Journal of Molecular Catalysis a-Chemical* 2004, 214 (1), 129-132.
23. Fischer, E.; Speier, A., *Berichte der deutschen chemischen Gesellschaft* 1895, 28, 3252-3258.
24. Remme, N.; Koschek, K.; Schneider, C., *Synlett* 2007, (3), 491-493.
25. Neises, B.; Steglich, W., *Angewandte Chemie-International Edition in English* 1978, 17 (7), 522-524.
26. Albertsson, A. C.; Varma, I. K., *Biomacromolecules* 2003, 4 (6), 1466-1486.
27. Nuyken, O.; Pask, S. D., *Polymers* 2013, 5 (2), 361-403.
28. Kurcok, P.; Kowalczyk, M.; Hennek, K.; Jedlinski, Z., *Macromolecules* 1992, 25 (7), 2017-2020.
29. Stridsberg, K. M.; Ryner, M.; Albertsson, A. C., *Degradable Aliphatic Polyesters* 2002, 157, 41-65.
30. Labet, M.; Thielemans, W., *Chemical Society Reviews* 2009, 38 (12), 3484-3504.
31. Nigam, P. S.; Singh, A., *Progress in Energy and Combustion Science* 2011, 37 (1), 52-68.
32. Albertsson, A. C.; Varma, I. K., *Degradable Aliphatic Polyesters* 2002, 157, 1-40.
33. Woodruff, M. A.; Hutmacher, D. W., *Progress in Polymer Science* 2010, 35 (10), 1217-1256.
34. Shuai, X. T.; Ai, H.; Nasongkla, N.; Kim, S.; Gao, J. M., *Journal of Controlled Release* 2004, 98 (3), 415-426.
35. Darney, P. D.; Klaisle, C. M.; Monroe, S. E.; Cook, C. E.; Phillips, N. R.; Schindler, A., *Fertility and Sterility* 1992, 58 (1), 137-143.
36. Yang, K. K.; Wang, X. L.; Wang, Y. Z., *Journal of Macromolecular Science-Polymer Reviews* 2002, C42 (3), 373-398.
37. Im, J. N.; Kim, J. K.; Kim, H.-K.; In, C. H.; Lee, K. Y.; Park, W. H., *Polymer Degradation and Stability* 2007, 92 (4), 667-674.

38. Song, L.; Shen, Y.; Hou, J.; Lei, L.; Guo, S.; Qian, C., *Colloids and Surfaces a-Physicochemical and Engineering Aspects* 2011, 390 (1-3), 25-32; Tang, D.-L.; Song, F.; Chen, C.; Wang, X.-L.; Wang, Y.-Z., *Nanotechnology* 2013, 24 (14).
39. Tamada, J.; Langer, R., *Journal of Biomaterials Science-Polymer Edition* 1992, 3 (4), 315-353; Kumar, N.; Langer, R. S.; Domb, A. J., *Advanced Drug Delivery Reviews* 2002, 54 (7), 889-910.
40. Albertsson, A. C.; Carlfors, J.; Stureson, C., *Journal of Applied Polymer Science* 1996, 62 (4), 695-705.
41. Albertsson, A. C.; Eklund, M., *Journal of Applied Polymer Science* 1995, 57 (1), 87-103.
42. Zhang, Z.; Kuijjer, R.; Bulstra, S. K.; Grijpma, D. W.; Feijen, J., *Biomaterials* 2006, 27 (9), 1741-1748.
43. Gabriele, B.; Mancuso, R.; Salerno, G.; Ruffolo, G.; Costa, M.; Dibenedetto, A., *Tetrahedron Letters* 2009, 50 (52), 7330-7332; Darensbourg, D. J.; Moncada, A. I.; Choi, W.; Reibenspies, J. H., *Journal of the American Chemical Society* 2008, 130 (20), 6523-6533.
44. Zhang, Y.; Zhuo, R. X., *Biomaterials* 2005, 26 (14), 2089-2094; Jiang, X.; Sha, X.; Xin, H.; Chen, L.; Gao, X.; Wang, X.; Law, K.; Gu, J.; Chen, Y.; Jiang, Y.; Ren, X.; Ren, Q.; Fang, X., *Biomaterials* 2011, 32 (35), 9457-9469.
45. Habraken, W. J. E. M.; Zhang, Z.; Wolke, J. G. C.; Grijpma, D. W.; Mikos, A. G.; Feijen, J.; Jansen, J. A., *Biomaterials* 2008, 29 (16), 2464-2476.
46. Amsden, B. G.; Timbart, L.; Marecak, D.; Chapanian, R.; Tse, M. Y.; Pang, S. C., *Journal of Controlled Release* 2010, 145 (2), 109-115.
47. Danquah, M.; Fujiwara, T.; Mahato, R. I., *Biomaterials* 2010, 31 (8), 2358-2370.
48. Park, S. H.; Choi, B. G.; Joo, M. K.; Han, D. K.; Sohn, Y. S.; Jeong, B., *Macromolecules* 2008, 41 (17), 6486-6492.
49. *Monomers, Polymers and Composites from Renewable Resources* 2008, 1-553; MN, B.; A, G., *Monomers, Polymers and Composites from Renewable Resources* 2008, 1-553.
50. Vilela, C.; Sousa, A. F.; Fonseca, A. C.; Serra, A. C.; Coelho, J. F. J.; Freire, C. S. R.; Silvestre, A. J. D., *Polymer Chemistry* 2014, 5 (9), 3119-3141.
51. Miller, S. A., *Acs Macro Letters* 2013, 2 (6), 550-554.
52. Holmberg, A. L.; Reno, K. H.; Wool, R. P.; Epps, T. H., III, *Soft Matter* 2014, 10 (38), 7405-7424.

53. Trzaskowski, J.; Quinzler, D.; Baehrle, C.; Mecking, S., *Macromolecular Rapid Communications* 2011, 32 (17), 1352-1356.
54. Krasko, M. Y.; Shikanov, A.; Ezra, A.; Domb, A. J., *Journal of Polymer Science Part a-Polymer Chemistry* 2003, 41 (8), 1059-1069.
55. Sokolsky-Papkov, M.; Domb, A. J., *Polymers for Advanced Technologies* 2008, 19 (6), 671-679; Sokolsky-Papkov, M.; Golovanevski, L.; Domb, A. J.; Weiniger, C. F., *Pharmaceutical Research* 2009, 26 (1), 32-39.
56. Tueruenc, O.; Meier, M. A. R., *Macromolecular Rapid Communications* 2010, 31 (20), 1822-1826.
57. Meier, M. A. R.; Metzger, J. O.; Schubert, U. S., *Chemical Society Reviews* 2007, 36 (11), 1788-1802.
58. Gandini, A., *Macromolecules* 2008, 41 (24), 9491-9504.
59. Goerz, O.; Ritter, H., *Polymer International* 2013, 62 (5), 709-712.
60. Guo, B.; Chen, Y.; Lei, Y.; Zhang, L.; Zhou, W. Y.; Rabie, A. B. M.; Zhao, J., *Biomacromolecules* 2011, 12 (4), 1312-1321.
61. Fu, J.; Fiegel, J.; Krauland, E.; Hanes, J., *Biomaterials* 2002, 23 (22), 4425-4433; Najafi, F.; Sarbolouki, M. N., *Biomaterials* 2003, 24 (7), 1175-1182.
62. Papadimitriou, S.; Papageorgiou, G. Z.; Kanaze, F. I.; Georgarakis, M.; Bikiaris, D. N., *Journal of Nanomaterials* 2009; Zhang, S. P.; Yang, J.; Liu, X. Y.; Chang, J. H.; Cao, A. M., *Biomacromolecules* 2003, 4 (2), 437-445.
63. Ba, C. Y.; Yang, J.; Hao, Q. H.; Liu, X. Y.; Cao, A., *Biomacromolecules* 2003, 4 (6), 1827-1834.
64. Liu, J.; Jiang, Z.; Zhang, S.; Saltzman, W. M., *Biomaterials* 2009, 30 (29), 5707-5719.
65. Namazi, H.; Adell, M., *Biomaterials* 2005, 26 (10), 1175-1183.
66. Adeli, M.; Rasoulian, B.; Saadatmehr, F.; Zabihi, F., *Journal of Applied Polymer Science* 2013, 129 (6), 3665-3671.
67. Yang, J.; Webb, A. R.; Ameer, G. A., *Advanced Materials* 2004, 16 (6), 511-+.
68. Yang, J.; Webb, A. R.; Pickerill, S. J.; Hageman, G.; Ameer, G. A., *Biomaterials* 2006, 27 (9), 1889-1898.
69. Wittlich, P.; Themann, A.; Vorlop, K. D., *Biotechnology Letters* 2001, 23 (6), 463-466.
70. Zhou, C.-H.; Beltramini, J. N.; Fan, Y.-X.; Lu, G. Q., *Chemical Society Reviews* 2008, 37 (3), 527-549.

71. Behr, A.; Eilting, J.; Irawadi, K.; Leschinski, J.; Lindner, F., *Green Chemistry* 2008, 10 (1), 13-30.
72. .
73. Bettinger, C. J.; Orrick, B.; Misra, A.; Langer, R.; Borenstein, J. T., *Biomaterials* 2006, 27 (12), 2558-2565; Sundback, C. A.; Shyu, J. Y.; Wang, Y. D.; Faquin, W. C.; Langer, R. S.; Vacanti, J. P.; Hadlock, T. A., *Biomaterials* 2005, 26 (27), 5454-5464; Rai, R.; Tallawi, M.; Grigore, A.; Boccaccini, A. R., *Progress in Polymer Science* 2012, 37 (8), 1051-1078.
74. Wang, Y. D.; Kim, Y. M.; Langer, R., *Journal of Biomedical Materials Research Part A* 2003, 66A (1), 192-197.
75. Sun, Z.-J.; Chen, C.; Sun, M.-Z.; Ai, C.-H.; Lu, X.-L.; Zheng, Y.-F.; Yang, B.-F.; Dong, D.-L., *Biomaterials* 2009, 30 (28), 5209-5214.
76. Kallinteri, P.; Higgins, S.; Hutcheon, G. A.; St Pourcain, C. B.; Garnett, M. C., *Biomacromolecules* 2005, 6 (4), 1885-1894; Kulshrestha, A. S.; Gao, W.; Gross, R. A., *Macromolecules* 2005, 38 (8), 3193-3204; Yang, Y.; Lu, W.; Cai, J.; Hou, Y.; Ouyang, S.; Xie, W.; Gross, R. A., *Macromolecules* 2011, 44 (7), 1977-1985; Halpern, J. M.; Urbanski, R.; Weinstock, A. K.; Iwig, D. F.; Mathers, R. T.; von Recum, H. A., *Journal of Biomedical Materials Research Part A* 2014, 102 (5), 1467-1477.
77. Makadia, H. K.; Siegel, S. J., *Polymers* 2011, 3 (3), 1377-1397.
78. Wu, X. S., *Encyclopedic handbook of biomaterials and bioengineering, Part A: Materials, Vols. 1 and 2* 1995, 1015-1054; Tsuji, H., *Macromolecular Bioscience* 2005, 5 (7), 569-597; Nicolas, J.; Mura, S.; Brambilla, D.; Mackiewicz, N.; Couvreur, P., *Chemical Society Reviews* 2013, 42 (3), 1147-1235; Avgoustakis, K., *Current Drug Delivery* 2004, 1 (4), 321-333.
79. Jain, R. A., *Biomaterials* 2000, 21 (23), 2475-2490.
80. Park, T. G., *Biomaterials* 1995, 16 (15), 1123-1130; Lawrence, M. J.
81. Kirby, G. T. S.; White, L. J.; Rahman, C. V.; Cox, H. C.; Qutachi, O.; Rose, F. R. A. J.; Hutmacher, D. W.; Shakesheff, K. M.; Woodruff, M. A., *Polymers* 2011, 3 (1), 571-586.
82. Lee, J. Y.; Bashur, C. A.; Goldstein, A. S.; Schmidt, C. E., *Biomaterials* 2009, 30 (26), 4325-4335.
83. Arora, G.; Shukla, J.; Ghosh, S.; Maulik, S. K.; Malhotra, A.; Bandopadhyaya, G., *Plos One* 2012, 7 (3).
84. Lee, H.; Lee, K.; Park, T. G., *Bioconjugate Chemistry* 2008, 19 (6), 1319-1325; Nam, Y. S.; Kang, H. S.; Park, J. Y.; Park, T. G.; Han, S. H.; Chang, I. S., *Biomaterials* 2003, 24 (12), 2053-2059.

85. Jhunjhunwala, S.; Raimondi, G.; Thomson, A. W.; Little, S. R., *Journal of Controlled Release* 2009, *133* (3), 191-197.
86. Danhier, F.; Ansorena, E.; Silva, J. M.; Coco, R.; Le Breton, A.; Preat, V., *Journal of Controlled Release* 2012, *161* (2), 505-522; Cheng, J.; Teply, B. A.; Sherifi, I.; Sung, J.; Luther, G.; Gu, F. X.; Levy-Nissenbaum, E.; Radovic-Moreno, A. F.; Langer, R.; Farokhzad, O. C., *Biomaterials* 2007, *28* (5), 869-876.
87. Jiang, H. L.; Hu, Y. Q.; Li, Y.; Zhao, P. C.; Zhu, K. J.; Chen, W. L., *Journal of Controlled Release* 2005, *108* (2-3), 237-243.
88. Song, Z.; Feng, R.; Sun, M.; Guo, C.; Gao, Y.; Li, L.; Zhai, G., *Journal of Colloid and Interface Science* 2011, *354* (1), 116-123.
89. Johansen, P.; Men, Y.; Audran, R.; Corradin, G.; Merkle, H. P.; Gander, B., *Pharmaceutical Research* 1998, *15* (7), 1103-1110; Thomas, C.; Gupta, V.; Ahsan, F., *Pharmaceutical Research* 2010, *27* (5), 905-919.
90. Fonseca, C.; Simoes, S.; Gaspar, R., *Journal of Controlled Release* 2002, *83* (2), 273-286; Avgoustakis, K.; Beletsi, A.; Panagi, Z.; Klepetsanis, P.; Karydas, A. G.; Ithakissios, D. S., *Journal of Controlled Release* 2002, *79* (1-3), 123-135.
91. van de Weert, M.; Hennink, W. E.; Jiskoot, W., *Pharmaceutical Research* 2000, *17* (10), 1159-1167; Zhu, G. Z.; Mallery, S. R.; Schwendeman, S. P., *Nature Biotechnology* 2000, *18* (1), 52-57.
92. Jeong, Y.-I.; Na, H.-S.; Seo, D.-H.; Kim, D.-G.; Lee, H.-C.; Jang, M.-K.; Na, S.-K.; Roh, S.-H.; Kim, S.-I.; Nah, J.-W., *International Journal of Pharmaceutics* 2008, *352* (1-2), 317-323.
93. Murata, N.; Takashima, Y.; Toyoshima, K.; Yamamoto, M.; Okada, H., *Journal of Controlled Release* 2008, *126* (3), 246-254; Patil, Y.; Panyam, J., *International Journal of Pharmaceutics* 2009, *367* (1-2), 195-203.
94. Zhang, D. H.; Hillmyer, M. A.; Tolman, W. B., *Biomacromolecules* 2005, *6* (4), 2091-2095.
95. Wanamaker, C. L.; Tolman, W. B.; Hillmyer, M. A., *Biomacromolecules* 2009, *10* (2), 443-448.
96. Hillmyer, M. A.; Tolman, W. B., *Accounts of Chemical Research* 2014, *47* (8), 2390-2396.
97. Lowe, J. R.; Martello, M. T.; Tolman, W. B.; Hillmyer, M. A., *Polymer Chemistry* 2011, *2* (3), 702-708.
98. Martello, M. T.; Burns, A.; Hillmyer, M., *Acs Macro Letters* 2012, *1* (1), 131-135.

99. Olsen, P.; Borke, T.; Odelius, K.; Albertsson, A.-C., *Biomacromolecules* 2013, 14 (8), 2883-2890.
100. Hong, M.; Chen, E. Y. X., *Macromolecules* 2014, 47 (11), 3614-3624.
101. Tempelaar, S.; Mespouille, L.; Dubois, P.; Dove, A. P., *Macromolecules* 2011, 44 (7), 2084-2091; Chen, W.; Yang, H.; Wang, R.; Cheng, R.; Meng, F.; Wei, W.; Zhong, Z., *Macromolecules* 2010, 43 (1), 201-207.
102. Moore, T.; Adhikari, R.; Gunatillake, P., *Biomaterials* 2005, 26 (18), 3771-3782.
103. Kumar, A.; Kalra, B.; Dekhterman, A.; Gross, R. A., *Macromolecules* 2000, 33 (17), 6303-6309.
104. van der Meulen, I.; de Geus, M.; Antheunis, H.; Deumens, R.; Joosten, E. A. J.; Koning, C. E.; Heise, A., *Biomacromolecules* 2008, 9 (12), 3404-3410.
105. Liu, J.; Jiang, Z.; Zhang, S.; Liu, C.; Gross, R. A.; Kyriakides, T. R.; Saltzman, W. M., *Biomaterials* 2011, 32 (27), 6646-6654.
106. Slivniak, R.; Domb, A. J., *Biomacromolecules* 2005, 6 (3), 1679-1688.
107. Pratt, R. C.; Lohmeijer, B. G. G.; Long, D. A.; Waymouth, R. M.; Hedrick, J. L., *Journal of the American Chemical Society* 2006, 128 (14), 4556-4557.
108. Tang, M.; White, A. J. P.; Stevens, M. M.; Williams, C. K., *Chemical Communications* 2009, (8), 941-943.
109. Urakami, H.; Guan, Z., *Biomacromolecules* 2008, 9 (2), 592-597.
110. Gustafson, T. P.; Lonneckker, A. T.; Heo, G. S.; Zhang, S.; Dove, A. P.; Wooley, K. L., *Biomacromolecules* 2013, 14 (9), 3346-3353.
111. Mikami, K.; Lonneckker, A. T.; Gustafson, T. P.; Zinnel, N. F.; Pai, P.-J.; Russell, D. H.; Wooley, K. L., *Journal of the American Chemical Society* 2013, 135 (18), 6826-6829.
112. Simon, J.; Olsson, J. V.; Kim, H.; Tenney, I. F.; Waymouth, R. M., *Macromolecules* 2012, 45 (23), 9275-9281.
113. Brignou, P.; Gil, M. P.; Casagrande, O.; Carpentier, J.-F.; Guillaume, S. M., *Macromolecules* 2010, 43 (19), 8007-8017.
114. Trivedi, R.; Kompella, U. B., *Nanomedicine* 2010, 5 (3), 485-505.
115. Gaucher, G.; Dufresne, M. H.; Sant, V. P.; Kang, N.; Maysinger, D.; Leroux, J. C., *Journal of Controlled Release* 2005, 109 (1-3), 169-188.

116. Lu, Y.; Park, K., *International Journal of Pharmaceutics* 2013, 453 (1), 198-214.
117. Torchilin, V. P., *Pharmaceutical Research* 2007, 24 (1), 1-16.
118. Nishiyama, N.; Kataoka, K., *Pharmacology & Therapeutics* 2006, 112 (3), 630-648.
119. Gref, R.; Luck, M.; Quellec, P.; Marchand, M.; Dellacherie, E.; Harnisch, S.; Blunk, T.; Muller, R. H., *Colloids and Surfaces B-Biointerfaces* 2000, 18 (3-4), 301-313.
120. Sutton, D.; Nasongkla, N.; Blanco, E.; Gao, J., *Pharmaceutical Research* 2007, 24 (6), 1029-1046.
121. Torchilin, V. P., *Journal of Controlled Release* 2001, 73 (2-3), 137-172.
122. Kauzmann, W., *Advances in Protein Chemistry* 1959, 14, 1-63; Schellman, J. A., *Protein Science* 2010, 19 (3), 363-371.
123. Kwon, G. S.; Kataoka, K., *Advanced Drug Delivery Reviews* 1995, 16 (2-3), 295-309.
124. Kataoka, K.; Harada, A.; Nagasaki, Y., *Advanced Drug Delivery Reviews* 2001, 47 (1), 113-131.
125. Matsumura, Y.; Hamaguchi, T.; Ura, T.; Muro, K.; Yamada, Y.; Shimada, Y.; Shirao, K.; Okusaka, T.; Ueno, H.; Ikeda, M.; Watanabe, N., *British Journal of Cancer* 2004, 91 (10), 1775-1781.
126. Matsumura, Y., *Japanese Journal of Clinical Oncology* 2008, 38 (12), 793-802.
127. Uchino, H.; Matsumura, Y.; Negishi, T.; Koizumi, F.; Hayashi, T.; Honda, T.; Nishiyama, N.; Kataoka, K.; Naito, S.; Kakizoe, T., *British Journal of Cancer* 2005, 93 (6), 678-687.
128. Kim, S. C.; Kim, D. W.; Shim, Y. H.; Bang, J. S.; Oh, H. S.; Kim, S. W.; Seo, M. H., *Journal of Controlled Release* 2001, 72 (1-3), 191-202.
129. Roesler, A.; Vandermeulen, G. W. M.; Klok, H.-A., *Advanced Drug Delivery Reviews* 2012, 64, 270-279.
130. Torchilin, V. P., *Cellular and Molecular Life Sciences* 2004, 61 (19-20), 2549-2559.
131. Kedar, U.; Phutane, P.; Shidhaye, S.; Kadam, V., *Nanomedicine-Nanotechnology Biology and Medicine* 2010, 6 (6), 714-729.
132. Oerlemans, C.; Bult, W.; Bos, M.; Storm, G.; Nijssen, J. F. W.; Hennink, W. E., *Pharmaceutical Research* 2010, 27 (12), 2569-2589.

133. Aliabadi, H. M.; Lavasanifar, A., *Expert opinion on drug delivery* 2006, 3 (1), 139-62.
134. Allen, C.; Han, J. N.; Yu, Y. S.; Maysinger, D.; Eisenberg, A., *Journal of Controlled Release* 2000, 63 (3), 275-286.
135. Jee, J.-P.; McCoy, A.; Mecozzi, S., *Pharmaceutical Research* 2012, 29 (1), 69-82.
136. Gou, M.; Men, K.; Shi, H.; Xiang, M.; Zhang, J.; Song, J.; Long, J.; Wan, Y.; Luo, F.; Zhao, X.; Qian, Z., *Nanoscale* 2011, 3 (4), 1558-1567.
137. *Cancer Nanotechnology: Methods and Protocols* 2010, 624.
138. Brannon-Peppas, L.; Blanchette, J. O., *Advanced Drug Delivery Reviews* 2004, 56 (11), 1649-1659; Bae, Y. H.; Park, K., *Journal of Controlled Release* 2011, 153 (3), 198-205.
139. Danhier, F.; Feron, O.; Preat, V., *Journal of Controlled Release* 2010, 148 (2), 135-146.
140. Peer, D.; Karp, J. M.; Hong, S.; FaroKhazad, O. C.; Margalit, R.; Langer, R., *Nature Nanotechnology* 2007, 2 (12), 751-760.
141. Maeda, H.; Bharate, G. Y.; Daruwalla, J., *European Journal of Pharmaceutics and Biopharmaceutics* 2009, 71 (3), 409-419.
142. Torchilin, V., *Advanced Drug Delivery Reviews* 2011, 63 (3), 131-135.
143. Maeda, H.; Wu, J.; Sawa, T.; Matsumura, Y.; Hori, K., *Journal of Controlled Release* 2000, 65 (1-2), 271-284.
144. Jain, R. K., *Advanced Drug Delivery Reviews* 2012, 64, 353-365.
145. Maeda, H., *Bioconjugate Chemistry* 2010, 21 (5), 797-802.
146. Fang, J.; Nakamura, H.; Maeda, H., *Advanced Drug Delivery Reviews* 2011, 63 (3), 136-151.
147. Yuan, F.; Chen, Y.; Dellian, M.; Safabakhsh, N.; Ferrara, N.; Jain, R. K., *Proceedings of the National Academy of Sciences of the United States of America* 1996, 93 (25), 14765-14770.
148. Padera, T. P.; Stoll, B. R.; Tooredman, J. B.; Capen, D.; di Tomaso, E.; Jain, R. K., *Nature* 2004, 427 (6976), 695-695.
149. Noguchi, Y.; Wu, J.; Duncan, R.; Strohmalm, J.; Ulbrich, K.; Akaike, T.; Maeda, H., *Japanese Journal of Cancer Research* 1998, 89 (3), 307-314.
150. Nishiyama, N.; Okazaki, S.; Cabral, H.; Miyamoto, M.; Kato, Y.; Sugiyama, Y.; Nishio, K.; Matsumura, Y.; Kataoka, K., *Cancer Research* 2003, 63 (24), 8977-8983.

151. Hamaguchi, T.; Matsumura, Y.; Suzuki, M.; Shimizu, K.; Goda, R.; Nakamura, I.; Nakatomi, I.; Yokoyama, M.; Kataoka, K.; Kakizoe, T., *British Journal of Cancer* 2005, 92 (7), 1240-1246; Kato, K.; Chin, K.; Yoshikawa, T.; Yamaguchi, K.; Tsuji, Y.; Esaki, T.; Sakai, K.; Kimura, M.; Hamaguchi, T.; Shimada, Y.; Matsumura, Y.; Ikeda, R., *Investigational New Drugs* 2012, 30 (4), 1621-1627.
152. Abouzeid, A. H.; Patel, N. R.; Torchilin, V. P., *International Journal of Pharmaceutics* 2014, 464 (1-2), 178-184.
153. Danson, S.; Ferry, D.; Alakhov, V.; Margison, J.; Kerr, D.; Jowle, D.; Brampton, M.; Halbert, G.; Ranson, M., *British Journal of Cancer* 2004, 90 (11), 2085-2091.
154. Li, Y.; Yang, F.; Chen, W.; Liu, J.; Huang, W.; Jin, M.; Gao, Z., *Chemical & Pharmaceutical Bulletin* 2012, 60 (9), 1146-1154.
155. Kim, T. Y.; Kim, D. W.; Chung, J. Y.; Shin, S. G.; Kim, S. C.; Heo, D. S.; Kim, N. K.; Bang, Y. J., *Clinical Cancer Research* 2004, 10 (11), 3708-3716.
156. Bertrand, N.; Wu, J.; Xu, X.; Kamaly, N.; Farokhzad, O. C., *Advanced Drug Delivery Reviews* 2014, 66, 2-25; Byrne, J. D.; Betancourt, T.; Brannon-Peppas, L., *Advanced Drug Delivery Reviews* 2008, 60 (15), 1615-1626.
157. Jhaveri, A. M.; Torchilin, V. P., *Frontiers in pharmacology* 2014, 5, 77-77.
158. Perche, F.; Patel, N. R.; Torchilin, V. P., *Journal of Controlled Release* 2012, 164 (1), 95-102.
159. Zhao, J.; Mi, Y.; Feng, S.-S., *Biomaterials* 2013, 34 (13), 3411-3421.
160. Goldenberg, D. M.; Sharkey, R. M., *Expert Opinion on Biological Therapy* 2012, 12 (9), 1173-1190; Kamaly, N.; Xiao, Z.; Valencia, P. M.; Radovic-Moreno, A. F.; Farokhzad, O. C., *Chemical Society Reviews* 2012, 41 (7), 2971-3010.
161. Vinogradov, S.; Batrakova, E.; Li, S.; Kabanov, A., *Bioconjugate Chemistry* 1999, 10 (5), 851-860; Sawant, R. R.; Jhaveri, A. M.; Koshkaryev, A.; Zhu, L.; Qureshi, F.; Torchilin, V. P., *Molecular Pharmaceutics* 2014, 11 (2), 375-381.
162. Yue, J.; Liu, S.; Wang, R.; Hu, X.; Xie, Z.; Huang, Y.; Jing, X., *Molecular Pharmaceutics* 2012, 9 (7), 1919-1931.
163. Miura, Y.; Takenaka, T.; Toh, K.; Wu, S.; Nishihara, H.; Kano, M. R.; Ino, Y.; Nomoto, T.; Matsumoto, Y.; Koyama, H.; Cabral, H.; Nishiyama, N.; Kataoka, K., *Acs Nano* 2013, 7 (10), 8583-8592; Nasongkla, N.; Shuai, X.; Ai, H.; Weinberg, B. D.; Pink, J.;

- Boothman, D. A.; Gao, J. M., *Angewandte Chemie-International Edition* 2004, 43 (46), 6323-6327.
164. Ma, P. a.; Liu, S.; Huang, Y.; Chen, X.; Zhang, L.; Jing, X., *Biomaterials* 2010, 31 (9), 2646-2654.
165. Yang, R.; Meng, F.; Ma, S.; Huang, F.; Liu, H.; Zhong, Z., *Biomacromolecules* 2011, 12 (8), 3047-3055.
166. Xu, W.; Siddiqui, I. A.; Nihal, M.; Pilla, S.; Rosenthal, K.; Mukhtar, H.; Gong, S., *Biomaterials* 2013, 34 (21), 5244-5253.
167. Ross, J. F.; Chaudhuri, P. K.; Ratnam, M., *Cancer* 1994, 73 (9), 2432-2443; Hilgenbrink, A. R.; Low, P. S., *Journal of Pharmaceutical Sciences* 2005, 94 (10), 2135-2146.
168. Sudimack, J.; Lee, R. J., *Advanced Drug Delivery Reviews* 2000, 41 (2), 147-162.
169. Lu, Y.; Low, P. S., *Advanced Drug Delivery Reviews* 2012, 64, 342-352.
170. Qiu, L.-Y.; Yan, L.; Zhang, L.; Jin, Y.-M.; Zhao, Q.-H., *International Journal of Pharmaceutics* 2013, 456 (2), 315-324.
171. Kim, D.; Gao, Z. G.; Lee, E. S.; Bae, Y. H., *Molecular Pharmaceutics* 2009, 6 (5), 1353-1362.
172. Yoo, H. S.; Park, T. G., *Journal of Controlled Release* 2004, 96 (2), 273-283.

Chapter 2 Materials and Methods

2.1 Materials

General chemicals

All chemicals used in this project were purchased from Sigma-Aldrich unless specifically stated. The detailed list of chemicals with their purity as stated by the manufacturer was described below.

N,N'-dicyclohexylcarbodiimide (99%), 4-(dimethylamino)pyridine (99%), sodium trifluoroacetate (98%), poly(ethylene glycol) monomethyl ether ($M_n \sim 550$), pyrene ($\geq 99\%$), δ -decalactone ($\geq 98\%$), 1,5,7-triazabicyclo[4.4.0]dec-5-ene (TBD) (98%), poly(ethylene glycol) (M_n -4000), poly(ethylene glycol) monomethyl ether (M_n -5000), propargyl alcohol (99%), cis-1,3-O-benzylidene glycerol (97%), benzoic acid ($\geq 99.5\%$), pyrene ($\geq 99\%$), ϵ -caprolactone (97%), ω -pentadecalactone ($\geq 98\%$), novozymes-435 ($\geq 5,000$ U/g, recombinant, expressed in *Aspergillus niger*), Nile red (technical grade), Curcumin ($\geq 99.5\%$), Amphotericin B ($\sim 80\%$), Tween 80, 2,2'-bipyridyl ($\geq 99\%$), p-toluenesulfonyl chloride ($\geq 99\%$), sodium azide ($\geq 99.5\%$), anhydrous pyridine (99.8%), folic acid ($\geq 97\%$), rhodamine B isothiocyanate (mixed isomer), *N*-hydroxysuccinimide (98%), triethylamine ($\geq 99\%$), copper (I) bromide (99.9%). Sodium ascorbate and ortho phosphoric acid (85%) was purchased from Fluka. N₃-

PEG-NH₂.TFA salt was purchased from JenKemUSA which has ≥ 95 % of amine substitution and >90 % of azide substitution. δ -decalactone was passed through basic alumina before use. PEG4K, mPEG5K, δ -decalactone and ϵ -caprolactone were dehydrated by azeotropic distillation using anhydrous toluene. Novozymes-435 was dried under vacuum at 50°C for 24 hours before use. All other materials were used as received unless otherwise stated.

All other solvents were purchased from Fischer Scientific UK except deuterated solvents and dimethylacetamide, which were purchased from Sigma Aldrich.

Cells and Cell Culture reagents

Opti-MEM[®], reduced serum media and Alamar Blue[®] were purchased from Life Technologies, UK. RPMI-1640 Medium was procured from Sigma Aldrich. A549, MCF-7 and HCT116 cell lines were obtained from the ATCC and the media used for general maintenance was RPMI-1640 supplement with 2 mM L-glutamine and 10% fetal bovine serum.

2.2 Instruments and Methods

Fourier Transform Infrared (FTIR) Spectroscopy

FTIR analysis of polymers was performed on Cary 630 Agilent FTIR spectroscopy. A small quantity of sample was directly

placed on clean crystal present in the sample holder. A 'real-time' spectrum will appear on the screen, which was then analysed using MicroLab software. A background spectra was also collected before placing sample.

Nuclear Magnetic Resonance (NMR)

NMR analysis was performed on a Bruker NMR spectrometer at 400 MHz (^1H) and 101 MHz (^{13}C) in deuterated solvent. Spectra were analysed using MestReNova 6.0.2 copyright© 2009 Mestrelab Research S.L. All chemical shifts were recorded in ppm using residual solvent as an internal standard (CDCl_3 : δH 7.26, δC 77.16, DMSO-d_6 : δH 2.50, δC 39.52).

MALDI-TOF Mass Spectrometry (MALDI-MASS)

Matrix-assisted laser desorption/ionization time-of-flight (MALDI-TOF) mass spectroscopy was performed on an Ultraflex III MALDI-TOF spectrometer with N_2 laser of 337 nm and pulses of 3 ns. Trans-2-[3-(4-tert-Butylphenyl)-2-methyl-2-propenylidene] malononitrile (DCTB) was used as the matrix and Sodium trifluoroacetate was used as dopant. Samples were prepared by mixing 5mg/mL of sample in 10mg/mL of matrix in a suitable solvent (acetone or acetonitrile).

Size Exclusion Chromatography (SEC)

The number-average molecular weight (M_n), weight average molecular weight (M_w) and molecular weight distribution (polydispersity, M_w/M_n) were measured by SEC. Molecular weight analysis was performed on a Polymer Laboratories GPC 50 spectrometer fitted with a differential refractive index detector. The eluent was HPLC grade CHCl_3 at 30 °C with a flow rate of 1 mL min^{-1} . The instrument was fitted with a Polymer Labs PLgel guard column (50 × 7.5 mm, 8 μm) followed by a pair of PLgel Mixed-D columns (300 × 7.5 mm, 8 μm). Column calibration was achieved using narrow polystyrene standards of known M_p in the range of 100 Da-500 kDa. Molecular weight and polydispersity were calculated using Polymer Labs Cirrus 3.0 software.

Some samples were also run on a SEC having HPLC grade tetrahydrofuran as eluent. The instrument used was Polymer Laboratories (PL-120) spectrometer equipped with RI detector and calibrated with linear polymethylmethacrylate (PMMA) standards. The columns used were PLgel Mixed-C (30 cm, 2 in series) with a guard column of PL Gel M and analysis was performed at 40°C, with flow rate of 1ml/min.

Differential Scanning calorimeter (DSC)

A TA-Q2000 DSC (TA instruments), was used to determine the melting temperature (T_m) and glass transition temperature (T_g) of polymers. Typically, the sample (5–15 mg) was weighed into a Tzero DSC pan and capped with a Tzero DSC lid which was then sealed with a Tzero press (TA instruments) using a Black Tzero lower die and a flat upper die. In a typical run, two cycles of experiment were run and the temperature was increased from -90 to 200 ° C at a rate of 10 ° C/min and the results obtained from the second cycle were reported.

Dynamic light scattering (DLS) and Zeta Potential

DLS is a well-established technique for measuring the size and size distribution of samples of nano-materials. It measures the scattered laser light at different intensities caused by the Brownian motion of particles in a diluted suspension. Analysis of these intensity fluctuations gives the velocity of the Brownian motion, which can be converted into particle size using the Stokes-Einstein relationship.

The z-average diameter and the Polydispersity Index (PdI) of micelles were measured by DLS using a NanoZS instrument (Malvern, UK). The measurements were carried out at 25 ° C using 633 nm (4 mW) wavelength laser. The scattered light was detected at an angle of 173 °.

Zeta Potential was measured using a NanoZS instrument (Malvern, UK) *via* a Laser Doppler Micro-electrophoresis technique. An electric field was applied to the dispersion of particles, which induced movement at a certain velocity. This velocity was measured using phase analysis light scattering to give the value of electrophoretic mobility from which zeta potential and zeta potential distribution were calculated. Data analysis was carried out using zetasizer software version 7.03 and mean values were obtained from three measurements.

Transmission Electron Microscopy (TEM)

TEM was used to determine the size and morphology of the micelles. Samples were imaged using a FEI Tecnai G2 electron microscope. One drop of sample in water, typically 25-50 µg/mL was dropped onto a copper grid and allow to dry in air. Samples were then imaged on TEM in bright field at high tension of 100 Kv using TIA imaging software without staining.

Rotary Evaporator

A Buchi rotavapor R-200 equipped with a B490 heating bath was used to remove organic solvent under reduced pressure.

Freeze Drier

An Edwards Modulyo freeze drier equipped with an Edwards high vacuum pump was used to remove water from samples.

All samples were frozen with liquid nitrogen before placing in drier.

Fluorescence Spectroscopy

Fluorescence spectra were recorded using a Cary Eclipse Fluorescence spectrophotometer (Varian). The intensity was measured against appropriate blank solutions at room temperature with the excitation and emission slit widths of 5 nm.

Ultraviolet-visible Spectroscopy (uv/vis)

Samples for UV-vis absorbance were analysed on a Beckman Coulter DU 800 UV spectrophotometer using capped quartz cuvettes. A sample volume of 700 μ l was used for all measurements after appropriate dilutions.

Critical Micelle Concentration (CMC) determination

The CMC values of amphiphilic block copolymers were determined using the pyrene 1:3 ratio method¹. Pyrene showed five different peaks in its fluorescence spectra (figure 2-1) whose intensities are totally dependent on the surrounding environment (i.e. polarity) experienced by the pyrene molecule. Consequently, when pyrene moves from a polar region to a nonpolar region the intensity of first peak (I_1) at 373 nm is observed to reduce, while that of the third peak

intensity (I_3) at 384 nm rises and thus gives an idea of the environment facing by the pyrene in experimental solutions². This difference in the peak intensity was used to determine the CMC of surfactants. When micelles start forming in experimental solution, they provide a hydrophobic region to the pyrene, which leads to decrease in the intensity of peak 1 or the ratio of peak 1st to 3rd.

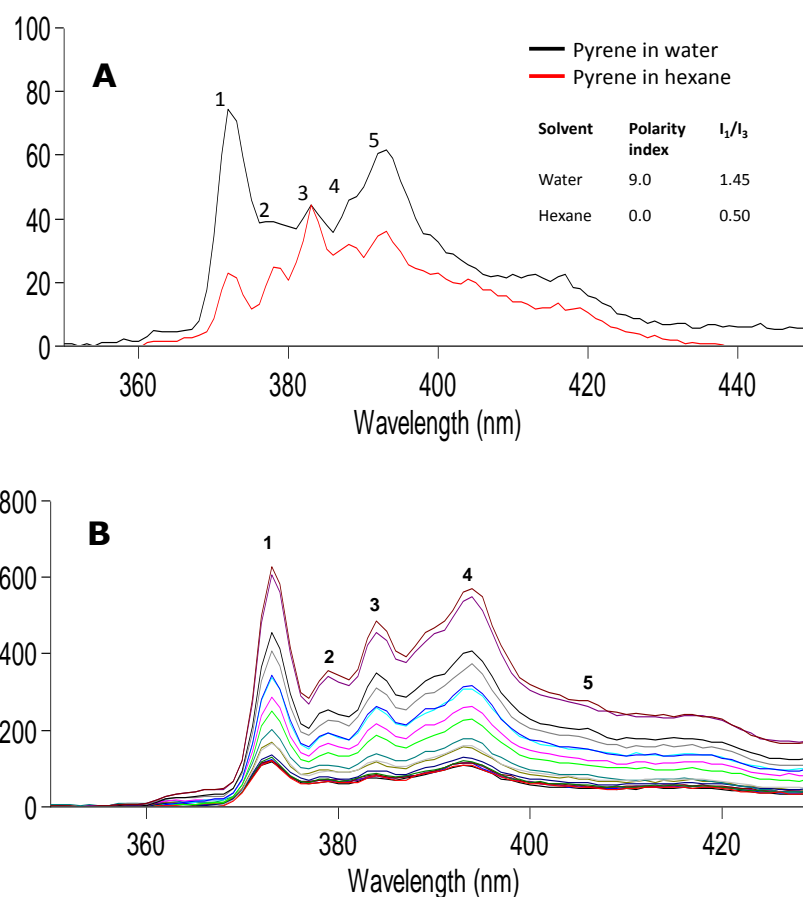


Figure 2-1 Pyrene fluorescence spectra in (A) solvents with different polarity and (B) in different concentration of amphiphilic block copolymer in water

Briefly, a stock solution of pyrene was made in acetone and a pre-calculated quantity contains 6×10^{-7} M of pyrene was transferred into 22 vials followed by evaporation of acetone under a slow stream of nitrogen. Different concentrations (from 0.001 to 50 $\mu\text{g}/\text{mL}$) of polymer solutions in water were then added in each vial and left overnight (in the dark) with agitation to equilibrate. Fluorescence spectra of solutions were then recorded in the range of 350 to 420 nm at an excitation wavelength of 335 nm. The intensities of emitted light at 373 nm (I_1) and 384 nm (I_3) were used to calculate the pyrene 1:3 ratio and plotted against the concentration of polymer used (log scale). All measurements were carried out in triplicate at $25.0 \pm 1^\circ\text{C}$ and mean value with error was reported.

Drug Content and Encapsulation Efficiency

Drug content weight percent (DC wt%) and percent encapsulation efficiency (EE %) in the samples were calculated using the formula below:

$$\text{DC wt\%} = \frac{\text{Amount of drug loaded}}{\text{Amount of polymer used}} \times 100$$

$$\text{EE\%} = \frac{\text{Weight of loaded drug}}{\text{Weight of drug in feed}} \times 100$$

2.3 References

1. Aguiar, J.; Carpena, P.; Molina-Bolivar, J. A.; Ruiz, C. C., *Journal of Colloid and Interface Science* 2003, 258 (1), 116-122.
2. Dong, D. C.; Winnik, M. A., *Canadian Journal of Chemistry-Revue Canadienne De Chimie* 1984, 62 (11), 2560-2565.

**Chapter 3 Synthesis and
Characterisation of
Homopolymers and Block
Copolymers based on δ -
Decalactone**

3.1 Introduction

Ring opening polymerisation (ROP) is a widely used, industrially important synthesis methodology to obtain polyesters with high molecular weight. Unlike polycondensation, ROP does not always require high temperature or long reaction time. The conversion rate observed in ROP is generally high without the need to remove any side products or the use of exactly stoichiometric amount of monomers¹. Lactides and lactones are the most important and investigated category of monomers used to make polyesters by ROP. Polymers and copolymers of lactides are well established materials, which are currently marketed for various applications². Poly(caprolactone) synthesised from ϵ -caprolactone is another class of extensively studied biodegradable and less-toxic polymer which is cheap and commercially available³.

Poly(caprolactone) and its copolymers are amongst the most studied polymers in biomedical applications but the long degradation time and non-renewable monomer source restrict their extensive use^{4,5}. Hence, monomers and polymers from natural/renewable resources are of increasing importance. However, many polymers derived directly from natural resources have limitations; for example, batch to batch

variability in terms of molecular weight, lack of addressable chemical functionalities and limited scope to alter the physical and chemical properties. Consequently, polymers synthesised in the laboratory using monomers obtained from renewable resources are attractive materials, which can address the problems of unsustainable feedstocks and unfavourable application properties.

Poly(lactic acid) (PLA) and poly(lactic-co-glycolic acid) (PLGA) are Food and Drug Administration (FDA) approved polymers, obtained from renewable monomers, however their applicability has been limited by certain disadvantages. For instance, the use of PLGA in medical implants can cause local irritation by releasing excessive acid upon degradation. In the case of PLGA-derived drug delivery materials, the production of excessive acid from PLGA degradation can cause deleterious effects on loaded acid sensitive drugs^{6,7}. In addition, the loading of hydrophobic drugs into PLA or PLGA matrices has been reported to be low, which was suggested due to the lower hydrophobicity of these polymers compared to long chain polyesters^{8, 9}. Therefore, more hydrophobic derivatives of lactide and resulting copolymer have been prepared^{8, 9} however, the synthesis procedure is tedious and expensive in terms of monomer cost. Considering these limitations there is

an urgent need to develop a polymeric system, which can be produced from cheap renewable monomers *via* easy synthesis methodologies.

δ -Decalactone is a FDA approved flavouring agent¹⁰ (FDA 21 CFR -172.515) but its applicability in biomedical fields has not yet been demonstrated. This commercially available compound is obtained from the plant *Cryptocarya massoy*¹¹ and therefore can be considered as a renewable monomer. We selected this monomer to explore its potential in drug delivery applications due to its renewable source; commercial availability and the presence of an alkyl side chain. The presence of an alkyl chain in monomer structure could generate a highly hydrophobic polymer, which may be useful to achieve better drug loading than other currently-used polymers^{9, 12}. The first ROP of δ -decalactone was reported by Dong *et. al* in 1999 using lipase PSL (*Pseudomonas* sp.) as a catalyst with 87% conversion (M_n - 9,000) after 480 hrs¹³. Additionally, despite the high efficiency of enzymes in ROP for polymer preparation, some drawbacks remain. For instance:

- a) Enzymes are expensive compared to other ROP catalysts and therefore use of enzymes is limited for large scale synthesis¹⁴.
- b) Required in high concentration to initiate ROP¹⁵.

- c) Dilution of polymers with solvent is desirable when removing enzyme at the end of the reaction, leading to an additional step in purification¹⁵.
- d) Limited use at high temperatures (melt polymerization)¹⁶.
- e) Poor control of molecular weight due to trans-esterification reactions¹⁶.

Considering these limitations, a highly efficient organic catalyst named 1,5,7-Triazabicyclo[4.4.0]dec-5-ene (TBD) has been reported as an alternative for ROP of macrolactones and hindered lactones which addresses many of the problems associated with enzyme catalysts^{17, 18}. TBD is a bicyclic guanidine base, first synthesised by McKay and Kreling in 1957. It is reported to be a very efficient catalyst for various reactions like acyl transfer¹⁹, aldol reaction²⁰, Michael reactions²¹, ring opening polymerization²² etc. TBD can be recovered by CO₂ treatment reported by Cota *et. al.* and therefore could be used in more batches to catalyse reactions²⁰. In addition, an active organic catalyst like TBD for ROP is preferable compared to metal catalysts due to reported higher catalytic efficiency and easier purification^{22, 23}.

More recently, Martello *et. al* reported the ROP of δ -decalactone to synthesise high molecular weight poly(decalactone) (PDL) under mild conditions using TBD¹⁸.

Following the work of Martello *et. al.*, it was postulated to synthesise block copolymers of PDL, using TBD as catalyst, and then to evaluate the potential of these block copolymers for drug delivery applications.

In this chapter, the synthesis of novel amphiphilic block copolymers has been reported *via* ROP of δ -decalactone initiated by poly(ethylene glycol) (M_n -4000) (PEG) and mono methoxy poly(ethylene glycol) (M_n -5000) (mPEG). The reaction was performed under mild conditions in the absence of solvent as a step towards a metal free "green" synthesis approach²⁴. The PEG initiators were chosen to provide hydrophilic blocks, which, when combined with the hydrophobic decalactone blocks, would generate amphiphilic copolymers. In turn, self-assembly of these copolymers was expected to occur in water providing micelle-like structures with hydrophobic cores for drug incorporation and hydrophilic shells to provide colloidal stability and resistance to protein attachment in biological media. This design provided a framework for materials intended for use in various pharmaceutical applications²⁵.

Homopolymers of δ -decalactone were also synthesised using initiators like glycerol, propargyl alcohol and cis-1,3-O-benzylideneglycerol (BZD) to compare the properties with

novel block copolymers of PDL. Initiators such as BZD and or propargyl alcohol are of further interest due to the presence of end functional groups, which could be later used to introduce desirable properties by post polymerisation functionalization. A block copolymer of ϵ -caprolactone using mPEG as initiator was also synthesised for comparative studies.

Lactone rings of larger size than ϵ -caprolactone have been rather less investigated for the preparation of more hydrophobic polyesters and only a few reports have been published for ROP of macrolactones. Therefore, a macrolactone (*i.e.* ω -pentadecalactone) was explored in the current study to make block copolymers. ω -pentadecalactone is a FDA approved flavouring agent/food additive (FDA 21 CFR -172.515), found naturally in angelica root oil²⁶ and commercial quantities of the monomer are produced synthetically. The applications of homopolymers of ω -pentadecalactone *i.e.* poly(pentadecalactone) (PPDL) have previously been limited due to poor solubility in non-chlorinated organic solvents and high crystallinity²⁷. ROP of ω -pentadecalactone has been well studied and therefore it was hypothesised that making copolymers of ω -pentadecalactone with δ -decalactone could produce materials of better solubility and intermediate crystallinity, thus enhancing its applicability

for biomedical use²⁸. In addition, it has been reported that ROP of macrolactones has been successful using enzyme catalysts, despite the above-mentioned limitations²⁹. Therefore, to provide comparison with other catalytic routes, a copolymer of ω -pentadecalactone was synthesised using Novozyme-435 as a catalyst and diblock copolymer of PDL as initiator. The resulting polymer was expected to contain a soft part (amorphous PDL) and a hard part (crystalline PPDL) thus was anticipated to have mixed physicochemical properties³⁰ which could be tunable by changing the molar ratio of starting materials.

3.2 General Synthesis Method for δ -Decalactone Polymers

3.2.1 Synthesis of δ -Decalactone Homopolymers

Poly(decalactone) was synthesised via ROP of δ -decalactone in bulk according to the reported procedure¹⁸. Briefly, δ -decalactone (10 g, 58.73 mmol) was transferred into a flask containing an initiating alcohol *i.e.* either BZD (0.10 g, 0.58 mmol) or propargyl alcohol (0.03 g, 0.58 mmol) or glycerol (Gly) (0.05 g, 0.58 mmol). The mixture was stirred for 10-15 minutes to make a homogeneous mixture. TBD (0.20 g, 1.45 mmol) was then added under a nitrogen atmosphere and the mixture was allowed to react for 11 hrs at desired

temperature (See table 3-1). The obtained viscous liquid was then quenched by adding benzoic acid (0.35g, 2.90 mmol) solution in acetone, precipitated in cold methanol and the residual solvent was evaporated under vacuum. Polymer BZD-PDL propargyl-PDL and Gly-PDL were recovered as colourless viscous liquid with the percentage yield of 78.21% (7.90 g) 76.07% (7.63 g) and 80.39 (8.08 g) respectively.

BZD-PDL -: ^1H NMR (400 MHz, CDCl_3) δ 7.53 – 7.42 (aromatic-CH, m, 2H), 7.38 – 7.30 (aromatic-CH, m, 3H), 5.52 (aromatic-C-CH-O, s, 1H), 4.94 – 4.78 (CH-O-CO, m, 89H), 4.68 (CH_2 -CH-O-CO, dd, 1H), 4.31 – 4.09 (O-CH $_2$ -CH, m, 4H), 3.64 – 3.48 (CH_2 -CH-OH, m, 4H), 2.37 – 2.18 (O-CO-CH $_2$, m, 178H), 1.76 – 1.38 (CH $_2$ -CH $_2$ -CH-CH $_2$, m, 535H), 1.27 (CH $_2$ -CH $_2$ -CH $_2$ -CH $_3$, m, 546H), 0.96 – 0.76 (CH $_3$, t, 282H).

^{13}C NMR (101 MHz, CDCl_3) δ 172.98 (CH-O-CO, CH $_2$ -CH-O-CO), 137.25 (aromatic-C-CH-O) 128.98 (aromatic-CH), 128.19 (aromatic-CH), 125.97 (aromatic-CH), 101.15 (aromatic-C-CH-O), 73.62 (CH $_2$ -CH-O-CO, CH $_2$ -CH-OH), 71.21 (O-CH $_2$ -CH), 69.04 (CH $_2$ -CH-O-CO), 34.14 (CH-CH $_2$ -CH $_2$), 33.91 (CH $_2$ -CH-O-CO, CH $_2$ -CH-OH), 33.43 (O-CO-CH $_2$), 31.60 (CH $_2$ -CH $_2$ -CH $_3$), 24.89 (CH-CH $_2$ -CH $_2$), 22.48 (O-CO-CH $_2$ -CH $_2$), 20.77 (CH $_2$ -CH $_3$), 13.94 (CH $_2$ -CH $_3$)

Propargyl-PDL -: ^1H NMR (400 MHz, CDCl_3) δ 4.94 – 4.78 (CH-O-CO , m, 87H), 4.67 ($\text{C-CH}_2\text{-O}$, s, 2H), 3.64-3.48 ($\text{CH}_2\text{-CH-OH}$, m, 4H), 2.48 (CH-C , s, 1H), 2.37 – 2.18 (O-CO-CH_2 , m, 174H), 1.76 – 1.38 ($\text{CH}_2\text{-CH}_2\text{-CH-CH}_2$, m, 522H), 1.38 – 1.14 ($\text{CH}_2\text{-CH}_2\text{-CH}_2\text{-CH}_3$, m, 526H), 0.96-0.76 ($\text{CH}_2\text{-CH}_3$, t, 270H).

^{13}C NMR (101 MHz, CDCl_3) δ 173.04 (CH-O-CO , $\text{CH}_2\text{-O-CO}$), 77.23 (CH-C-CH_2), 75.86 (CH-C-CH_2), 73.69 ($\text{CH}_2\text{-CH-O-CO}$, $\text{CH}_2\text{-CH-OH}$), 34.19 ($\text{CH-CH}_2\text{-CH}_2$), 33.94 ($\text{CH}_2\text{-CH-O-CO}$, $\text{CH}_2\text{-CH-OH}$), 33.46 (O-CO-CH_2), 31.64 ($\text{CH}_2\text{-CH}_2\text{-CH}_3$), 24.93 ($\text{CH-CH}_2\text{-CH}_2$), 22.52 ($\text{O-CO-CH}_2\text{-CH}_2$), 20.79 ($\text{CH}_2\text{-CH}_3$), 13.98 ($\text{CH}_2\text{-CH}_3$)

Gly-PDL -: ^1H NMR (400 MHz, CDCl_3) δ 5.29 – 5.15 (CH-O-CO , m, 1H), 4.86 (CH-O-CO , m, 88H), 4.26 ($\text{CH-CH}_2\text{-O-CO}$, m, 2H), 4.19 – 4.00 ($\text{CH-CH}_2\text{-O-CO}$, m, 2H), 3.54 ($\text{CH}_2\text{-CH-OH}$, m, 4H), 2.29 (O-CO-CH_2 , m, 176H), 1.73 – 1.38 ($\text{CH}_2\text{-CH}_2\text{-CH-CH}_2$, m, 528H), 1.37 – 1.15 ($\text{CH}_2\text{-CH}_2\text{-CH}_2\text{-CH}_3$, m, 532H), 0.97 – 0.74 ($\text{CH}_2\text{-CH}_3$, t, 277H).

^{13}C NMR (101 MHz, CDCl_3) δ 173.02 (CH-O-CO , $\text{CH}_2\text{-O-CO}$), 73.67 ($\text{CH}_2\text{-CH-O-CO}$, $\text{CH}_2\text{-CH-OH}$), 71.27 ($\text{CH-CH}_2\text{-O-CO}$), 59.52 (CH-OH), 34.18 ($\text{CH-CH}_2\text{-CH}_2$), 33.94 ($\text{CH}_2\text{-CH-O-CO}$, $\text{CH}_2\text{-CH-OH}$), 33.46 (O-CO-CH_2), 31.76 ($\text{CH}_2\text{-CH}_2\text{-CH}_3$), 24.9 ($\text{CH-CH}_2\text{-CH}_2$), 22.51 ($\text{O-CO-CH}_2\text{-CH}_2$), 20.39 ($\text{CH}_2\text{-CH}_3$), 13.88 ($\text{CH}_2\text{-CH}_3$).

3.2.2 Synthesis of Block Copolymers of δ -Decalactone

A di-block (AB type) copolymer of δ -decalactone was synthesised using mPEG ($M_n \sim 5000$) as initiator. Briefly, mPEG (11.2 g, 2.24 mmol) was added in a flask containing δ -decalactone (57.2 g, 336 mmol) and the content was heated to 50°C and stirred for 10 min to make a homogeneous mixture. TBD (1.17 g, 8.4 mmol) was then added and the mixture was allowed to react for 7 hrs at 50°C. The reaction mixture was then cooled, quenched by adding benzoic acid (2.05 g, 16.8 mmol) solution in acetone and polymer was precipitated in cold methanol followed by removal of residual solvent in *vacuo*. The obtained dry material was again precipitated in petroleum ether and any residual solvent was evaporated under vacuum to yield a wax-like material (mPEG-b-PDL). The ratio of monomer to initiator was changed to obtain copolymers with different molar masses. A similar procedure was followed to synthesise tri-block (PDL-b-PEG-b-PDL, ABA type) copolymer of δ -decalactone (4.25 g, 25.0 mmol) using PEG (1 g, 0.25 mmol) as initiator (see table 3-1). Copolymer mPEG-b-PDL and PDL-b-PEG-b-PDL were recovered as a wax-like material with the percentage yield of 67.60% (46.24 g) and 69.71% (3.66 g) respectively.

mPEG-b-PDL -: ^1H NMR (400 MHz, CDCl_3) δ 4.95-4.84 (CH-O-CO, m, 37H), 4.27 – 4.17 ($\text{CH}_2\text{-O-CO}$, t, 2H), 3.65 ($\text{O-CH}_2\text{-CH}_2\text{-O}$, s, 497H), 3.38 (O-CH_3 , s, 3H), 2.32 (O-CO-CH_2 , m, 75H), 1.75 – 1.40 ($\text{CH}_2\text{-CH}_2\text{-CH-CH}_2$, m, 222H), 1.39 – 1.18 ($\text{CH}_2\text{-CH}_2\text{-CH}_2\text{-CH}_3$, m, 227H), 0.95 – 0.77 ($\text{CH}_2\text{-CH}_3$, t, 138H).

^{13}C NMR (101 MHz, CDCl_3) δ 173.04 (CH-O-CO, $\text{CH}_2\text{-O-CO}$), 73.67 ($\text{CH}_2\text{-CH-O-CO}$, $\text{CH}_2\text{-CH-OH}$), 70.57 ($\text{CH}_2\text{-CH}_2\text{-O}$), 65.96 ($\text{CH}_2\text{-O-CO}$) 57.86 (O-CH_3), 34.19 ($\text{CH-CH}_2\text{-CH}_2$), 33.94 ($\text{CH}_2\text{-CH-O-CO}$, $\text{CH}_2\text{-CH-OH}$), 33.47 (O-CO-CH_2), 31.64 ($\text{CH}_2\text{-CH}_2\text{-CH}_3$), 24.93 ($\text{CH-CH}_2\text{-CH}_2$), 22.52 ($\text{O-CO-CH}_2\text{-CH}_2$), 20.80 ($\text{CH}_2\text{-CH}_3$), 13.99 ($\text{CH}_2\text{-CH}_3$)

FTIR wavenumber (cm^{-1}): 2858 (C-H, stretching), 1729 (C=O, stretching), 1341 (C-H, bending), 1106 (C-O, Stretching).

PDL-b-PEG-b-PDL -: ^1H NMR (400 MHz, CDCl_3) δ 4.97 – 4.80 (CH-O-CO, m, 37H), 4.24 ($\text{CH}_2\text{-O-CO}$, t, 4H), 3.66 ($\text{O-CH}_2\text{-CH}_2\text{-O}$, s, 409H), 2.41 – 2.18 (O-CO-CH_2 , m, 78H), 1.75 – 1.39 ($\text{CH}_2\text{-CH}_2\text{-CH-CH}_2$, m, 218H), 1.37 – 1.12 ($\text{CH}_2\text{-CH}_2\text{-CH}_2\text{-CH}_3$, m, 226H), 0.97 – 0.77 ($\text{CH}_2\text{-CH}_3$, t, 140H).

^{13}C NMR (101 MHz, CDCl_3) δ 173.05 (CH-O-CO, $\text{CH}_2\text{-O-CO}$), 73.70 ($\text{CH}_2\text{-CH-O-CO}$, $\text{CH}_2\text{-CH-OH}$), 70.56 ($\text{CH}_2\text{-CH}_2\text{-O}$), 64.11 ($\text{CH}_2\text{-O-CO}$), 34.20 ($\text{CH-CH}_2\text{-CH}_2$), 33.94 ($\text{CH}_2\text{-CH-O-CO}$, $\text{CH}_2\text{-CH-OH}$), 33.47 (O-CO-CH_2), 31.65 ($\text{CH}_2\text{-CH}_2\text{-CH}_3$), 24.95 (CH-

CH₂-CH₂), 22.52 (O-CO-CH₂-CH₂), 20.79 (CH₂-CH₃), 13.99 (CH₂-CH₃)

3.2.3 Synthesis of Block Copolymer of ϵ -Caprolactone

A di-block (AB type) copolymer of ϵ -caprolactone was synthesised using mPEG as initiator and TBD as catalyst¹⁷. Briefly, mPEG (6 g, 1.2 mmol) was added in a flask containing ϵ -caprolactone (7 g, 61.3 mmol), heated to 110°C and stirred for 10 min to make a uniform mixture under a nitrogen atmosphere. TBD (0.17 g, 1.2 mmol) was dissolved in anhydrous acetone (500 μ l) and added to the mixture *via* a syringe and reaction was continued for 10 minutes under nitrogen atmosphere. The reaction mixture was cooled, quenched by adding benzoic acid (0.29 g, 2.4 mmol) solution in acetone and the resultant polymer was precipitated in cold methanol followed by precipitation in diethyl ether. The residual solvent was evaporated under vacuum to obtain purified material. Copolymer mPEG-b-PCL was recovered as an off-white powder with the percentage yield of 93.84% (12.20 g).

¹H NMR (400 MHz, CDCl₃) δ 4.24 (CH₂-O-CO, t, 2H), 4.07 (CH₂-O-CO, t, 100H), 3.66 (O-CH₂-CH₂-O, s, 522H), 3.40 (O-CH₃, s, 3H), 2.33 (O-CO-CH₂, t, 100H), 1.74 – 1.58 (CH₂-CH₂-CH₂, m, 200H), 1.46 – 1.32 (CH₂-CH₂-CH₂, m, 100H).

^{13}C NMR (101 MHz, CDCl_3) δ 173.51 ($\text{CH}_2\text{-O-CO}$), 70.57 ($\text{CH}_2\text{-CH}_2\text{-O}$), 64.13 ($\text{CH}_2\text{-O-CO}$), 57.69 (O-CH_3), 34.11 (O-CO-CH_2), 28.35 ($\text{CH}_2\text{-CH}_2\text{-CH}_2$), 25.52 ($\text{CH}_2\text{-CH}_2\text{-CH}_2$), 24.57 ($\text{CH}_2\text{-CH}_2\text{-CH}_2$)

3.2.4 Copolymer Synthesis of ω -Pentadecalactone with mPEG-b-PDL (ABC Type)

A copolymer of ω -pentadecalactone was synthesised using mPEG-b-PDL as initiator via a reported procedure³¹. Briefly, mPEG-b-PDL (2.9 g, 0.26 mmol) and ω -pentadecalactone (0.75 g, 3.12 mmol) were dissolved in anhydrous toluene (10mL) and transferred into a flask containing Novozyme-435 (0.075 g, 10% weight of pentadecalactone). The reaction mixture was then heated to 70°C and allowed to react for 3 hrs, then cooled and an excess of cold acetone was added. The reaction mixture was then filtered to remove the catalyst, and concentrate up to the volume of 30mL. The solution was again filtered to remove insoluble copolymer and homopolymer, if any. The filtrate was then concentrated and precipitated in cold methanol to remove any unconverted monomer followed by drying in vacuum. Copolymer mPEG-b-PDL-b-PPDL was recovered as a white sticky solid with the percentage yield of 61.37% (2.24 g).

mPEG-b-PDL-b-PPDL-:¹H NMR (400 MHz, CDCl₃) δ 4.88 (CH-O-CO, m, 38H), 4.28 – 4.17 (CH₂-O-CO, t, 2H), 4.08 (CH₂-O-CO, m, 14H), 3.66 (O-CH₂-CH₂-O, s, 505H), 3.39 (O-CH₃, s, 3H), 2.32 (O-CO-CH₂, m, 92H), 1.77 – 1.42 (CH₂-CH₂-CH-CH₂, O-CO-CH₂-CH₂, m, 243H), 1.28 (CH₂-CH₂-CH₂-CH₃, CH₂-CH₂, m, 374H), 0.88 (CH₂-CH₃, t, 121H).

¹³C NMR (101 MHz, CDCl₃) δ 173.98 (CH-O-CO-CH₂), 173.03 (CH-O-CO), 73.68 (CH₂-CH-O-CO), 70.56 (CH₂-CH₂-O), 64.38 (CH₂-O-CO), 58.58 (O-CH₃), 34.40 (O-CO-CH₂), 34.19 (CH-CH₂-CH₂), 33.94 (CH₂-CH-O-CO), 33.46 (O-CO-CH₂), 31.64 (CH₂-CH₂-CH₃), 29.77 – 29.00 (pentadecalactone-CH₂), 28.65 (pentadecalactone-CH₂), 25.93 (pentadecalactone-CH₂), 24.98 (CH-CH₂-CH₂, pentadecalactone-CH₂), 22.51 (O-CO-CH₂-CH₂), 20.81 (CH₂-CH₃), 13.98 (CH₂-CH₃).

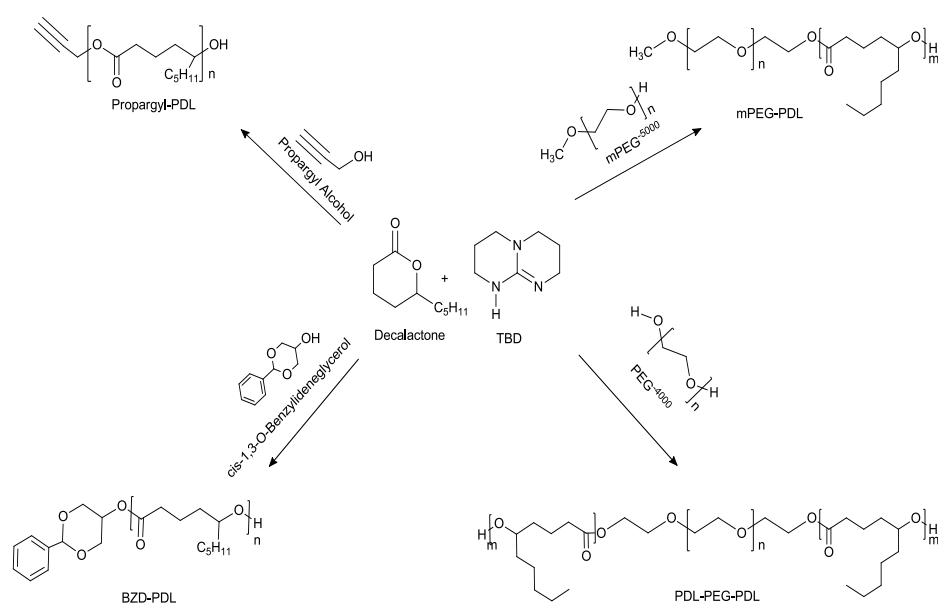
3.3 Results

3.3.1 Synthesis and Characterisation of Homopolymers of δ-Decalactone

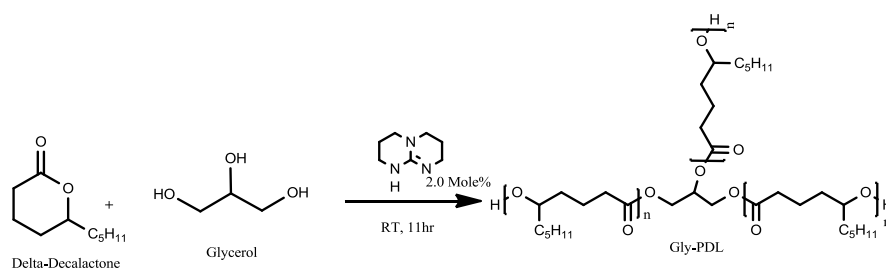
The synthetic route for synthesis of poly(decalactone) (PDL) homopolymer is shown in scheme 3-1. ROP of δ-decalactone was performed at either 5°C or at room temperature to generate homopolymers with end-terminal functionality. Conversion was monitored using ¹H NMR by integrating the peak at 4.3 ppm corresponding to the proton adjacent to the

cyclic ester in monomer (figure 3-1, position 1) and 4.9 ppm which corresponds to the proton adjacent to the ester bond in polymer (figure 3-3, position 8). Characterisation data was obtained after precipitating the quenched reaction mixture in cold methanol, which removed the unconverted monomer and inactive catalyst (figure 3-2).

(I)



(II)



Scheme 3-1 Ring opening polymerization of δ -decalactone catalysed by TBD using different initiators. (RT – room temperature)

The pure polymer was separated from methanol by centrifugation and any solvent residue was removed under vacuum. The obtained polymer of δ -decalactone was

amorphous and therefore no melting point was observed in DSC analysis, while T_g of the polymer was $\sim -54^\circ\text{C}$ (table 3-1, figure 3-4).

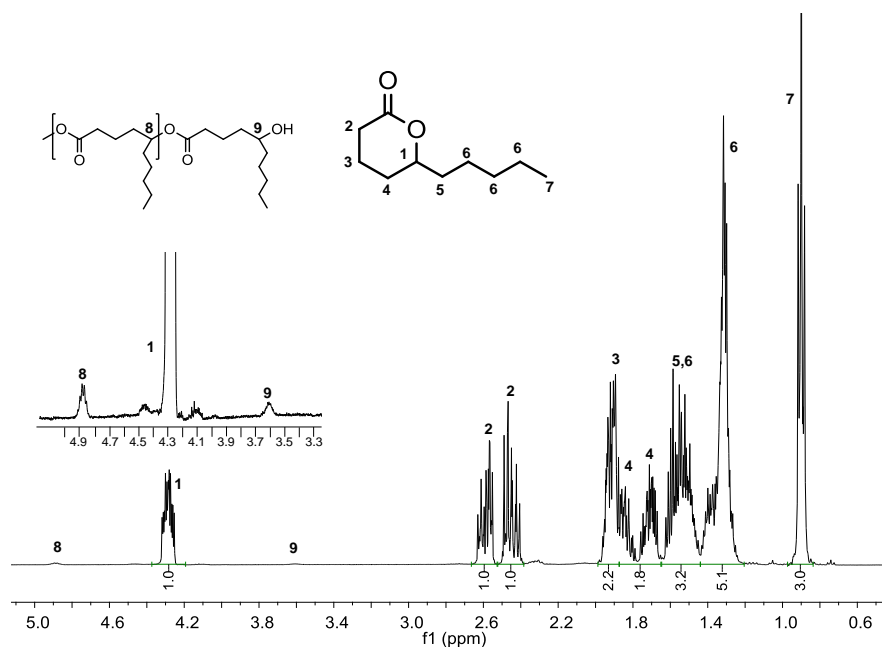


Figure 3-1 $^1\text{H NMR}$ of δ -decalactone acquired in CDCl_3 . Inset showing zoomed spectra between 3.3 and 5.0 ppm.

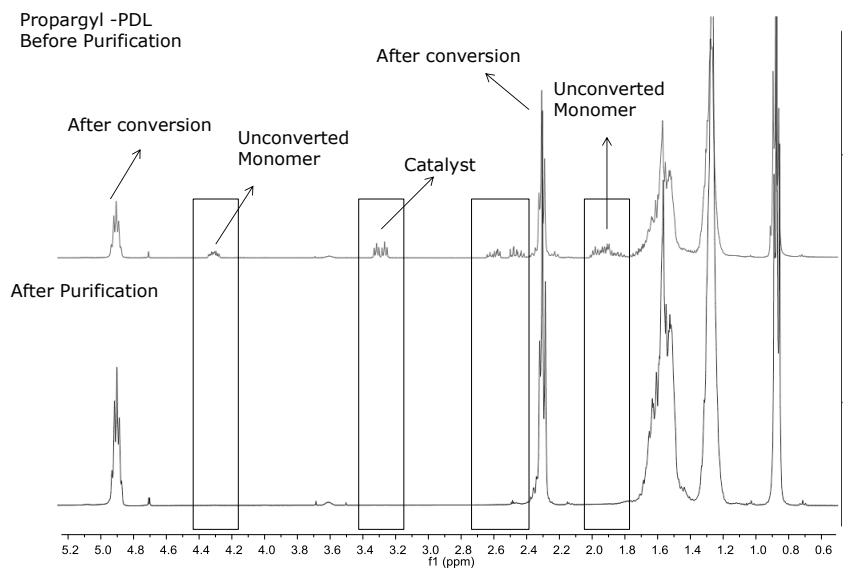


Figure 3-2 $^1\text{H NMR}$ spectra of propargyl PDL before and after purification of polymer. Purification was done by precipitating the quenched reaction mixture in cold methanol

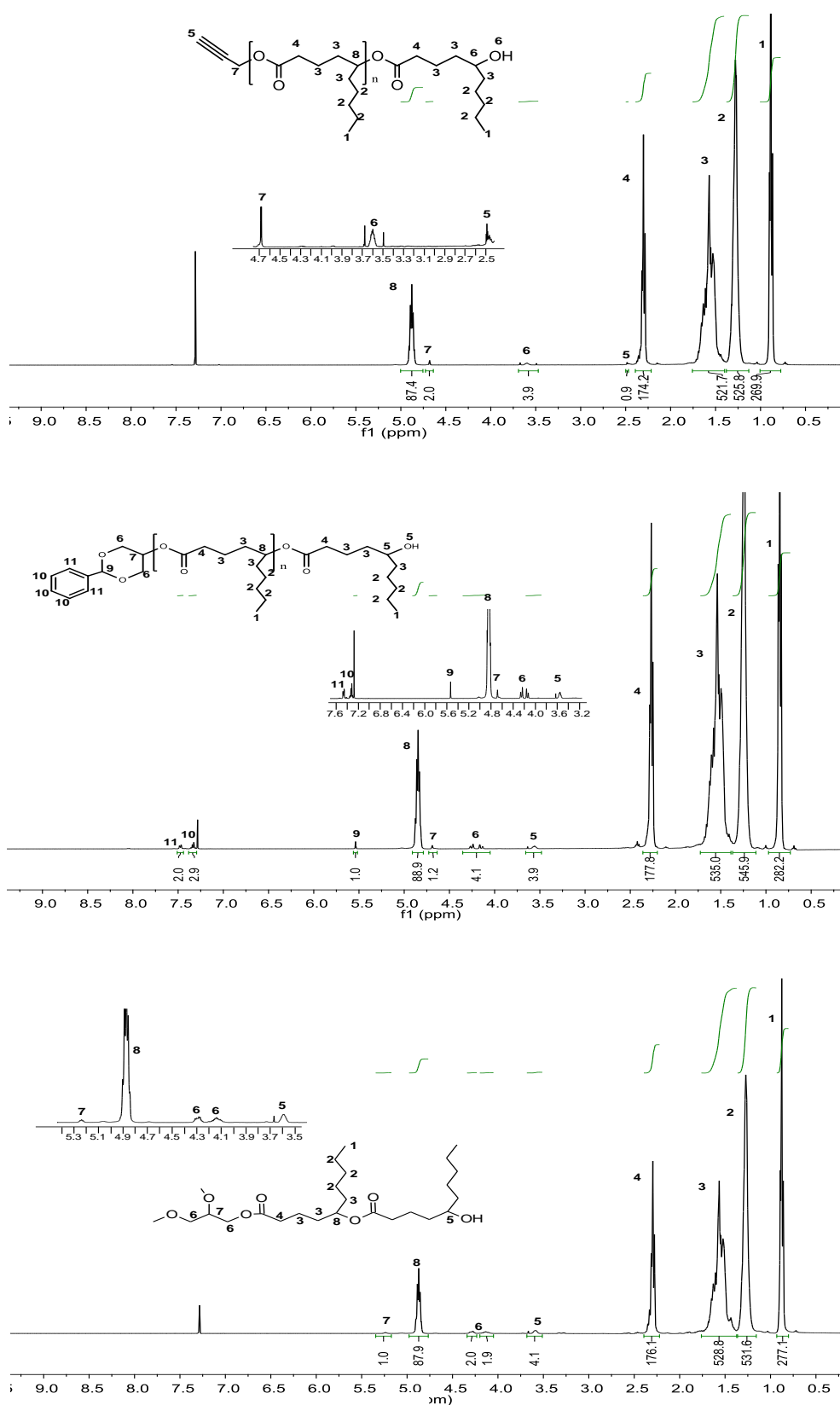


Figure 3-3 ^1H NMR spectra of propargyl-PDL, BZD-PDL and Gly-PDL acquired in CDCl_3 .

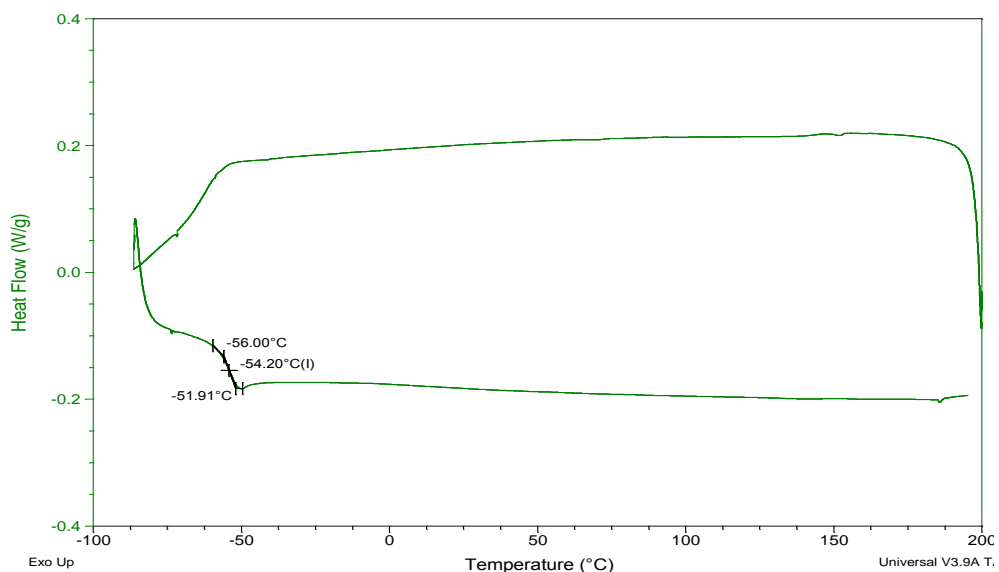


Figure 3-4 DSC plot of propargyl PDL. The presented trace was acquired from second cycle.

^1H NMR of the synthesised polymers with assigned peaks are shown in figure 3-3. Proton integration of peaks at 4.9 ppm and 4.67 ppm (for propargyl-PDL), or 5.52 and 4.68 ppm (for BZD-PDL) were used to calculate the molecular weight of polymer. Carbon NMR was also acquired to characterise the structure and to check the purity however; the peaks of carbons present in the initiators were not prominent compared to the signals of the carbons of PDL backbone (figure 3-5). The peak positions in NMR for poly(decalactone) were matched with the previously reported values suggesting the successful synthesis of polymer¹⁸.

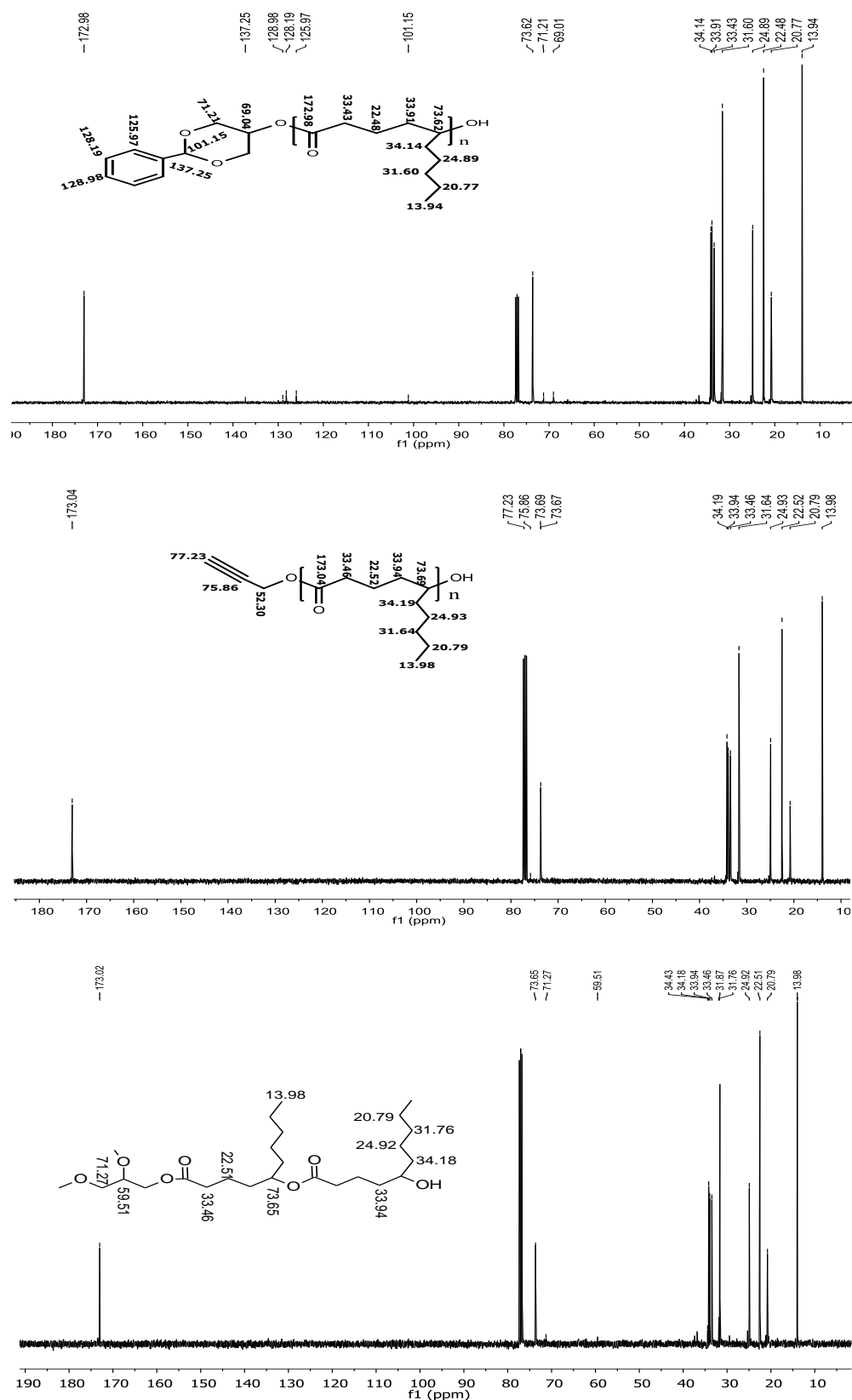


Figure 3-5 ^{13}C NMR of BZD-PDL, propargyl-PDL and Gly-PDL acquired in CDCl_3 .

Size exclusion chromatography (SEC) using chloroform as eluent and polystyrene as reference polymer gave a unimodal size distribution with narrow polydispersity for all polymers. However, the M_n observed by SEC was almost half compared to the molecular weight calculated by proton NMR (table 3-1, figure 3-6). Additionally, the integral of the end group proton resonance at 3.5 ppm in ^1H NMR was observed to be double that of the expected integrals. These data indicates either presence of an additional initiator or chain cleavage due to back biting (transesterification) obstructing the synthesis of polymer up to target molecular weight. However, SEC traces obtained (THF as eluent) using PMMA as reference polymer gave the M_n values, which matched with the calculated molecular weight by NMR (figure 3-7).

Syntheses of polymers were also tried in the presence of solvents (chloroform, toluene, and acetonitrile) in attempts to improve polymerisation control. However, it was found that TBD was not an effective catalyst while used in the above mentioned solvents for ROP of δ -decalactone. A decrease in the catalytic efficiency of TBD for the ROP of lactide in some solvents has also been reported earlier²².

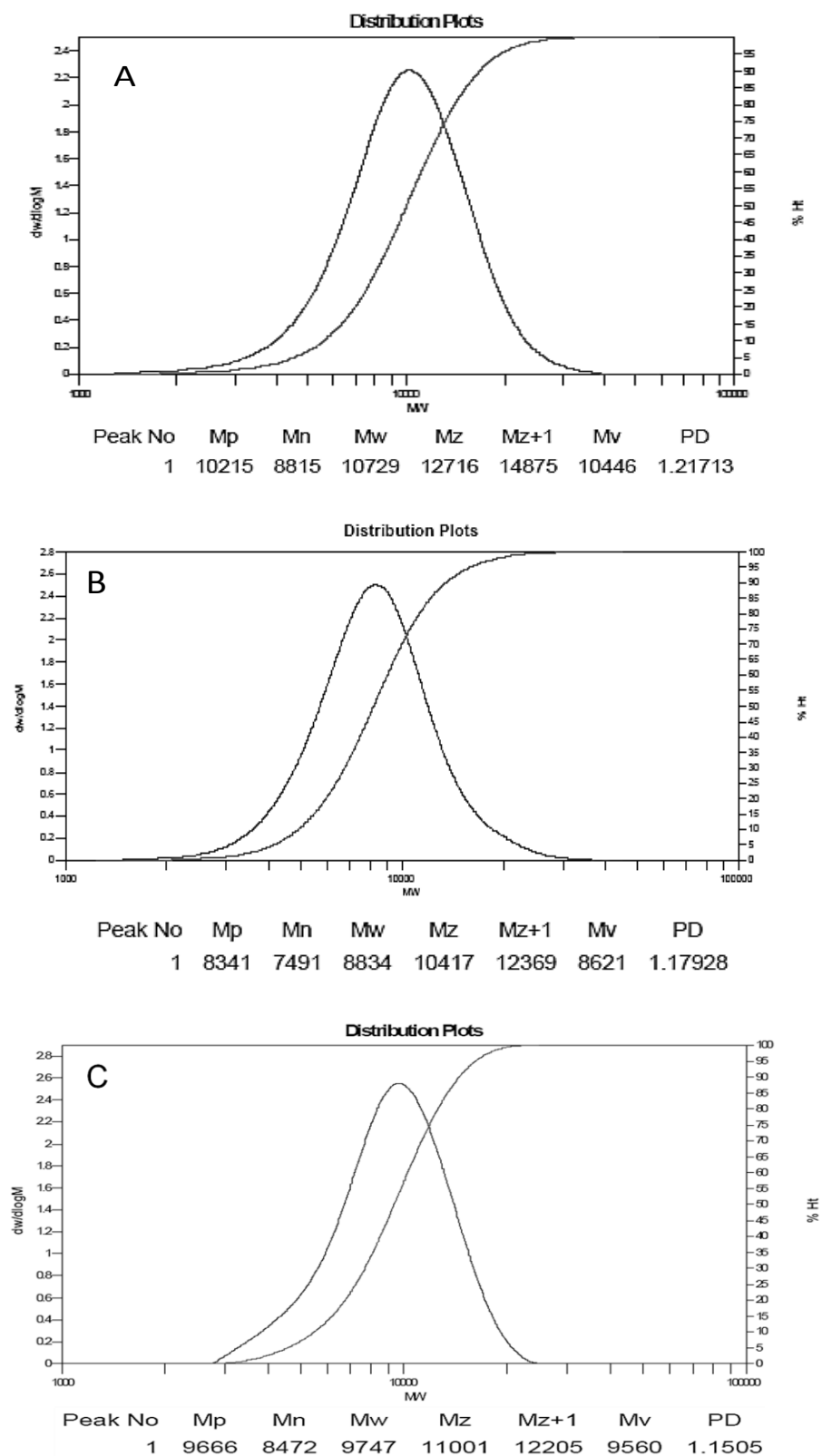


Figure 3-6 SEC traces of (A) BZD-PDL, (B) propargyl-PDL and (C) Gly-PDL, which were acquired using chloroform as eluent and molecular weight was calculated against polystyrene as internal standard.

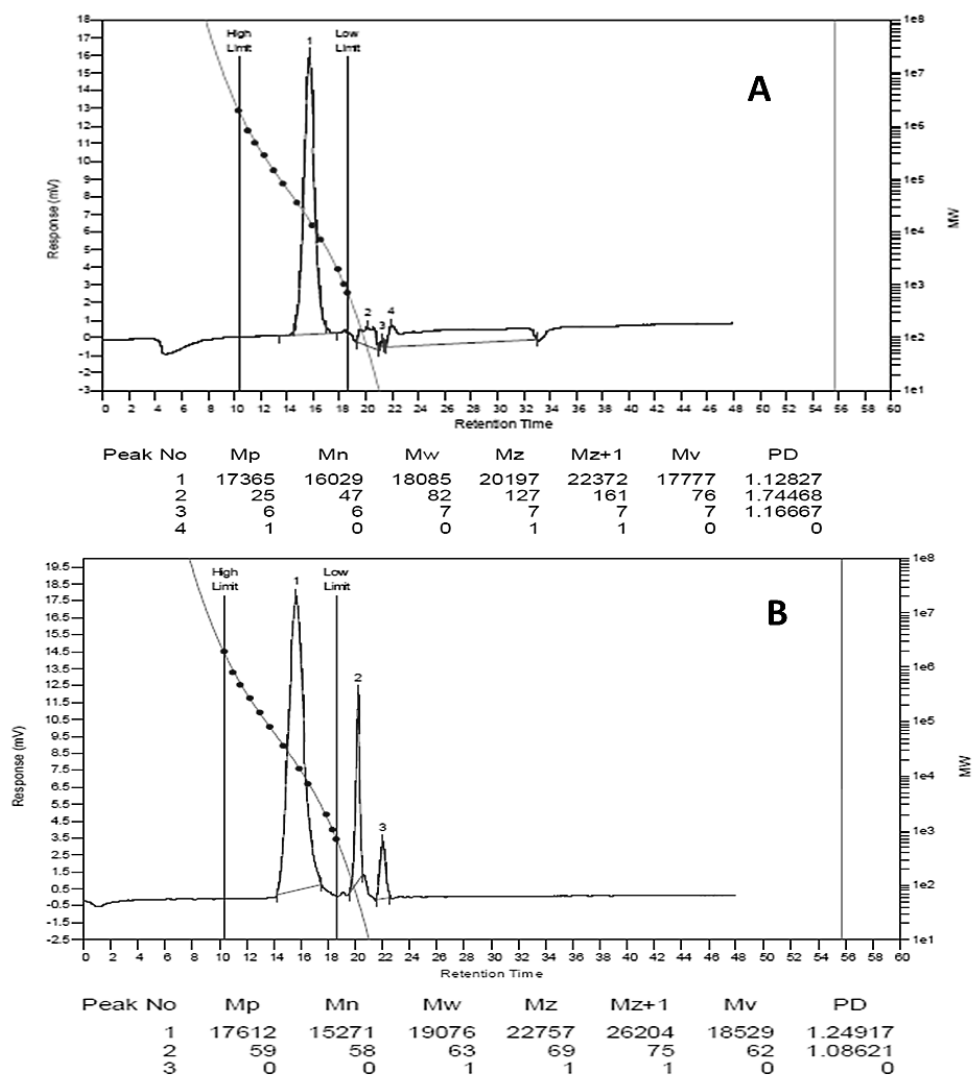


Figure 3-7 SEC traces of (A) BZD-PDL and (B) propargyl-PDL using THF as eluent. Molecular weight was calculated against PMMA as internal standard.

Run	Initiator	M/I ratio	Temp. (°C)	Time (hrs)	Catalyst (Mole%)	Conversion by NMR (%)	M_n by NMR (KDa)	M_n by SEC (Chloroform) (KDa)	M_w/M_n	T_g (°C)	T_m (°C)
1	Cis-1,3-O-Benzylidene Glycerol	100	5	11	2.5	89	15.3	8.8	1.21	ND	ND
2	Propargyl Alcohol	100	RT	11	2.5	87	14.8	7.5	1.18	-54.2	ND
3	Glycerol	100	RT	11	2.0	88	15.1	8.5	1.15	ND	ND
4	Poly(Ethylene Glycol)	150	40	8	2.5	89	10.3	16.2	1.15	-53.3	47.0
5	Poly(Ethylene Glycol) methyl ether	150	50	7	2.5	91	11.3	19.5	1.17	-54.6	54.6
6*	Poly(Ethylene Glycol) methyl ether	52	110	10 min	2.0	99	10.7	19.3	1.31	ND	ND
7 [§]	mPEG-b-PDL	12	70	3	10.0 (% wt)	98	12.9	21.8	1.25	-52.7	54.7, 88.0

Table 3-1 Summary of experimental details and molecular weight obtained after ROP of δ -decalactone, * ϵ -caprolactone and [§] ω -pentadecalactone. (ND- not determined, M/I - monomer/initiator, T_g - glass transition temperature, T_m - melting temperature).

3.3.2 Synthesis and Characterisation of Block Copolymers of δ -Decalactone

Block copolymers of δ -decalactone were synthesised at a temperature above the melting point of polyethylene glycol to avoid the use of added solvents in reaction (scheme 3-1). The target molecular weight of PDL chain for both copolymers was 5 KDa. It was observed that increases in the catalyst loading accelerate the conversion rate. Reaction kinetics was monitored by ^1H NMR and SEC, and the acquired data suggested that the reaction followed first order kinetics. No back-biting/transesterification reaction was observed regardless of the time and concentration of catalyst (up to 5 mol% to monomer) (figure 3-8, 3-9 and table 3-2). Onset of homopolymer formation was observed from the very beginning of the reaction (figure 3-8). These data suggested that the homo-polymerisation was because of a competing ROP initiated by an unknown initiator and not by a transesterification reaction (chain cleavage via backbiting during polymerisation).

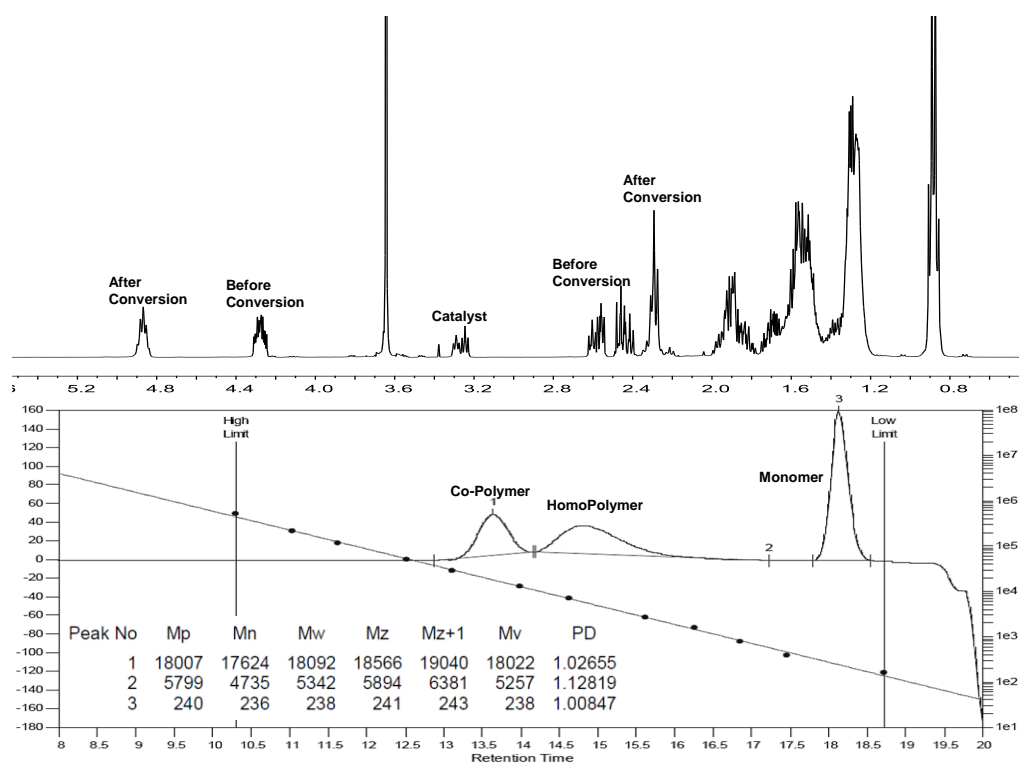


Figure 3-8 ^1H NMR spectrum and SEC trace of mPEG-b-PDL (during kinetic study) after 9 hrs containing 5% of TBD as catalyst. SEC trace was obtained using chloroform as eluent and polystyrene as internal standard whereas ^1H NMR was acquired in CDCl_3 .

Time	Conversion by NMR (%)	M_n by SEC	by PD Peak 1	M_n by SEC	by PD Peak 2
15 min	14.88	12596	1.02	1172	1.36
30 min	20.97	13700	1.02	1662	1.37
1 hr	34.78	15214	1.02	2814	1.23
1.5 hr	45.02	15847	1.02	3312	1.21
2 hr	52.28	16384	1.02	3878	1.16
3 hr	61.60	17232	1.02	4451	1.14
4 hr	68.60	17315	1.02	4576	1.13
5.5 hr	69.77	17647	1.02	4659	1.13
9hr	69.84	17624	1.02	4735	1.12

Table 3-2 Data obtained from the kinetic study of mPEG-b-PDL synthesis. As shown in figure 3-8, peak 1 and 2 are corresponds to copolymer and homopolymer respectively. SEC traces were obtained using chloroform as eluent and polystyrene as internal standard (PD – Polydispersity).

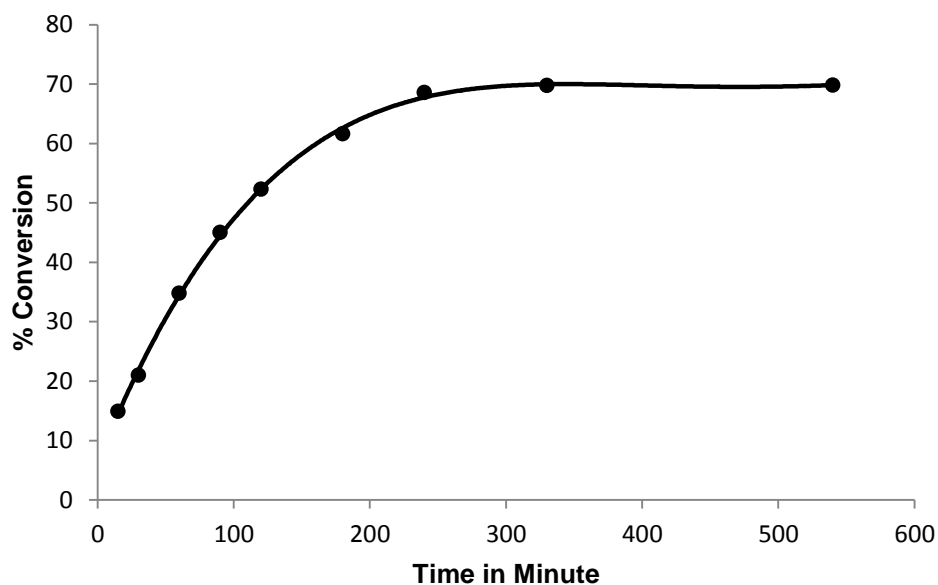


Figure 3-9 Reaction kinetics for ROP of δ -decalactone using mPEG as initiator and TBD (5 mole%) as catalyst. Maximum 70% conversion was observed in this reaction.

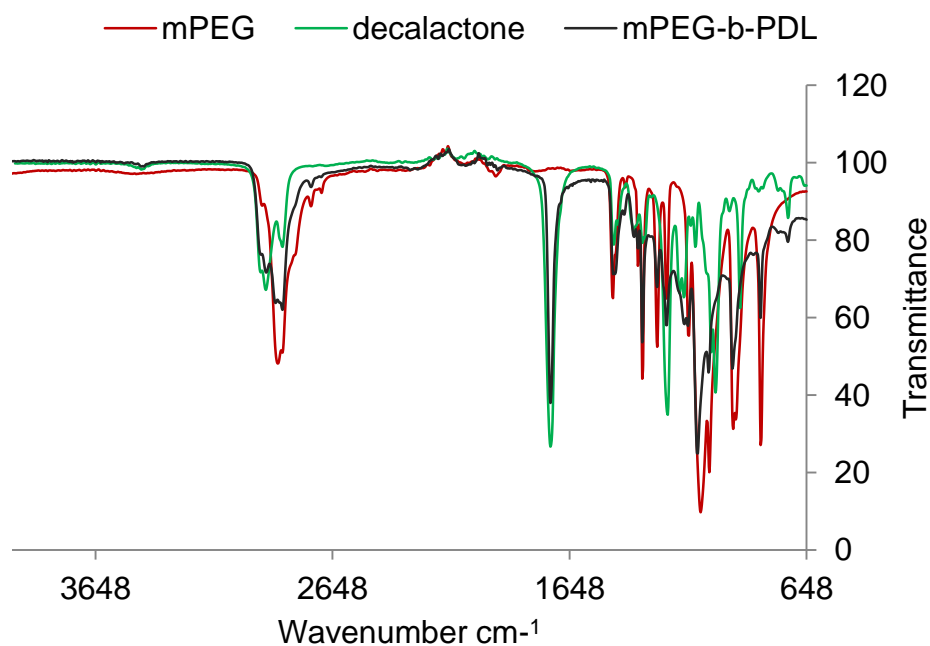


Figure 3-10 Overlapped FTIR spectra of mPEG, δ -decalactone and mPEG-b-PDL copolymer.

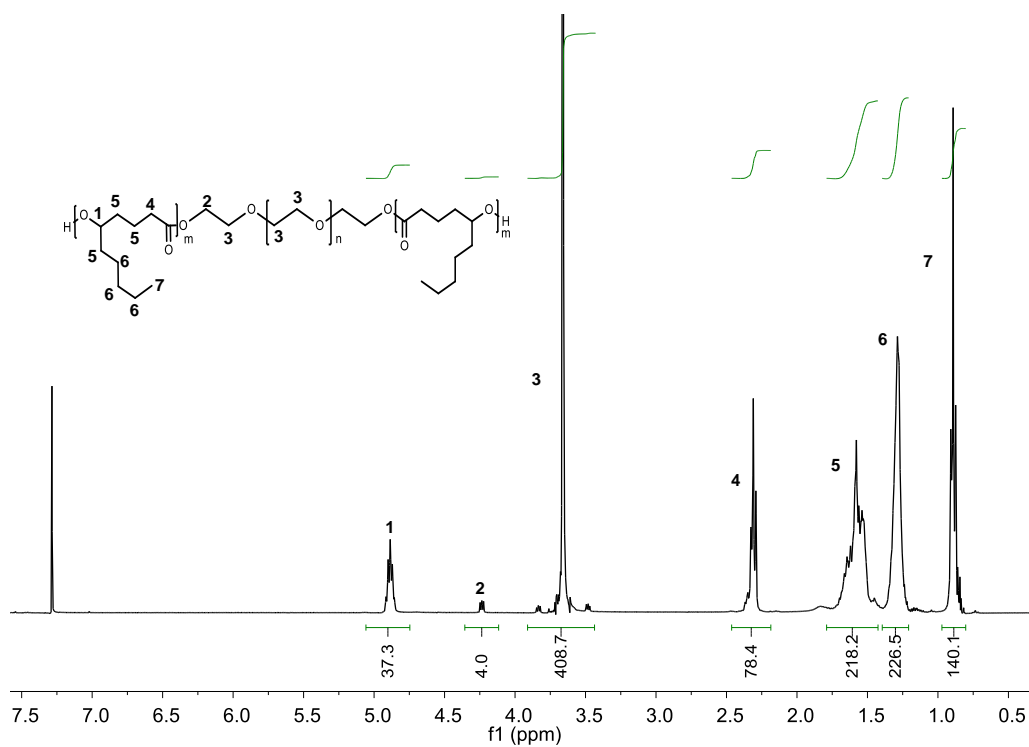
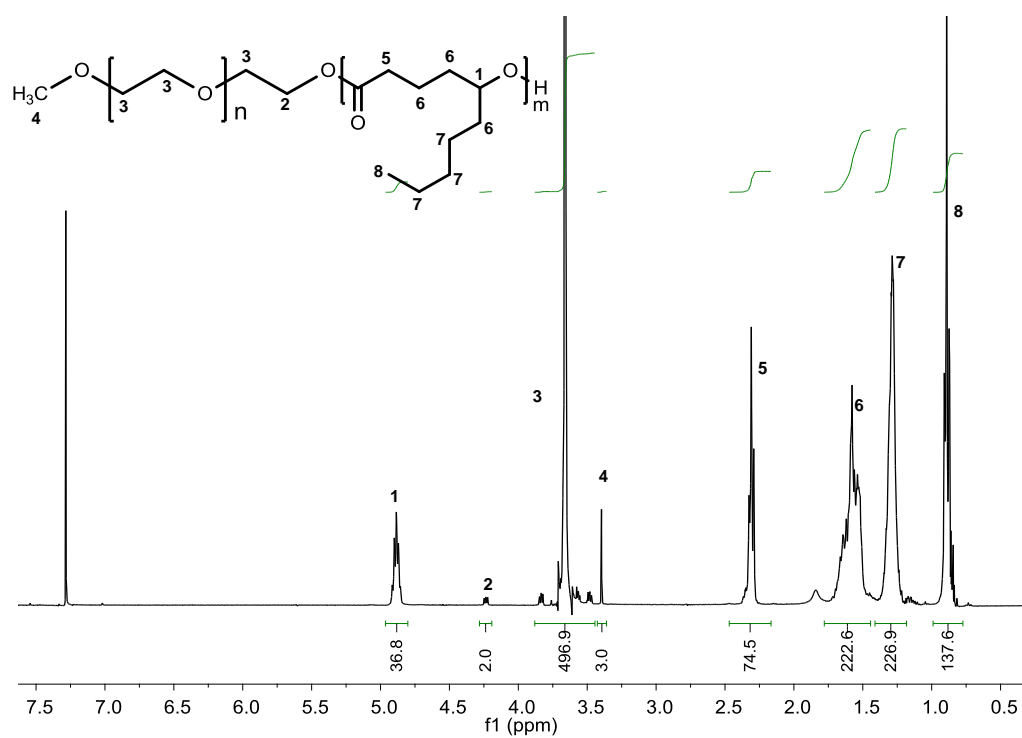


Figure 3-11 $^1\text{H NMR}$ of mPEG-b-PDL and PDL-b-PEG-b-PDL copolymer acquired in CDCl_3

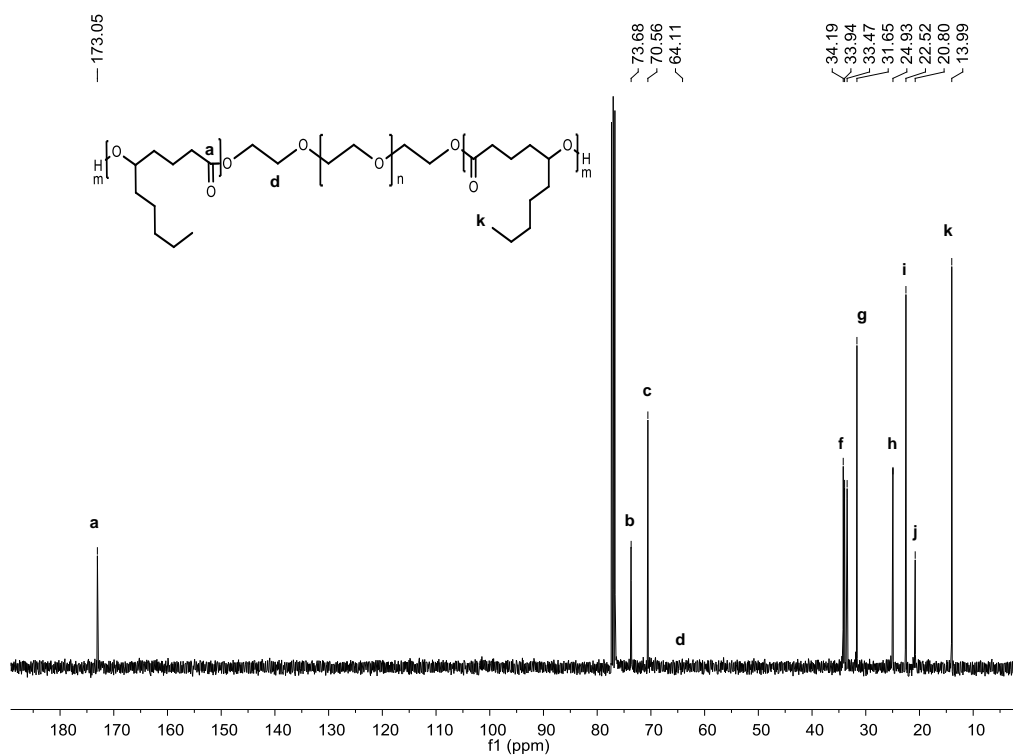
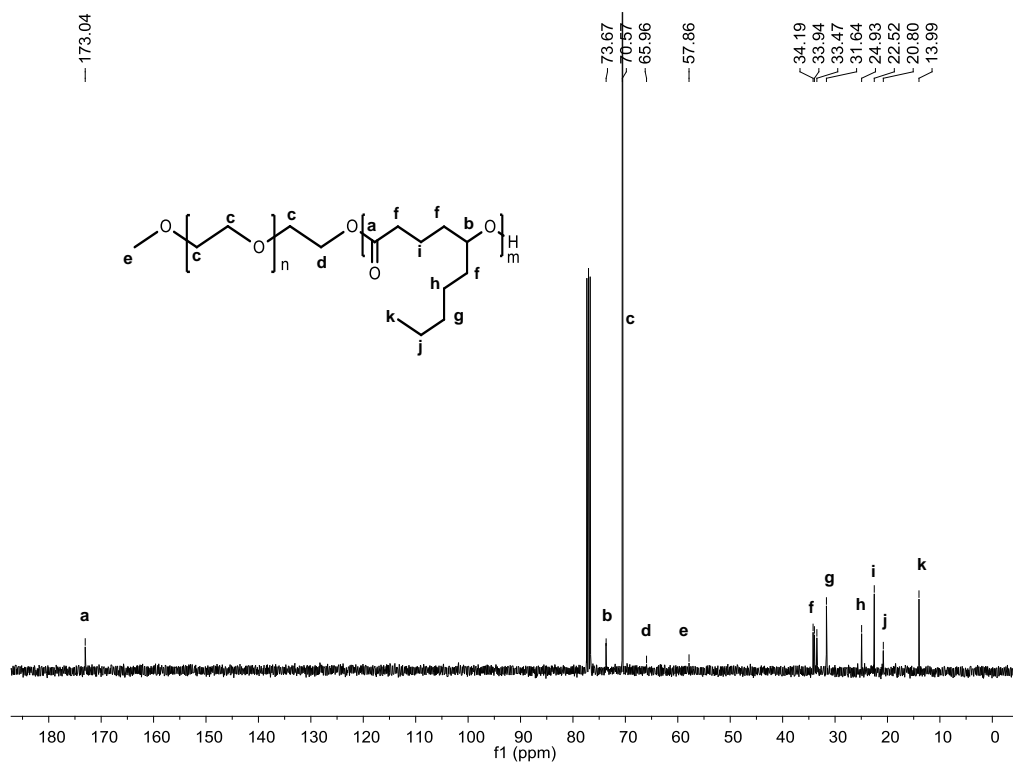


Figure 3-12 Carbon¹³ NMR of mPEG-b-PDL and PDL-b-PEG-b-PDL copolymer acquired in CDCl₃.

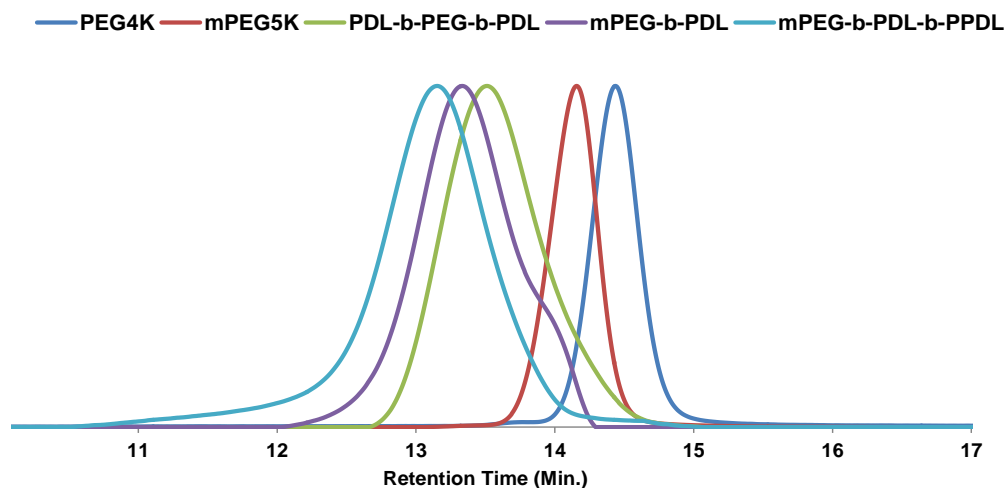


Figure 3-13 SEC traces of initiators and different block copolymers of δ -decalactone, which were obtained using chloroform as eluent and polystyrene as internal standard.

The PDL homopolymer was separated from block copolymers by washing the reaction mixture with excess of petroleum ether (2-3 times). PDL is freely soluble in petroleum ether whereas PEG is insoluble, and hence PDL block copolymers were precipitated leaving homopolymer PDL in ether. FTIR, ^1H NMR and ^{13}C NMR of the synthesised block copolymers with assigned peaks are shown in figure 3-10, 3-11 and 3-12. Molecular weights were calculated through ^1H NMR by comparing the number of protons adjacent to the PDL ester link at 4.9 ppm with respect to protons of initiator (PEG) at 3.6 (3.3 ppm with mPEG) and the protons adjacent to the ester bond created after ring opening of decalactone by PEG-OH at 4.2 ppm.

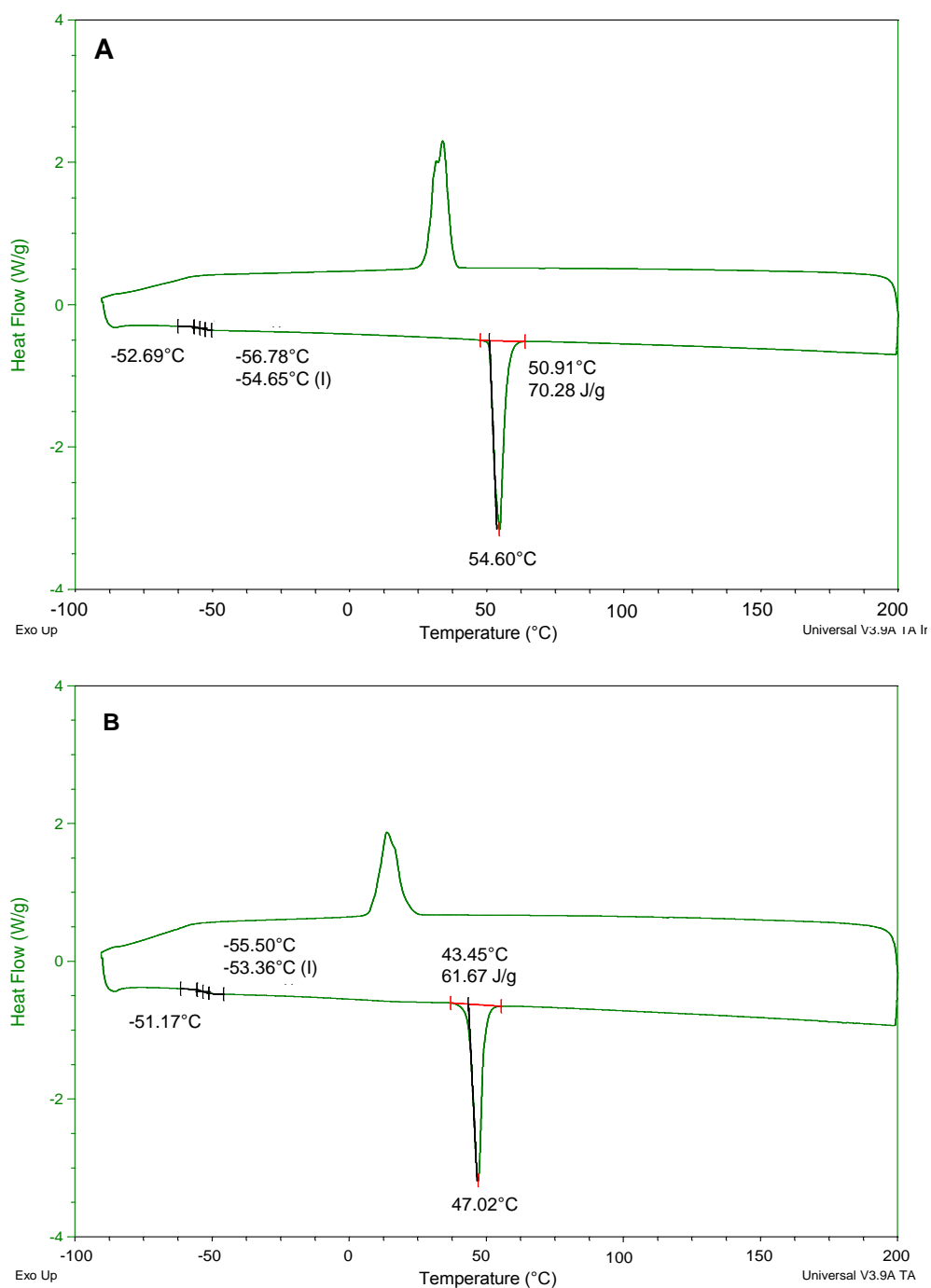
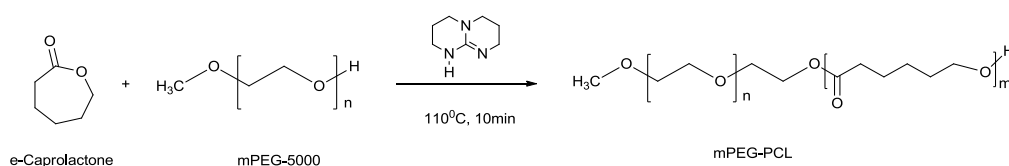


Figure 3-14 DSC plot of (A) mPEG-b-PDL and (B) PDL-b-PEG-b-PDL, obtained from second cycle.

Both copolymer showed unimodal distribution in SEC traces however, tailing was detected for mPEG-b-PDL (figure 3-13), which might be due to the presence of some free mPEG. Number average molecular weight (M_n) determined by SEC for

copolymers were almost twice those of the molecular weight calculated by ^1H NMR (table 3-1). Synthesised copolymers were also characterised by DSC to determine the change in thermal properties. The block copolymers showed the melting points corresponding to PEG, as well as a low glass transition temperatures (T_g) attributed to amorphous PDL, thus suggesting the formation of a semicrystalline polymer (figure 3-14). The number average molecular weight (M_n) by SEC, molecular weight by NMR, T_g , melting temperature (T_m) and other experimental details are summarised in table 3-1. The molecular weight calculated by ^1H NMR was used for the calculations in further experiments.

3.3.3 Synthesis and Characterisation of block Copolymer of ϵ -Caprolactone



Scheme 3-2 Ring opening polymerization of ϵ -caprolactone using TBD as catalyst

The synthetic route to produce poly(caprolactone) is shown in scheme 3-2. Approximately 99% of monomer was converted to polymer in 10 minutes of reaction time at 110°C . The target molecular weight for mPEG-b-PCL was aimed to be similar to the mPEG-b-PDL (*i.e.* 10 KDa), in order to carry out the

appropriate comparison of this copolymer with novel block copolymers of δ -decalactone.

mPEG-b-PCL was characterised by NMR and by SEC to check the purity of obtained polymer and to determine the molecular weight (figure 3-15,3-16). Molecular weight was calculated by ^1H NMR through the integral of the protons of initiator, protons adjacent to the caprolactone ester bond and the protons adjacent to the ester bond created after ring opening of caprolactone by PEG-OH at 3.4, 4.0 and 4.2 ppm respectively. The peak positions in NMR were matched with the previously reported values¹⁷. The obtained characterisation results are reported in table 3-1. The characterisation data suggested the successful synthesis of pure mPEG-b-PCL copolymer having an approximate molecular weight of 10 KDa.

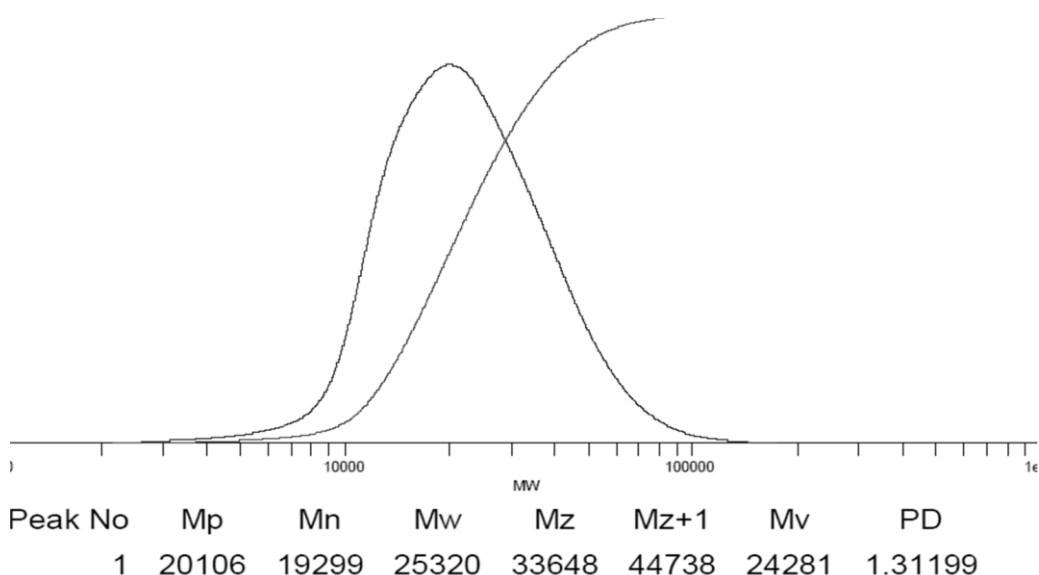


Figure 3-15 SEC trace of mPEG-b-PCL obtained using chloroform as eluent and polystyrene as internal standard.

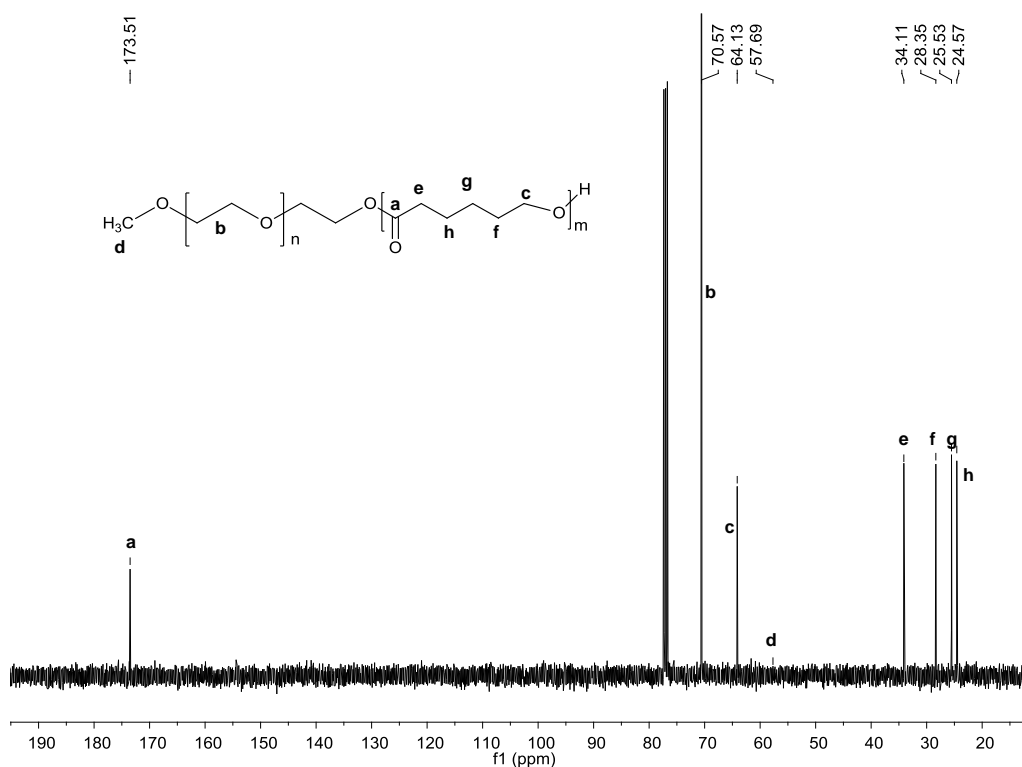
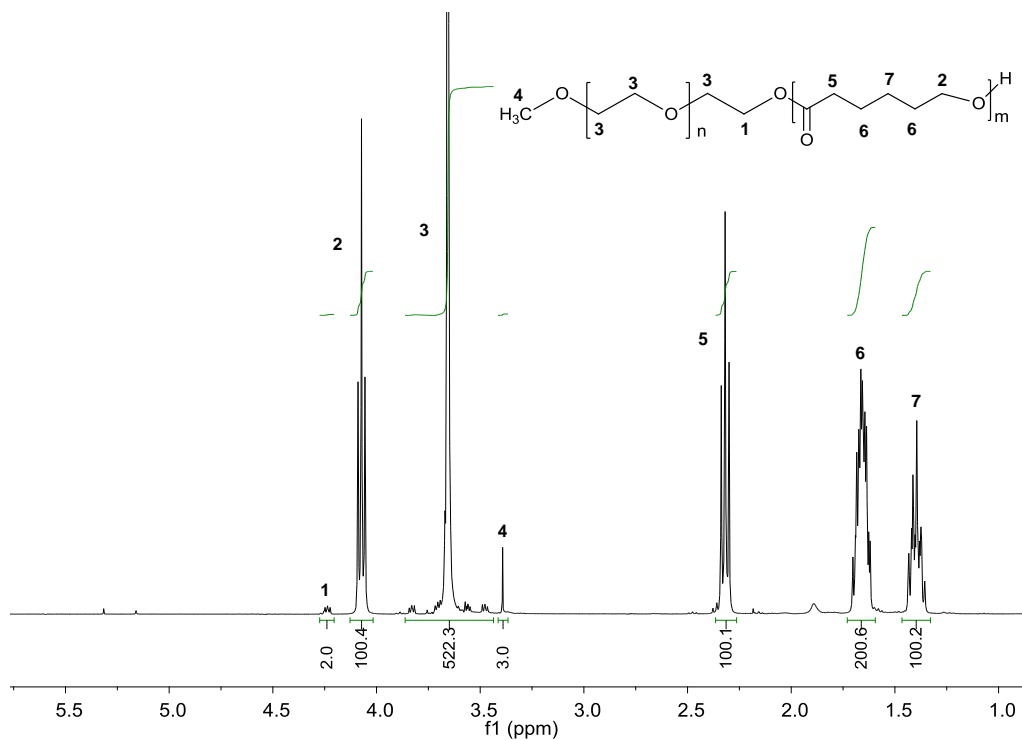
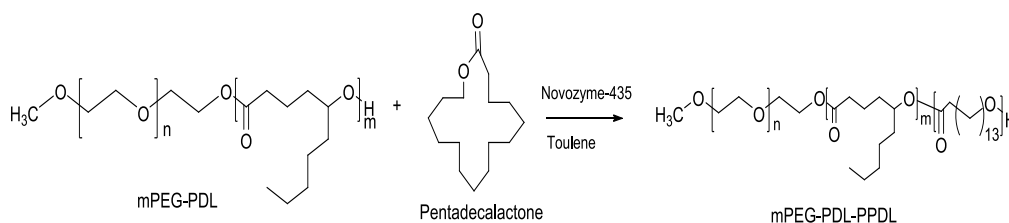


Figure 3-16 $^1\text{H NMR}$ and $^{13}\text{C NMR}$ of mPEG-b-PCL in chloroform-d.

3.3.4 Synthesis and Characterisation of block Copolymer of ω -Pentadecalactone

The synthesis of block copolymers of ω -pentadecalactone using mPEG-b-PDL as initiator was performed by following a reported method³¹ (scheme 3-3). Novozyme 435 is a well-established catalyst for the ring opening polymerization of ω -pentadecalactone and hence gave successful conversion of monomer to polymer in this study³². Reaction was performed in anhydrous toluene at 70°C, which resulted in 98% conversion of monomer to polymer in 3 hrs. The reaction was conducted in an inert atmosphere to avoid any initiation from water. The conversion of monomer to copolymer (mPEG-b-PDL-b-PPDL) was monitored by ¹HNMR in which, appearance of at 4.08 ppm suggested the ring opening polymerisation of ω -pentadecalactone. No change in peak positions of mPEG-b-PDL in ¹HNMR spectrum was observed after addition of PPDL block.



Scheme 3-3 Ring opening polymerization of ω -pentadecalactone using lipase as catalyst

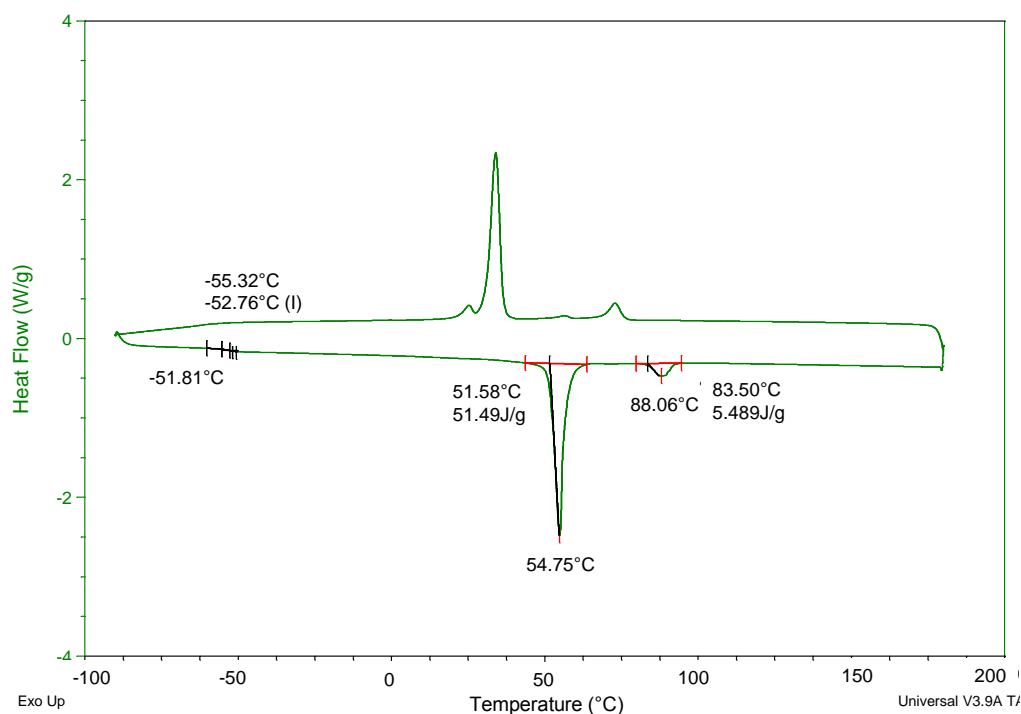


Figure 3-18 DSC plot of mPEG-b-PDL-b-PPDL, which was obtained from second cycle.

The physical state of polymer was changed from a waxy material (mPEG-b-PDL) to a sticky solid (mPEG-b-PDL-b-PPDL) after incorporation of the poly(pentadecalactone) block. The ^1H NMR of copolymer was obtained in chloroform-d and the peaks positions of PPDL block were matched with the previously reported results³² (figure 3-17). Integrals of methylene protons in ^1H NMR at 4.0, 4.8 and 3.3 ppm were used to calculate the experimental molecular weight of copolymer, which was 12.9 KDa whereas M_n obtained by SEC was 21.8 KDa with M_w/M_n (PDI) of 1.25 (table 3-1, figure 3-13).

This block copolymer was further characterized by ^{13}C NMR and DSC to confirm the structure and to determine the effect on thermal properties due to the presence of poly(penta decalactone) (PPDL) block. Peak positions of the PPDL block in ^{13}C NMR spectra were also matched with the reported values³² (figure 3-17). The T_g of mPEG-b-PDL-b-PPDL copolymer did not change when compared to mPEG-b-PDL however the graph showed two distinct melting peaks which corresponded to the individual PEG and PPDL blocks (figure 3-18). The melting temperature observed for the PPDL block was $\sim 88^\circ\text{C}$ after polymerisation with mPEG-b-PDL while the T_g of this block (PPDL) was not detectable by DSC²⁷. Characterisation data obtained for this copolymer confirmed the successful synthesis and purification of the desired triblock copolymer (ABC type).

3.4 Discussion

Synthesis of homopolymers and copolymers of δ -decalactone were performed under mild conditions using a procedure reported by Martello *et. al.* with slight modification in order to develop a green synthesis approach. In contrast to the synthesis procedure reported by Martello *et. al.*, any conversion of monomer to polymer was not observed using catalyst quantities less than 1.5 mol% to the monomer.

Though, it was observed that reactions at low temperature gave higher conversion and no further reaction occurred after a certain conversion (maximum 91% after which thermodynamic equilibrium was achieved). This latter result was analogous to those reported by Martello *et. al*¹⁸.

Poly(decylactone) homopolymers were prepared to understand the difference in physicochemical properties compared to copolymers of PDL. During the synthesis of copolymers of δ -decylactone, the formation of poly(decylactone) homopolymer suggested the presence of an initiator additional to the added PEG or alcohol in reaction mixture. The most probable reasons that can be associated with the additional polymer synthesis are:

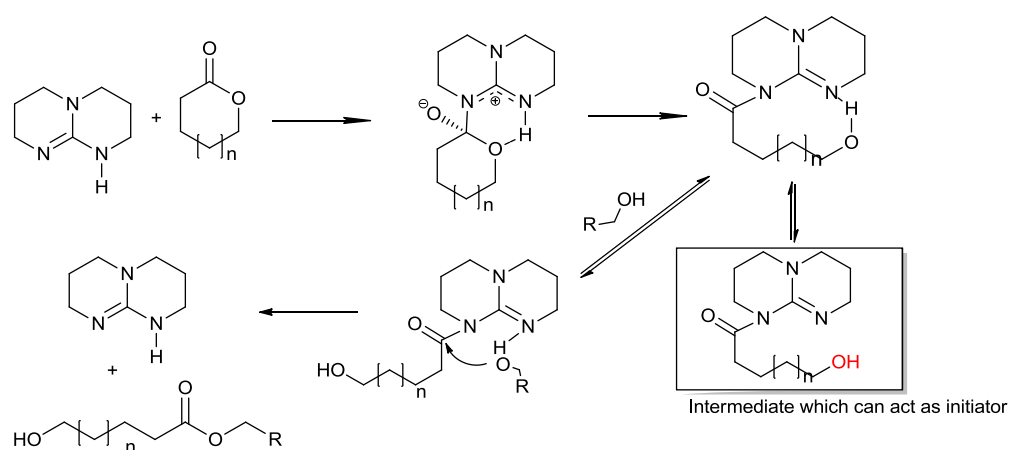
1. Impurities present in the commercial available monomer.

The purity of δ -decylactone was checked by ¹HNMR and a peak at 3.5 ppm in spectrum suggested the existence of open form of the lactone ring with hydroxyl end group (figure 3-1 inset). This hydroxyl group could have acted as initiator, which could not be separated during the purification procedure for the monomer.

2. Traces of water present. It may have been that the starting materials were not dried completely during the drying

procedure and hence residual water could have acted as initiator.

3. Mechanism of TBD for ROP proposed by Pratt *et al.*²². There is a reversible step in which an alcohol group is generated (shown in red in scheme 3-4) which can potentially act as initiator for other molecules activated by TBD. Jaffredo *et al.* used TBD as catalyst as well as initiator for the ROP of β -butyrolactone³³ suggested that TBD has potential to act as a initiator.



Scheme 3-4 Ring opening mechanism of TBD suggested by Pratt *et al.*²²

Fortunately, the difference in solubility of co-polymers and homo-polymers in ether offered a route to separate the desired co-polymer from the homopolymer impurity. Due to the formation of undesired homopolymer during synthesis, the target molecular weight would not achieve based on degree of polymerisation. Representative molecular weight determination using ¹HNMR was only feasible with pure

copolymers because of the absence of undesired homopolymer in samples. In case of propargyl-PDL, BZD-PDL and GLY-PDL, M_n observed by SEC was considered as the molecular weight of polymer which half to the molecular weight calculated by $^1\text{HNMR}$. In contrast, M_n detected by SEC for copolymers were almost twice to the molecular weight calculated by $^1\text{HNMR}$. This may have been because of the interaction of PEG with SEC column (PLgel Mixed-D). The M_n of PEG itself detected by SEC was almost twice the molecular weight reported by supplier (PEG4000 M_n -7.7 KDa, mPEG5000 M_n - 10.8 KDa).

The main objective of the project is to synthesise the amphiphilic block copolymers of δ -decalactone and to evaluate their ability as drug delivery carriers. Therefore, an extensive study of the chemistry behind the polymer formation from additional initiator was not pursued. Other catalysts such as stannous octanoate and scandium triflate were also investigated for ROP of δ -decalactone. Nevertheless, TBD was proved to be the most effective catalyst for the ROP of δ -decalactone. All the obtained characterisation data suggested the successful synthesis and purification of block copolymers of δ -decalactone.

TBD was reported as a very efficient catalyst for the ROP of ϵ -caprolactone¹⁷ and therefore it was used for the synthesis of

copolymer of ϵ -caprolactone. Compared to the ROP of δ -decalactone, no polymer synthesis from additional initiator was observed during ROP of ϵ -caprolactone with TBD as catalyst. This finding suggested that the impurity present in the monomer δ -decalactone could be the probable initiator which caused the formation of the homopolymer of Poly(decalactone) during copolymer synthesis.

After the successful synthesis of copolymers of δ -decalactone and ϵ -caprolactone, ROP of ω -pentadecalactone was investigated. The solubility of poly(pentadecalactone) (PPDL) in organic solvents (especially non-chlorinated) has been considered as a major issue limiting its applicability in drug delivery. Hence, the aim was to make a copolymer of pentadecalactone, which would be soluble in acetone and other similar solvents preferable in pharmaceutical industries³⁴. To do this, ROP of ω -pentadecalactone using mPEG-b-PDL as initiator was tried with TBD (1 mole% to monomer) at 110°C in bulk¹⁷. During the reaction it was found that at higher temperature the chain of mPEG-b-PDL was cleaved and the ring of decalactone was regenerated as detected by ¹HNMR (figure 3-19). Based on this result it was concluded that TBD was not a good catalyst in the selected conditions for copolymer synthesis. The depolymerisation

(reversible) process observed with poly(δ -decalactone) could be associated with the thermodynamic equilibrium of δ -decalactone with TBD at high temperature¹⁸.

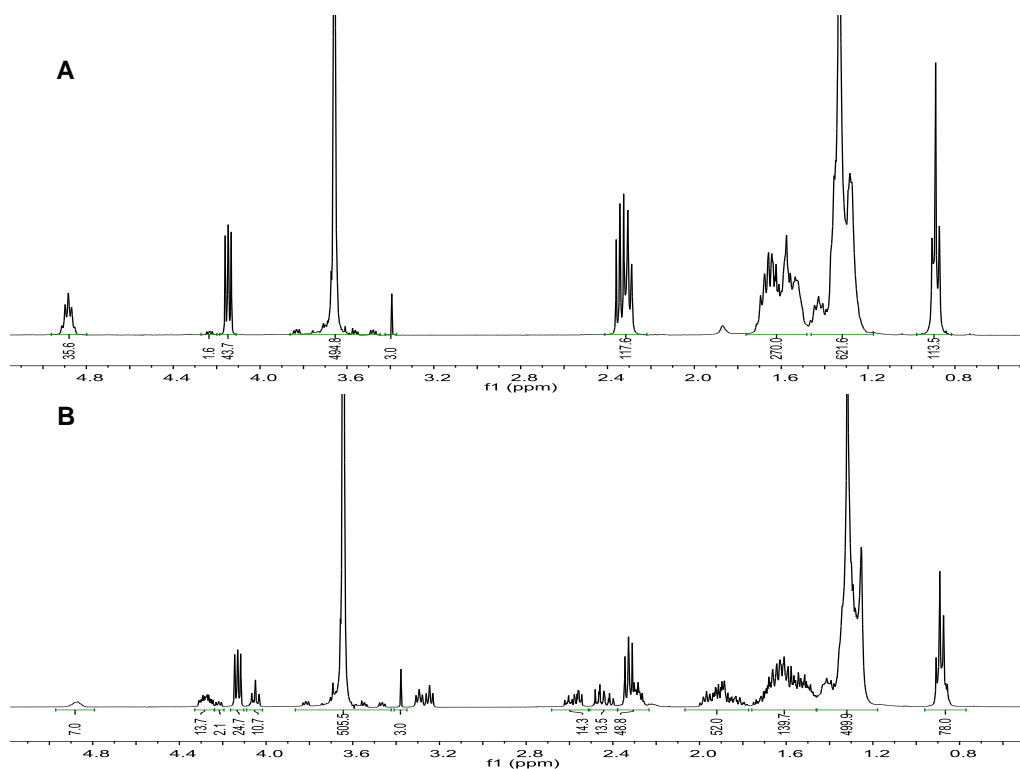


Figure 3-19 ¹H NMR spectra of (A) at 0 hr and (B) after conversion of the reaction mixture obtained during the attempt of ROP of ω -pentadecalactone using TBD as catalyst and mPEG-b-PDL as initiator.

Tin (II) trifluoromethanesulfonate was another catalyst tried (1 mole% to monomer) for copolymer synthesis but no conversion was observed at 110°C. Stannous octanoate as catalyst (1 mole% to monomer) was also investigated for the same but only 10-15% of conversion (by ¹H NMR) was observed in 2 days. Finally, the use of lipase as catalyst gave the desired product without any side reactions.

The molecular weight of poly(pentadecalactone) block was varied in attempt to modulate solubility of the final copolymer in acetone. It was found that increasing in the PPDL block molecular weight above 2 KDa in the mPEG-b-PDL-b-PPDL copolymer reduced its solubility in acetone. Therefore, a PPDL block of less than 2 KDa molecular weight was targeted to synthesise the subsequent copolymer. This copolymer was also characterised by NMR, SEC and DSC however, the synthesis confirmation of such triblock copolymer with NMR alone is difficult. Absence of substantial change in peak positions of poly(pentadecalactone) block after copolymerisation in NMR spectrum reduce the efficiency of this technique as a tool of synthesis confirmation. A physical mixture of mPEG-b-PDL and PPDL could generate a similar spectrum. Therefore, the synthesis confirmation is mainly relying on SEC and a clear shift in SEC trace of mPEG-b-PDL-b-PPDL compared to mPEG-b-PDL confirmed the synthesis of desired copolymer. It was expected that the incorporation of crystalline block (PPDL) to mPEG-b-PDL could have increased the crystallinity of mPEG-b-PDL. However, the determination of exact change in percent crystallinity was not possible since two melting temperatures were observed.

3.5 Conclusion

In this chapter, successful synthesis of homopolymers and novel block copolymers based on renewable monomers *via* ROP using organic (TBD) and enzyme (Novozymes-435) catalysts has been reported. Small molecule initiators such as propargyl alcohol, *cis*-1,3-O-benzylidenediglycerol were successfully initiated the polymerisation of δ -decalactone at room temperature in the absence of solvents. However, it was observed that polymers could also be obtained without using an added alcohol initiator under certain circumstances. The reason for this unexpected polymerisation was not fully investigated owing to time constraint.

Block copolymers (mPEG-*b*-PDL and PDL-*b*-PEG-*b*-PDL) were synthesised at temperature above the melting point of PEG to avoid the use of solvents. All block copolymers were successfully separated from homopolymer contamination by washing them with ether. Characterisation data of the resultant purified polymers were established by FTIR, NMR, SEC and DSC. The acquired data suggested the successful synthesis and purification of the desired products. Copolymers of PEG with PDL displayed both T_m and T_g in thermal analysis, indicated the presence of both crystalline and amorphous regions. A diblock copolymer (*i.e.* mPEG-*b*-PCL) of

poly(caprolactone) of similar molecular weight was also synthesised using TBD as catalyst and characterised fully. This copolymer will be used as a standard for comparison in future formulation studies.

Novozymes-435 was found to be an effective catalyst for the ROP of ω -pentadecalactone to generate an ABC type of triblock copolymer (mPEG-b-PDL-b-PPDL). It was observed that increases in the molecular weight of poly(pentadecalactone) block above 2 kDa decreased the solubility of the resultant copolymer in acetone. The polydispersity index detected by SEC for all synthesised novel block copolymers was found to be less than 1.3.

The synthesis of polymers and copolymers of δ -decalactone was performed using organic catalysts under mild conditions without using any solvents except in the case of copolymerisation of ω -pentadecalactone. The investigated procedure for the synthesis of novel amphiphilic copolymers of δ -decalactone can thus be considered as a more sustainable and less environmentally-costly method compared to the standard routes to synthesise amphiphilic block copolymers.

3.6 References

1. Edlund, U.; Albertsson, A. C., *Advanced Drug Delivery Reviews* **2003**, *55* (4), 585-609.
2. Dechy-Cabaret, O.; Martin-Vaca, B.; Bourissou, D., *Chemical Reviews* **2004**, *104* (12), 6147-6176; Tsuji, H., *Macromolecular Bioscience* **2005**, *5* (7), 569-597; Avgoustakis, K., *Current Drug Delivery* **2004**, *1* (4), 321-333.
3. Labet, M.; Thielemans, W., *Chemical Society Reviews* **2009**, *38* (12), 3484-3504; Wei, X.; Gong, C.; Gou, M.; Fu, S.; Guo, Q.; Shi, S.; Luo, F.; Guo, G.; Qiu, L.; Qian, Z., *International Journal of Pharmaceutics* **2009**, *381* (1), 1-18.
4. Woodruff, M. A.; Hutmacher, D. W., *Progress in Polymer Science* **2010**, *35* (10), 1217-1256.
5. Lam, C. X. F.; Hutmacher, D. W.; Schantz, J.-T.; Woodruff, M. A.; Teoh, S. H., *Journal of Biomedical Materials Research Part A* **2009**, *90A* (3), 906-919.
6. Kang, J. C.; Schwendeman, S. P., *Biomaterials* **2002**, *23* (1), 239-245.
7. Meyer, F.; Wardale, J.; Best, S.; Cameron, R.; Rushton, N.; Brooks, R., *Journal of Orthopaedic Research* **2012**, *30* (6), 864-871.
8. Yin, M.; Baker, G. L., *Macromolecules* **1999**, *32* (23), 7711-7718; Trimaille, T.; Moller, M.; Gurny, R., *Journal of Polymer Science Part a-Polymer Chemistry* **2004**, *42* (17), 4379-4391.
9. Trimaille, T.; Mondon, K.; Gurny, R.; Moeller, M., *International Journal of Pharmaceutics* **2006**, *319* (1-2), 147-154.
10. Adams, T. B.; Greer, D. B.; Doull, J.; Munro, I. C.; Newberne, P.; Portoghese, P. S.; Smith, R. L.; Wagner, B. M.; Weil, C. S.; Woods, L. A.; Ford, R. A., *Food and Chemical Toxicology* **1998**, *36* (4), 249-278.
11. Rali, T.; Wossa, S. W.; Leach, D. N., *Molecules* **2007**, *12* (2), 149-154.
12. Bachhav, Y. G.; Mondon, K.; Kalia, Y. N.; Gurny, R.; Moeller, M., *Journal of Controlled Release* **2011**, *153* (2), 126-132.
13. Dong, H.; Cao, S. G.; Li, Z. Q.; Han, S. P.; You, D. L.; Shen, J. C., *Journal of Polymer Science Part a-Polymer Chemistry* **1999**, *37* (9), 1265-1275.
14. Gross, R. A.; Kumar, A.; Kalra, B., *Chemical Reviews* **2001**, *101* (7), 2097-2124.

15. Wosnick, J. H.; Faucher, S.; Pereira, L., *Abstracts of Papers of the American Chemical Society* **2010**, 240.
16. van der Meulen, I.; Gubbels, E.; Huijser, S.; Sablong, R.; Koning, C. E.; Heise, A.; Duchateau, R., *Macromolecules* **2011**, 44 (11), 4301-4305.
17. Bouyahyi, M.; Pepels, M. P. F.; Heise, A.; Duchateau, R., *Macromolecules* **2012**, 45 (8), 3356-3366.
18. Martello, M. T.; Burns, A.; Hillmyer, M., *Acs Macro Letters* **2012**, 1 (1), 131-135.
19. Kiesewetter, M. K.; Scholten, M. D.; Kirn, N.; Weber, R. L.; Hedrick, J. L.; Waymouth, R. M., *Journal of Organic Chemistry* **2009**, 74 (24), 9490-9496.
20. Cota, I.; Medina, F.; Sueiras, J. E.; Tichit, D., *Tetrahedron Letters* **2011**, 52 (3), 385-387.
21. Ye, W. P.; Xu, J. Y.; Tan, C. T.; Tan, C. H., *Tetrahedron Letters* **2005**, 46 (40), 6875-6878.
22. Pratt, R. C.; Lohmeijer, B. G. G.; Long, D. A.; Waymouth, R. M.; Hedrick, J. L., *Journal of the American Chemical Society* **2006**, 128 (14), 4556-4557.
23. Dove, A. P., *Acs Macro Letters* **2012**, 1 (12), 1409-1412; Simon, L.; Goodman, J. M., *Journal of Organic Chemistry* **2007**, 72 (25), 9656-9662.
24. Helou, M.; Miserque, O.; Brusson, J.-M.; Carpentier, J.-F.; Guillaume, S. M., *Chemistry-a European Journal* **2010**, 16 (46), 13805-13813.
25. Alexander, C., *Faraday Discussions* **2013**, 166, 449-452.
26. McGinty, D.; Letizia, C. S.; Api, A. M., *Food and Chemical Toxicology* **2011**, 49, S193-S201.
27. Jiang, Z.; Azim, H.; Gross, R. A.; Focarete, M. L.; Scandola, M., *Biomacromolecules* **2007**, 8 (7), 2262-2269.
28. Liu, J.; Jiang, Z.; Zhang, S.; Saltzman, W. M., *Biomaterials* **2009**, 30 (29), 5707-5719; Liu, J.; Jiang, Z.; Zhang, S.; Liu, C.; Gross, R. A.; Kyriakides, T. R.; Saltzman, W. M., *Biomaterials* **2011**, 32 (27), 6646-6654; Van der Mee, L.; Antens, A.; Van de Kruijs, B.; Palmans, A. R. A.; Meijer, E. W., *Journal of Polymer Science Part a-Polymer Chemistry* **2006**, 44 (7), 2166-2176.
29. Kobayashi, S., *Proceedings of the Japan Academy Series B-Physical and Biological Sciences* **2010**, 86 (4), 338-365; van der Meulen, I.; de Geus, M.; Antheunis, H.; Deumens, R.; Joosten, E. A. J.; Koning, C. E.; Heise, A., *Biomacromolecules* **2008**, 9 (12), 3404-3410.

-
30. Tang, D.; Macosko, C. W.; Hillmyer, M. A., *Polymer Chemistry* **2014**, 5 (9), 3231-3237.
 31. Kumar, A.; Kalra, B.; Dekhterman, A.; Gross, R. A., *Macromolecules* **2000**, 33 (17), 6303-6309.
 32. Bisht, K. S.; Henderson, L. A.; Gross, R. A.; Kaplan, D. L.; Swift, G., *Macromolecules* **1997**, 30 (9), 2705-2711.
 33. Jaffredo, C. G.; Carpentier, J.-F.; Guillaume, S. M., *Macromolecular Rapid Communications* **2012**, 33 (22), 1938-1944.
 34. Alfonsi, K.; Colberg, J.; Dunn, P. J.; Fevig, T.; Jennings, S.; Johnson, T. A.; Kleine, H. P.; Knight, C.; Nagy, M. A.; Perry, D. A.; Stefaniak, M., *Green Chemistry* **2008**, 10 (1), 31-36; Henderson, R. K.; Jimenez-Gonzalez, C.; Constable, D. J. C.; Alston, S. R.; Inglis, G. G. A.; Fisher, G.; Sherwood, J.; Binks, S. P.; Curzons, A. D., *Green Chemistry* **2011**, 13 (4), 854-862.

**Chapter 4 Evaluation of
Surfactant Properties of Novel
Amphiphilic Block Copolymers of
Poly(Decalactone)**

4.1 Introduction

Aqueous solubility of active pharmaceutical ingredients (API) is one of the important determining factors affecting their absorption *in vivo*. Poor absorption and therefore low bioavailability after oral administration is often attributed to the poor aqueous solubility of drugs. On average approximately 40% of drugs available in the market and around 75% of drugs currently in development stage are poorly soluble in water¹. The approaches generally utilised to solubilise the drugs in water include the use of co-solvents, solid dispersions, surfactants, dendrimers etc¹.

Micelles/surfactants are widely used drug delivery vehicles used to enhance the bioavailability of pharmaceutically active ingredients^{1, 2}. However, small surfactant molecules with generally high critical micelle concentration (CMC) values can dissociate upon dilution in the bloodstream and thus can release the loaded drug before reaching the target site³. To address this problem, polymeric micelles having low CMC values have been developed and some have been successfully utilised to solubilise hydrophobic drugs³. Many academic science papers have been published in this field, indicating the potential of polymeric micelles as effective drug delivery carriers^{4,5,6}.

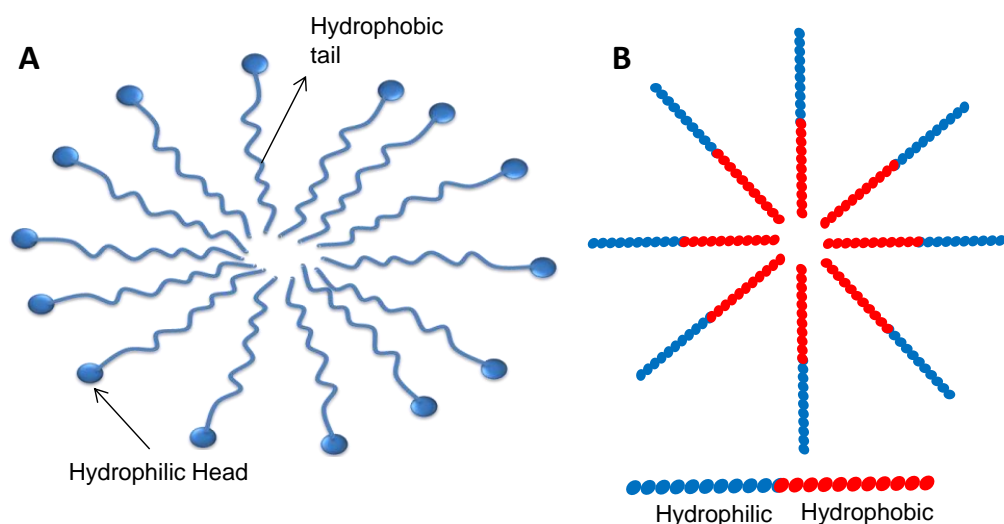


Figure 4-1 Proposed assembly of (A) low molecular weight surfactant and (B) amphiphilic block polymer after dispersion in water.

Amphiphilic block copolymers with a hydrophobic and a hydrophilic block are readily self-assembled into micelles in aqueous media to generate core shell structures (figure 4-1) and can have low CMC values⁷. The use of PEG (hydrophilic polymer) to generate a hydrophilic 'corona' has been reported to hinder the uptake of micelles by the reticulo endothelial system (RES) thus improving the circulatory time of polymeric micelles *in vivo*^{4, 6}. Long circulating drug delivery systems are useful in cancer therapy because of their accumulation in tumor by the Enhanced Permeability and Retention (EPR) effect⁸. Several core forming blocks (hydrophobic polymers) such as poly(caprolactone) (PCL), poly(lactide) PLA, poly(lactide-co-glycolide) (PLGA), poly(propylene oxide), poly(L-lysine), poly(styrene), poly(aspartic acid) etc. have been successfully utilised to synthesise amphiphilic block

copolymers^{3, 6, 7}. However, hydrophobic polymer obtained from renewable/sustainable feedstocks offers advantages over those polymers which are synthesised from petrochemicals sources in terms of low-toxicity and source of origin⁹.

The amphiphilic block copolymers derived from renewable lactic acid and glycolic acid with PEG has been the polymers of choice for various pharmaceutical applications to date. Micelles prepared from PLA and PLGA block copolymers with hydrophilic PEG-type shells have already shown their potential in solubility enhancement¹⁰, sustained release¹¹, tumor targeting¹², stimuli-responsive drug delivery¹³ etc. However, continuous efforts are in place to develop other sustainable polymers which can overcome certain problems associated with PLA and PLGA block copolymers such as sub-optimal degradation profile¹⁴ and poor drug loading¹⁵.

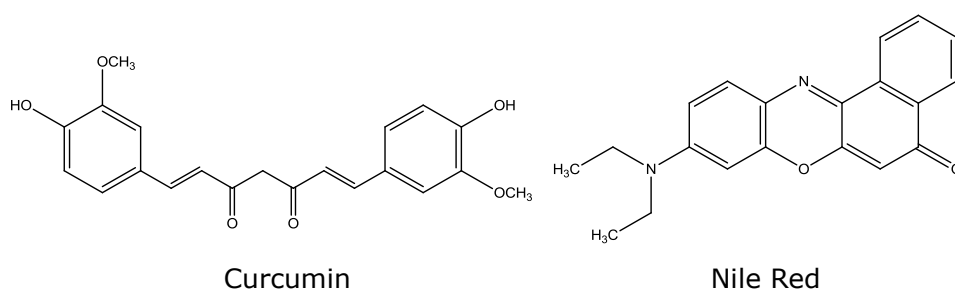
The successful synthesis of novel amphiphilic block copolymers with alkyl side chains using renewable monomers were reported in chapter 3. The aim of the studies performed in this chapter is to evaluate the efficiency of those synthesised novel block copolymers to encapsulate hydrophobic drug-like molecules. The results obtained from these amphiphilic block copolymers micelles were compared with block copolymer micelles of mPEG-b-PCL in terms of size,

loading efficiency and release profile. Poly(caprolactone) block copolymer was selected for the comparative studies because of its source of origin (petroleum) and its prior investigation for drug delivery applications, against which the novel PDL block copolymers could be evaluated.

Micelles of block copolymers were fabricated using a revised nano-precipitation method¹⁶ as this offers advantages over the other methods such as dialysis, emulsion and solvent evaporation⁶. For instance, with the solvent evaporation (film method) method, incomplete reconstitution of the polymeric film was observed in aqueous solvent resulting in polymer loss and consequently decreases in the micelles efficiency⁶. Hence, the solvent evaporation method was considered not suitable for the PDL block copolymers because of their expected high hydrophobicity. Emulsion methods for micelle preparation were not preferred because they generally require the use of volatile water immiscible solvents such as dichloromethane (DCM) and chloroform^{5, 6}. In the dialysis method, use of organic solvents in dialysis bag is required to fabricate micelles. However, solvents other than DMSO are not recommended for use with the regenerated cellulose membrane and none of the solvents commonly used for the preparation of micelles using dialysis method were

recommended for use with the cellulose membrane. The commonly used non-volatile organic solvents in the dialysis method are DMF, DMSO and DMAc,^{17,18} which generally removed from the formulation by dialysis. Since these solvents are not compatible with dialysis membrane and thus could damage the membrane that can cause undesired loss of micelles formulation in release medium.

To check the efficiency of poly(decalactone) micelles in encapsulation of hydrophobic molecules, Nile Red (NR) was chosen as a model hydrophobic compound. The aqueous solubility of NR is less than $1\mu\text{g}/\text{mL}$ ¹⁹ and therefore it is a good candidate for the evaluation of polymeric micelles as encapsulate. Additionally, NR loaded micelles can be used for various imaging studies, if needed²⁰.



Curcumin was selected as a model drug to evaluate the encapsulation efficiency and release behaviour using novel PDL block copolymer micelles. Curcumin is a natural chemotherapeutic agent obtained from the rhizome of the *Curcuma longa* Linn. It has attracted much attention recently

due to its various claimed pharmacological properties combined with lack of systemic toxicity at high dose²¹. However, the therapeutic use of curcumin has been hampered due to its low aqueous solubility and poor *in vivo* stability. Numerous literature precedence is available discussing the applications and drawbacks associated with the use of curcumin as well as the approaches to overcome those drawbacks^{22,23}. It was proposed that the encapsulation of curcumin in nano-sized drug delivery carriers could be a better approach to overcome the solubility and stability problems associated with curcumin^{24, 25}. Several nano-sized formulations like nanoparticles, micelles, nanogels, liposomes were reported previously to enhance the solubility, stability and thus bioavailability of curcumin^{24,25}.

Recently mixed micelles formulation using Pluronic (PEO-PPO-PEO) co-polymers was reported for the improved delivery of curcumin^{26, 27}. It has been also demonstrated that mixed micelles prepared from two or more different block copolymers were able to enhance the formulation stability and drug loading efficiency compared to the micelles prepared from single block copolymer²⁸. Therefore, curcumin loaded mixed micelle formulation was also prepared using mPEG-b-PDL and mPEG-b-PCL copolymer.

4. 2 Methods

4.2.1 Determination of CMC of Poly(decalactone) and Poly(caprolactone) Block Copolymers Micelles

The CMC of block copolymers of poly(decalactone) (*i.e.* mPEG-b-PDL, PDL-b-PEG-b-PDL and mPEG-b-PDL-b-PPDL) and Poly(caprolactone) (mPEG-b-PCL) were determined by using the pyrene 1:3 fluorescence ratio method²⁹. The results were analysed using GraphPad Prism software (version 6.4). Detailed procedures for CMC determination are described in chapter 2.

4.2.2 Empty and Dye/Drug Loaded Micelles Preparation from PDL and PCL Block Copolymers

Micelles of synthesised block copolymers were prepared by a single-step nano-precipitation method with minor modification³⁰. Briefly, block copolymer (50 mg) of PDL or PCL was dissolved in 5 mL of acetone and this solution was added drop-wise into 10 mL of HPLC grade water under stirring (1000 rpm). The solution was then stirred for 3 hrs at room temperature and left overnight (open vial) to ensure the complete removal of acetone. The micellar solution was then filtered through a membrane syringe filter (pore size: 220 nm) (Millex-LG, Millipore Co., USA) and the filtrate was used for

the analysis of size and zeta potential after appropriate dilutions.

Drug or dye-loaded micelles were prepared by a similar method used to prepare blank micelles. Briefly, curcumin (2 mg) or Nile red (NR) (1 mg) was dissolved along with the polymer (50 mg) in acetone (5 mL) and added drop wise into HPLC grade water (10 mL). The micellar solution was stirred for 3 hrs and then stored overnight to remove the traces of acetone. Curcumin is light sensitive and hence the whole process was performed in the dark (vials covered using aluminium foil). Mixed micelles using mPEG-b-PDL and mPEG-b-PCL copolymer were prepared to understand the effect on curcumin loading content and release pattern. Mixed micelles were fabricated by physical mixing³¹ of both copolymer (25 mg each) in acetone (5mL) and the method described above was employed to obtain curcumin-loaded mixed micelles.

The unencapsulated NR was removed by filtering the micellar solution through a membrane filter (pore size: 220 nm). Curcumin loaded micelles were purified by passing through PD10 Desalting Column (Sephadex G-25 Medium, GE Healthcare Life Sciences) in order to retain material of < 5K molecular weight and hence the collected solution was free from any unencapsulated drug. The curcumin-loaded micelles

were filtered through a membrane filter (pore size: 220 nm, Millex-LG, Millipore Co., USA). Purified micelle solutions were then used for further characterisation. A part of the micellar solution was freeze dried for the determination of drug content. A pictorial presentation of preparation, purification and characterisation of curcumin loaded micelles is shown in figure 4-2.

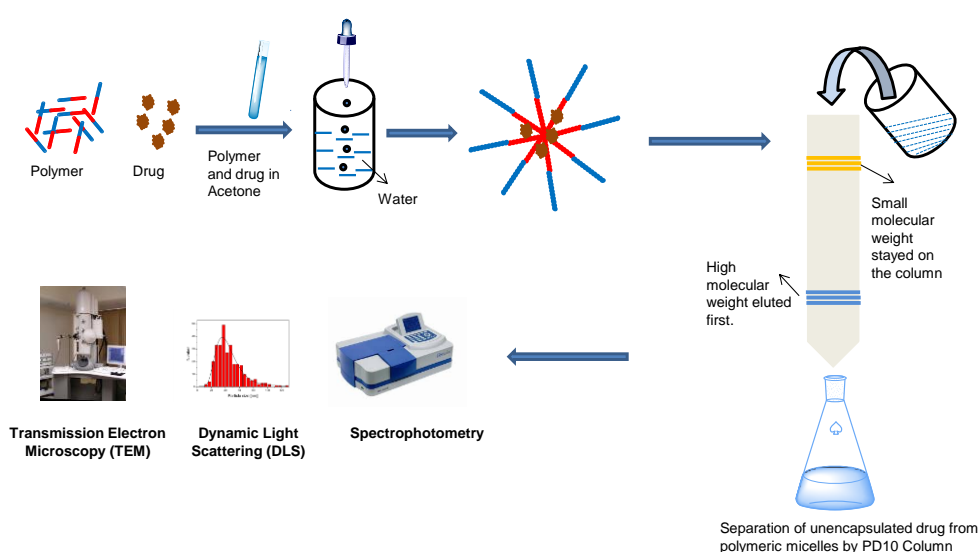


Figure 4-2 Pictorial representation of preparation, purification and characterisation of curcumin loaded micelles

4.2.3 Preparation of Nano-emulsion from homopolymer of Poly(decalactone)

An end-functional homopolymer of poly(decalactone) *i.e.* propargyl-PDL was used to make an oil-in-water nanoemulsion³² for comparative studies with blank micelles. Briefly, a solution of propargyl-PDL (50 mg) in 5 mL of acetone was added drop-wise into 10 mL of HPLC grade water

under stirring (1000 rpm). This procedure formed dispersed droplets of poly(decalactone) due to its immiscibility with water. The solution was then stirred for 3 hrs at room temperature and then stored overnight to remove the traces of acetone. The nanoemulsion was then filtered through a membrane syringe filter (pore size: 220 nm) (Millex-LG, Millipore Co., USA) and the filtrate was used for size and zeta potential analysis after appropriate dilutions. No stabiliser was used during the preparation of nanoemulsion.

4.2.4 Characterisation of micelles for size, zeta potential and surface morphology

For the size and polydispersity index measurements, micelle samples (50µg/mL) in HPLC grade water were analysed using a Malvern NanoZS instrument. The Z-average size (d.nm) has been reported, which was calculated by the instrument using the formula below³³.

$$\text{Z-average diameter (Dz)} = \frac{\sum S_i}{\sum (S_i/D_i)}$$

Where, S_i is the scattered intensity from particle i and D_i is the diameter of particle i obtained using the Stokes-Einstein equation.

Surface zeta potential was measured from same instrument in HEPES 10mM buffer (pH-7.4). TEM was performed to confirm

the size and to determine the surface morphology. Samples were imaged on TEM grids without staining.

The full experimental procedures for these methods are reported in chapter 2. All the measurements were performed on three different batches and the mean values were reported.

4.2.5 Determination of Drug Content, Curcumin Stability and *in vitro* Release behaviour from Micelles.

Drug Content (DC) and Encapsulation Efficiency (EE) of drug/dye in micelles were determined by dissolving a known amount of freeze dried sample (5-10 mg) of micelles in acetone followed by quantification of the drug/dye concentration. For the determination of NR concentration, the UV absorption of sample solutions was recorded at λ_{\max} of 541 nm using a UV spectrophotometer. The amount of NR was calculated using a standard calibration curve of NR (figure 4-3).

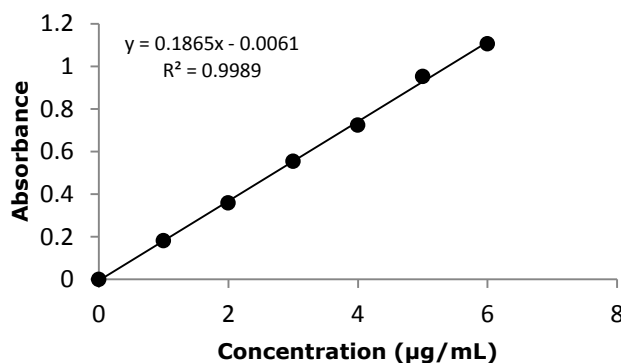


Figure 4-3 Standard calibration curve of Nile red. The UV-Vis absorbance of Nile red solution (in acetone) was measured at wavelength of 541nm.

For curcumin analysis, samples were excited at a fixed wavelength ($\lambda_{\text{ex}} = 420 \text{ nm}$) and emission spectra were recorded in a range of 450 to 650nm³⁴ using a fluorescence spectrophotometer. The excitation and emission slit widths were selected at 5 nm and the emission intensity at 524 nm was selected for drug content calculations. Amounts of curcumin present in the samples were then calculated using a standard calibration curve of curcumin (figure 4-4).

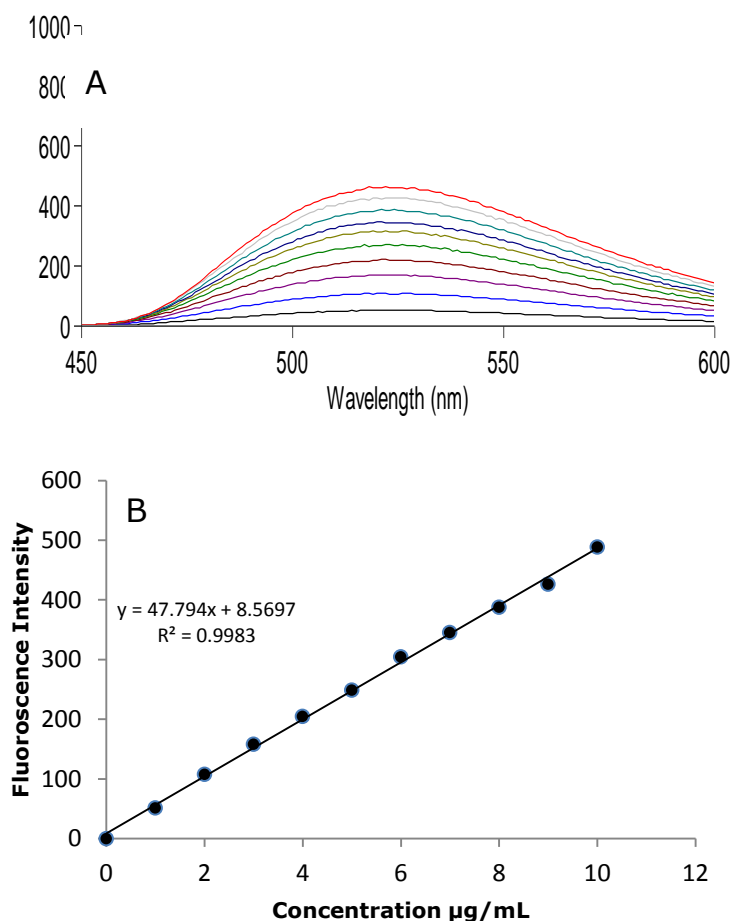


Figure 4-4 (A) Fluorescence emission spectra of curcumin at different concentration in acetone ($\lambda_{\text{ex}} = 420 \text{ nm}$) and (B) Standard calibration curve of curcumin. The fluorescence emission of curcumin solution (in acetone) was measured at wavelength of 524nm.

DC and EE were calculated using the formula reported in chapter 2 and the results were reported as mean \pm standard deviation (SD) from three different batches.

The ability of mPEG-b-PDL micelles to protect the curcumin from degradation at physiological pH was tested using a reported method³⁵. Freeze dried micelles containing curcumin equivalent to 100 μ g, were redispersed in 2mL of PBS (pH 7.4) and incubated at 37°C. For the preparation of control samples, free curcumin (100 μ g) was dissolved in 2mL of phosphate buffer saline (PBS) with the aid of methanol and incubated at 37° C³⁵. At predetermined time intervals, 100 μ L of the sample was withdrawn and diluted with acetone up to 1 mL. The amount of remaining curcumin was then determined using a fluorescence spectrophotometer by following the similar parameters used to determine DC.

The release profile of curcumin from micelles was determined by a dialysis method³⁵. Briefly, a calculated quantity of curcumin-loaded freeze dried micelles equivalent to 350 μ g of curcumin was dissolved in PBS (2mL) (pH-7.4). The micelle solution in PBS was then placed in dialysis tubing (Float-A-Lyzer) having the molecular weight cut off (mwco) of 3.5-5 KDa. The samples were dialysed against 500 mL of PBS (pH 7.4) at 37°C. The release media was replaced with fresh PBS

every 24 hrs. The volume of solution in the dialysis tubing was measured at appropriate time intervals (every 6-12 hrs), and restored to the original with PBS, if necessary. Samples (100 μL) were withdrawn directly from the dialysis tubing at predetermined time intervals and the volume of solution in the dialysis tubing was restored with fresh solvent. Samples were analysed after diluting with acetone using a fluorescence spectrophotometer to calculate the amount of curcumin remaining in the micelles.

4.3 Results

4.3.1 Determination of CMC of Poly(decalactone) and Poly(caprolactone) Block Copolymer Micelles

The CMC values of PDL-b-PEG-b-PDL, mPEG-b-PDL, mPEG-b-PCL and mPEG-b-PDL-b-PPDL were determined by plotting the graph between polymer concentration versus I_1 and I_3 peak intensity ratio of pyrene. The data (mean values) used to plot the graph is presented in table 4-1. The obtained curve was fitted using nonlinear regression (Sigmoidal, 4PL, X is on log scale) to determine the CMC value (figure 4-5). The inflection point (IC50) of the sigmoidal curve suggesting the abrupt change in values was considered as the CMC value of the polymer. Further, 95%-confidence intervals of the CMCs were plotted to visualise any statistical difference in obtained CMC

values (figure 4-6). The CMC range detected for poly(decylactone) copolymers overlapped each other, suggested no statistical significant differences among them. The CMC value observed for mPEG-b-PCL was approximately 2.5 times higher compared to the novel poly(decylactone) block copolymers micelles (table 4-2).

Concentration ($\mu\text{g/mL}$)	I_1/I_3 PDL	mPEG-b- PDL	I_1/I_3 PDL-b-PEG- b-PDL	I_1/I_3 PDL-b-PPDL	mPEG-b- PCL
0.001	1.5153		1.5269	1.5562	1.5469
0.005	1.5145		1.5278	1.55331	1.5457
0.01	1.5126		1.5249	1.5493	1.5379
0.05	1.5019		1.5216	1.5391	1.5313
0.1	1.4908		1.4995	1.5245	1.5211
0.3	1.4562		1.4829	1.507	1.5179
0.5	1.439		1.4709	1.4933	1.5084
0.8	1.4331		1.4663	1.4708	1.4997
1	1.4253		1.4434	1.4381	1.4757
2	1.3801		1.4159	1.3596	1.4391
4	1.3355		1.3746	1.3087	1.4061
6	1.3185		1.3609	1.3021	1.3850
8	1.3179		1.3467	1.2984	1.3618
10	1.3105		1.3427	1.2976	1.3439
15	1.3042		1.3384	1.2967	1.3347
20	1.3009		1.3330	1.2955	1.3258
25	1.297		1.3324	1.2934	1.3165
30	1.2924		1.3328	1.2896	1.3131
35	1.2916		1.3341	1.2877	1.3077
40	1.2919		1.3316	1.2878	1.3073
45	1.291		1.3307	1.2871	1.3070
50	1.2927		1.3309	1.2873	1.3080

Table 4-1 Intensity ratio of peak 1 and 3 of pyrene fluorescence spectrum acquired using different concentration of polymer in water.

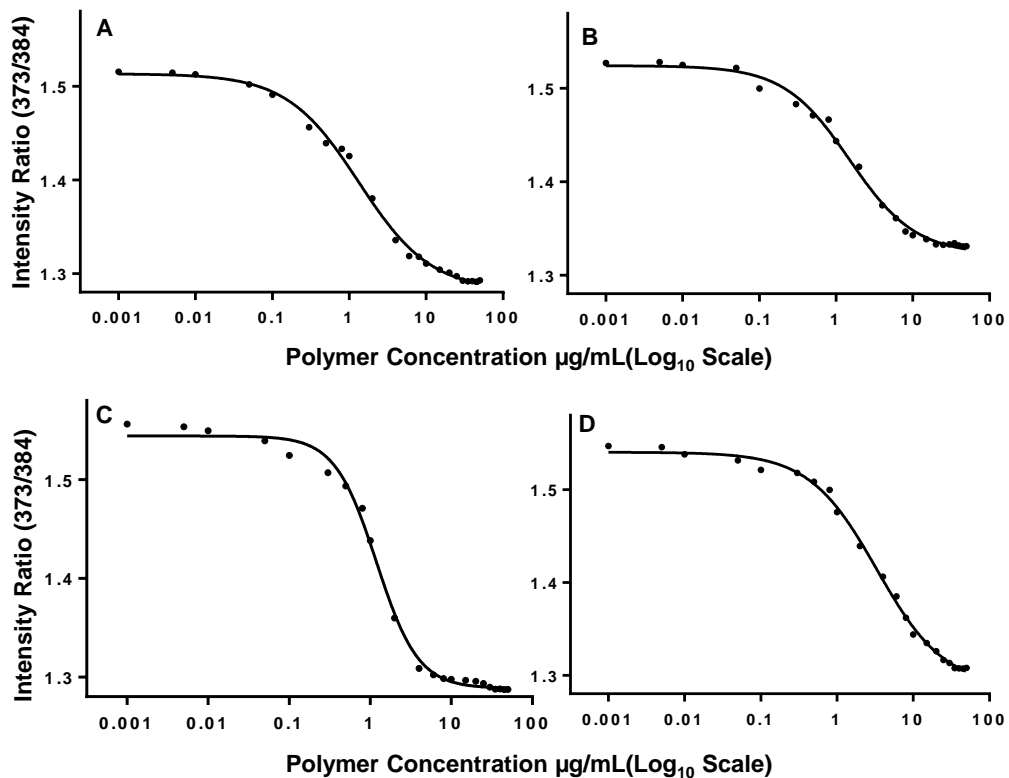


Figure 4-5 CMC plot for (A) mPEG-b-PDL, (B) PDL-b-PEG-b-PDL, (C) mPEG-b-PDL-b-PPDL and (D) mPEG-b-PCL obtained by pyrene 1:3 peak ratio method.

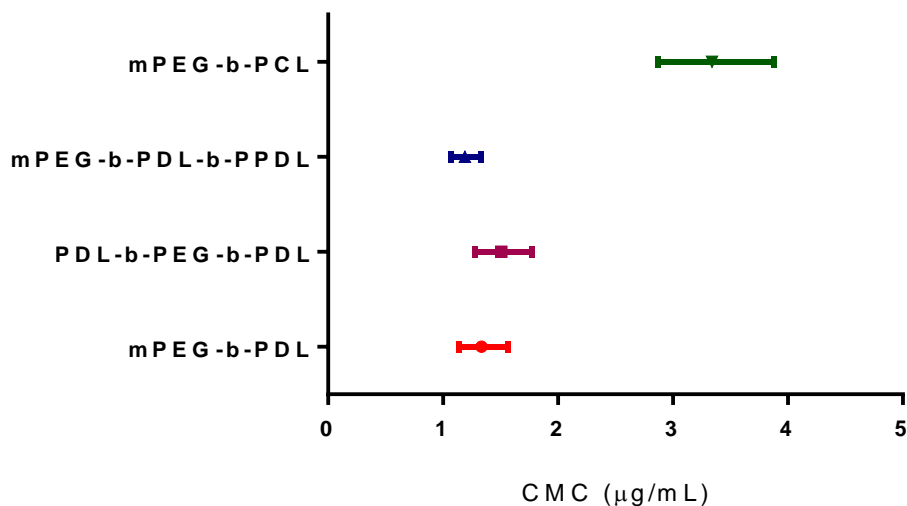


Figure 4-6 Comparison of 95% confidence interval (IC50) of the CMC values of synthesised copolymers. IC50 value was obtained by non-linear curve fitting of CMC plot (sigmoidal, 4PL).

Sample	CMC ($\mu\text{g/mL}$)	Z- average size (d/nm) ($\pm\text{SD}$) (Blank)	PdI (Blank)	Zeta Potential (mv) ($\pm\text{SD}$)	Z- average size (d/nm) ($\pm\text{SD}$) (NR Loaded)	PdI (NR Loaded)	Z-average size (d/nm) ($\pm\text{SD}$) (Curcumin Loaded)	PdI (Curcumin Loaded)	Zeta Potential (mv) ($\pm\text{SD}$) (Curcumin Loaded)
^a Propargyl PDL	NA	149 \pm 4	0.04 \pm 0.02	-70.5 \pm 3.0	NA	NA	NA	NA	NA
PDL-b- PEG-b-PDL	1.50	163 \pm 7	0.26 \pm 0.03	-6.8 \pm 2.6	58 \pm 5	0.32 \pm 0.02	123 \pm 7	0.28 \pm 0.03	-7.3 \pm 0.9
mPEG-b- PDL	1.33	34 \pm 4	0.12 \pm 0.02	-3.1 \pm 0.8	38 \pm 3	0.17 \pm 0.02	40 \pm 3	0.14 \pm 0.02	-2.8 \pm 1.2
mPEG-b- PDL-b- PPDL	1.19	85 \pm 5	0.28 \pm 0.01	-2.5 \pm 0.8	83 \pm 4	0.38 \pm 0.02	101 \pm 9	0.28 \pm 0.02	-3.2 \pm 1.8
mPEG-b- PCL	3.34	36 \pm 3	0.14 \pm 0.02	-1.2 \pm 1.2	NA	NA	40 \pm 2	0.12 \pm 0.02	0.1 \pm 1.3

Table 4-2 Characterization data of polymeric micelles prepared from block copolymers of Poly(decalactone) and Poly(caprolactone). (CMC- critical micelles concentration, d/nm – diameter in nanometer, NA - Not applicable, SD- Standard deviation, PdI – polydispersity index, mv – millivolt, NR- Nile Red). ^aNano-emulsion preparation of homopolymer.

4.3.2 Preparation and Characterisation of Empty Micelles.

Nano-precipitation method was previously employed successfully for the incorporation of hydrophobic molecules inside micellar cores^{36, 37} and therefore this method is chosen for micelles preparation in the current study.

Micelle solutions were filtered through a membrane filter in order to remove precipitates (if any) after complete removal of acetone. The recoveries of micellar suspension after filtration for mPEG-b-PDL, mPEG-b-PCL and PDL-b-PEG-b-PDL copolymer were ranged from 90 to 95%. However, the recovery of the micelle suspension of mPEG-b-PDL-b-PPDL was approximately 60% only. The Z-average size (in diameter) and polydispersity index obtained by DLS for empty amphiphilic block copolymers micelles are reported in table 4-2. The mean particle size (Z-average size) produced by the DLS instrument was used here for the comparison. The Z-average size is the intensity weighted harmonic mean size and the best value to report as defined by the International Organisation for Standardization in ISO 13321 and ISO 22412³⁸.

Sample Name	Mean Size by Intensity (% intensity in bracket)		Mean Size by Volume (\pm SD)
	Peak 1 (d/nm)	Peak 2 (d /nm)	Peak 1 (d/nm)
PDL-b-PEG-b-PDL (Blank)	32.7 (47.2%)	224.6 (52.8%)	29.0 \pm 3.0
PDL-b-PEG-b-PDL (NR loaded)	49.9 (77.4%)	365.4 (22.6%)	31.0 \pm 2.0
PDL-b-PEG-b-PDL (Curcumin loaded)	44.3 (55.4%)	143.7 (44.6%)	36.0 \pm 2.0

Table 4-3 Average size by intensity and volume of PDL-b-PEG-b-PDL micelles in bimodal size distribution curve. (SD - standard deviation, d/nm - diameter of micelles in nanometer, NR - Nile Red)

Size detected for empty mPEG-b-PCL micelles was comparable to the size of mPEG-b-PDL micelles (table 4-2, figure 4-7). Intensity size distribution curve observed for mPEG-b-PDL and mPEG-b-PCL micelles was unimodal whereas micelles prepared from PDL-b-PEG-b-PDL gave bimodal distribution curve (figure 4-7). The average size by intensity detected for each peak along with the intensity percentage in bimodal distribution curve is shown in table 4-3. The bigger size micelles were expected in this sample due to the cloudy appearance of purified micellar solution (figure 4-8).

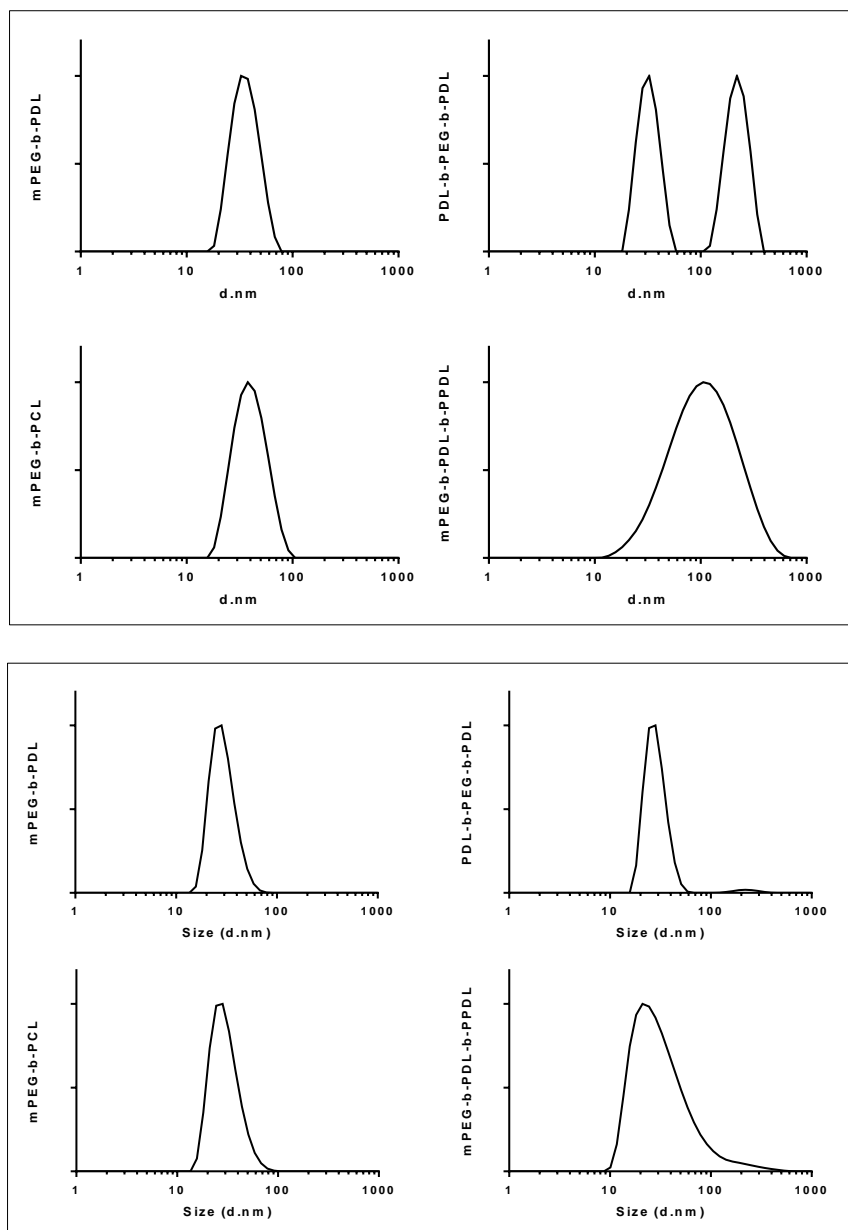


Figure 4-7 Size distributions by intensity (top) and by volume (bottom) of blank micelles determined by DLS method in water.

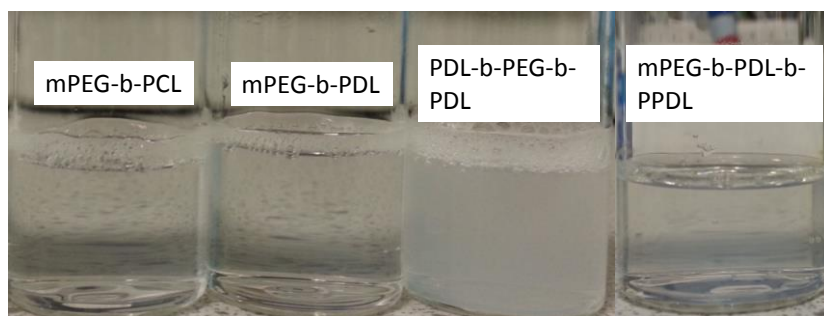


Figure 4-8 Physical appearance of purified blank micelles in water obtained from different copolymers via nanoprecipitation method.

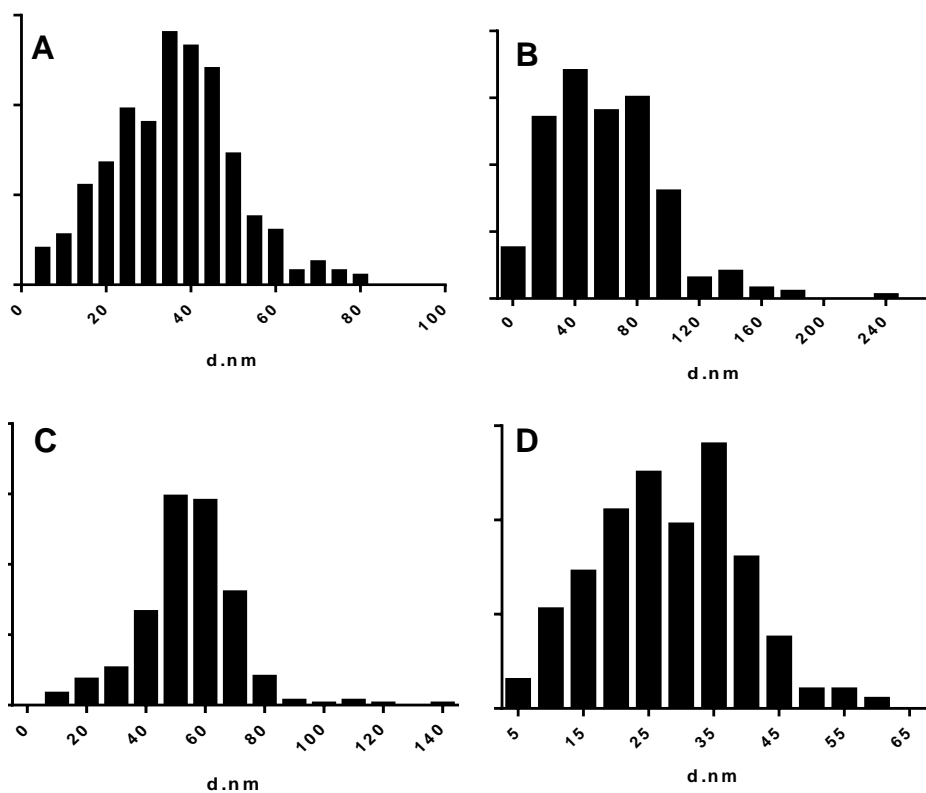
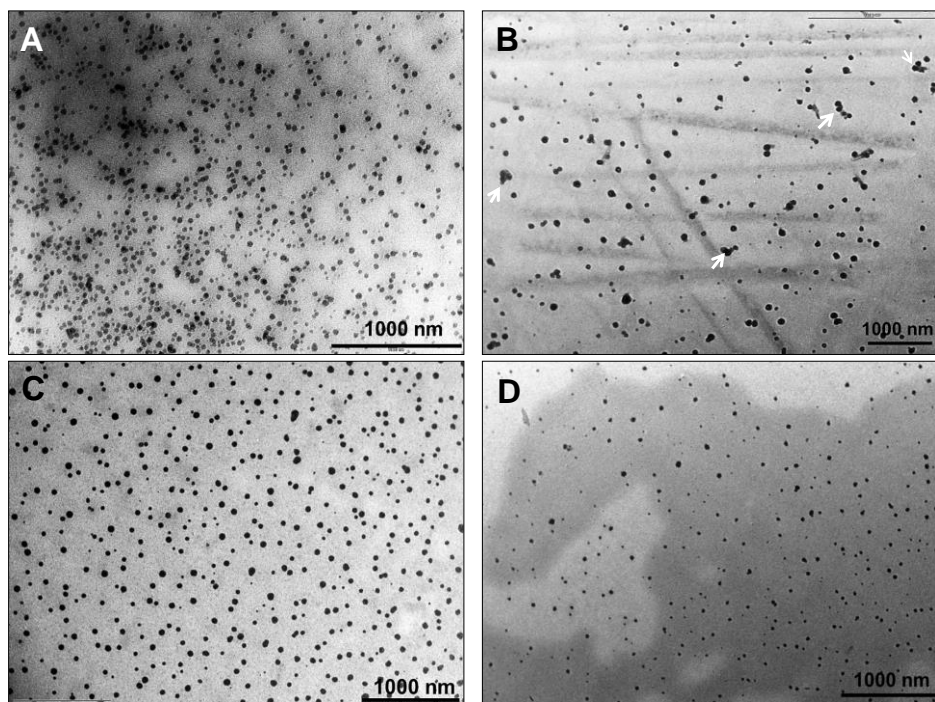


Figure 4-9 TEM images and size distribution histogram (analysed using ImageJ software) of empty (A) mPEG-b-PDL, (B) PDL-b-PEG-b-PDL, (C) mPEG-b-PDL-b-PPDL and (D) mPEG-b-PCL micelles. Arrow represents the presence of clusters in PDL-b-PEG-b-PDL micelles sample. Scale bar – 1000nm

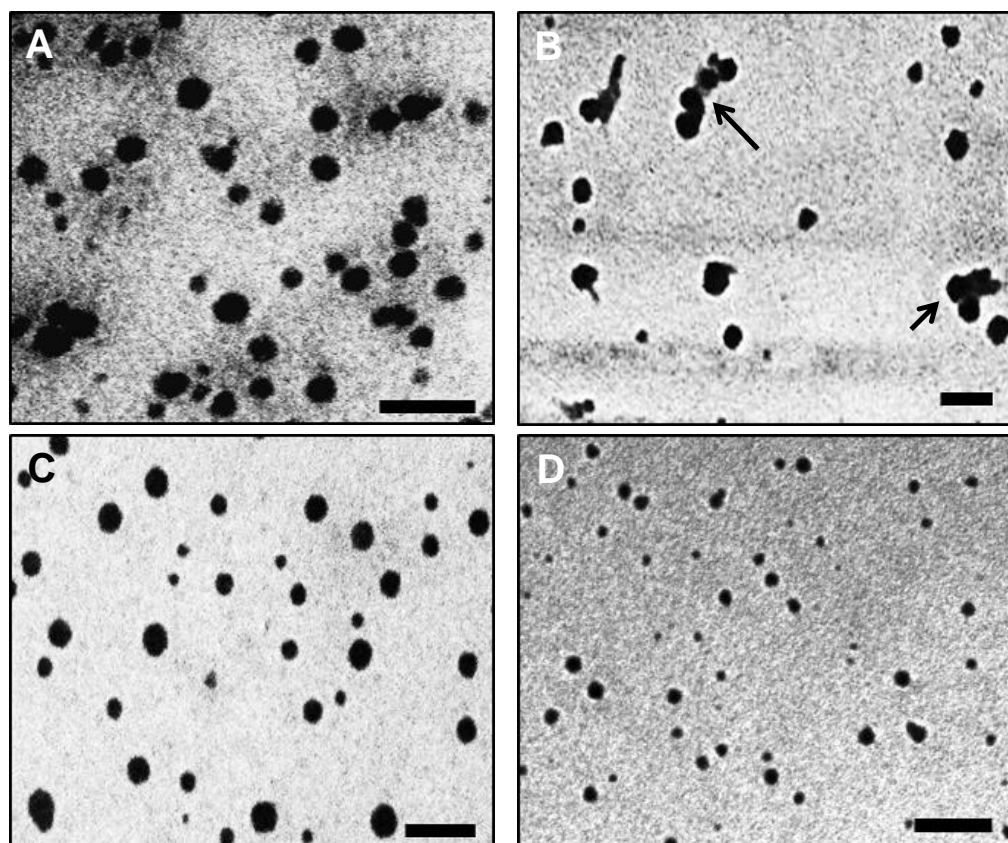


Figure 4-10 TEM images of empty (A) mPEG-b-PDL, (B) PDL-b-PEG-b-PDL, (C) mPEG-b-PDL-b-PPDL and (D) mPEG-b-PCL micelles. Scale bar – 200nm. Arrow represents the presence of clusters in PDL-b-PEG-b-PDL sample.

Micelles prepared from mPEG-b-PDL-b-PPDL copolymer gave the broadest size distribution determined by DLS with high polydispersity index when compared to the other PDL block copolymers (table 4-2, figure 4-7). However, the average size by volume detected for this sample was 41 ± 4 nm. The presence of small numbers of large size micelles increased the polydispersity and the Z-average size.

All micelles samples were also imaged on TEM and were found that the micelles obtained from amphiphilic block copolymers were of roughly spherical in shape (figure 4-9, 4-10). TEM

image of mPEG-b-PDL-b-PPDL displayed the presence of a broad size range in the sample whereas mPEG-b-PDL and mPEG-b-PCL possessed narrower and more uniform size distribution (figure 4-9, 4-10). TEM image of the sample PDL-b-PEG-b-PDL indicated the presence of some aggregates (clusters) of the micelles. Thus, it can be hypothesised that the bimodal distribution observed in the DLS analysis for this sample was due to the clusters formation (figure 4-10). Size histogram plotted using TEM images suggested that none of the micelles exhibits the size greater than 60 and 80 nm in mPEG-b-PDL and mPEG-b-PCL samples respectively. However, as expected PDL-b-PEG-b-PDL and mPEG-b-PDL-b-PPDL samples contains micelles of bigger size.

Size detected for the nanoemulsion prepared from propargyl-PDL homopolymer was found to be the biggest if the clusters of PDL-b-PEG-b-PDL micelles were ignored (table 4-2, figure 4-11). This was might be due to the absence of any stabiliser (surfactant) in the nano-emulsion formulation³⁹.

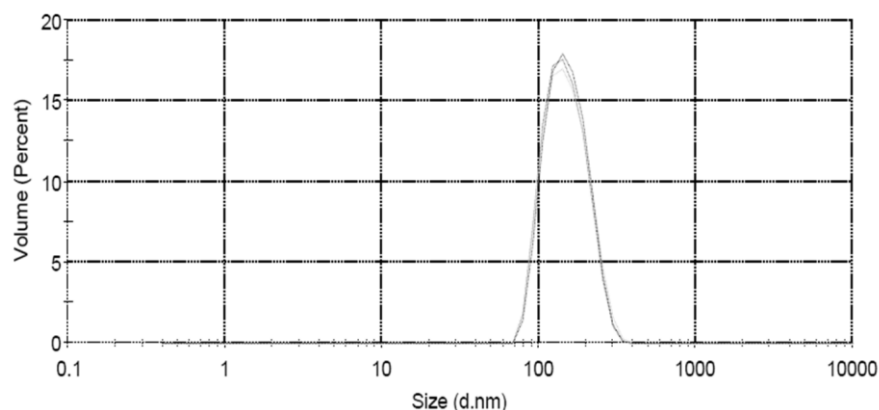


Figure 4-11 Size distribution spectrum (by volume) of propargyl-PDL nano emulsion. Nano-emulsion was prepared by dispersing oily propargyl-PDL polymer in water by following nanoprecipitation method.

Surface charge is one of the fundamental parameters known to affect the stability of colloidal suspension and can be defined as the repulsion or attraction between particles based on the presence of surface charge. The zeta potential is the measure of the surface charge that exists on a particle. It is well established that particles with zeta potentials above ± 30 mV are generally considered as stable in aqueous suspension⁴⁰. The zeta potential detected for nano-emulsion (globules) prepared from poly(decalactone) homopolymer in HEPES buffer (10mM, pH-7.4) was -70.5 ± 3.0 mv, which suggested an excellent stability of this formulation (table 4-2, figure 4-12). The zeta potential values measured for amphiphilic block copolymers micelles were close to neutral. However, PDL-b-PEG-b-PDL gave slight negative value

compared to the other block copolymer micelles (table 4-2, figure 4-13).

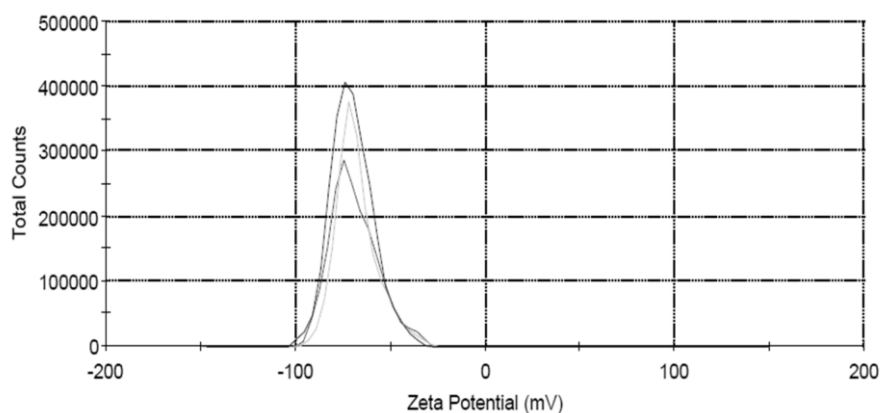


Figure 4-12 Zeta potential spectrum of propargyl-PDL nano emulsion measured in 10mM HEPES (pH-7.4) buffer.

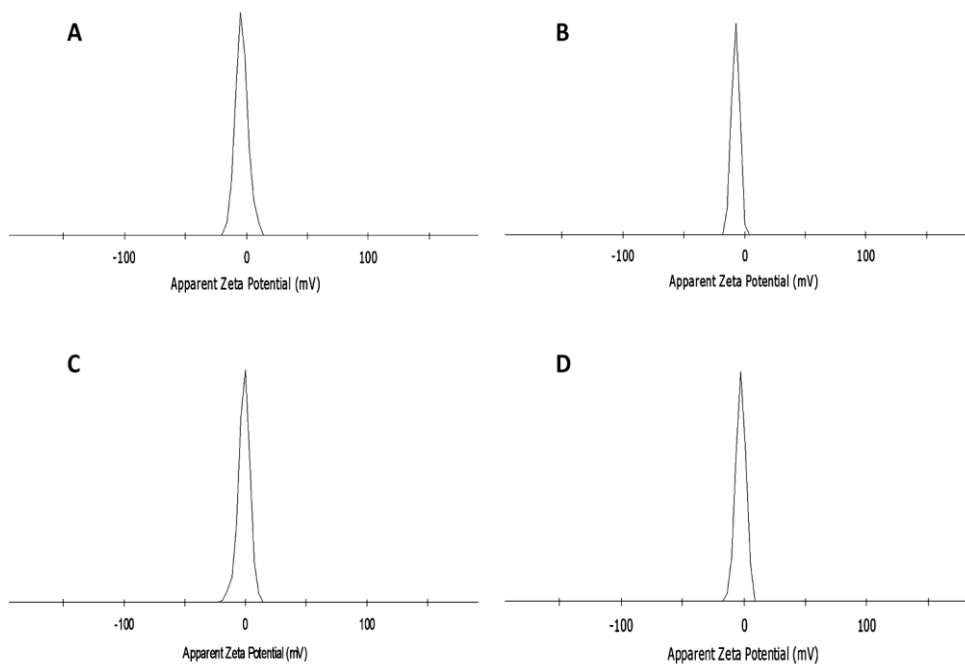


Figure 4-13 Zeta potential curve of (A) mPEG-b-PDL, (B) PDL-b-PEG-b-PDL, (C) mPEG-b-PCL and (D) mPEG-b-PDL-b-PPDL micelles acquired using Zeta sizer instrument in HEPES 10mM buffer (pH – 7.4).

PEG as a hydrophilic block has been reported to mask the charge of the micelles core and hence the micelles with PEG as corona gave the neutral surface charge⁴¹. Thus, the difference in zeta potential value between micelles and nano-emulsion suggested the assembly of amphiphilic block copolymers with PDL as core and PEG as corona. PEGylated particles have been generally regarded as sterically stabilised rather than electrostatically (charge) stabilised⁴².

4.3.3 Characterisation of Drug/Dye loaded Micelles.

The self-assembly behaviour of novel poly(decylactone) block copolymer micelles and ability to act as a model drug carrier was evaluated by using Nile red dye (NR)⁴³.

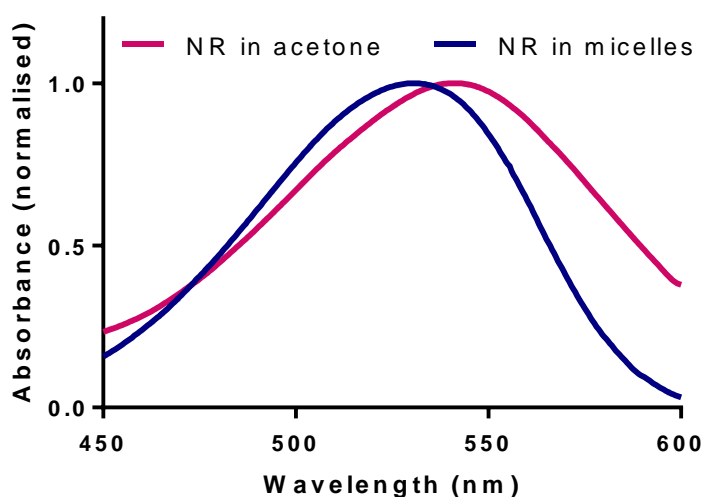


Figure 4-14 UV-Visible absorbance spectra of Nile red (NR) in acetone and micelles. Micelles sample contains encapsulated NR in mPEG-b-PDL micelles dispersed in water.

NR was extensively used to check the self-assembly behaviour of amphiphilic block copolymers⁴⁴. The absorption maxima of NR strongly depend on the polarity of the surrounding environment. Generally the λ_{\max} of NR shifts from a high value to low value with a decrease in the polarity of surrounding media⁴⁴. A clear shift in λ_{\max} (*i.e.* 531 nm) of NR (encapsulated in micelles) was observed when compared with the maximum absorption of dye in acetone solution (λ_{\max} - 541 nm). This result suggested the localisation of NR inside the hydrophobic PDL core of the micelles⁴³ (figure 4-14).

Further, the amount of NR encapsulated in each micelle formulation was calculated using UV-visible spectroscopy. A control sample (water only) showed no solubilisation of NR suggesting the highly hydrophobic behaviour of this dye (figure 4-15). The micelles fabricated from PDL-b-PEG-b-PDL copolymer displayed the maximum dye content (0.81 ± 0.01 wt%) among the tested poly(decalactone) micelles (figure 4-15). The loading percentages were compared using one-way ANOVA with Tukey's correction for multiple comparisons. Using $P < 0.05$ as a statistical significance threshold, only PDL-b-PEG-b-PDL indicated significantly higher loading compared to the other formulations. The rest of formulations did not significantly differ in their dye content (0.69 ± 0.01 and 0.71

± 0.01 wt% for mPEG-b-PDL and mPEG-b-PDL-b-PPDL respectively).

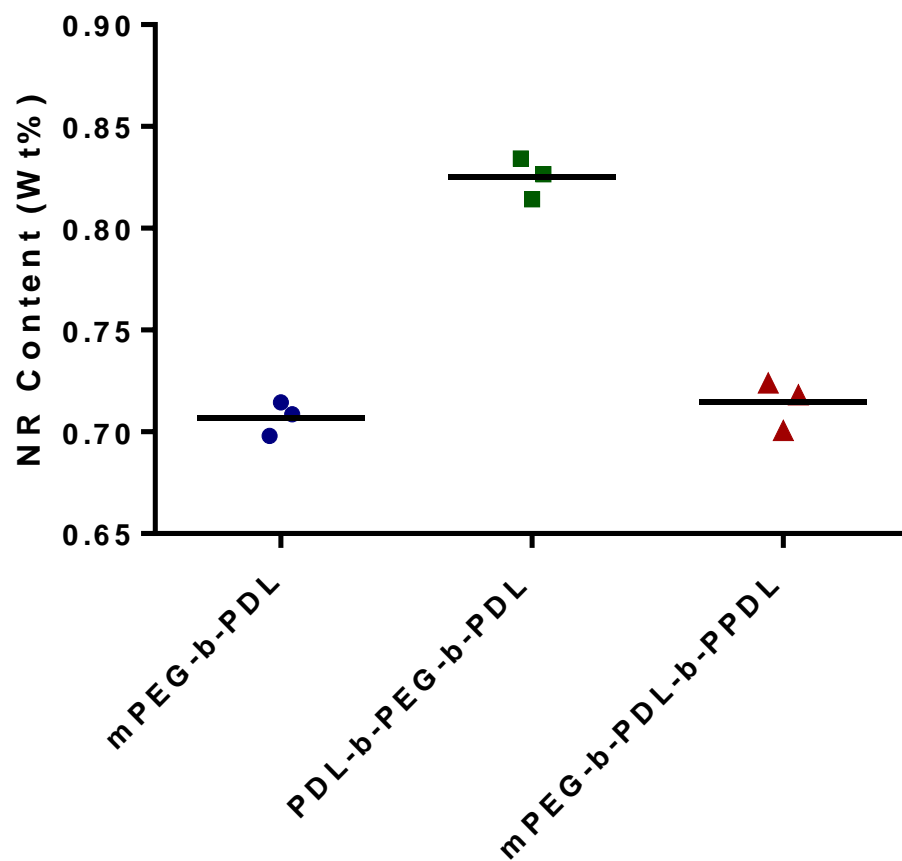
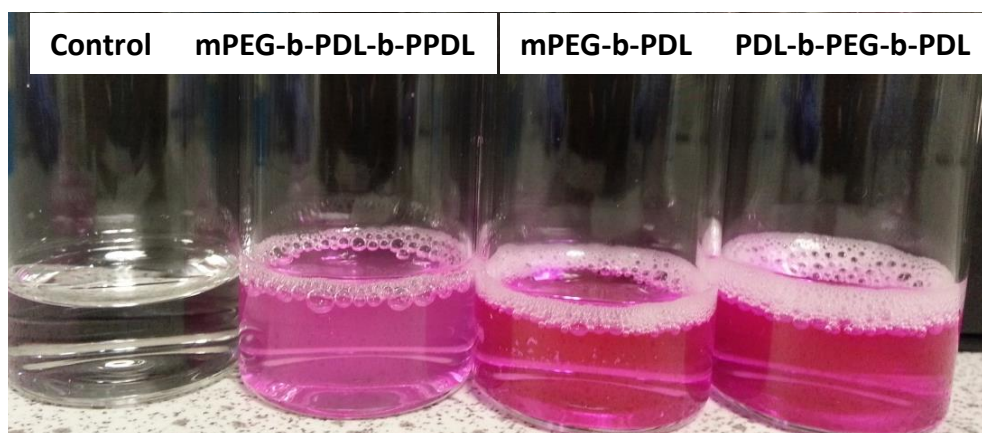


Figure 4-15 (Top) Appearance of micellar solutions and control (formulation without polymer) after Nile red loading and (Bottom) NR content in different polymeric micelles estimate by UV-Visible Spectroscopy. Dots represent separate individual values and bar represents the mean value (n=3).

No significant differences in Z-average sizes of the micelles were observed after NR loading except with PDL-b-PEG-b-PDL micelles (table 4-2). The Z-average size detected by DLS is very sensitive to small changes in the sample distribution, e.g. the presence of a small proportion of aggregates (clusters). Therefore, the reduction in Z-average size of PDL-b-PEG-b-PDL micelles after loading was attributed to the reduction in the percentage of scattered intensity of second peak (observed due to clusters) (table 4-3, figure 4-16D). Due to this reason, the mean size by volume was compared for PDL-b-PEG-b-PDL micelles and no significant difference in size was observed after NR loading (table 4-3, figure 4-16).

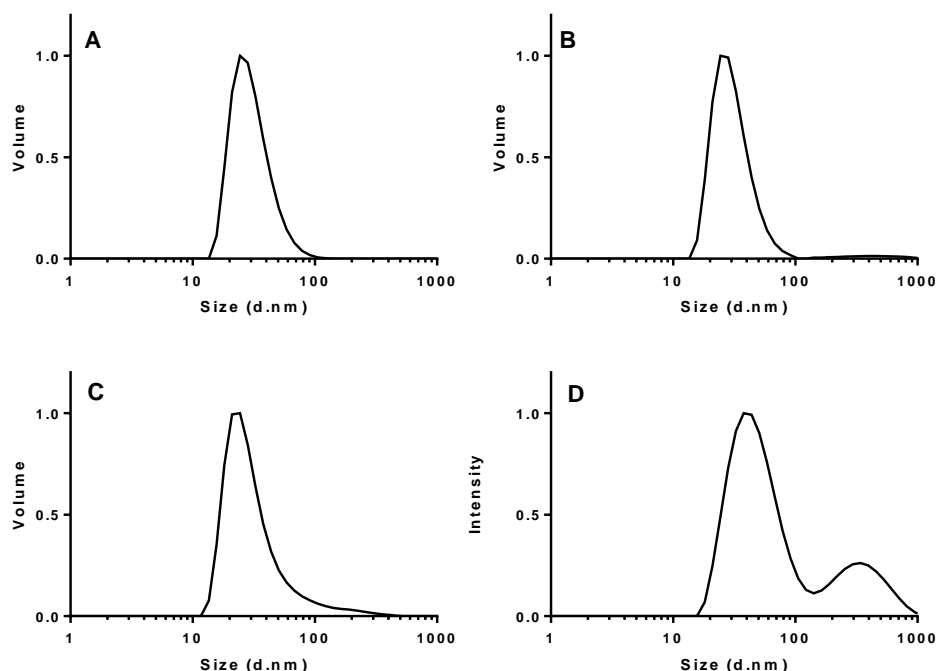


Figure 4-16 Size distribution curve by volume of (A) mPEG-b-PDL, (B) PDL-b-PEG-b-PDL, (C) mPEG-b-PDL-b-PPDL and by intensity of (D) PDL-b-PEG-b-PDL copolymer micelles in water after NR loading.

To further check the surfactant properties of these copolymers, a curcumin loading and release study was performed. Due to the poor stability of curcumin in alkaline conditions and low aqueous solubility (0.6 µg/ml), it was chosen as a model drug to assess the encapsulation efficiency of the novel surfactants²⁴. Curcumin was loaded into the polymeric micelle cores via hydrophobic interactions during the process of self-assembly of the polymer in water. The unencapsulated curcumin was separated from micelles by passing through a PD10 desalting (Sephadex) column. However, loss of curcumin loaded micelles was observed with this method when compared with the purification performed by filtration using syringe filter (0.22 µm). Therefore, all micelles purification were subsequently performed by filtration to avoid loss of material. Similar encapsulation study was performed with mPEG-b-PCL block copolymer micelles for comparison.

The cloudy appearance of PDL-b-PEG-b-PDL micelles solution after purification indicates the presence of clusters in this sample. The loss in volume of mPEG-b-PDL-b-PPDL micelles solution was observed after filtration (reduced due to the filter blockage) (figure 4-17). Purified micelles were analysed using DLS and TEM to determine the size after curcumin loading.

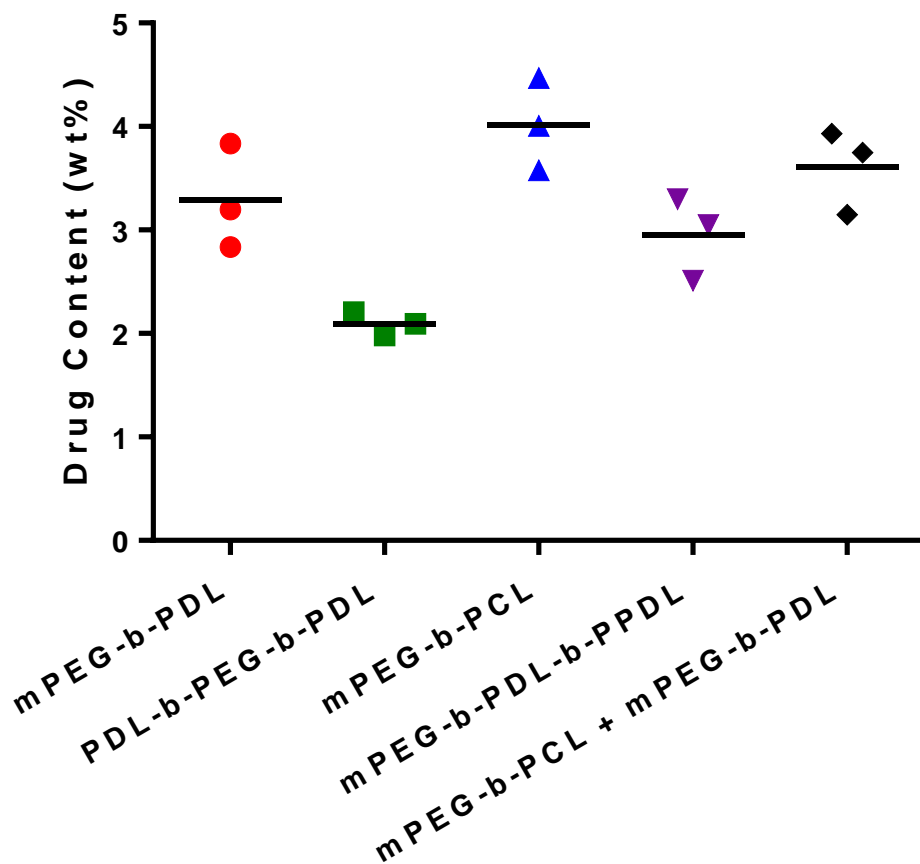
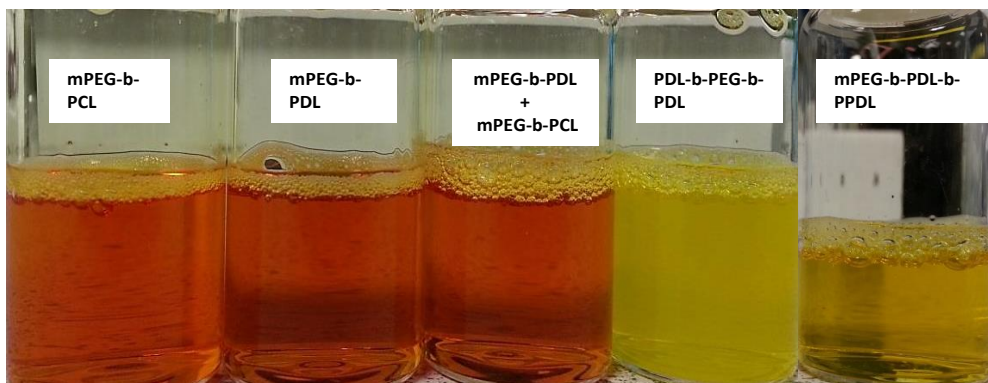


Figure 4-17 Polymer micelles after curcumin loading (Top) and curcumin content in polymeric micelles (Bottom). Dots represent separate individual values and bar represents the mean value (n=3).

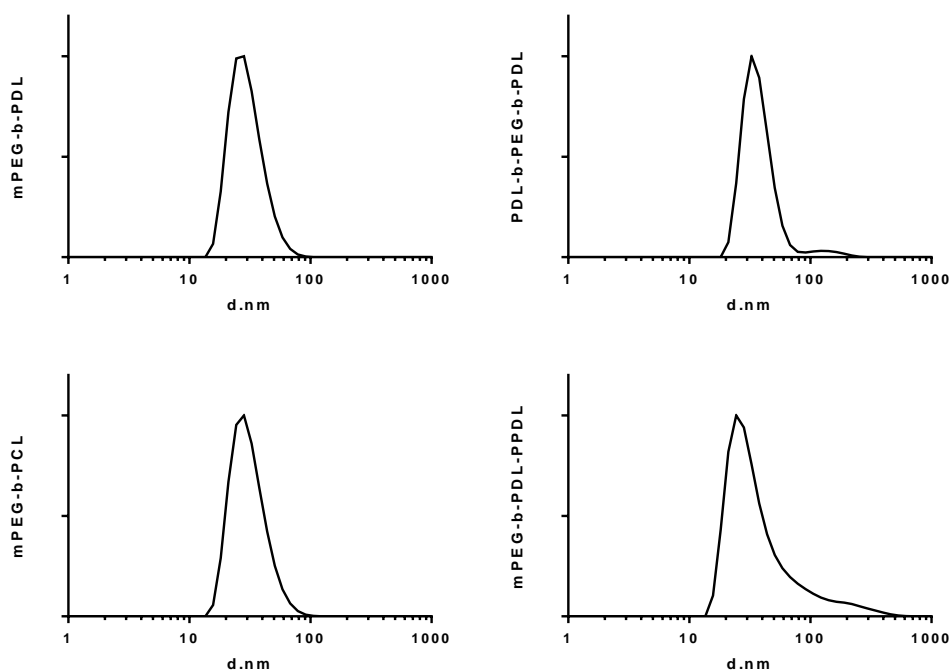


Figure 4-18 Size distribution by volume of the micelles in water after loading of Curcumin. The Z-average size detected for mPEG-b-PDL, PDL-b-PEG-b-PDL, mPEG-b-PCL and mPEG-b-PDL-b-PPDL was 40 ± 3 nm, 123 ± 7 nm, 40 ± 2 nm, and 100 ± 9 nm respectively

Slight increases in the Z-average sizes (except with PDL-b-PEG-b-PDL micelles) of the micelles were observed after curcumin loading when compared to the empty micelles. The increase in the size of the micelles after curcumin loading has also been reported previously^{30, 35, 45, 46}. In contrast, reduction in Z-average size of PDL-b-PEG-b-PDL micelles was observed after curcumin loading (table 4-2). This behaviour was due to the reduction in the percent intensity of the second peak (figure 4-18, table 4-3).

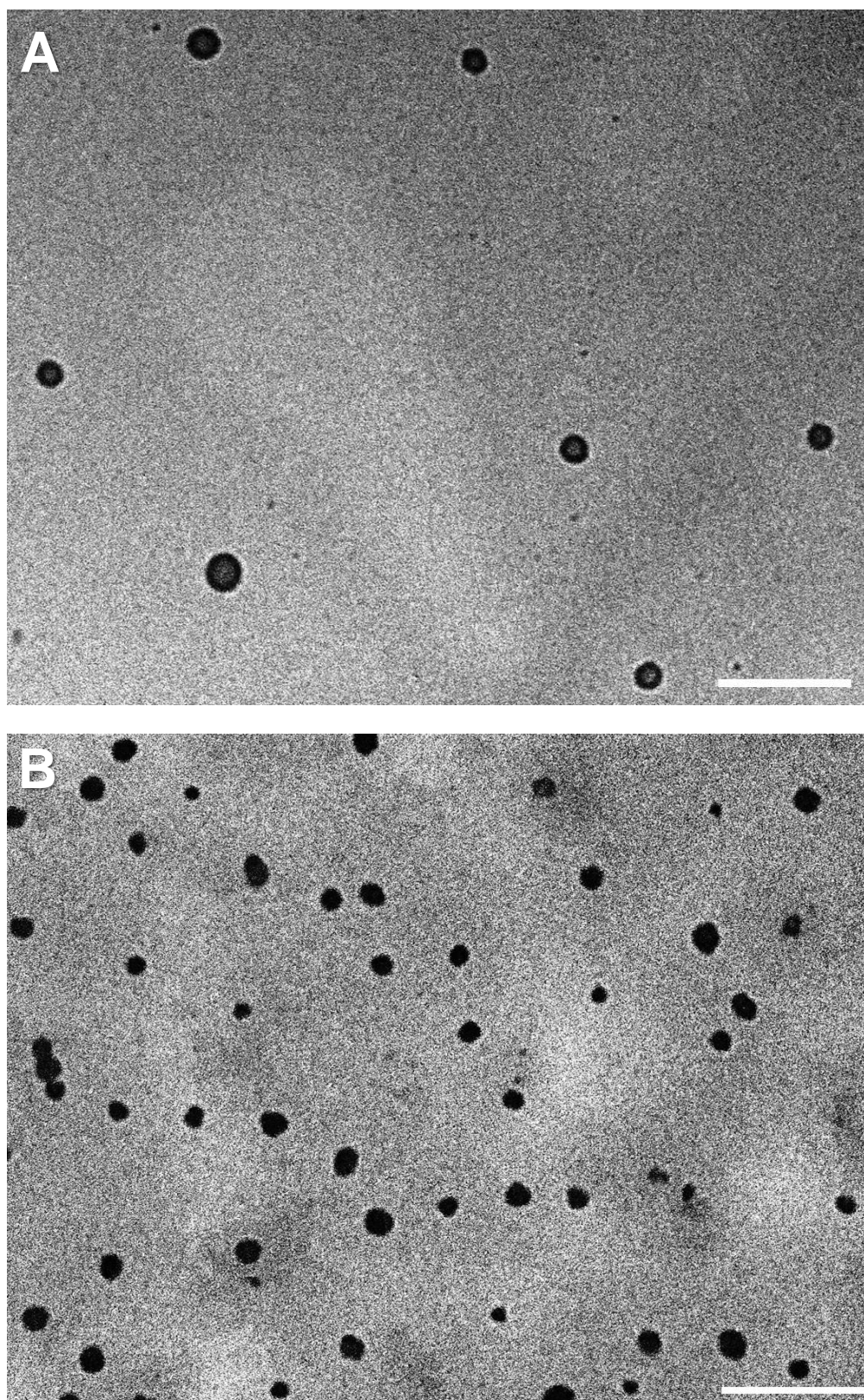


Figure 4-19 TEM images of curcumin loaded micelles of (A) mPEG-b-PDL and (B) mPEG-b-PCL copolymer. Scale bar - 200nm

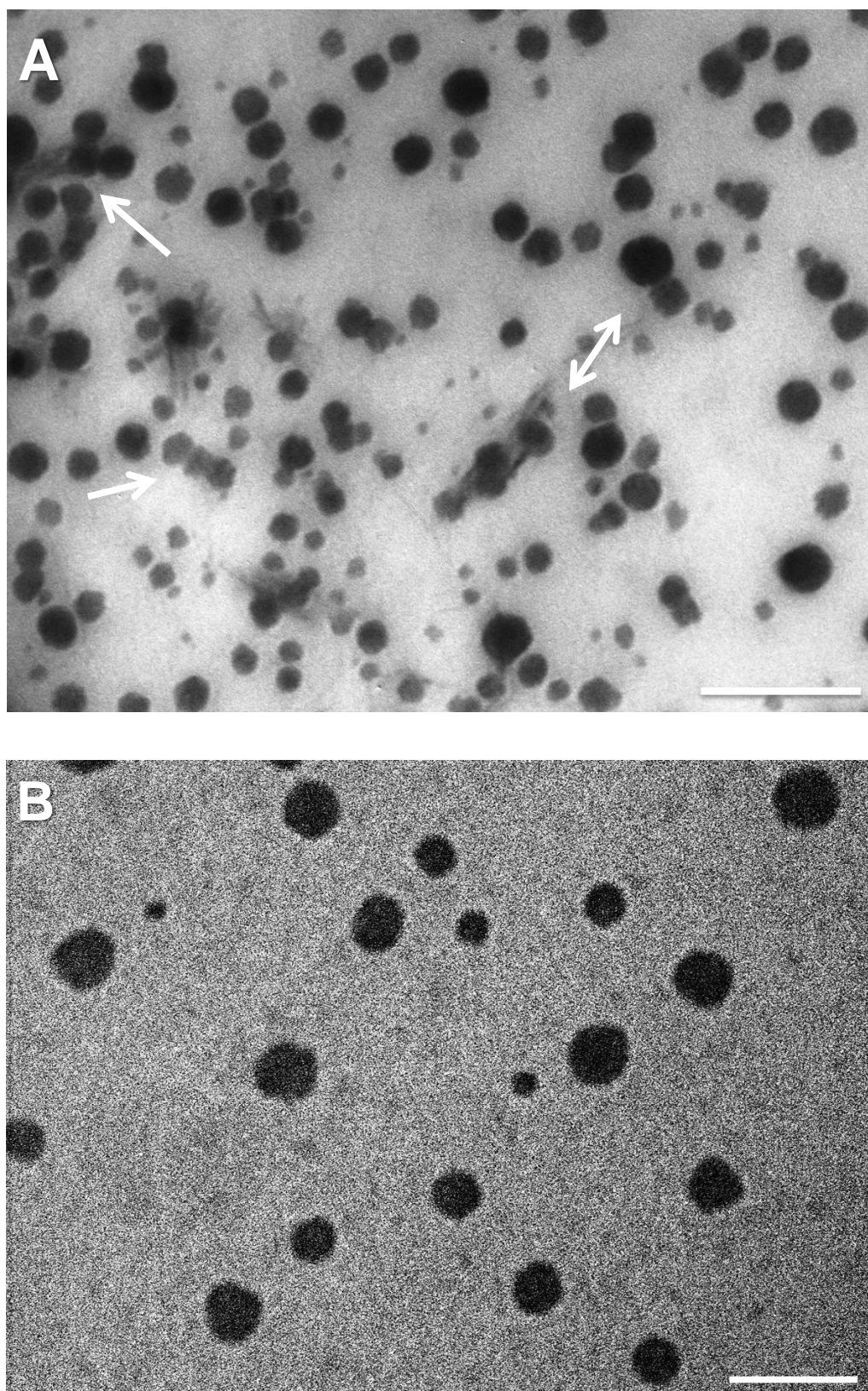


Figure 4-20 TEM images of curcumin loaded micelles of (A) PDL-b-PEG-b-PDL and (B) mPEG-b-PDL-b-PPDL copolymer. Scale bar - 200nm. Arrows represents the aggregates.

TEM images further confirmed the size and suggested that the obtained micelles are spherical in shape with smooth surfaces (Figure 4-19 and 4-20). Again, the presence of clusters (aggregates) in PDL-b-PEG-b-PDL micelles was evident *via* TEM images (Figure 4-20A). No significant difference in surface charge compared to blank micelles confirms the presence of curcumin in the micellar core, which was shielded by the PEG corona (Table 4-2).

The curcumin content and encapsulation efficiency in amphiphilic block copolymers micelles are shown in figure 4-17 and 4-21. The micelles fabricated from mPEG-b-PCL copolymer demonstrated the drug content of 4.0 ± 0.4 weight %, with an encapsulation efficiency of 80.3 ± 8.9 %. The drug content found for mPEG-b-PDL micelles was 3.3 ± 0.5 weight %. Curcumin content in PDL-b-PEG-b-PDL micelles was found to be least (2.1 ± 0.1 weight %) when compared with other studied polymeric micelles. The micelles prepared from mPEG-b-PDL-b-PPDL copolymer showed a drug content of 2.6 ± 0.1 weight %.

Mixed micelles of mPEG-b-PDL and mPEG-b-PCL (1:1) were also prepared to assess any advantage which could be gained by physical mixing of two different amphiphilic block copolymers on the loading and release of curcumin²⁸. The

sizes observed for mixed micelles were almost identical to the sizes observed for mPEG-b-PDL and mPEG-b-PCL micelles. Curcumin content observed in the mixed micelles was 3.6 ± 0.4 weight % (figure 4-17).

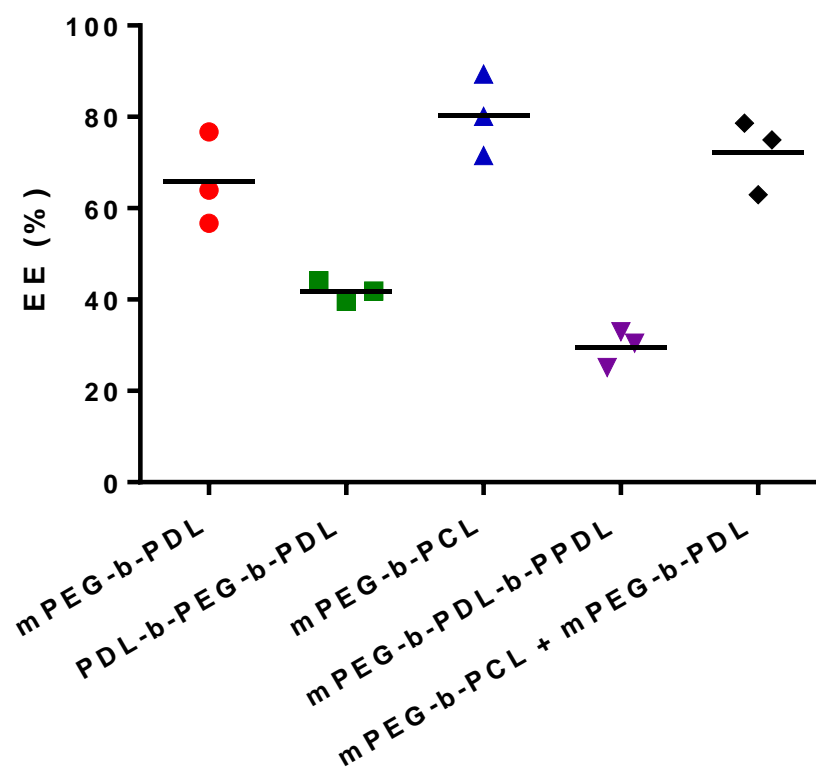


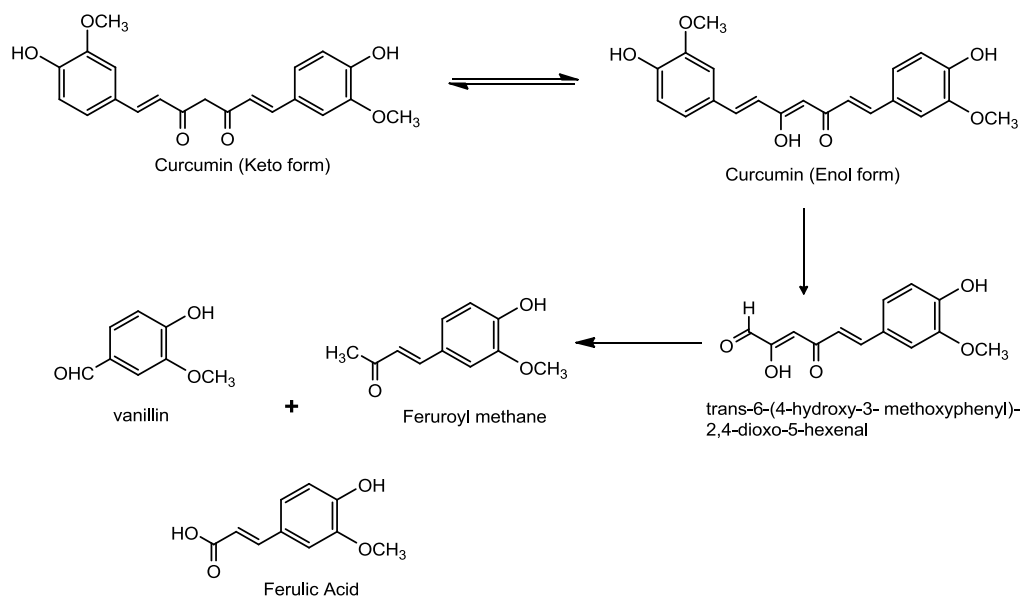
Figure 4-21 Percent encapsulation efficiency (EE%) observed for curcumin in different polymeric micelles

The loading percentages were further compared using one-way ANOVA with Tukey's correction for multiple comparisons. Using $P < 0.05$ as a statistical significance threshold, only PDL-b-PEG-b-PDL micelles loading content showed significant differences when compared to the other formulations. The rest of formulations did not significantly differ in their drug content. Encapsulation efficiency followed the similar pattern

as loading content except for mPEG-b-PDL-b-PPDL micelles in which approximately 40% of loaded polymeric micelles were lost during purification by filtration (figure 4-21).

4.3.4 Curcumin Stability Study and *In vitro* Release Behaviour from Block Copolymers Micelles

It has been reported that curcumin undergoes hydrolytic degradation at alkaline pH⁴⁷. The degradation mechanism of curcumin in PBS is presented in scheme 4-1^{47, 48}.



Scheme 4-1 Degradation products of curcumin observed after its hydrolysis in 0.1 M phosphate buffer, (pH 7.2) at 37°C^{47, 49}.

Hence, evaluation of the degradation rate of curcumin encapsulated in nano-carriers is an important parameter, which needs to be established. mPEG-b-PDL performed better compared to other PDL block copolymers in terms of size and loading, and therefore it was selected for the curcumin

stability study. The stabilities of free curcumin and curcumin loaded in micelles were tested for 10 hrs. Free curcumin was degraded/ hydrolysed completely in 2 hrs whereas only 3% of encapsulated curcumin was degraded after 2 hrs (figure 4-22). After 10 hrs, 10 % degradation of encapsulated curcumin was observed.

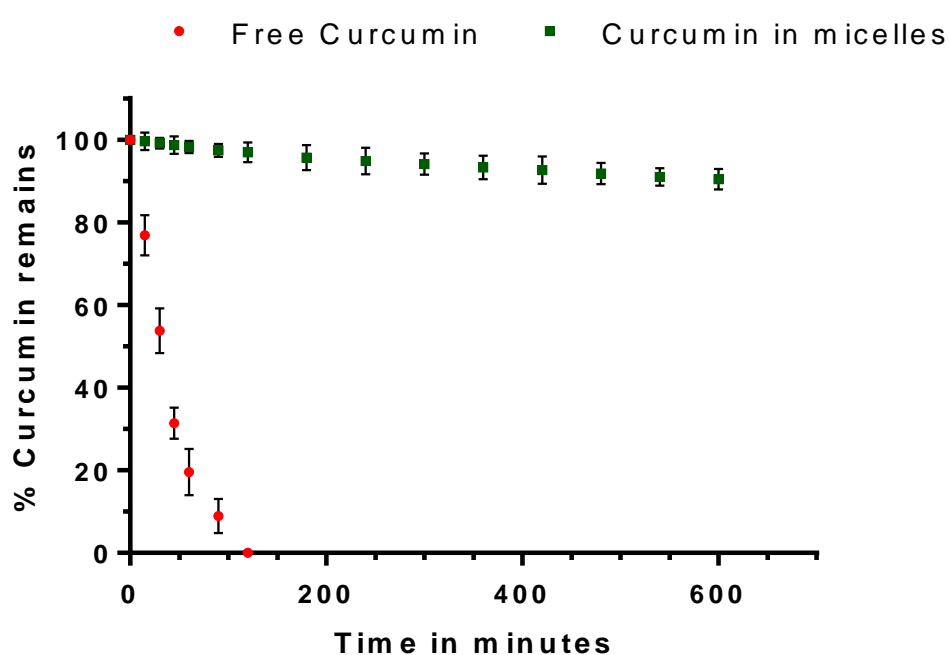


Figure 4-22 Plot representing the percentage of curcumin remains with respect to time of free curcumin and curcumin loaded in micelles incubated in PBS (pH-7.4) at 37°C.

Determination of the release pattern of loaded drug from a drug delivery carrier is an important parameter, which needs to be assessed before performing any *in vivo* experiments. This experiment was intended to show how quickly a carrier system releases the encapsulated content to the surroundings.

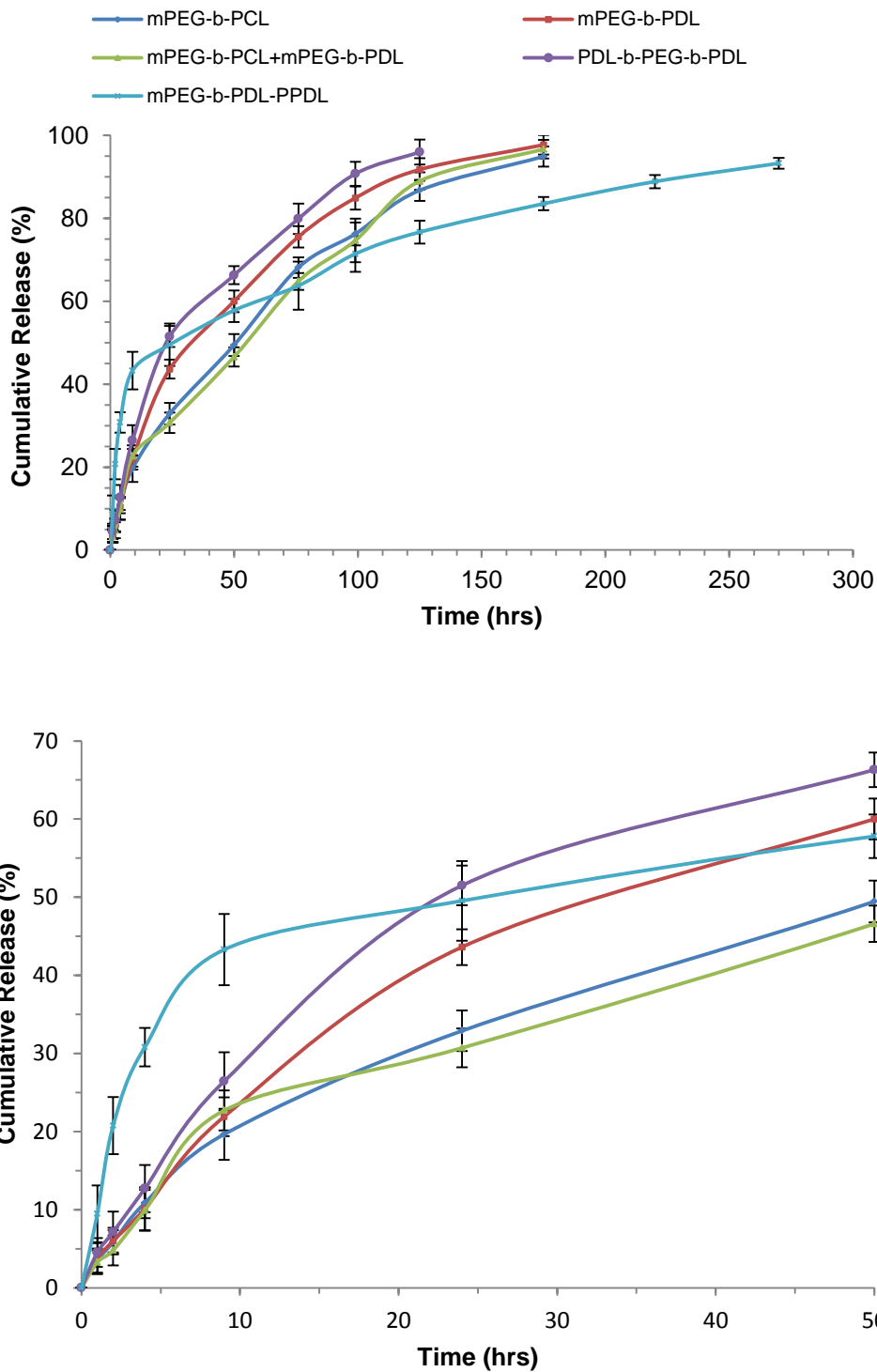


Figure 4-23 *In-vitro* release pattern of curcumin from different block copolymer micelles (top) and zoomed graph showing the release pattern observed in first 50 hrs (bottom) using PBS as release media at 37°C

Generally a controlled release pattern from a polymeric system is desirable to justify its potential as a drug delivery carrier⁵⁰. Curcumin showed rapid degradation in the chosen release medium and therefore samples were collected directly from the dialysis tube to avoid any error due to drug degradation³⁵. The release patterns of curcumin from the different amphiphilic block copolymers micelles are presented in figure 4-23.

Initial burst release of curcumin was observed in all samples where 43% of release was observed with mPEG-b-PDL-b-PPDL micelles and 19% of release was noticed with mPEG-b-PCL micelles in first 9 hrs. More than 95 % of curcumin was released from mPEG-b-PDL, mPEG-b-PCL and mPEG-b-PDL + mPEG-b-PCL micelles after 175 hrs however, mPEG-b-PDL-b-PPDL micelles showed only 83% release. Micelles of PDL-b-PEG-b-PDL copolymer displayed rapid release (96 % after 125 hrs) compared to the release pattern observed with mPEG-b-PDL-b-PPDL micelles (93 % after 270hrs). In summary, faster release was observed with micelles containing PDL block as core when compared to PCL or PPDL as core forming block. The rapid release from the mPEG-b-PDL could be useful in the cases where incomplete release of drug was observed⁵¹.

4.4 Discussions

It is well established that the CMCs of amphiphilic block copolymers decrease with increase in the hydrophobicity⁵. As per the molecular weight calculated by ¹HNMR, the hydrophobicity sequences of PDL block copolymers are mPEG-b-PDL < PDL-b-PEG-b-PDL < mPEG-b-PDL-b-PPDL. However, no significant differences in CMCs were observed due to the minor difference in the hydrophobic chain molecular weight (figure 4-6) but, if mean values were compared, mPEG-b-PDL-b-PPDL demonstrated the lowest CMC value as predicted based on hydrophobic block content. CMC value calculated for mPEG-b-PCL micelles was matched with the previously reported value where the hydrophobic to hydrophilic block ratio were similar^{52, 53}.

CMC values generated by the pyrene method for novel block copolymers of poly(decylactone) were lower compared to the well-established amphiphilic block copolymer of poly(caprolactone). The reason for significantly lower CMC values for PDL block copolymer micelles compared to the similar molecular weight poly (caprolactone) copolymer attributed to the presence of an additional hydrophobic alkyl side chain on PDL structure. A similar phenomenon was reported earlier in which copolymers of poly (lactide)

synthesised by using alkyl chain substituted lactide monomer displayed lower CMC compared to their un-substituted analogues⁴³. It has been known that polymers with low CMC values are more stable *in vivo* thus preventing the premature release of loaded therapeutic agents before reaching the target sites^{2, 54}. Therefore, it can be hypothesised that the novel poly(decylactone) block copolymers could perform better when compared to the poly(caprolactone) block copolymers.

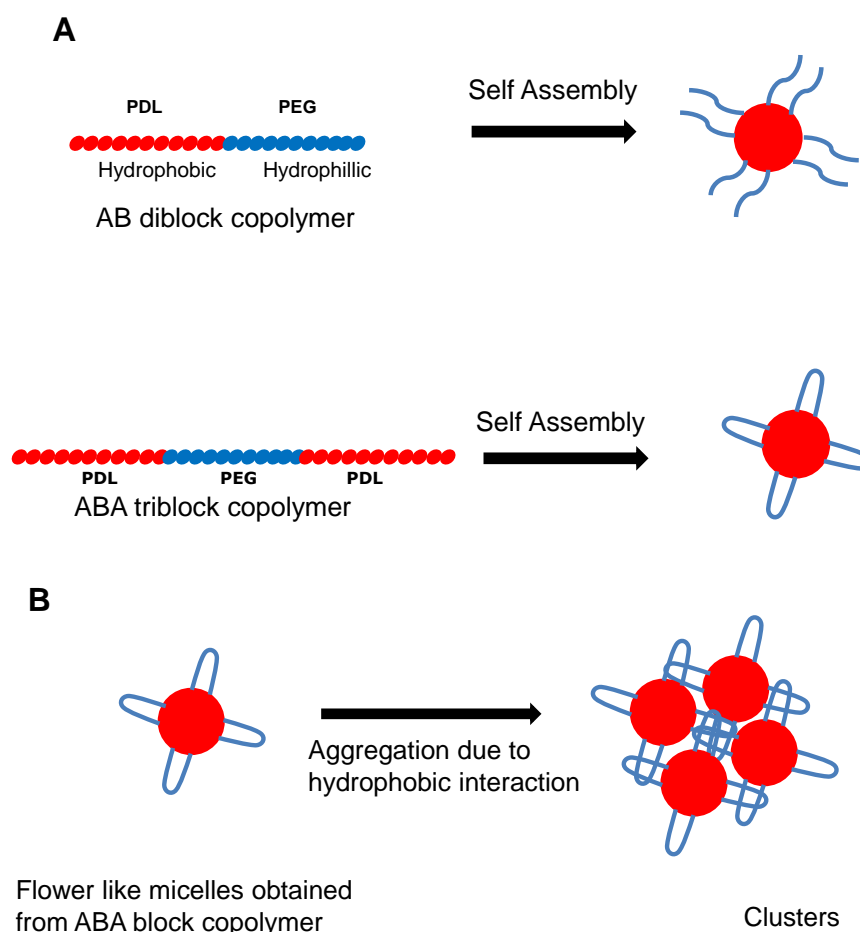


Figure 4-24 (A) Proposed assembly of synthesized di-block and tri-block copolymer in water and (B) the formation of cluster from triblock copolymer micelles.

The average sizes detected for the empty mPEG-b-PDL micelles were similar to the sizes of empty mPEG-b-PCL micelles. Similar sizes micelles were expected to generate from both AB type copolymer due to comparable hydrophobic to hydrophilic ratio. The average sizes detected for mPEG-b-PCL micelles were also matched with the sizes reported in literatures^{24, 37, 52, 55}.

A bimodal size distribution observed with ABA type copolymer (PDL-b-PEG-b-PDL) was probably due to the hydrophobic-hydrophobic interaction between cores of the micelles which led in aggregation⁵⁶ (figure 4-24). It has been proposed that an ABA type block copolymer can assemble in flowered shaped micelle⁵⁷. This could lead to decrease in the length of PEG chain, which separates the core from surrounding environment. In addition, the PDL-b-PEG-b-PDL copolymer was synthesised using a small chain PEG ($M_n - 4000$) and hence was expected to have a less dense corona. A slight negative zeta potential of PDL-b-PEG-b-PDL micelles also confirmed the presence of a less dense shell of PEG. It was reported that PEG imparts steric stability to micelles by minimizing the interfacial free energy of the micellar core and by inhibiting hydrophobic inter-micellar attractions⁵⁸. Thus, due to the presence of a less dense shell, some aggregation

was observed with triblock copolymers, which in turn gave bimodal size distribution³.

Similar phenomena was reported earlier with PCL-b-PEG-b-PCL micelles in which the presence of aggregates (clusters) was proposed⁵⁹. Cluster formation was also reported with poly(t-butyl methacrylate) ABA block-copolymer micelles⁶⁰ and polystyrene-b-poly(ethylene oxide) block copolymer micelles⁶¹. Clusters of micelles may have different bio-distribution and could be eliminated through the RES system from the body and thus would have impaired performance *in vivo*⁶². Hence, it could be possible that PDL-b-PEG-b-PDL micelles would not perform well *in vivo* compared to other PDL block copolymer micelles due to its tendency of clusters formation.

The large size observed with mPEG-b-PDL-b-PPDL micelles may be attributed to the poor solubility of copolymer in acetone. Addition of crystalline PPDL block⁶³ in mPEG-b-PDL copolymer reduced the overall solubility of the resultant copolymer (figure 4-25). Due to the high polydispersity of mPEG-b-PDL-b-PPDL copolymer (M_w/M_n by SEC – 1.25), there is a possibility of existence of some copolymer chains with high molecular weight PPDL blocks. These particular copolymers chains with poor solubility in acetone could be

responsible for generating bigger size micelles. Acetone is not a good solvent for poly(pentadecalactone) block and thus, this component of the copolymer would have been in a more collapsed state and possibly formed aggregates in acetone. During nano-precipitation, these collapsed chains present in the acetone (aggregates) produced larger size micelles⁶⁴ and thus gave broad size distribution.

Additionally, the presence of particles of diameter above the pore size of filter (*i.e.* 220 nm) in sample was responsible for the blockage of syringe filter. Therefore, 2-3 units of syringe filter were employed to filter the mPEG-b-PDL-b-PPDL micellar suspension, which potentially caused the loss of micellar suspension due to the retention/absorption of some material on each syringe filter thus gave low recovery.

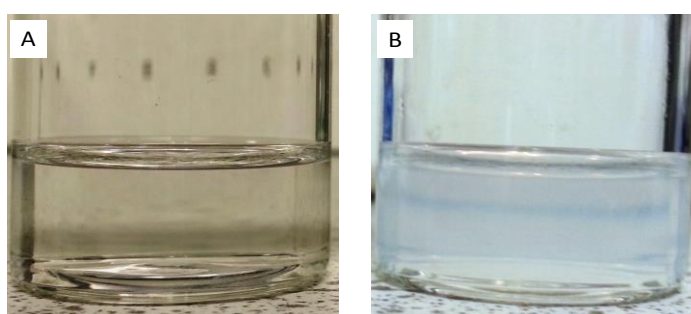


Figure 4-25 Physical appearance of (A) mPEG-b-PDL and (B) mPEG-b-PDL-b-PPDL copolymer (50mg each) in 5mL acetone

No significant differences in mean sizes of novel block copolymer micelles were observed after NR loading except with PDL-b-PEG-b-PDL micelles. This discrepancy was due to

the reduction in the intensity of clusters after NR loading, which reduced the overall mean size. NR loading study proposed that these novel micelles are able to encapsulate hydrophobic moieties inside their core and can act as solubilisation tool. Based on this result, curcumin encapsulation study was also performed to further evaluate the drug incorporation efficiency of the polymer micelles. In contrast to NR loading results, PDL-b-PEG-b-PDL micelles demonstrated lower loading of curcumin compared to other block copolymers. This behaviour could be attributed to the core compatibility with a particular drug. The ability of a hydrophobic core to encapsulate a drug mainly depends upon its compatibility with the drug molecule^{3, 65}. It was assumed that curcumin could be less compatible with PDL polymer and therefore micelles with PDL core forming block demonstrated low loading compared to micelles with PCL core.

Curcumin content observed with mPEG-b-PCL micelles in this study was significantly less when compared with previously reported results. In most of the reported studies, curcumin loadings with amphiphilic block copolymers of poly(caprolactone) of similar hydrophobic to hydrophilic block ratios were found to be more than 7.0 weight %^{45, 66-68}. However, there were some studies, in which the curcumin

loading using poly(caprolactone) block copolymer was reported to be less than 5.0 weight %^{30, 35, 68}.

The variation in the results of curcumin loading with mPEG-b-PCL micelles might have been due to the different parameters used for loading in the various individual studies. Encapsulation procedure, drug to polymer ratio, molecular weight of polymer, solvent used etc. can significantly influence the loading content^{30, 35, 66, 68}. Since, the objective of current study was to compare the loading results obtained from novel and well established block copolymers rather than maximise specific drug loading. Thus, the optimisation of the formulation parameters was not performed to achieve the maximum drug loading.

Curcumin loading observed with mixed micelles suggested that mixing of the novel renewable copolymer (mPEG-b-PDL) with a copolymer synthesised from non-renewable feedstock (mPEG-b-PCL) could produce similar results when compared with the results obtained from poly(caprolactone) copolymer alone. Thus, mixed micelle approach might be useful to reduce the amount of non-renewable copolymer in the overall formulation. Further optimisation of loading parameters could produce better results but was not studied in current work due to time constraints.

The degradation rate of curcumin encapsulated in mPEG-b-PDL micelles was slower compared to free drug, suggesting that the curcumin was located inside the highly hydrophobic PDL core. Due to this reason, the direct contact of curcumin with PBS was hampered thus, the hydrolytic degradation rate was reduced. The mPEG-b-PDL micelle's ability to protect the degradation of curcumin was similar to the mPEG-b-PCL micelles reported by Ma et.al.³⁵

In release experiment, Burst release observed from all micelles could be attributed to the presence of some amount of curcumin on the exterior part (surface) of the PDL block. The initial burst release of curcumin from polymeric micelles was also reported earlier in which 30-40 % of drug was released within 10 hrs^{26, 45, 69}. On the basis of the release results, it can be proposed that the diffusion mechanism was mainly responsible for the release of curcumin from the studied micelles. It has been reported that polymers with low T_m , T_g value and low crystallinity release their loaded content rapidly^{70, 71}. Therefore, the drug permeated faster from the amorphous PDL core compared to semicrystalline (PCL) or crystalline (PPDL) core polymeric micelles⁷². A similar release pattern has been reported with PLGA nano carriers where

increase in the composition of D, L -PLA (amorphous polymer) increased the release rate of loaded drug^{12, 73}.

Delayed release observed from mPEG-b-PDL-b-PPDL micelles was most likely due to the restricted diffusion of drug from the more crystalline poly(pentadecalactone) core⁷⁴. Similar phenomena were observed earlier with poly(propylene succinate-co-caprolactone) copolymer nanoparticles where mixing of crystalline polymer with amorphous polymer decreased the release rate compared to the release observed from the amorphous polymer only⁷¹.

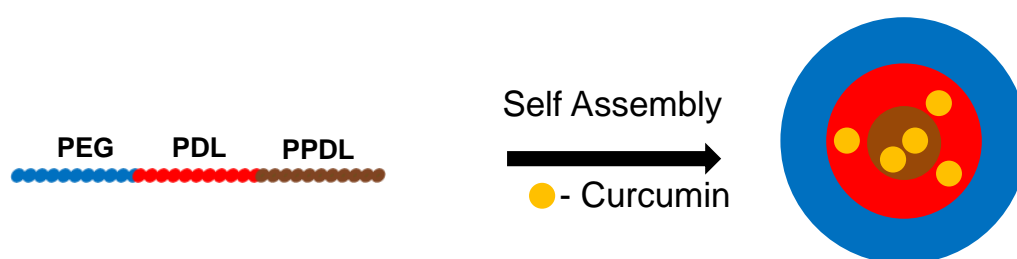


Figure 4-26 Proposed encapsulation of curcumin in mPEG-b-PDL-b-PPDL copolymer micelles. Due to the layered hydrophobic core, curcumin can be localised at PDL and PPDL core.

A significant percentage of burst release observed with mPEG-b-PDL-b-PPDL micelles might have been associated with the presence of some larger size micelles. In this formulation, the drug molecules that were located in the PDL core, from the big micelles permeated (diffused) faster due to the large surface area when compared to the small size micelles (figure 4-26).

The release rate observed for mPEG-b-PCL micelles in this study was more sustained than previously reported release pattern for mPEG-b-PCL micelles of similar molecular weight³⁵. This difference in release pattern can be attributed to the concentration of curcumin, sample withdrawal method and release media used for the study. It was reported that when higher drug concentration was used for the release study, a more sustained release pattern was observed⁷⁵. Additionally, the release pattern could be different in the different release media, based on the partition coefficient of the drug at different pH.

4.5 Conclusion

In this chapter, the self-assembly and encapsulation behaviour of novel poly(decalactone) block copolymer micelles was demonstrated. These novel amphiphilic block copolymers possess low CMC values compared to the similar molecular weight mPEG-b-PCL copolymer. The CMC values of novel amphiphilic block copolymers range between 1.07-1.77 µg/mL in water, calculated from pyrene fluorescence method. Micelles of amphiphilic block copolymers were prepared by nano-precipitation method and no significant difference in size of mPEG-b-PDL and mPEG-b-PCL micelles were observed. Micelles obtained from PDL-b-PEG-b-PDL copolymer gave a

bimodal size distribution, in which the second peak was due to the formation of clusters. The Z-average size detected for mPEG-b-PDL-b-PPDL copolymer micelles were significantly higher when compared with mPEG-b-PDL micelles. The difference in size of these micelles was attributed to the change in solubility of mPEG-b-PDL-b-PPDL copolymer in acetone, which in turn produced some large size micelles. Micelles fabricated from all block copolymers were of roughly spherical in shape as evident by TEM images. The zeta potential obtained in HEPES buffer (10mM, pH-7.4) for block copolymer micelles was almost neutral except for PDL-b-PEG-b-PDL micelles, which was slightly negative due to the less dense PEG corona. It was hypothesised that due to the less dense corona, the micelles obtained from PDL-b-PEG-b-PDL block copolymer were prone to aggregates thus gave large size micelles.

All novel block copolymers were successfully encapsulated Nile red and curcumin. A shift in UV-Vis absorbance maxima of NR suggested the self-assembly of block copolymer in water with PDL core. NR and curcumin loading did not significantly change the diameter of micelles except in case of PDL-b-PEG-b-PDL where reduction in clusters volume led to decrease in average diameter. No significant difference in curcumin

loading content was observed with mPEG-b-PDL and mPEG-b-PDL-b-PPDL micelles when compared to the well-established mPEG-b-PCL copolymer micelles. Micelles of mPEG-b-PDL were also demonstrated its ability to reduce degradation of curcumin at physiological pH. *In vitro* release studies of curcumin loaded micelles suggested that micelles having the more amorphous poly(decalactone) core gave the faster release compared to semicrystalline poly(caprolactone) and poly(pentadecalactone) core.

From the results obtained in different studies, it was concluded that the overall performance of novel mPEG-b-PDL copolymer micelles was better (in terms of size, loading and release) when compared with the other PDL block copolymers studied in this work. Additionally, the performance of mPEG-b-PDL micelles was almost equivalent to the mPEG-b-PCL micelles. Therefore, mPEG-b-PDL copolymer was selected for further evaluation of its drug delivery capability.

4.6 References

1. Williams, H. D.; Trevaskis, N. L.; Charman, S. A.; Shanker, R. M.; Charman, W. N.; Pouton, C. W.; Porter, C. J. H., *Pharmacological Reviews* **2013**, 65 (1), 315-499.
2. Rangel-Yagui, C. O.; Pessoa, A.; Tavares, L. C., *Journal of Pharmacy and Pharmaceutical Sciences* **2005**, 8 (2), 147-163.
3. Lu, Y.; Park, K., *International Journal of Pharmaceutics* **2013**, 453 (1), 198-214.
4. Torchilin, V. P., *Pharmaceutical Research* **2007**, 24 (1), 1-16.
5. Gaucher, G.; Dufresne, M. H.; Sant, V. P.; Kang, N.; Maysinger, D.; Leroux, J. C., *Journal of Controlled Release* **2005**, 109 (1-3), 169-188.
6. Aliabadi, H. M.; Lavasanifar, A., *Expert opinion on drug delivery* **2006**, 3 (1), 139-62.
7. Torchilin, V. P., *Journal of Controlled Release* **2001**, 73 (2-3), 137-172.
8. Maeda, H.; Wu, J.; Sawa, T.; Matsumura, Y.; Hori, K., *Journal of Controlled Release* **2000**, 65 (1-2), 271-284.
9. Warwel, S.; Bruse, F.; Demes, C.; Kunz, M.; Klaas, M. R. G., *Chemosphere* **2001**, 43 (1), 39-48.
10. Hagan, S. A.; Coombes, A. G. A.; Garnett, M. C.; Dunn, S. E.; Davis, M. C.; Illum, L.; Davis, S. S.; Harding, S. E.; Purkiss, S.; Gellert, P. R., *Langmuir* **1996**, 12 (9), 2153-2161.
11. Lee, J. Y.; Cho, E. C.; Cho, K., *Journal of Controlled Release* **2004**, 94 (2-3), 323-335.
12. .
13. Kohori, F.; Sakai, K.; Aoyagi, T.; Yokoyama, M.; Sakurai, Y.; Okano, T., *Journal of Controlled Release* **1998**, 55 (1), 87-98.
14. Miller, S. A., *Acs Macro Letters* **2013**, 2 (6), 550-554.
15. Kallinteri, P.; Higgins, S.; Hutcheon, G. A.; St Pourcain, C. B.; Garnett, M. C., *Biomacromolecules* **2005**, 6 (4), 1885-1894.
16. Schubert, S.; Delaney, J. T., Jr.; Schubert, U. S., *Soft Matter* **2011**, 7 (5), 1581-1588.
17. Kim, S. Y.; Shin, I. L. G.; Lee, Y. M.; Cho, C. S.; Sung, Y. K., *Journal of Controlled Release* **1998**, 51 (1), 13-22.
18. Zhang, J. X.; Yan, M. Q.; Li, X. H.; Qiu, L. Y.; Li, X. D.; Li, X. J.; Jin, Y.; Zhu, K. J., *Pharmaceutical Research* **2007**, 24 (10), 1944-1953.

19. Castro, G. R.; Larson, B. K.; Panilaitis, B.; Kaplan, D. L., *Applied Microbiology and Biotechnology* **2005**, 67 (6), 767-770.
20. Chen, W.; Meng, F.; Li, F.; Ji, S.-J.; Zhong, Z., *Biomacromolecules* **2009**, 10 (7), 1727-1735.
21. Aggarwal, B. B.; Kumar, A.; Bharti, A. C., *Anticancer Research* **2003**, 23 (1A), 363-398.
22. Anand, P.; Kunnumakkara, A. B.; Newman, R. A.; Aggarwal, B. B., *Molecular Pharmaceutics* **2007**, 4 (6), 807-818.
23. Goel, A.; Kunnumakkara, A. B.; Aggarwal, B. B., *Biochemical Pharmacology* **2008**, 75 (4), 787-809.
24. Naksuriya, O.; Okonogi, S.; Schiffelers, R. M.; Hennink, W. E., *Biomaterials* **2014**, 35 (10), 3365-3383.
25. Yallapu, M. M.; Jaggi, M.; Chauhan, S. C., *Drug Discovery Today* **2012**, 17 (1-2), 71-80.
26. Zhao, L.; Du, J.; Duan, Y.; Zang, Y. n.; Zhang, H.; Yang, C.; Cao, F.; Zhai, G., *Colloids and Surfaces B-Biointerfaces* **2012**, 97, 101-108.
27. Saxena, V.; Hussain, M. D., *Journal of Biomedical Nanotechnology* **2013**, 9 (7), 1146-1154.
28. Attia, A. B. E.; Ong, Z. Y.; Hedrick, J. L.; Lee, P. P.; Ee, P. L. R.; Hammond, P. T.; Yang, Y.-Y., *Current Opinion in Colloid & Interface Science* **2011**, 16 (3), 182-194.
29. Aguiar, J.; Carpena, P.; Molina-Bolivar, J. A.; Ruiz, C. C., *Journal of Colloid and Interface Science* **2003**, 258 (1), 116-122.
30. Gou, M.; Men, K.; Shi, H.; Xiang, M.; Zhang, J.; Song, J.; Long, J.; Wan, Y.; Luo, F.; Zhao, X.; Qian, Z., *Nanoscale* **2011**, 3 (4), 1558-1567.
31. Bae, Y.; Diezi, T. A.; Zhao, A.; Kwon, G. S., *Journal of Controlled Release* **2007**, 122 (3), 324-330.
32. Mason, T. G.; Wilking, J. N.; Meleson, K.; Chang, C. B.; Graves, S. M., *Journal of Physics-Condensed Matter* **2006**, 18 (41), R635-R666; Kentish, S.; Wooster, T. J.; Ashokkumar, A.; Balachandran, S.; Mawson, R.; Simons, L., *Innovative Food Science & Emerging Technologies* **2008**, 9 (2), 170-175.
33. Thomas, J. C., *Journal of Colloid and Interface Science* **1987**, 117 (1), 187-192.
34. Leung, M. H. M.; Kee, T. W., *Langmuir* **2009**, 25 (10), 5773-5777.
35. Ma, Z.; Haddadi, A.; Molavi, O.; Lavasanifar, A.; Lai, R.; Samuel, J., *Journal of Biomedical Materials Research Part A* **2008**, 86A (2), 300-310.

36. Aliabadi, H. M.; Elhasi, S.; Mahmud, A.; Gulamhusein, R.; Mahdipoor, P.; Lavasanifar, A., *International Journal of Pharmaceutics* **2007**, 329 (1-2), 158-165.
37. Shuai, X. T.; Ai, H.; Nasongkla, N.; Kim, S.; Gao, J. M., *Journal of Controlled Release* **2004**, 98 (3), 415-426.
38. Kaszuba, M.; McKnight, D.; Connah, M.; McNeil-Watson, F.; Nobbmann, U.
39. Tadros, T.; Izquierdo, R.; Esquena, J.; Solans, C., *Advances in Colloid and Interface Science* **2004**, 108, 303-318.
40. Freitas, C.; Muller, R. H., *International Journal of Pharmaceutics* **1998**, 168 (2), 221-229.
41. Merdan, T.; Kunath, K.; Petersen, H.; Bakowsky, U.; Voigt, K. H.; Kopecek, J.; Kissel, T., *Bioconjugate Chemistry* **2005**, 16 (4), 785-792; Lai, S. K.; O'Hanlon, D. E.; Harrold, S.; Man, S. T.; Wang, Y.-Y.; Cone, R.; Hanes, J., *Proceedings of the National Academy of Sciences of the United States of America* **2007**, 104 (5), 1482-1487.
42. Ishida, T.; Ichikawa, T.; Ichihara, M.; Sadzuka, Y.; Kiwada, H., *Journal of Controlled Release* **2004**, 95 (3), 403-412; Salmaso, S.; Caliceti, P., *Journal of drug delivery* **2013**, 2013, 374252-374252; Sweet, D. M.; Kolhatkar, R. B.; Ray, A.; Swaan, P.; Ghandehari, H., *Journal of Controlled Release* **2009**, 138 (1), 78-85.
43. Trimaille, T.; Mondon, K.; Gurny, R.; Moeller, M., *International Journal of Pharmaceutics* **2006**, 319 (1-2), 147-154.
44. Wyszogrodzka, M.; Haag, R., *Chemistry-a European Journal* **2008**, 14 (30), 9202-9214.
45. Shao, J.; Zheng, D.; Jiang, Z.; Xu, H.; Hu, Y.; Li, X.; Lu, X., *Acta Biochimica Et Biophysica Sinica* **2011**, 43 (4), 267-274.
46. Wang, K.; Zhang, T.; Liu, L.; Wang, X.; Wu, P.; Chen, Z.; Ni, C.; Zhang, J.; Hu, F.; Huang, J., *International journal of nanomedicine* **2012**, 7, 4487-97.
47. Wang, Y. J.; Pan, M. H.; Cheng, A. L.; Lin, L. I.; Ho, Y. S.; Hsieh, C. Y.; Lin, J. K., *Journal of Pharmaceutical and Biomedical Analysis* **1997**, 15 (12), 1867-1876.
48. Sharma, R. A.; Gescher, A. J.; Steward, W. P., *European Journal of Cancer* **2005**, 41 (13), 1955-1968.
49. Priyadarsini, K. I., *Journal of Photochemistry and Photobiology C-Photochemistry Reviews* **2009**, 10 (2), 81-95.
50. Uhrich, K. E.; Cannizzaro, S. M.; Langer, R. S.; Shakesheff, K. M., *Chemical Reviews* **1999**, 99 (11), 3181-3198.

51. Shaikh, J.; Ankola, D. D.; Beniwal, V.; Singh, D.; Kumar, M. N. V. R., *European Journal of Pharmaceutical Sciences* **2009**, *37* (3-4), 223-230.
52. Xie, W.; Zhu, W.; Shen, Z., *Polymer* **2007**, *48* (23), 6791-6798.
53. Gao, X.; Wang, B.; Wei, X.; Rao, W.; Ai, F.; Zhao, F.; Men, K.; Yang, B.; Liu, X.; Huang, M.; Gou, M.; Qian, Z.; Huang, N.; Wei, Y., *International Journal of Nanomedicine* **2013**, *8*, 971-982.
54. Sezgin, Z.; Yuksel, N.; Baykara, T., *European journal of pharmaceuticals and biopharmaceutics : official journal of Arbeitsgemeinschaft fur Pharmazeutische Verfahrenstechnik e.V* **2006**, *64* (3), 261-8; Gaucher, G.; Marchessault, R. H.; Leroux, J.-C., *Journal of Controlled Release* **2010**, *143* (1), 2-12.
55. Wang, B.-L.; Shen, Y.-m.; Zhang, Q.-w.; Li, Y.-l.; Luo, M.; Liu, Z.; Li, Y.; Qian, Z.-y.; Gao, X.; Shi, H.-s., *International journal of nanomedicine* **2013**, *8*, 3521-31.
56. Cammas, S.; Suzuki, K.; Sone, C.; Sakurai, Y.; Kataoka, K.; Okano, T., *Journal of Controlled Release* **1997**, *48* (2-3), 157-164.
57. Lee, E. S.; Oh, K. T.; Kim, D.; Youn, Y. S.; Bae, Y. H., *Journal of Controlled Release* **2007**, *123* (1), 19-26; Maiti, S.; Chatterji, P. R., *Langmuir* **1997**, *13* (19), 5011-5015.
58. Otsuka, H.; Nagasaki, Y.; Kataoka, K., *Advanced Drug Delivery Reviews* **2012**, *64*, 246-255.
59. Ge, H. X.; Hu, Y.; Jiang, X. Q.; Cheng, D. M.; Yuan, Y. Y.; Bi, H.; Yang, C. Z., *Journal of Pharmaceutical Sciences* **2002**, *91* (6), 1463-1473.
60. Kotsis, N.; Siakali-Kioulafa, E.; Pitsikalis, M., *European Polymer Journal* **2008**, *44* (8), 2687-2694.
61. Bronstein, L. M.; Chernyshov, D. M.; Timofeeva, G. I.; Dubrovina, L. V.; Valetsky, P. M.; Khokhlov, A. R., *Langmuir* **1999**, *15* (19), 6195-6200.
62. Allen, C.; Maysinger, D.; Eisenberg, A., *Colloids and Surfaces B-Biointerfaces* **1999**, *16* (1-4), 3-27.
63. Jiang, Z.; Azim, H.; Gross, R. A.; Focarete, M. L.; Scandola, M., *Biomacromolecules* **2007**, *8* (7), 2262-2269.
64. Galindo-Rodriguez, S.; Allemann, E.; Fessi, H.; Doelker, E., *Pharmaceutical Research* **2004**, *21* (8), 1428-1439.
65. Letchford, K.; Liggins, R.; Burt, H., *Journal of Pharmaceutical Sciences* **2008**, *97* (3), 1179-1190.

66. Feng, R.; Song, Z.; Zhai, G., *International Journal of Nanomedicine* **2012**, *7*, 4089-4098; Mohanty, C.; Acharya, S.; Mohanty, A. K.; Dilnawaz, F.; Sahoo, S. K., *Nanomedicine* **2010**, *5* (3), 433-449.
67. Song, L.; Shen, Y.; Hou, J.; Lei, L.; Guo, S.; Qian, C., *Colloids and Surfaces a-Physicochemical and Engineering Aspects* **2011**, *390* (1-3), 25-32.
68. Gong, C.; Deng, S.; Wu, Q.; Xiang, M.; Wei, X.; Li, L.; Gao, X.; Wang, B.; Sun, L.; Chen, Y.; Li, Y.; Liu, L.; Qian, Z.; Wei, Y., *Biomaterials* **2013**, *34* (4), 1413-1432.
69. Bisht, S.; Feldmann, G.; Soni, S.; Ravi, R.; Karikar, C.; Maitra, A.; Maitra, A., *Journal of Nanobiotechnology* **2007**, *5*, 3-Article No.: 3.
70. Karavelidis, V.; Giliopoulos, D.; Karavas, E.; Bikiaris, D., *European Journal of Pharmaceutical Sciences* **2010**, *41* (5), 636-643.
71. Papadimitriou, S.; Bikiaris, D., *Journal of Controlled Release* **2009**, *138* (2), 177-184.
72. Teng, Y.; Morrison, M. E.; Munk, P.; Webber, S. E.; Prochazka, K., *Macromolecules* **1998**, *31* (11), 3578-3587.
73. Jain, R. A., *Biomaterials* **2000**, *21* (23), 2475-2490.
74. Liu, J.; Jiang, Z.; Zhang, S.; Liu, C.; Gross, R. A.; Kyriakides, T. R.; Saltzman, W. M., *Biomaterials* **2011**, *32* (27), 6646-6654; Liu, J.; Jiang, Z.; Zhang, S.; Saltzman, W. M., *Biomaterials* **2009**, *30* (29), 5707-5719.
75. Soo, P. L.; Luo, L. B.; Maysinger, D.; Eisenberg, A., *Langmuir* **2002**, *18* (25), 9996-10004; Layre, A.; Couvreur, P.; Chacun, H.; Richard, J.; Passirani, C.; Requier, D.; Benoit, J. P.; Gref, R., *Journal of Controlled Release* **2006**, *111* (3), 271-280.

Chapter 5 Novel

Poly(Decalactone) Micelles for

Solubilisation and Controlled

Delivery of Amphotericin B

5.1 Introduction

Amphotericin B (AmpB) is a polyene antibiotic from *Streptomyces nodosus*, a filamentous bacterium, and the compound was first isolated in 1955 at the Squibb Institute for Medical Research. AmpB is a reliable broad spectrum antifungal and antiprotozoal drug which is widely used against life threatening systemic infection such as visceral leishmaniasis¹. AmpB is insoluble in water and therefore the conventional intravenous formulation of AmpB contains sodium deoxycholate (surfactant) to enhance its aqueous solubility. However, sodium deoxycholate, used for the solubilisation of amphotericin B has been known to be haemolytic². Additionally, this conventional formulation is known to cause nephrotoxicity^{3,1}. Therefore, to increase the efficacy and to reduce the systemic toxicity of AmpB, various lipid formulations of AmpB has been developed and a few of them are commercially available^{1,4}. However, numerous other nano-sized carriers such as micelles², nanospheres⁵, carbon nanotubes⁶, nanosuspensions⁷, nanoparticles⁸ etc. have also been evaluated for the delivery of AmpB.

It has been reported that micellar formulations of AmpB performed better than its commercially available analogue. For instance, micelles of poly(ethylene oxide)-block-poly(L-

aspartate) and its derivatives^{2,9,10} have been extensively studied for the delivery of AmpB and found to be more effective (*in vitro* and *in vivo*) compared to the commercially available Fungizone[®] (a formulation of amphotericin B containing sodium deoxycholate)^{2,9,10}. In addition to the poly(L-aspartate), micelles fabricated using other hydrophobic blocks such as PLGA¹¹, PCL¹², phospholipid¹³ etc. has also been tested for the delivery of AmpB. Considering the advantages of micellar formulations over the conventional formulations of AmpB, it was decided to evaluate the potential of novel poly(decalactone) block copolymer micelles for AmpB delivery.

Good solubility of drug and polymer in common water miscible volatile organic solvent (preferably acetone and tetrahydrofuran) is must for the effective loading via nanoprecipitation. Encapsulation of AmpB using a nanoprecipitation method is generally a complex procedure, which always requires a co-solvent. The commonly used co-solvents are dimethyl sulfoxide (DMSO) and methanol. However, the mixture of acetone and methanol required an additional step of pH adjustment to dissolve the AmpB completely¹⁴. Similarly, when non-volatile DMSO has been used as a co-solvent, additional steps such as dialysis or

washing were required to remove the solvent from final formulation¹¹. A polymer, which is soluble in methanol, could avoid the additional steps required to load AmpB *via* nanoprecipitation. In the view of this, a lipid formulation of AmpB has been reported, which was fabricated *via* nanoprecipitation using methanol as solvent¹⁵. The co-polymer mPEG-b-PDL is soluble in methanol and therefore it was proposed that the encapsulation of AmpB *via* nanoprecipitation using this copolymer might be possible.

Polymers containing ester group in their backbone have the ability to perform a certain role for a specific period and be subsequently degraded into low molecular weight products, which can be easily eliminated from the body via metabolic pathways^{16,17}. The hydrolytic degradation of a poly(esters) is also known to affect the release rate of the encapsulated material and can be tuned to control drug release¹⁸. Most of the poly(esters) used for *in vivo* drug delivery can be degraded in the human body by acid or base catalysed hydrolysis in the presence or absence of esterase enzymes¹⁹. Since mPEG-b-PDL is a novel but highly hydrophobic polyester, and therefore it was expected that it might undergo a very slow hydrolytic degradation. Hence, a preliminary *in*

vitro degradation study was performed to investigate the degradation profile of the mPEG-b-PDL polymeric micelles.

Another important parameter that needs to be addressed before the use of a new material *in vivo* is its cytotoxicity. Primary toxicity evaluation of new polymers has been generally done on human cell lines to determine their suitability for *in vivo* use²⁰. Being a new polymer, the mPEG-b-PDL formulation was tested to evaluate its effects on human cell lines. Alamar Blue assay was selected for the evaluation of the effects of polymers on cells. This assay is a simple and rapid test in which commercially available Alamar Blue[®] reagent^{21, 22}, which is a water soluble nontoxic dye, is used to assess metabolic activity of cells. The assay was chosen in place of the common 3-(4,5-dimethylthiazol-2-yl)-2,5-diphenyl-tetrazolium bromide (MTT) metabolic activity assay because, unlike the MTT test, re-use of cells is possible for further investigations which might be important for reasons of time in this study²¹. Previously reported mPEG-b-PCL copolymer was also tested using the same protocol for a comparative study²³.

5.2 Methods

5.2.1 Preparation and Characterisation of Blank and Amphotericin B loaded Micelles:

Empty and drug loaded micelles of mPEG-b-PDL and mPEG-b-PCL (50 mg each) were prepared and characterised by similar methods used for curcumin (see chapter 4). Methanol (5mL) was used as organic solvent instead of acetone to solubilise polymer and drug. The initial amount of AmpB used for the encapsulation study was 2 mg. The mPEG-b-PCL copolymer produced a hazy solution in methanol due to its poor solubility whereas mPEG-b-PDL gave transparent solution (figure 5-1). All micellar formulations were purified by filtration (0.22 μ m) in order to remove free drug and aggregates. Drug content (DC) in micelles was determined by dissolving the known amount of freeze dried sample in methanol followed by quantification of the AmpB using UV-Vis spectrophotometry. Freeze dried mPEG-b-PCL micelles formed precipitates after reconstitution in methanol and therefore, samples were sonicated for 2 minutes and then centrifuged (2 min.) at 5000 rpm to remove precipitates. A similar method was followed for mPEG-b-PDL micelles samples for proper comparison. Supernatant (methanol) was collected from each sample and analysed at $\lambda_{\text{max}} = 405 \text{ nm}$ *via* UV-Vis spectrophotometry. The amount of

AmpB was then calculated using standard calibration curve, which was prepared from UV analysis of AmpB solutions in methanol (Dilutions – 1 to 10 $\mu\text{g} / \text{mL}$). DC and EE was calculated using the formula reported in chapter 2.

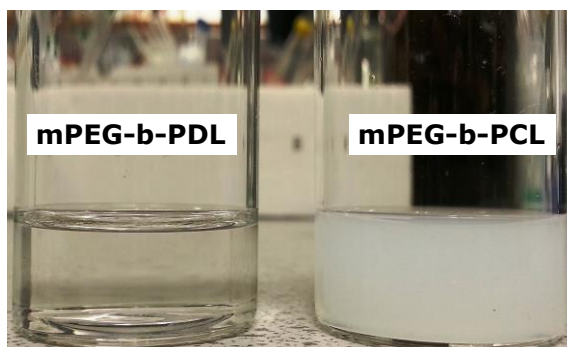


Figure 5-1 Physical appearance of solution of mPEG-b-PDL and mPEG-b-PCL copolymer (50 mg each) after being dissolved in 5mL of methanol.

5.2.2 *In vitro* Release Study of Amphotericin B from Block Copolymers Micelles

To facilitate the solubilisation of AmpB, a release study was performed in modified release media *i.e.* water containing Tween 80 (1% v/v)^{24,25}. A calculated amount of AmpB loaded freeze dried micelles, equivalent to 200 μg of AmpB were redispersed in HPLC grade water (2 mL). The solution was then placed in a dialysis tubing (Slide-A-Lyzer, 3.5 KDa mwco, Thermo Scientific) and dialysed against 10 mL of release media at 37°C. The whole release media was replaced with fresh media at a predetermined time interval to maintain sink condition. Collected release media (samples) was freeze dried. The dried samples were then dissolved in methanol (1 mL)

and analysed on UV-Vis spectrophotometer (λ_{\max} -405 nm). The amount of released AmpB was then calculated using a standard calibration curve of AmpB (figure 5-2). Control samples were prepared by dissolving 200 μg of AmpB in 2 mL of water (containing 2% v/v of Tween 80, Control A). An additional control experiment was also setup by adding 50 μl of mPEG-b-PDL copolymer solution in acetone (100 mg of mPEG-b-PDL in 1mL of acetone) to the control "A". The solution was then bubbled with nitrogen to remove acetone. This sample was assigned as control "B" (figure 5-3). The AmpB release pattern from control samples was analysed by following the identical method used for mPEG-b-PDL micelles.

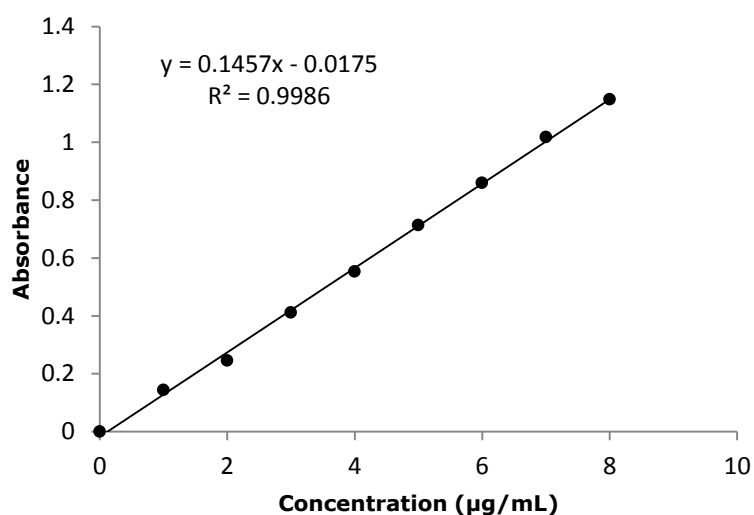


Figure 5-2 Standard calibration curve of Amphotericin B. The UV absorbance of Amphotericin B solution (in methanol containing 10% v/v Tween 80) was measured at wavelength of 405 nm.

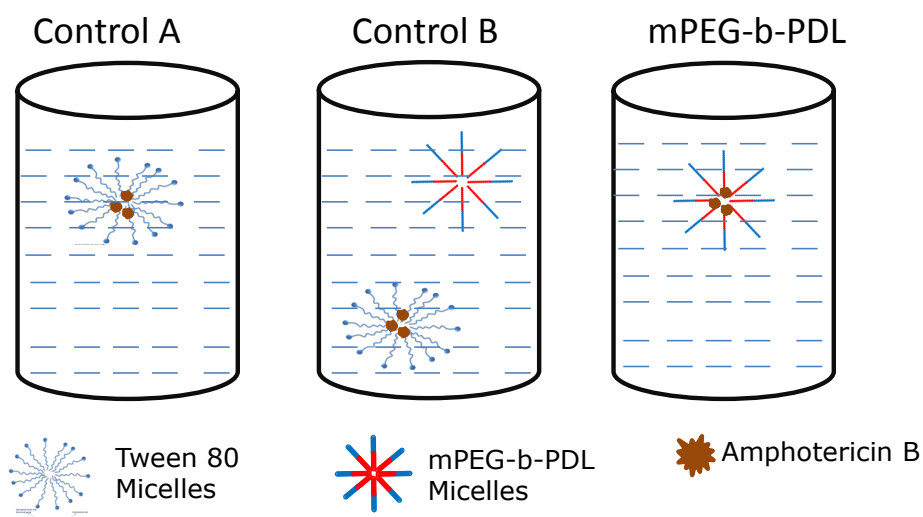


Figure 5-3 Sample distribution for release study. Control A contained AmpB in water having Tween 80 (2% v/v). Control B sample contained mPEG-b-PDL co-polymer (5mg) in control A. mPEG-b-PDL sample contained AmpB loaded mPEG-b-PDL micelles in water. All samples contained 200 μg of AmpB.

5.2.3 *In vitro* Degradation Study of mPEG-b-PDL Micelles

The degradation profile of empty mPEG-b-PDL micelles was assessed in two different pH (*i.e.* pH – 7.4 and 4.0) at 37° C. To perform this study, freeze dried empty micelles (8 mg) were redispersed in 1 mL of acetate buffer (pH – 4.0, 10mM) and phosphate buffer (pH – 7.4, 10mM) separately. The samples (6 each for both pH) were then incubated at 37°C using a water bath. At predetermined time intervals, one sample vial from each pH was collected and freeze dried. The freeze dried samples were then dissolved in chloroform, filtered and analysed by SEC to determine the change in molecular weight.

5.2.4 *In vitro* Cytotoxicity Study of mPEG-b-PDL and mPEG-b-PCL Micelles

The Alamar Blue cell viability assay was performed to determine the toxicity of the empty micelles on HCT116 colon cancer cells. This study was kindly performed by Dr. Laura Purdie. Cells were seeded at 10,000 cells per well in a 96 well plate. After 48 hrs, the media (RPMI-1640, 10 % FBS, 2mM L-Glutamine) was replaced with fresh 200µl of Opti-MEM[®]. The stock solution of micelles (mPEG-PDL and mPEG-b-PCL) (5 mg/mL) was diluted in water as required to make the final concentration of 3.5, 7.0, 14.0 and 21.0 µg/µL. Micelle solutions (15 µL) were then added to the media (treated cells) and in three wells, only water (15 µL) was added as negative control (untreated cells). Three wells with no cells were also set up on the same plate containing Opti-MEM[®] only, as a background control. The plate was then incubated for 24 hrs in a humidified incubator at 37 °C (5% CO₂). After 24 hrs, the media was replaced with 110 µL of 1:10 Alamar Blue reagent in OptiMEM. The plate was then incubated for 1 hr followed by fluorescence measurement at the excitation wavelength of 594 nm and emission wavelength of 610 nm using a fluorescence plate reader (Molecular Devices Flexstation 3 plate reader). The background fluorescence was subtracted

from all of the cell readings. Considering the negative control as 100 % cell viability, calculations were performed to determine the percentage of cells which were actively metabolising (and thus viable) in each sample.

Two-Way ANOVA analysis was performed for multiple comparison (Sidak test), to evaluate any significant differences in the samples.

All experiments were done in triplicate and results were reported as mean with standard deviations. GraphPad Prism 6 was used to analyse the data.

5.3 Results

5.3.1 Preparation and Characterisation of Blank and Amphotericin B loaded Micelles

The appearance of micelle solutions before and after purification is shown in figure 5-4. The mPEG-b-PCL copolymer, due to its poor solubility in methanol, produced large size particles after nanoprecipitation method (figure 5-4A). However, during purification of micellar suspension, particles above 220 nm sizes were removed (figure 5-4B). The recovery of micellar suspension after filtration was approximately 30-40% for mPEG-b-PCL copolymer whereas 90-95% of mPEG-b-PDL micellar suspension was recovered.

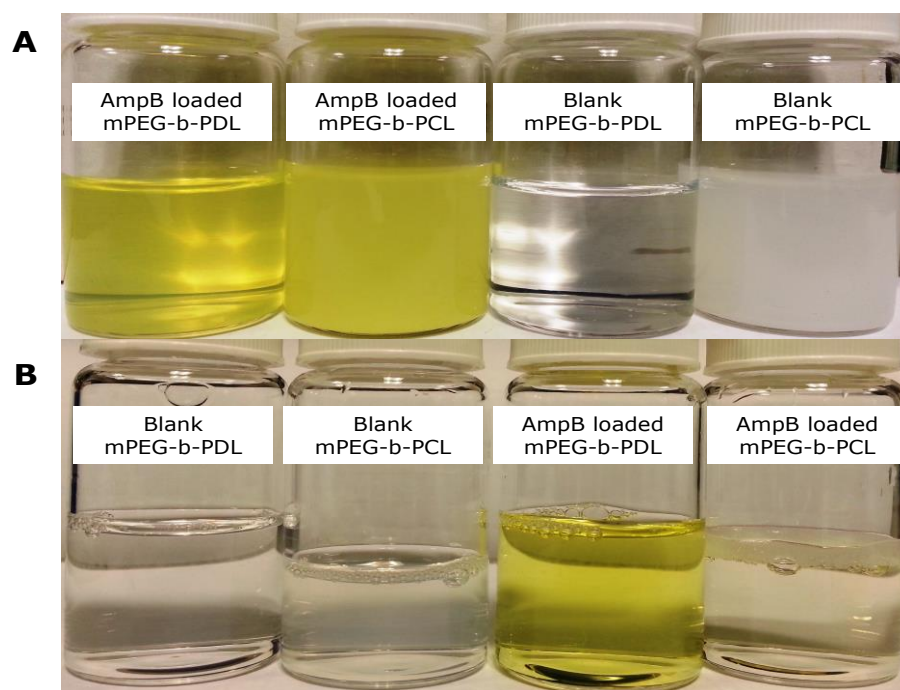


Figure 5-4 Physical appearance of micellar suspension (obtained *via* nanoprecipitation method) in water (A) before and (B) after filtration through 0.22 μm syringe filter.

Sample	Z-average size (d/nm) (\pm SD)	PdI	Zeta Potential (mv) (\pm SD)
mPEG-b-PDL (Blank)	41 \pm 2	0.15 \pm 0.01	-2.4 \pm 1.3
mPEG-b-PDL (Loaded)	44 \pm 3	0.16 \pm 0.02	-2.8 \pm 1.1
mPEG-b-PCL (Blank)	36 \pm 2	0.30 \pm 0.03	-0.3 \pm 1.7
mPEG-b-PCL (Loaded)	32 \pm 3	0.26 \pm 0.02	-1.2 \pm 1.0

Table 5-1 Characterisation data of micelles prepared by nanoprecipitation method using methanol as an organic solvent. (d/nm-diameter in nanometre, SD-standard deviation, PdI-polydispersity index, mv- millivolt).

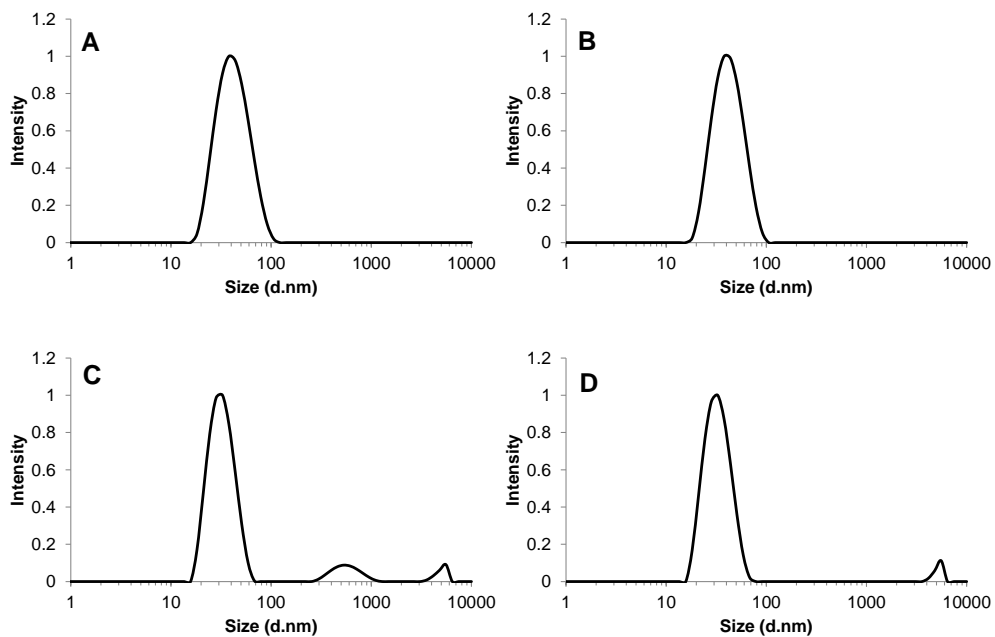


Figure 5-5 Size distribution curve by intensity of (A) Blank mPEG-b-PDL, (B) AmpB loaded mPEG-b-PDL, (C) Blank mPEG-b-PCL and (D) AmpB loaded mPEG-b-PCL micelles.

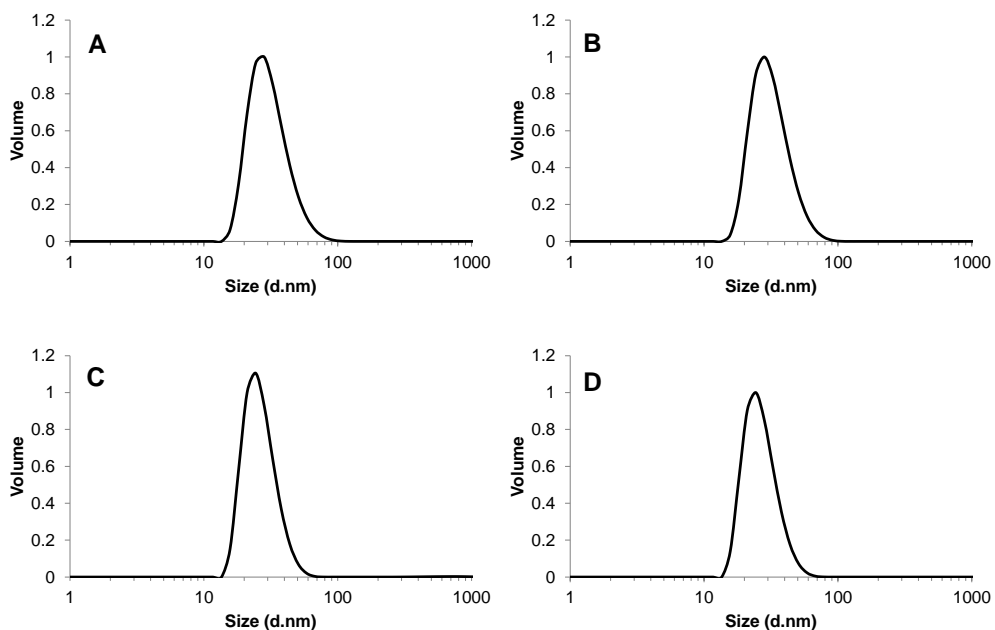


Figure 5-6 Size distribution curve by volume of (A) Blank mPEG-b-PDL, (B) AmpB loaded mPEG-b-PDL, (C) Blank mPEG-b-PCL and (D) AmpB loaded mPEG-b-PCL micelles.

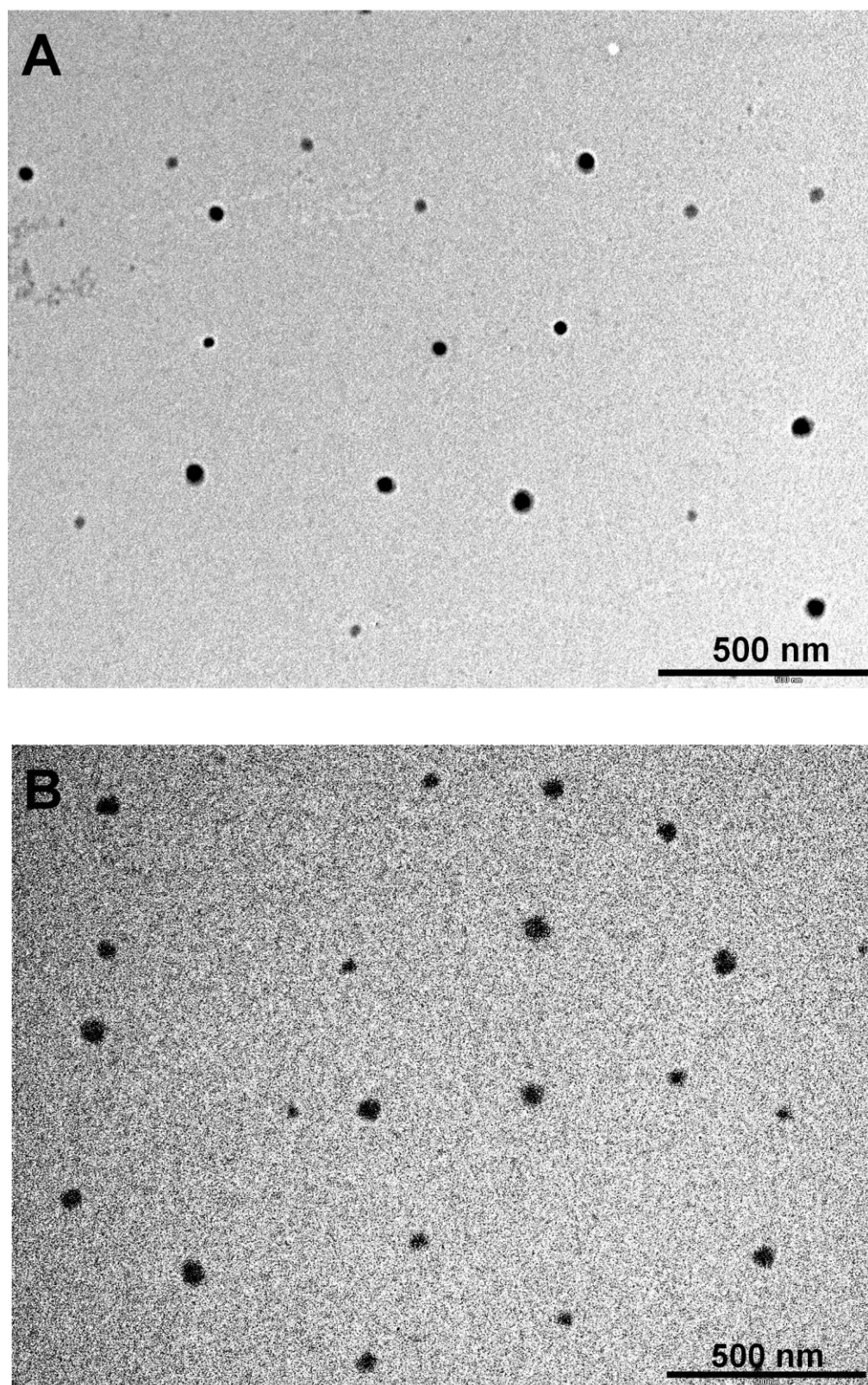


Figure 5-7 TEM image of (A) blank mPEG-b-PDL and (B) AmpB loaded mPEG-b-PDL micelles. The images were taken without staining. Scale bar - 500 nm

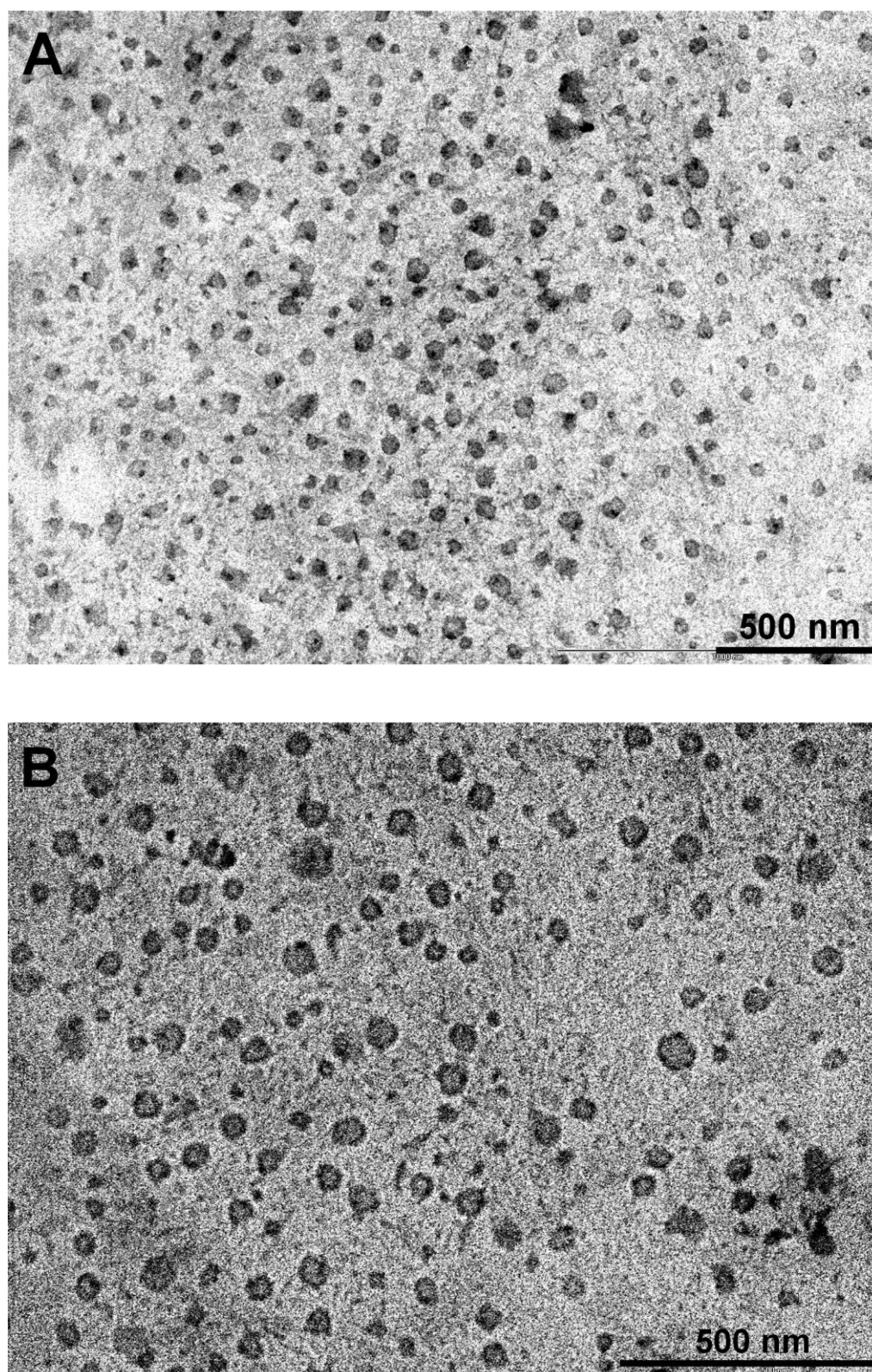


Figure 5-8 TEM image of (A) blank mPEG-b-PCL and (B) AmpB loaded mPEG-b-PCL micelles. The images were taken without staining. Scale bar 500 nm

The mean sizes detected by DLS for empty and AmpB loaded micelles are reported in table 5-1. No significant differences in the size of empty micelles were observed when compared with micelles prepared using acetone as solvent (in chapter 4). Furthermore, AmpB loading did not significantly change the size of the micelles when compared with blank micelles (table 5-1, figure 5-5 and 5-6). However, due to the broad size distribution, the polydispersity index observed for mPEG-b-PCL micelles was high.(figure 5-5). Interestingly, after loading of AmpB in mPEG-b-PCL micelles, a slight reduction in mean size and polydispersity index was observed.

Zeta potential detected for all micelles formulation in 10mM HEPES was almost neutral and no significant change in zeta potential was observed after AmpB loading (table 5-1). The TEM images of blank and AmpB loaded micelles confirmed the size and suggested that the prepared micelles are of roughly spherical in shape (figure 5-7 and 5-8).

The drug content and encapsulation efficiency observed for mPEG-b-PCL and mPEG-b-PDL micelles are presented in figure 5-9. The AmpB content found in mPEG-b-PDL micelles (3.5 ± 0.2 wt %) was 7.2 times higher than mPEG-b-PCL micelles (0.5 ± 0.1 wt %). The percentage encapsulation efficiency (EE%) found for mPEG-b-PDL micelles was 84.8 ± 4.7 %

whereas mPEG-b-PCL showed the EE% of 11.5 ± 1.7 % (figure 5-9 B).

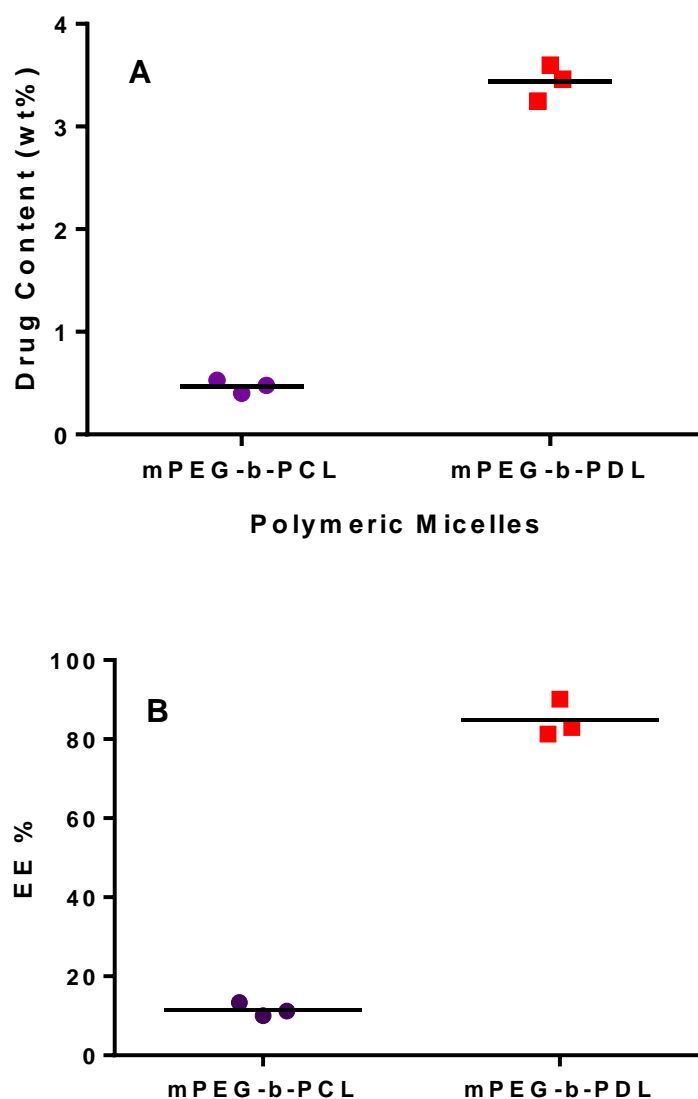


Figure 5-9 Graph represents (A) Amphotericin B content (weight % to polymer) and (B) encapsulation efficiency (EE%) observed in micelles, which was determined by UV-Vis spectrophotometer (λ_{\max} - 405 nm). Dots represent separate individual value and bar represents the mean value (n=3).

5.3.2 *In Vitro* Release Study of AmpB from Block Copolymer Micelles

Amphotericin B is poorly soluble in water ($< 0.5 \mu\text{g/mL}$)² and hence 1% v/v of Tween 80 was added in release media to enhance its solubility. The concentration of Tween 80 used was well above its CMC and hence it was expected that the Tween 80 micelles (mol. wt. 76 KDa)²⁶ were not diffused through the dialysis bag (mwco -3.5 to 5 KDa). Due to the poor loading of AmpB in mPEG-b-PCL micelles, this formulation was excluded from release study. Therefore, the release pattern of mPEG-b-PDL micelles was compared with the Tween 80 micelles formulation.

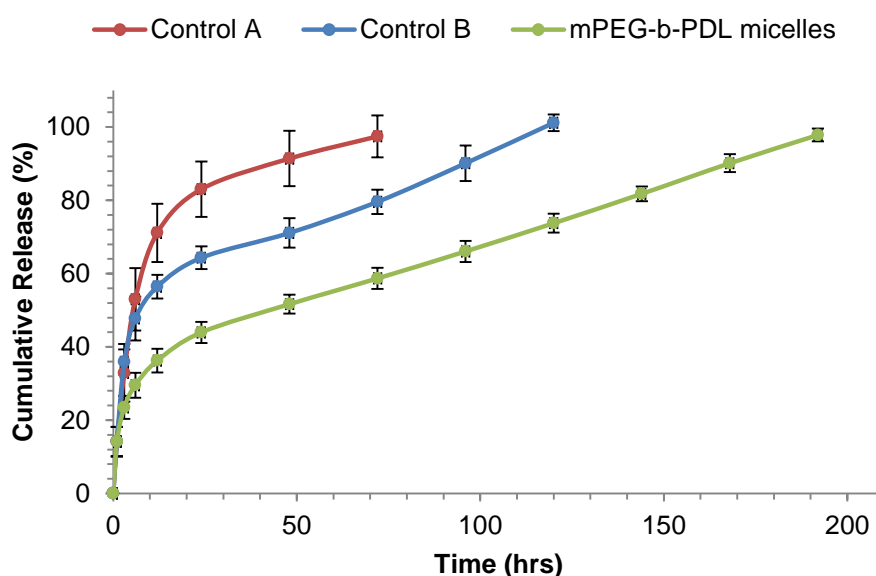


Figure 5-10 Cumulative release (%) of AmpB from different test formulations in water containing Tween 80 (1% v/v) at 37°C. Release study was performed by dialysis method and AmpB concentration was estimated by UV-Vis spectrophotometer.

Initial burst release of AmpB (30% approx. within 6 hrs) was observed with mPEG-b-PDL micelles followed by a slow-release phase, which continued for 8 days. In contrast, control "A" (Tween 80 micelles) released 100 % of AmpB in 3 days out of which 53 % of drug was released in first 6 hrs. However, in control "B" formulation, the release pattern observed was more sustained when compared to control "A" but was faster compared to mPEG-b-PDL micelles (figure 5-10). In the first 6 hrs, no significant difference in the percentage drug released was observed with control "B" when compared to control "A". However, probably due to the partition of AmpB after a certain time in to empty mPEG-b-PDL micelles, sustained release was observed with this control, which lasted for 5 days. If the percentage of burst release was ignored than all the three formulations demonstrated the similar pattern of drug release *i.e.* initial burst release followed by sustained release.

5.3.3 *In Vitro* Degradation Study of mPEG-b-PDL Micelles

Determination of the degradation time of a polyester is an important parameter to understand its fate inside the body and/or on long term storage in solution. A known degradation profile of a polymer could be useful to fabricate a drug

delivery carrier with predetermined release rate¹⁸. Therefore, in the current work, a preliminary study of hydrolytic degradation of mPEG-b-PDL micelles was performed for 4 months. Samples were analysed by SEC to determine the change in molecular weight (M_n). Here, NMR spectroscopy was not useful for molar mass determination because of the absence of substantial change in peak positions of poly(decylactone) after chain cleavage.

A SEC trace of mPEG-b-PDL micelles after 120 days and the loss of molecular weight (M_n) versus time are shown in figure 5-11 and 5-12 respectively. The change in M_n of peak at position 1 (figure 5-11) was monitored and used to plot the graph against time. As the degradation of polymer chain continued, the reduction in the M_n value of peak at position 1 was observed. Complete cleavage of the PDL block from mPEG block (M_n by SEC – 10.8K) was observed in 53 days at pH 4.0. High degradation rate at this pH was attributable to the acid-catalysed hydrolysis of ester bonds. However, at physiological pH (*i.e.* pH-7.4) only 16% drop in M_n was observed after 4 months from the initial value.

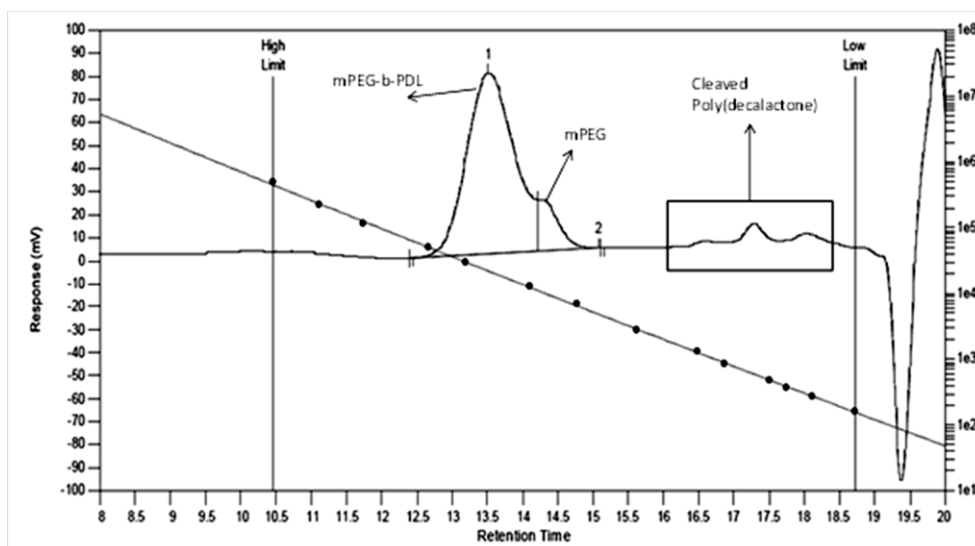


Figure 5-11 SEC trace of mPEG-b-PDL after 120 days of storage at pH 7.4 (temperature – 37°C). SEC instrument was calibrated using polystyrene standards and chloroform was used as mobile phase.

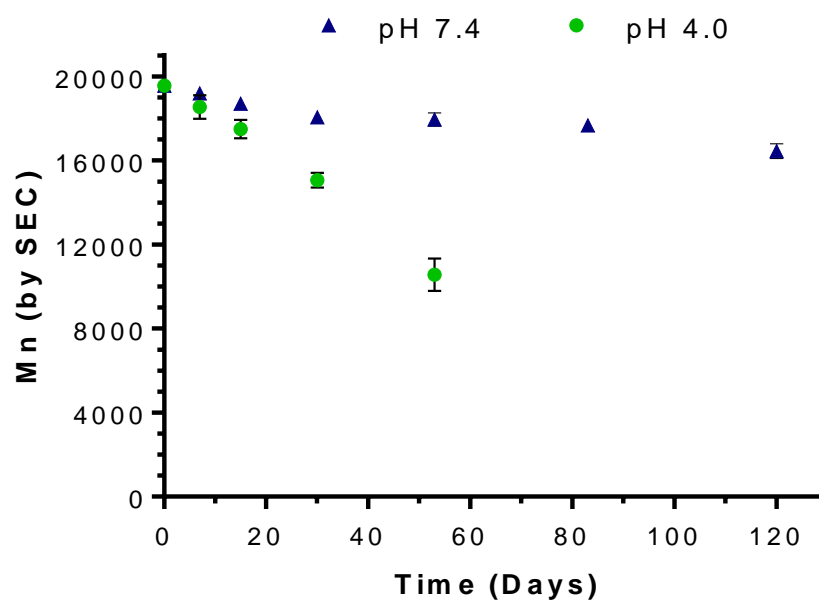


Figure 5-12 Loss in molecular weight (M_n) of mPEG-b-PDL micelles with time at two different pH as determined by SEC. SEC instrument was calibrated using polystyrene standard and chloroform was used as mobile phase.

5.3.4 Effect of Micelles on Cells Metabolic Activity by Alamar Blue Assay

The Alamar Blue assay is based on the measurement of the reduction of resazurin by viable cells due to their continuing metabolic activity²⁷. The oxidised non fluorescent Alamar Blue dye undergoes chemical reduction in the cell culture medium by mitochondrial enzymes and is converted into a pink fluorescent dye, resorufin^{21,22}. Fluorescence intensity of resorufin is directly related to the metabolic activity of cells.

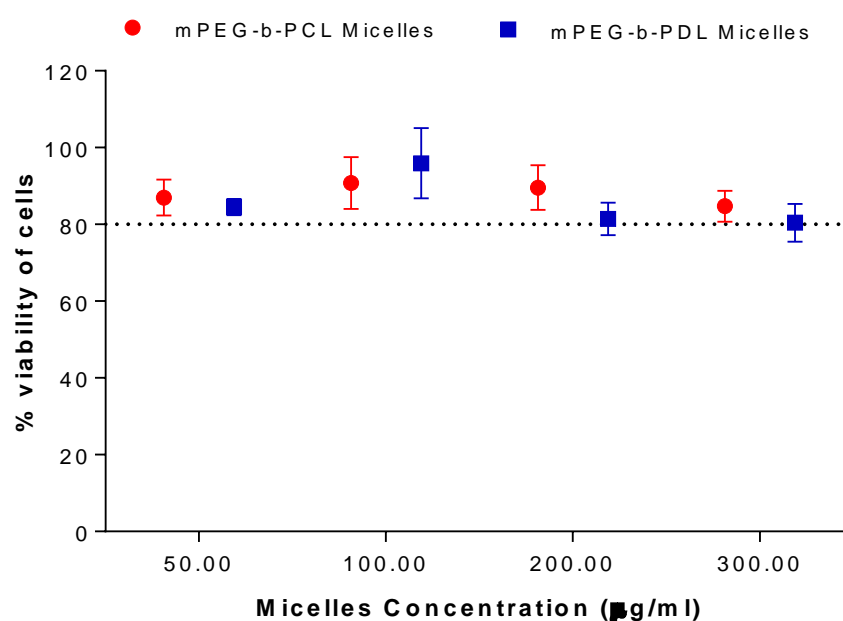


Figure 5-13 *In vitro* cytotoxicity of empty micelles formulations. The percent cell viability was calculated using Alamar Blue assay on HCT116 cell lines for 24 hrs.

The cytotoxicity of empty micelles was studied on HCT116 colon cancer cell lines for 24 hrs. The percent viability of cells, exposed to different concentrations of micelles formulation

(after 24 hrs) is shown in figure 5-13. No significant differences in percent viability of cells were observed between mPEG-b-PCL and mPEG-b-PDL micelles at any used concentration of micelles. Furthermore, not more than 20% cell death was observed in any cell culture treated with empty micelles after 24 hrs *in vitro*. These results suggested that the empty micelles were of relatively low toxicity to this cell line up to the concentration of 300 µg/mL.

5.4 Discussion

Empty and AmpB loaded mPEG-b-PDL micelles demonstrated no significant change in size when compared to micelles prepared using acetone as solvent. These results suggested that the solubility of mPEG-b-PDL copolymer is almost similar in acetone and methanol. However, large size micelles were observed with mPEG-b-PCL micelles due to the poor solubility of this copolymer in methanol. Similar result was earlier observed with mPEG-b-PDL-b-PPDL copolymer when micelles were fabricated using acetone as solvent. The presence of aggregates led to an increased polydispersity index for the mPEG-b-PCL micelles, but after AmpB loading, a reduction in size and polydispersity was observed. This behaviour might have been due to the hydrophobic interaction between PCL core and AmpB, which facilitated the assembly of mPEG-b-PCL

in water. Similar results have been reported with mPEG-b-PCL micelles when highly hydrophobic fenofibrate was loaded²⁸. A similar phenomenon was also observed earlier with PDL-b-PEG-b-PDL micelles, where loading of a hydrophobic drug decreased the size and polydispersity index (see chapter 4).

The encapsulation study results suggested that the performance of mPEG-b-PDL copolymer using the reported encapsulation procedure was superior compared to mPEG-b-PCL copolymer. Good solubility of mPEG-b-PDL in methanol and its higher hydrophobicity were the probable reasons, due to which a higher drug content in the novel polymeric micelles was observed. The EE observed with mPEG-b-PDL micelles for AmpB was higher than the previously reported micelles formulations having PLGA²⁹, PLA³⁰ or PCL^{31,12} as hydrophobic core. Although the drug content observed was low compared to the above mentioned polymers however, it can be improved by formulation optimisation. For instance, it has been reported that the loading content of AmpB in a polymeric drug delivery systems can be improved by increase in the initial quantity of drug used for loading^{11,2}.

An *in vitro* release experiment was performed using two control formulations to understand the role of drug partition between carrier and dispersed phase on release rate³². The

release rate obtained for control "B" formulation hypothesised that the partitioning of drug between the carrier and dispersed phase has an effect on the release rate determined by dialysis method.

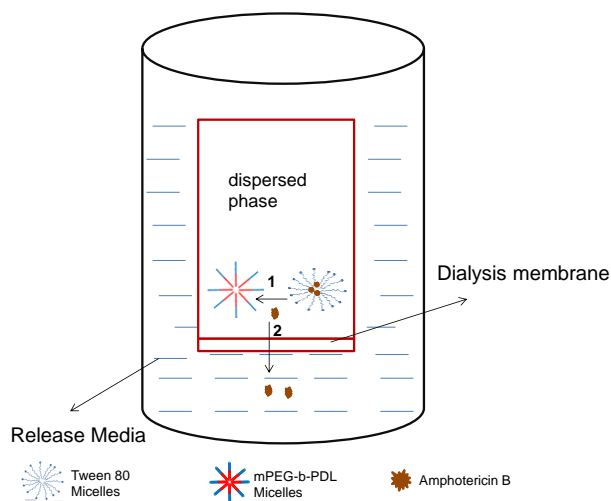


Figure 5-14 Pictorial presentation of control "B" showing the AmpB equilibration from Tween 80 micelles to mPEG-b-PDL micelles (step 1) and diffusion of AmpB in release media from dialysis membrane (step 2).

As shown in figure 5-14, the loaded drug after releasing from the Tween 80 micelles into dispersed phase, could either encapsulated back in to mPEG-b-PDL blank micelles (step 1) or diffuse out to release media (step 2). Due to the higher hydrophobicity of mPEG-b-PDL micelles core, drug migration from Tween 80 micelles towards mPEG-b-PDL micelles was expected. Consequently, a more sustained release pattern was observed with control "B" when compared with control "A". This phenomena indicates that a reversible binding of drug towards carrier (micelles) is possible before permeating through dialysis membrane, based on the partition coefficient

of drug between carrier and dispersed phase³³. Nevertheless, since the partition effect would have occurred in both formulations (*i.e.* in control "A" and mPEG-b-PDL micelles) and therefore it can be concluded that the mPEG-b-PDL micelles showed a more sustained release of AmpB compared to Tween 80 micelles. The release pattern observed with novel mPEG-b-PDL micelles was more controlled, compared to the earlier reported release pattern for AmpB in release media having Tween 80 as solubilising agent^{24,25}. The obtained results suggested that the mPEG-b-PDL micelles have potential to improve delivery of AmpB.

The preliminary *in vitro* degradation study suggested that the mPEG-b-PDL micelles were likely to undergo hydrolytic degradation. The degradation rate observed for mPEG-b-PDL copolymer at physiological pH (9 % after 30 days) was slower compared to two different reports on PEG-PLA block copolymers (27.6 %³⁴, 16.3 %³⁵ after 30 days). This might be due to the more pronounced steric effect (hindered ester groups) and higher hydrophobicity of the mPEG-b-PDL. However, it was found that the degradation rate of mPEG-b-PDL was faster than with PEG-PCL copolymers (9.0 % after 126 days³⁶, 4.1% after 56 days³⁷). It has been reported that amorphous polymers degrade faster than semicrystalline

polymers^{38,39}. Therefore, a more rapid degradation of the amorphous PDL block when compared to semicrystalline PCL block could be attributed to this difference in crystallinity.

The *in vitro* cell activity study results suggested that the mPEG-b-PDL micelles exhibited similar effects on a cancer cell line when compared to mPEG-b-PCL micelles. The similar cytocompatibility behaviour suggested that the PDL component was not different to PCL in its effects on cells, as in both cases the effects of PEG as corona were expected to be same.

5.5 Conclusion

In this study, the successful fabrication of mPEG-b-PDL micelles *via* a nanoprecipitation method using methanol as solvent was reported. No significant difference in average size was observed for mPEG-b-PDL micelles prepared using methanol as solvent when compared with the mPEG-b-PDL micelles fabricated using acetone. The encapsulation study of amphotericin B suggested that the mPEG-b-PDL micelles performed better in terms of drug loading than their counterpart mPEG-b-PCL micelles. The sustained release pattern was observed from mPEG-b-PDL micelles when compared with Tween 80 micelles as evident by *in vitro* release experiment. Additionally, with the help of an extra control (physically mixed copolymer) in release experiment, it

was demonstrated that the partition coefficient of a drug between carrier and dispersed phase was also a variable that influenced the release rate determined by the dialysis method. The investigated procedure for drug encapsulation proposed that these novel polymeric micelles could be useful for the encapsulation of highly hydrophobic drug molecules, which have good solubility in methanol (for ex. Paclitaxel) by nanoprecipitation method.

The preliminary degradation study suggested that the ester bond of mPEG-b-PDL was susceptible to hydrolytic degradation. However, from the results, it can be hypothesised that the presence of long alkyl chain (steric effect) could be responsible for the slow degradation of mPEG-b-PDL micelles. *In vitro* cell activity studies demonstrated that the novel mPEG-b-PDL and mPEG-b-PCL micelles were well tolerated by the studied HCT-116 human colon cancer cell.

Based on the conclusions made above, further investigation of mPEG-b-PDL micelles as a drug delivery vehicle was proposed. Actively targeted micelles in chemotherapy have been reported to be an efficient approach for the treatment of cancer⁴⁰. Therefore, in the subsequent study, preparation and evaluation of ligand tethered mPEG-b-PDL micelles for cancer therapy was proposed.

5.6 References

1. Barratt, G.; Bretagne, S., *International Journal of Nanomedicine* **2007**, 2 (3), 301-313.
2. Yu, B. G.; Okano, T.; Kataoka, K.; Kwon, G., *Journal of Controlled Release* **1998**, 53 (1-3), 131-136.
3. Torrado, J. J.; Espada, R.; Ballesteros, M. P.; Torrado-Santiago, S., *Journal of Pharmaceutical Sciences* **2008**, 97 (7), 2405-2425.
4. Vyas, S. P.; Gupta, S., *International Journal of Nanomedicine* **2006**, 1 (4), 417-432.
5. Espuelas, M. S.; Legrand, P.; Irache, J. M.; Gamazo, C.; Orecchioni, A. M.; Devissaguet, J. P.; Ygartua, P., *International Journal of Pharmaceutics* **1997**, 158 (1), 19-27.
6. Wu, W.; Wieckowski, S.; Pastorin, G.; Benincasa, M.; Klumpp, C.; Briand, J. P.; Gennaro, R.; Prato, M.; Bianco, A., *Angewandte Chemie-International Edition* **2005**, 44 (39), 6358-6362.
7. Kayser, O.; Olbrich, C.; Yardley, V.; Kiderlen, A. F.; Croft, S. L., *International Journal of Pharmaceutics* **2003**, 254 (1), 73-75.
8. Tiyaboonchai, W.; Woiszwilllo, J.; Middaugh, C. R., *Journal of Pharmaceutical Sciences* **2001**, 90 (7), 902-914.
9. Adams, M. L.; Andes, D. R.; Kwon, G. S., *Biomacromolecules* **2003**, 4 (3), 750-757.
10. Lavasanifar, A.; Samuel, J.; Sattari, S.; Kwon, G. S., *Pharmaceutical Research* **2002**, 19 (4), 418-422.
11. Choi, K.-C.; Bang, J.-Y.; Kim, P.-I.; Kim, C.; Song, C.-E., *International Journal of Pharmaceutics* **2008**, 355 (1-2), 224-230.
12. Falamarzian, A.; Lavasanifar, A., *Colloids and Surfaces B-Biointerfaces* **2010**, 81 (1), 313-320.
13. Jee, J.-P.; McCoy, A.; Mecozzi, S., *Pharmaceutical Research* **2012**, 29 (1), 69-82.
14. Das, S.; Suresh, P. K., *Nanomedicine-Nanotechnology Biology and Medicine* **2011**, 7 (2), 242-247.
15. Larabi, M.; Yardley, V.; Loiseau, P. M.; Appel, M.; Legrand, P.; Gulik, A.; Bories, C.; Croft, S. L.; Barratt, G., *Antimicrobial Agents and Chemotherapy* **2003**, 47 (12), 3774-3779.
16. Tsuji, H., *Macromolecular Bioscience* **2005**, 5 (7), 569-597.

17. Castilla-Cortazar, I.; Mas-Estelles, J.; Meseguer-Duenas, J. M.; Ivirico, J. L. E.; Mari, B.; Vidaurre, A., *Polymer Degradation and Stability* **2012**, 97 (8), 1241-1248.
18. Uhrich, K. E.; Cannizzaro, S. M.; Langer, R. S.; Shakesheff, K. M., *Chemical Reviews* **1999**, 99 (11), 3181-3198.
19. Ikada, Y.; Tsuji, H., *Macromolecular Rapid Communications* **2000**, 21 (3), 117-132.
20. Sgouras, D.; Duncan, R., *Journal of Materials Science-Materials in Medicine* **1990**, 1 (2), 61-68.
21. O'Brien, J.; Wilson, I.; Orton, T.; Pognan, F., *European Journal of Biochemistry* **2000**, 267 (17), 5421-5426.
22. Al-Nasiry, S.; Geusens, N.; Hanssens, M.; Luyten, C.; Pijnenborg, R., *Human Reproduction* **2007**, 22 (5), 1304-1309.
23. Wang, F.; Bronich, T. K.; Kabanov, A. V.; Rauh, R. D.; Roovers, J., *Bioconjugate Chemistry* **2005**, 16 (2), 397-405; Allen, C.; Han, J. N.; Yu, Y. S.; Maysinger, D.; Eisenberg, A., *Journal of Controlled Release* **2000**, 63 (3), 275-286.
24. Tiyafoonchai, W.; Limpeanchob, N., *International Journal of Pharmaceutics* **2007**, 329 (1-2), 142-149.
25. Zhou, W.; Wang, Y.; Jian, J.; Song, S., *International Journal of Nanomedicine* **2013**, 8, 3715-3728.
26. Zhang, H. J.; Yao, M.; Morrison, R. A.; Chong, S. H., *Archives of Pharmacal Research* **2003**, 26 (9), 768-772; Mohamed, A.; Mahfoodh, A.-S. M., *Colloids and Surfaces a-Physicochemical and Engineering Aspects* **2006**, 287 (1-3), 44-50.
27. Fields, R. D.; Lancaster, M. V., *American Biotechnology Laboratory* **1993**, 11 (4), 48-&.
28. Jette, K. K.; Law, D.; Schmitt, E. A.; Kwon, G. S., *Pharmaceutical Research* **2004**, 21 (7), 1184-1191.
29. Van de Ven, H.; Paulussen, C.; Feijens, P. B.; Matheussen, A.; Rombaut, P.; Kayaert, P.; Van den Mooter, G.; Weyenberg, W.; Cos, P.; Maes, L.; Ludwig, A., *Journal of Controlled Release* **2012**, 161 (3), 795-803.
30. Jain, J. P.; Kumar, N., *European Journal of Pharmaceutical Sciences* **2010**, 40 (5), 456-465.
31. Singh, P.; Gupta, A.; Jaiswal, A.; Dube, A.; Mishra, S.; Chaurasia, M. K., *Journal of Biomedical Nanotechnology* **2011**, 7 (1), 50-51.
32. Washington, C., *International Journal of Pharmaceutics* **1990**, 58 (1), 1-12.

33. Washington, C., *International Journal of Pharmaceutics* **1989**, 56 (1), 71-74.
34. Li, Y.; Qi, X. R.; Maitani, Y.; Nagai, T., *Nanotechnology* **2009**, 20 (5).
35. Stefani, M.; Coudane, J.; Vert, M., *Polymer Degradation and Stability* **2006**, 91 (11), 2554-2559.
36. Huang, M. H.; Li, S. M.; Hutmacher, D. W.; Schantz, J. T.; Vacanti, C. A.; Braud, C.; Vert, M., *Journal of Biomedical Materials Research Part A* **2004**, 69A (3), 417-427.
37. Cometa, S.; Bartolozzi, I.; Corti, A.; Chiellini, F.; De Giglio, E.; Chiellini, E., *Polymer Degradation and Stability* **2010**, 95 (10), 2013-2021.
38. Kister, G.; Cassanas, G.; Bergounhon, M.; Hoarau, D.; Vert, M., *Polymer* **2000**, 41 (3), 925-932.
39. Trimaille, T.; Gurny, R.; Moeller, M., *Journal of Biomedical Materials Research Part A* **2007**, 80A (1), 55-65.
40. Kim, D.; Gao, Z. G.; Lee, E. S.; Bae, Y. H., *Molecular Pharmaceutics* **2009**, 6 (5), 1353-1362; Bae, Y.; Jang, W. D.; Nishiyama, N.; Fukushima, S.; Kataoka, K., *Molecular Biosystems* **2005**, 1 (3), 242-250; Yoo, H. S.; Park, T. G., *Journal of Controlled Release* **2004**, 96 (2), 273-283.

**Chapter 6 Synthesis and
Characterisation of Folate tipped
Poly(decylactone) Micelles for
Receptor Mediated Tumor
Targeting**

6.1 Introduction

The delivery of an optimum concentration of a drug to the intended target site can minimise the systemic adverse reactions, reduce the dose, enhance its therapeutic efficiency and consequently improve patient compliance. Targeted drug delivery is crucial in cancer therapy and therefore extensive research is continuing to develop an effective treatment of cancer using targeted therapy. Although significant progress has been achieved for early stage cancer, the treatments are limited for advanced stage cancer^{1, 2}. In conventional chemotherapy for late stage cancers, cytotoxic agents have been used to kill cancer cells, often on the assumption that these are more rapidly proliferating than normal cells and thus more prone to internalise drugs. However, due to the lack of selectivity and high toxicity associated with many anticancer drugs, severe side effects are often observed. Targeted delivery of an anticancer drug to a tumor has been suggested to increase the therapeutic efficacy and minimise the systemic toxic effects of anticancer agents^{1, 2}. With the aid of drug targeting, selective killing of tumor cells is possible, leaving the normal cells unaffected and therefore fewer side effects are observed³. The strategy of drug targeting has been divided into "active" and "passive" categories.

Passive targeting is based on the Enhanced Permeation and Retention (EPR) effect⁴ in which drug-loaded polymeric nano-carriers accumulate in solid tumors. It has been reported that effective retention of drugs in tumors through the EPR effect is generally observed with higher molecular weight drug loaded nano-carriers (typically > 40 kDa)⁵. Additionally, in passive targeting, the bulk (>95%) of administered drug-loaded nano-carriers were found in other organs such as liver, lungs, and spleen⁶. Thus, it has been proposed that passive targeting is not very selective to tumors. Recently, Bae and Park suggested that the term "passive targeting" should be replaced with "blood circulation and extravasation," which is not limited to tumors only⁶.

Furthermore, it was reported that passive targeting is not very effective in multiple-drug resistance (MDR) tumors³. MDR is a condition in which cancer cells develop resistance towards one or more drugs. The overexpression of transporter proteins in cancer cells is responsible for MDR, as transporter protein frequently remove specific drugs from cancer cells. This leads to poor availability of the drug in tumors, which consequently reduces the effectiveness of treatment³. Moreover, variation in vascular permeability during tumor progression, tumor type

and in the anatomical location of tumors further limits the effectiveness of this approach for therapy in cancer^{2,7,6}.

Active targeting, also known as ligand-mediated targeting is another approach used for delivering cytotoxic agents to tumors. Active targeting has been suggested to be more effective when compared to passive targeting⁸. Superior antitumor activities of drug-loaded nano-carriers have been reported with active targeting due to their enhanced cellular internalisation *via* receptor-mediated endocytosis^{9,10}. Active targeting of drug-loaded nano-carriers can be achieved by attaching a ligand, on the surface of the polymers, which binds with appropriate receptors expressed at the target site *in vivo*. Commonly used ligands for tumor targeting are antibodies, proteins, peptides, nucleic acids, sugars, and small molecules such as vitamins^{10, 11}.

Among the different types of ligands utilised for the active targeting, folic acid (FA) as a ligand has been extensively studied in cancer therapy to deliver drug-loaded nano-carriers to tumor cells¹². FA, a vitamin, and its reduced form are essential components for the biosynthesis of nucleotide bases via one-carbon transfer reactions. Therefore, cell proliferation and survival largely depends on their ability to uptake FA. Cells normally endocytose the FA either by reduced folate

carrier or via the folate receptor (FR)¹³. Reduced folate carrier is present in all cells and is able to provide a sufficient quantity of FA for cell growth. However, in many cancer cells, the FR is overexpressed, so that malignant cells can compete for the required FA with normal cells when the supply of this vitamin is limited¹². Furthermore, the reduced folate carrier uptake mechanism is selective for the transportation of folate (reduced forms of folic acid) whereas FR favourably facilitates the uptake of folic acid (oxidised forms of folate)¹².

Therefore, a drug delivery carrier linked with folic acid has the ability to deliver its content specifically to cancer cells. Folic acid tipped carriers after binding to the FR present on to the cell surface have been shown to be taken up through receptor-mediated endocytosis. The overexpressed FR is present in many human cancers which include breast, ovarian, colorectal, endometrial, brain, kidney, and lung¹⁴.

In addition to the specific selectivity of folic acid to cancer cells its low immunogenicity, low molecular weight (mw – 441.4), aqueous solubility, high stability, low cost, ready availability and facile conjugation chemistry make it an attractive ligand for use in drug targeting^{15, 16}. Considering these advantages several folate-conjugated drug delivery carriers such as liposomes, nanoparticles, micelles, dendrimers, carbon

nanotubes have been investigated for targeted cancer therapy and has been reviewed recently^{16, 17}. Based on the excellent *in vitro* and *in vivo* results, a few folic acid conjugated drug delivery systems have been entered in clinical trials¹⁸.

Although liposomes, nanoparticles, and other drug delivery systems have been successfully used for the tumor targeting however, the use of polymeric micelles to deliver cytotoxic drug have their own advantages¹⁹ (refer chapter 1). Polymeric micelles have the ability to target tumor sites by active as well as passive mechanisms. Polymeric micelles after accumulation in tumors can selectively deliver the drugs to their subcellular targets by acting as intracellular "Trojan horses" thus; can overcome the drug resistance^{20, 21}. The selective release of drugs can be achieved by pH sensitive micelles, which only release their content in the endosome and lysosome of cell (acidic pH), after internalisation by endocytosis^{22, 23}. Furthermore, micelles have been shown to circumvent recognition by the drug efflux pump (such as P-glycoprotein) and thus can overcome multidrug resistance in cancer cells, which in turn enhanced the cellular concentration of drugs^{22, 24}. Attachment of a targeting ligand on the surface of polymeric micelles has been reported to enhance therapeutic

efficacy of a drug in cancer therapy by increasing its intracellular concentration^{23, 25}.

Folic acid-modified polymeric micelles have been widely studied for targeted therapy in cancer. Due to the functional group chemistry of FA, its conjugation with end-functionalised block copolymers is facile²⁰. For instance, Yoo and Park reported the synthesis of folate conjugated PEG-b-PLGA block copolymers by amide chemistry. Folic acid was attached to the end-functionalised PLGA-b-PEG-NH₂ via its γ -carboxyl group. *In vitro* cytotoxicity studies in KB cells showed that these micelles displayed high uptake as well as cytotoxicity compared to non-targeted micelles²⁶. In another study, FA was conjugated with a mPEG-b-PCL copolymer using similar chemistry but on the hydrophobic block (*i.e.* PCL). The obtained confocal images suggested that folate conjugated mPEG-b-PCL micelles were selectively taken up into MCF-7 cells by folate-receptor mediated endocytosis²⁷. Many reports have now been published proposing the effective treatment of cancer *via* folate conjugated polymeric micelles²⁸⁻³⁰. Therefore, it was hypothesised that FA conjugated PEG-b-PDL micelles could show their potential for targeted therapy in cancer.

In this chapter, fabrication of PEG-b-PDL block copolymer micelles conjugated with FA is reported. Folic acid was

conjugated onto the N_3 -PEG-NH₂ using a reported amidation reaction. Later this block was attached to the hydrophobic PDL block via click chemistry³¹. Rhodamine conjugated PEG-b-PDL copolymer was also synthesised for imaging purpose. A diblock copolymer (mPEG-b-PDL) was also synthesised using click chemistry for comparison studies. Mixed micelles of the functionalised and non-functionalised PEG-b-PDL copolymers were prepared and evaluated for the folate mediated targeting efficiency on human cancer cell lines *in vitro*.

6.2 Methods

6.2.1 Synthesis of Azide Terminated Poly(ethylene glycol) methyl ether

Synthesis of methoxy-PEG-N₃ using poly(ethylene glycol) methyl ether was accomplished in two steps *via* a reported procedure³².

Step (I) – Synthesis of tosylated poly(ethylene glycol) methyl ether: Poly(ethylene glycol) methyl ether ($M_n=5.0$ KDa, 2.00 g, 0.40 mmol) was dissolved in anhydrous pyridine (10.0 mL) and toluene sulfonyl chloride (0.76 g, 4.00 mmol) was added to the solution. The reaction mixture was then stirred for 24 hrs at room temperature under an inert atmosphere. The obtained solution was then precipitated four times in cold

diethyl ether and any solvent residue was removed under vacuum to obtain a white solid product (1.64 g, 82 %).

mPEG-OTs - ^1H NMR (400 MHz, CDCl_3) δ (ppm) 7.83 (Aromatic-CH, d, 2H), 7.35 (Aromatic-CH, d, 2H), 4.23 – 4.13 ($\text{CH}_2\text{-CH}_2\text{-O-Tosyl}$, t, 2H), 3.66 ($\text{O-CH}_2\text{-CH}_2\text{-O}$, s, 508H), 3.40 (O-CH_3 , s, 3H), 2.47 (Aromatic- CH_3 , s, 3H).

Step (II) – Synthesis of azide terminated poly(ethylene glycol) methyl ether: Tosylated poly(ethylene glycol) methyl ether (1.50 g, 0.25 mmol) was dissolved in DMSO (10.0 mL) and sodium azide (203.50 mg, 3.13 mmol) was added. The reaction mixture was then stirred for 24 hrs at room temperature under inert atmosphere. Dichloromethane (20.0 mL) was then added to the reaction mixture and the organic layer was washed with cold distilled water (50.0 mL x 3), then with cold 6 M hydrochloric acid solution (50.0 mL x 2) and again with cold distilled water (50.0 mL x 2). The organic layer was dried with anhydrous MgSO_4 and solvent was evaporated in vacuum. The obtained residue was then precipitated three times with cold diethyl ether. The solvent traces were then removed in vacuum to obtain an off white solid product (1.2 g, 78 %). The conversion of tosyl to azide product as calculated by $^1\text{HNMR}$ was 89%.

mPEG-N₃ - ¹H NMR (400 MHz, CDCl₃) δ (ppm) 3.67 (O-CH₂-CH₂-O, s, 508H), 3.43 – 3.36 (O-CH₃, CH₂-CH₂-N₃, m, 4.9H)

FTIR wavenumber (cm⁻¹) - 2873 (C-H, stretching), 2079 (N=N=N, stretching), 1464 (C-H, bending), 1091 (C-O, Stretching)

6.2.2 Synthesis of Folate Conjugated Poly(ethylene glycol)

Conjugation of folic acid on to the commercially available N₃-PEG-NH₂.TFA salt was done in single step using a reported method³³. Briefly, a solution of folic acid (0.055 g, 0.12 mmol) was prepared in anhydrous DMSO (2.0 mL) in the dark. Triethylamine (0.6 mL), *N,N'*-dicyclohexyl carbodiimide (DCC) (0.03 g, 0.15 mmol) and *N*-hydroxysuccinimide (NHS) (0.02 g, 0.15 mmol) were then added to the above prepared solution. The reaction mixture was than stirred overnight at room temperature in the dark (covered flask) under a nitrogen atmosphere. Separately, N₃-PEG-NH₂.TFA salt (0.25 g, 0.05 mmol) was dissolved in anhydrous DMSO (2.0 mL) contained triethylamine (0.1 mL) and stirred for 2 hrs. The solution of activated N₃-PEG-NH₂ was added to the solution of *N*-hydroxysuccinimidyl-ester of folic acid prepared above. The reaction mixture was then stirred for 24 hrs at room temperature in the dark. The obtained solution was then

precipitated several times in cold diethyl ether and any solvent residue was removed in vacuum. Recovered dry yellow solid was then dissolved in DCM (5.0 mL, a non-solvent for folic acid) and centrifuge in order to remove precipitate. Supernatant was collected after centrifugation and solvent was removed in vacuum. Further, the yielded product was dissolved in HPLC grade water (5.0 mL) and the pH was adjusted to 3.0 (approx.) using hydrochloric acid (1 M) to precipitate any remaining free folic acid. The solution was then filtered with 0.22 μ syringe filter and dialysed (MWCO of dialysis bag – 1000 Da) against PBS (pH-7.4) for 3 days to ensure complete removal of any free folic acid and then for 2 days against deionised (DI) water to remove salts (dialysis medium was changed in every 8 hrs). The final solution was then filtered and freeze dried to obtain the folate conjugate PEG-N₃ which was light yellow in colour (251 mg, 92 %). To determine the amount of conjugated folic acid, folate-PEG₅₀₀₀-N₃ (FA-PEG-N₃) was analysed on a UV-Vis spectrophotometer and the concentration of folic acid was calculated using a pre-prepared standard calibration curve of folic acid (PBS was used as solvent to prepare different concentration of folic acid solution) at λ_{max} of 280nm (figure 6-1 A).

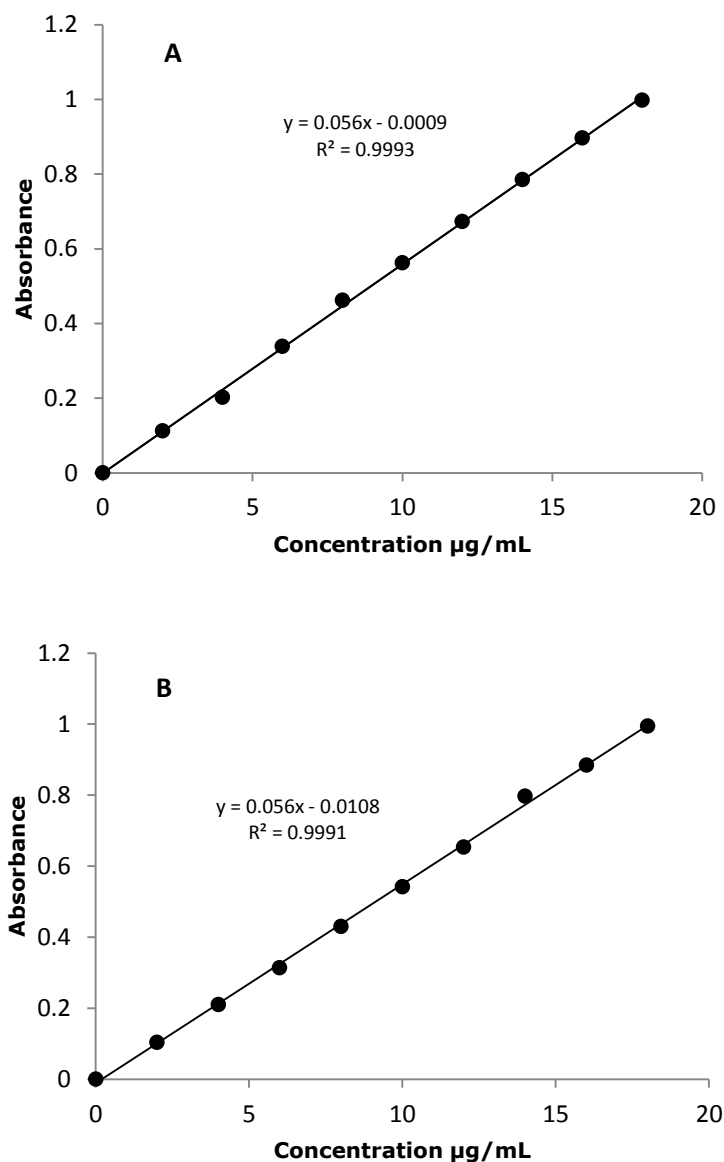


Figure 6-1 Standard calibration curve of (A) folic acid and (B) rhodamine B isothiocyanate. The UV-Vis absorbance of folic acid and rhodamine B isothiocyanate solution (in PBS) was measured at wavelength of 280 and 552 nm respectively.

FA-PEG-N₃ – ¹H NMR (400 MHz, DMSO-d₆ contained few drops of D₂O) δ (ppm) 8.65 (Ar-N-CH, d, 0.8H), 7.63 (Ar-CH, d, 1.7H), 6.64 (Ar-CH, d, 1.7H), 4.50 (NH-CH₂, d, 1.7H), 4.40 – 4.19 (CH₂-CH-COOH, m, 0.8H), 3.49 (O-CH₂-CH₂-O, s, 498H), 3.34 – 3.26 (CH₂-CH₂-N₃, m, 2H), 3.25 – 3.10 (CH₂-CH₂-NH-

COO, m, 1.6H), 2.43-2.10 ($\text{CH}_2\text{-CH}_2\text{-CH-COOH}$, m, 1.6H), 2.10-1.75 ($\text{CH}_2\text{-CH}_2\text{-CH-COOH}$, m, 2.0H).

MALDI-TOF MASS: $\text{N}_3\text{-PEG-NH}_2\text{.TFA}$ - m/z Calculated - 5000
Found- 4706 $[\text{M}]^+$

FA-PEG-N_3 - m/z Calculated - 5129, Found - 5176 $[\text{M} + 2\text{Na}]^+$.

6.2.3 Synthesis of Rhodamine B Conjugated Poly(ethylene glycol)

Conjugation of Rhodamine B *isothiocyanate* (RhB) on to commercially available $\text{N}_3\text{-PEG-NH}_2\text{.TFA}$ salt was done via a reported method³⁴. Briefly, $\text{N}_3\text{-PEG-NH}_2\text{.TFA}$ salt (0.25 g, 0.05 mmol) was dissolved in anhydrous DMSO (2.0 mL) that contained triethylamine (0.1 mL) and, the mixture stirred for 2 hrs. Rhodamine B *isothiocyanate* (0.053 g, 0.10 mmol) was then added to the above solution and the reaction mixture was stirred for 24 hrs at room temperature. The obtained solution was precipitated four times in cold diethyl ether and any solvent residue was evaporated under vacuum. The dried red solid was then dissolved in HPLC grade water (5.0 mL) and dialysed (MWCO of dialysis bag - 1000 Da) against DI water for 6 days (dialysis medium was changed in every 8 hrs) in order to remove free rhodamine B *isothiocyanate*. The obtained solution was then freeze dried to yield rhodamine

conjugated to PEG-N₃, which was red in colour (231 mg, 84 %). To determine the amount of rhodamine B, RhB-PEG₅₀₀₀-N₃ (RhB-PEG-N₃) was analysed on UV-Vis spectrophotometer and concentration of rhodamine B was calculated using a pre-prepared standard calibration curve of rhodamine at λ_{\max} of 552nm (figure 6-1 B).

¹HNMR (400 MHz, CDCl₃) δ (ppm) 6.76 – 6.25 (Ar-CH, m, 5.3H), 3.66 (O-CH₂-CH₂-O, s, 509H), 3.45 – 3.35 (CH₂-CH₂-N₃, m, 2H), 1.44 – 1.01 (-N-CH₂-CH₃, m, 11.4H)

¹HNMR (400 MHz, DMSO-d₆) δ (ppm) 10.57 (Ar-COOH, s, 0.5 H), 8.01 (Ar-CH, m, 2.7H), 6.87 (Ar-CH, m, 5.4H), 3.52 (O-CH₂-CH₂-O, s, 500H), 1.14 (-N-CH₂-CH₃, d, 11H)

MALDI-TOF MASS: RhB-PEG-N₃ – m/z Calculated – 5243, Found - 5361 [M +TFA]

6.2.4 Synthesis of Propargyl-PDL

Propargyl PDL was synthesised using a method reported in chapter 3. The degree of polymerisation selected for the synthesis of propargyl-PDL was 100. The M_n found by SEC was used for further calculations.

6.2.5 Synthesis of Block Copolymers via Click Chemistry

The block copolymers of PEG and PDL were synthesised using azide alkyne click chemistry³⁵. The reaction between azide of

PEG and alkyne of PDL was performed at room temperature using copper as catalyst to yield mPEG-b-PDL, FA-PEG-b-PDL and RhB-PEG-b-PDL. Briefly, propargyl-PDL (1.82 g, 0.24 mmol), mPEG-N₃ (0.48 g, 0.10 mmol) and 2,2'-Bipyridyl (0.02g, 0.10 mmol) were dissolved in 2.0 mL of dimethylacetamide (DMAc) under a nitrogen atmosphere. Copper (I) bromide (0.7 mg, 0.005 mmol) was then added to the above solution and the flask was sealed under nitrogen atmosphere. A saturated solution of sodium ascorbate (10 µl) in water was diluted to 100µl with DMAc and added to the reaction mixture. This is an additional precaution to prevent the oxidation of copper during the reaction. The reaction progress was monitored by ¹HNMR and complete conversion was observed after 48 hrs of stirring. The obtained solution was then precipitated four times in petroleum ether to remove excess of propargyl-PDL and 2,2'-bipyridyl. The precipitate was then dissolved in a minimum quantity of chloroform and centrifuged (15000 rpm, 2 min.) to remove copper and sodium ascorbate. The organic layer was collected and solvent was evaporated in vacuum to yield the product, which was a hard wax-like material (1.0 g, 87%). A similar procedure was followed to synthesise FA-PEG-b-PDL and RhB-PEG-b-PDL using FA-PEG-N₃ (200 mg) and RhB-PEG-N₃ (180 mg) respectively. The quantity of 2,2'-bipyridyl (1 equivalent) and

copper (I) bromide (0.05 equivalent) was calculated based on the amount of PEG used. The percentage yield observed for FA-PEG-b-PDL was 81% (398 mg) while 79% (361mg) yield was observed for RhB-PEG-b-PDL.

mPEG-b-PDL:

^1H NMR (400 MHz, CDCl_3) δ (ppm) 7.80 (Triazole-CH, s, 1H), 5.23 (COO-CH₂-Triazole, s, 2H), 5.02 – 4.78 (CH-O-CO, m, 42H), 4.66 – 4.46 (CH₂-CH₂-triazole, t, 2H), 3.93 – 3.86 (CH₂-CH₂-triazole, t, 2H), 3.66 (O-CH₂-CH₂-O, s, 507H), 3.39 (O-CH₃, s, 3H), 2.42 – 2.21 (O-CO-CH₂, m, 85H), 1.77 – 1.40 (CH₂-CH₂-CH-CH₂, m, 254H), 1.40 – 1.16 (CH₂-CH₂-CH₂-CH₃, m, 259H), 0.89 (CH₃, t, 129H).

FTIR wavenumber (cm^{-1}): 2858 (C-H, stretching), 1729 (C=O, stretching), 1341 (C-H, bending), 1103 (C-O, Stretching).

FA-PEG-b-PDL:

^1H NMR (400 MHz, CDCl_3) δ (ppm) 7.80 (Triazole-CH, s, 1H), 5.22 (COO-CH₂-Triazole, s, 2H), 5.00 – 4.80 (CH-O-CO, m, 42H), 4.65 – 4.49 (CH₂-CH₂-triazole, t, 2H), 3.96 – 3.87 (CH₂-CH₂-triazole, t, 2H), 3.65 (O-CH₂-CH₂-O, s, 500H), 2.48 – 2.19 (O-CO-CH₂, m, 86H), 1.89 – 1.40 (CH₂-CH₂-CH-CH₂, m, 253H), 1.40 – 1.14 (CH₂-CH₂-CH₂-CH₃, m, 259H), 1.03 – 0.76 (CH₃, t, 131H).

^1H NMR (400 MHz, DMSO- d_6) δ (ppm) 8.66 (Ar-N-CH, s, 1H), 8.06 (Triazole-CH, s, 1H), 7.66 (Ar-CH, s, 1.7H), 6.66 (Ar-CH, s, 2H), 4.96 – 4.60 (CH-O-CO, m, 42H), 4.54 (CH_2 - CH_2 -triazole, NH- CH_2 , d, 4H), 3.89 – 3.75 (CH_2 - CH_2 -triazole, m, 2H), 3.51 (O- CH_2 - CH_2 -O, s, 546H), 1.45 (CH_2 - CH_2 -CH- CH_2 , m, 247H), 1.20 (CH_2 - CH_2 - CH_2 - CH_3 , m, 246H), 0.80 (CH_3 , s, 133H).

RhB-PEG-b-PDL

^1H NMR (400 MHz, CDCl_3) δ (ppm) 7.80 (Triazole-CH, s, 1H), 5.22 (COO- CH_2 -Triazole, s, 2H), 4.89 (CH-O-CO, m, 42H), 4.61 – 4.51 (CH_2 - CH_2 -triazole, t, 2H), 3.95 – 3.87 (CH_2 - CH_2 -triazole, t, 2H), 3.66 (O- CH_2 - CH_2 -O, N- CH_2 - CH_3 s, 500H), 2.45 – 2.21 (O-CO- CH_2 , m, 85H), 1.78 – 1.40 (CH_2 - CH_2 -CH- CH_2 , m, 257H), 1.40 – 1.16 (CH_2 - CH_2 - CH_2 - CH_3 , N- CH_2 - CH_3 m, 270H), 1.00 – 0.78 (CH_3 , t, 133H).

^1H NMR (400 MHz, DMSO- d_6) δ (ppm) 8.24 (Ar-CH, s, 1H), 8.06 (Triazole-CH, s, 1H), 7.66 (Ar-CH, m, 1H), 7.54 – 7.38 (Ar-CH, m, 1H), 6.54 (Ar-CH, m, 6H), 5.05 – 4.60 (CH-O-CO, m, 43H), 4.54 (CH_2 - CH_2 -triazole, m, 2H).

6.2.6 Preparation and Characterisation of Mixed Micelles

Mixed micelles of synthesised functional copolymers were prepared by nanoprecipitation method. Two formulations of micelles were prepared using an automated syringe pump. The details of the polymers quantities used were as follow:

- **PDL Formulation** – Contained mPEG-b-PDL (10 mg) and RhB-PEG-b-PDL (0.5 mg)
- **PDLFA Formulation** – Contained mPEG-b-PDL (8 mg), FA-PEG-b-PDL (2 mg) and RhB-PEG-b-PDL (0.5 mg)

Briefly, calculated quantities (as above) of copolymers were dissolved in acetone (1.5 mL) and this solution was added drop-wise into PBS (3.0 mL) under stirring (1000rpm) using a syringe pump. The flow rate used was 0.25 mL/min. The samples were left under stirring for 3 hrs and then left aside for additional 2 hrs at room temperature to ensure complete removal of acetone. Both formulation was filtered through a 0.22 μ syringe filter and used for further analysis.

Micelle size and surface charge was measured using a Zetasizer Nano ZS instrument. The concentration of samples used for the analysis was 70 μ g/mL. Micelle size was measured in PBS and in RPMI while the surface charge was measured in HEPES buffer (pH- 7.4, 10mM). Further, the samples were imaged using TEM to confirm the size and to determine the

surface morphology. TEM samples (70 $\mu\text{g/mL}$) were prepared in HPLC grade water. The concentration of folic acid (λ_{max} – 280nm) and rhodamine B (λ_{max} – 552nm) present in the purified micelle solution was measured using UV-Vis spectroscopy. All UV-Vis absorbance were acquired in PBS and the concentration was calculated using a previously prepared standard calibration curve.

6.2.7 Cellular Uptake Studies

The cellular uptake studies was kindly performed by Dr. Laura Purdie and Lee Moir. Human cancer cell lines *i.e.* MCF-7 (FR+ve, breast cancer cell line) and A549 (FR-ve, human lung adenocarcinoma epithelial cell line) were cultured in RPMI-1640 (folate free) media containing 10% fetal bovine serum and 2 mM L-glutamine at 37° C with 5% CO₂. Cells were seeded at 35,000 cells per chamber in an eight chamber borosilicate glass chamber slide. The whole media were removed after 24 hrs and cells were then incubated for 2.5 hrs with PDL and PDLFA micelles (100 $\mu\text{g/mL}$ each) diluted in media with and without free folic acid (500 $\mu\text{g/mL}$ for competitive binding assay). After 2.5 hrs, media were removed from all chambers and cells were washed three times with PBS. To fix the cells, 4% paraformaldehyde (PFA) in PBS was added for 10 minutes at room temperature (RT).

After 10 minutes, PFA solution was removed and cells were washed three times with PBS and then treated with Hoechst (nuclear) stain for 5 minutes prior to imaging. Hoechst stain was removed after 5 minutes and the cells were washed with PBS. Control experiments were also performed at 4°C instead of 37°C to determine the energy-dependent uptake. The uptake of PDL and PDLFA micelles was then examined by Leica confocal microscope at emission wavelength of 580 nm.

6.3 Results

6.3.1 Synthesis and Characterisation of Block Copolymers

Scheme 6-1 illustrates the synthesis methodology used to prepare the desired azide terminated PEG. Functionalised block copolymers were synthesised using commercially available N_3 -PEG-NH₂.TFA while azide terminated mPEG was prepared in the laboratory to generate a non-targeted block copolymer. All block copolymers were synthesised in three steps i. e. (I) synthesis of desired azide terminated hydrophilic block (*i.e.* PEG), (II) synthesis of alkyne terminated hydrophobic block (*i.e.* PDL) and (III) linking of azide and alkyne terminated block by click chemistry.

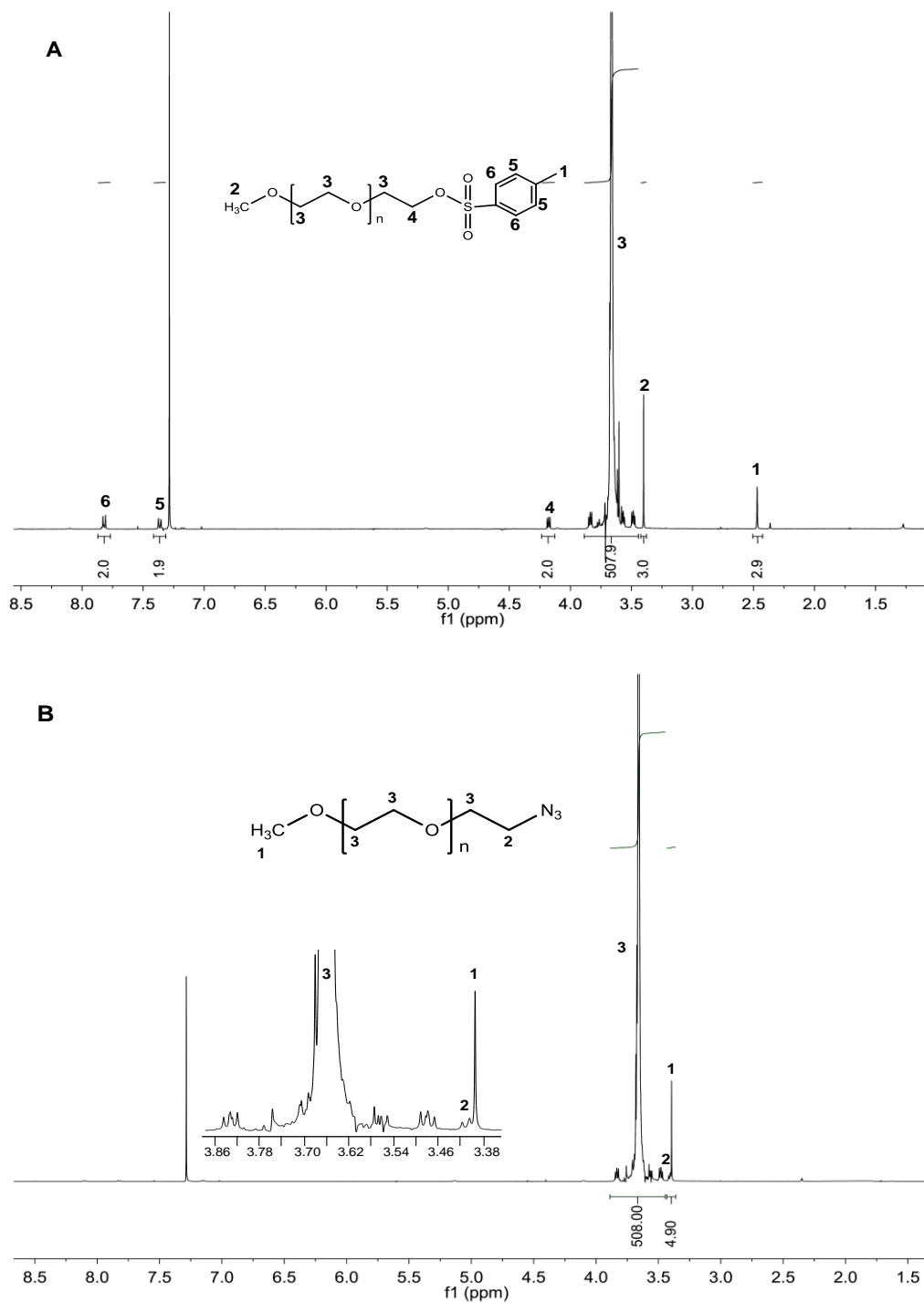


Figure 6-2 ^1H NMR spectra of (A) mPEG-OTs and (B) mPEG- N_3 acquired in chloroform- d . Inset in figure B showing the appearance of triplet peak at 3.4 ppm.

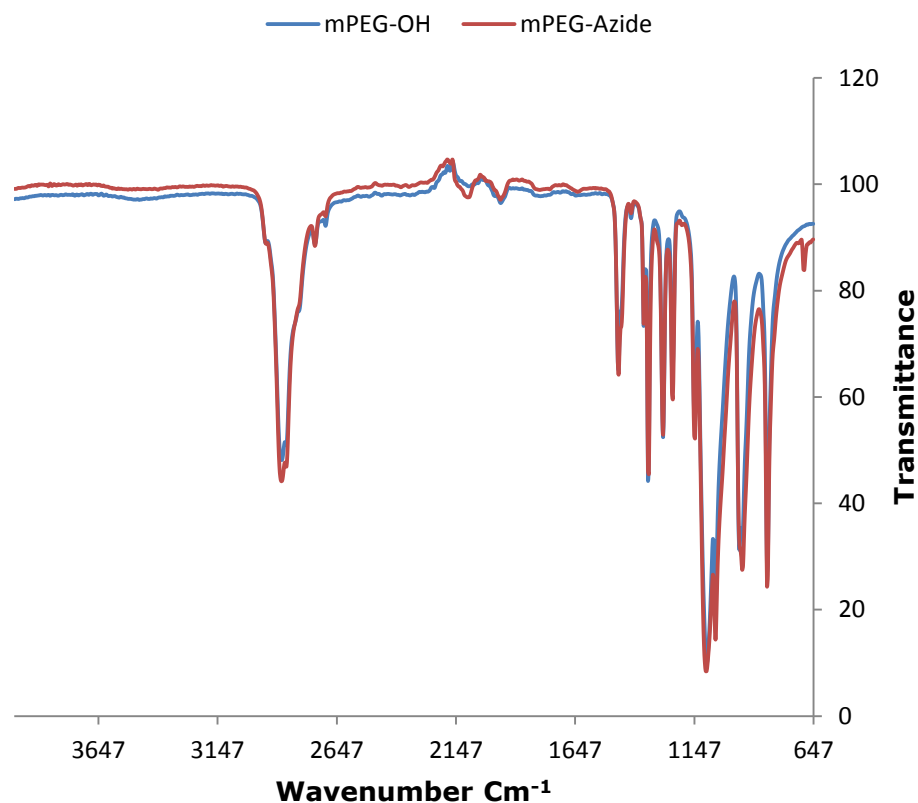


Figure 6-3 Overlapped FTIR spectra of mPEG₅₀₀₀-OH before and after azide conversion of hydroxyl group.

triplet at 3.3ppm (corresponding to the methylene proton next to azide, figure 6-2B, position 2) and disappearance of peak at 4.2 ppm suggested the successful conversion of intermediate into product (figure 6-2B). mPEG-N₃ was also characterised by FTIR and a peak detected at 2079 cm⁻¹ suggested the presence of azide group in sample (figure 6-3). However, the peak is not distinguishable and hence the synthesis confirmation is basically rely on NMR.

The conjugation of folic acid (FA) and rhodamine B *isothiocyanate* (RhB) to the amine group are well established

and facile reactions. FA and RhB were conjugated to the NH_2 -PEG- N_3 using reported mild reaction condition^{33, 34} (scheme 6-1 B, C).

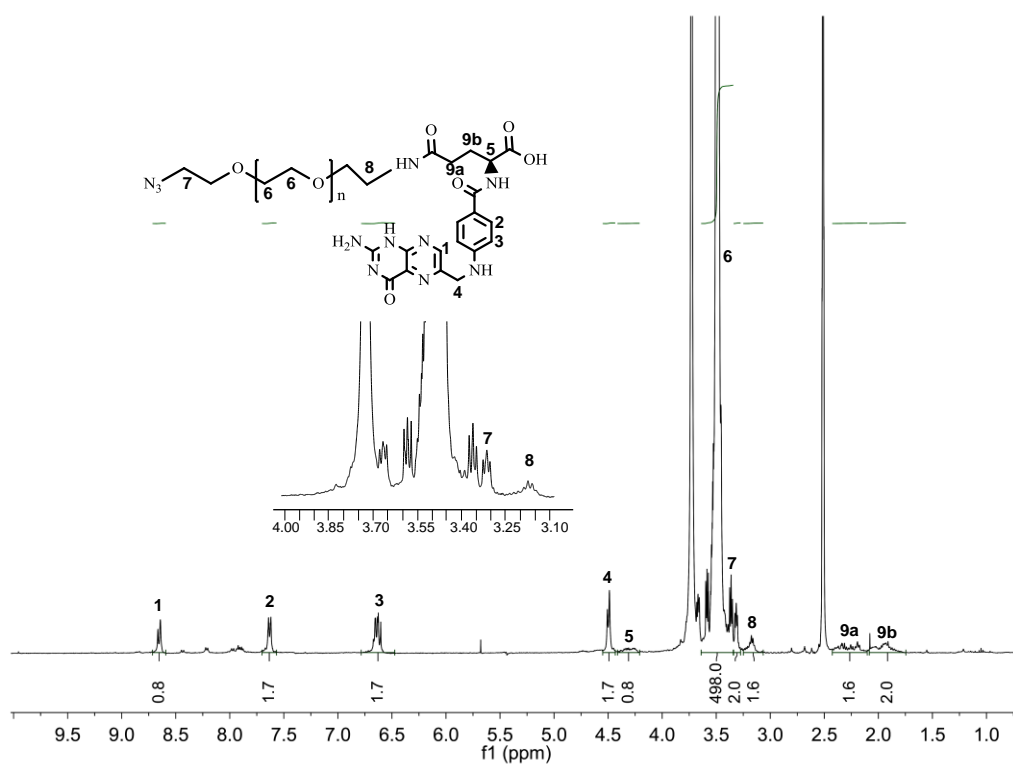


Figure 6-4 ^1H NMR of FA-PEG- N_3 in DMSO-d_6 that contained few drops of D_2O . The water peak generally observed at 3.3ppm in DMSO which was shifted to 3.7 due to the presence of D_2O .

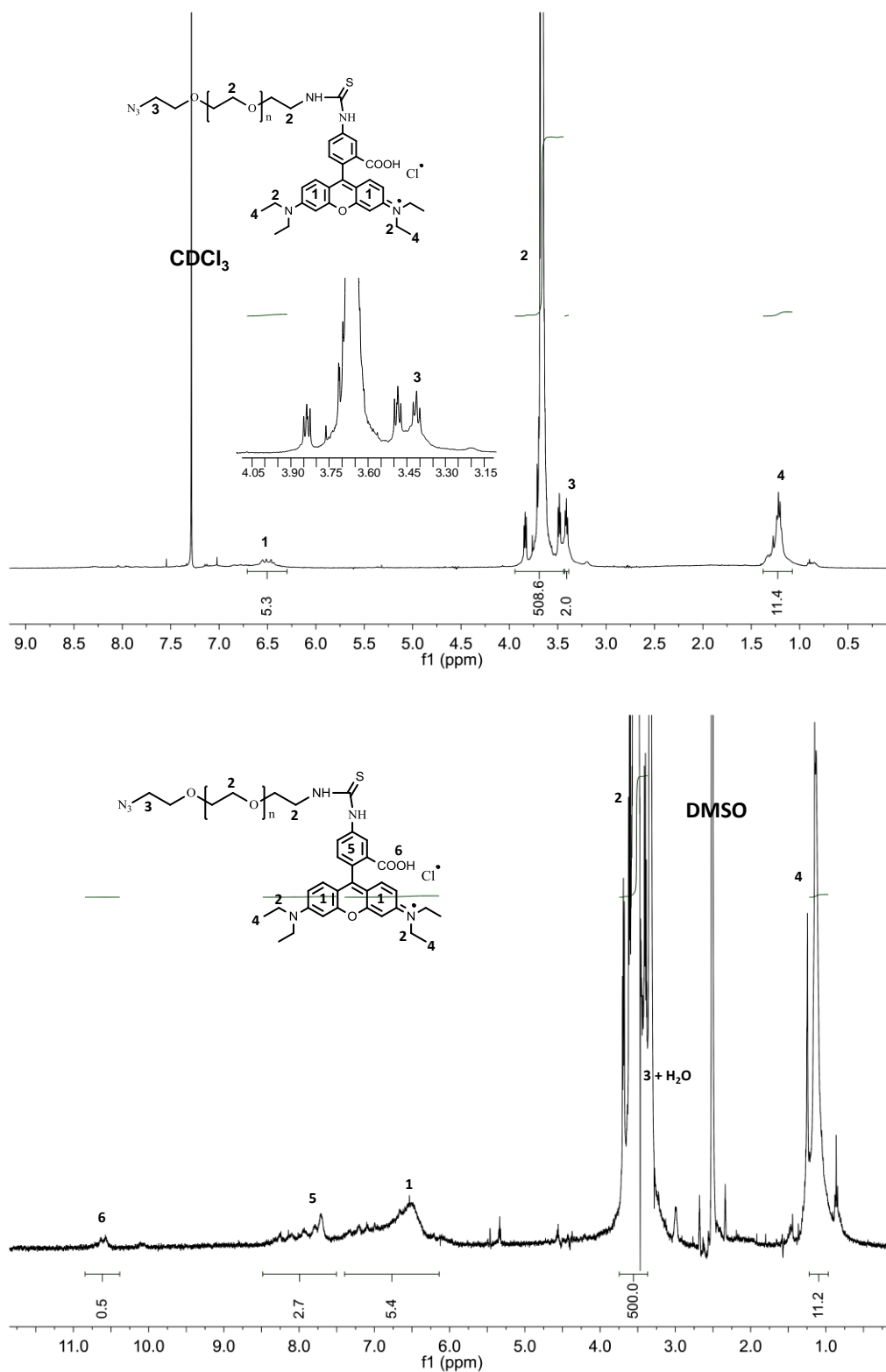


Figure 6-5 ¹H NMR of RhB-PEG-N₃ conjugate acquired in chloroform-d (top) and DMSO-d₆ (bottom). ¹H NMR spectra in DMSO-d₆ was acquired to visualise the peak of rhodamine B.

NH₂-PEG-N₃ was procured as a TFA salt and therefore it was treated with triethylamine before reaction to generate amine terminated PEG. Purified PEG conjugates (*i.e.* FA-PEG-N₃ and RhB-PEG-N₃) were characterised by ¹HNMR, MALDI-TOF MASS and SEC. Proton NMR spectrum of FA-PEG-N₃ was acquired in DMSO-d₆, which contained a few drops of D₂O to shift the residual water (present in DMSO-d₆) peak at 3.7 ppm. The methylene proton next to the azide group at 3.3 ppm was used as a standard for the comparative integration of other peaks (figure 6-4, position 7). The proton resonance and peak positions observed in the ¹HNMR spectrum of FA conjugated PEG were matched with the values reported in literatures^{30, 36}, which suggesting the successful conjugation of folic acid to PEG.

The conjugation of rhodamine B *isothiocyanate* with PEG was confirmed with ¹HNMR acquired in chloroform-d and DMSO-d₆. The proton resonance of other peaks with respect to the methylene proton next to the azide group of PEG (figure 6-5, position 3, acquired in CDCl₃) suggested the successful conjugation of RhB to PEG (figure 6-5). The peak positions observed for conjugated RhB were matched with the previous reported values³⁷. Further, FA-PEG-N₃ and RhB-PEG-N₃ were characterised by MASS and SEC. Changes in the peak shape

and position further confirmed the conjugation of FA and RhB to PEG as evident by MALDI-TOF MASS spectra (figure 6-6). The molecular weight (m/z) demonstrated by the highest peak (100% intensity) detected in MASS spectra was selected to represent the product molecular weight. The molecular weight detected by MASS technique for the conjugates were matched with the calculated molecular weight.

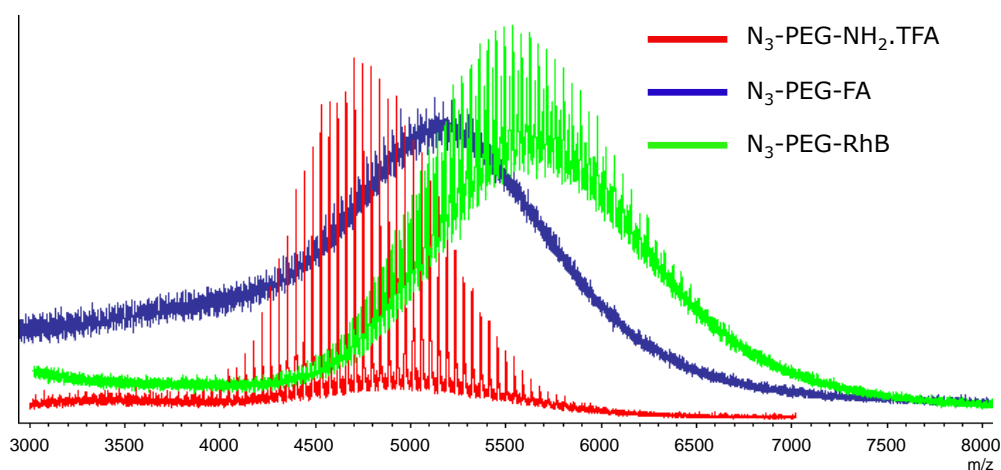


Figure 6-6 Overlapped MALDI-TOF MASS spectra of folic acid (FA), rhodamine B (RhB) conjugated PEG and non-conjugated PEG.

The M_n observed in SEC analysis for N_3 -PEG-FA ($M_n \sim 16.3$ KDa, PD-1.02) and N_3 -PEG-RhB ($M_n \sim 21.5$ KDa, PD-1.14) were more than the expected values but the change in retention time in SEC traces suggested the conjugation of FA and RhB on PEG ($M_n \sim 7.1$ KDa, PD-1.05) (figure 6-7). However, SEC traces suggested the presence of free PEG in the final product, which indicates incomplete conversion. The

PEG conjugates were used in the next step without further purification, considering that any azide terminated PEG will be converted into block copolymer in subsequent stage.

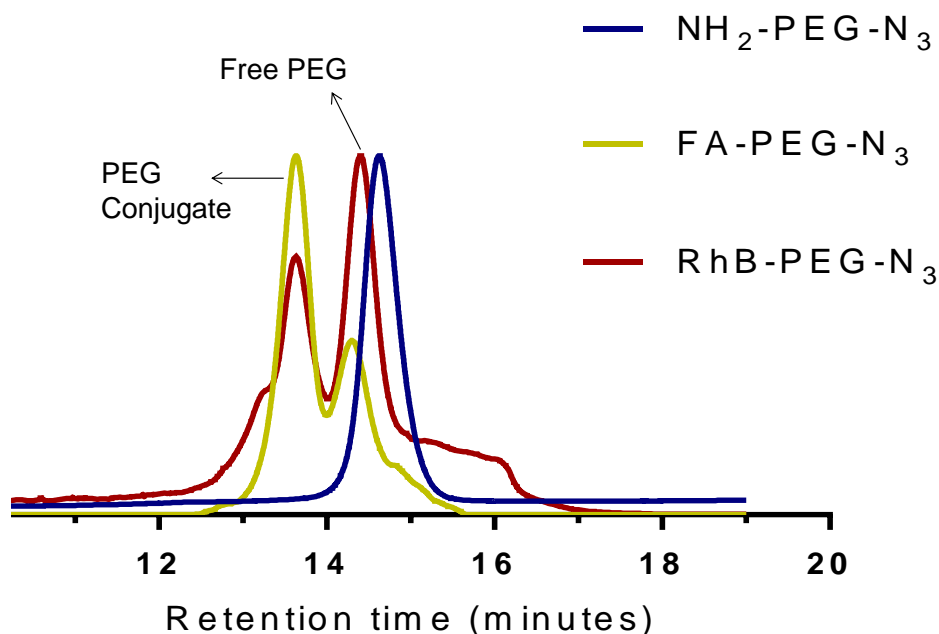


Figure 6-7 SEC trace of PEG conjugates and commercial PEG-azide. Chloroform was used as mobile phase and M_n was calculated against polystyrene polymer as reference

PEG conjugates of FA and RhB were further analysed on UV-Vis spectroscopy to determine the concentration of folic acid and Rhodamine B in samples. No change in λ_{max} was observed after the conjugation of FA and RhB with PEG as evident by UV-Vis spectra. According to the results, each milligram of FA-PEG-N_3 contained 81.84 μg of folic acid while 101.65 μg of rhodamine B was present in each milligram of RhB-PEG-N_3 . The percentage conversion calculated based on UV-vis results suggested 88 and 89.2% of conjugation of folic acid and

rhodamine B to PEG respectively. Based on the overall characterisation results, it can be concluded that desired PEG blocks were synthesised successfully. However, the final products contained some free PEG.

The hydrophobic block *i.e.* alkyne terminated PDL was synthesised by ROP of δ -decalactone using propargyl alcohol as initiator. The characterisation data has been already reported in chapter 3 and hence was not reproduced here.

The last step *i.e.* linking of PEG and PDL was done via a copper catalysed click reaction to fabricate the amphiphilic block copolymers (scheme 6-2). Excess of propargyl-PDL was used in the reactions to ensure complete consumption of azide terminated PEG. Copper was separated from the product by a simple solvent extraction process (figure 6-8).

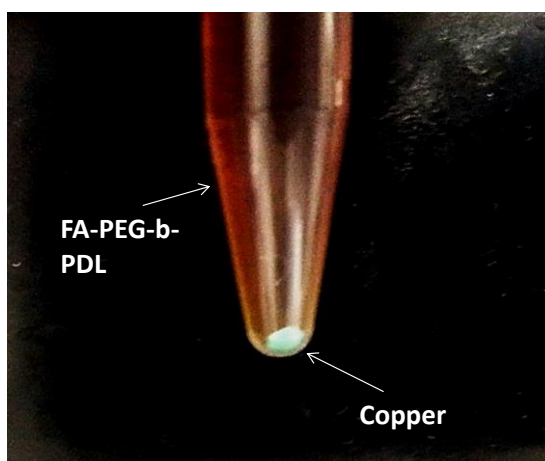
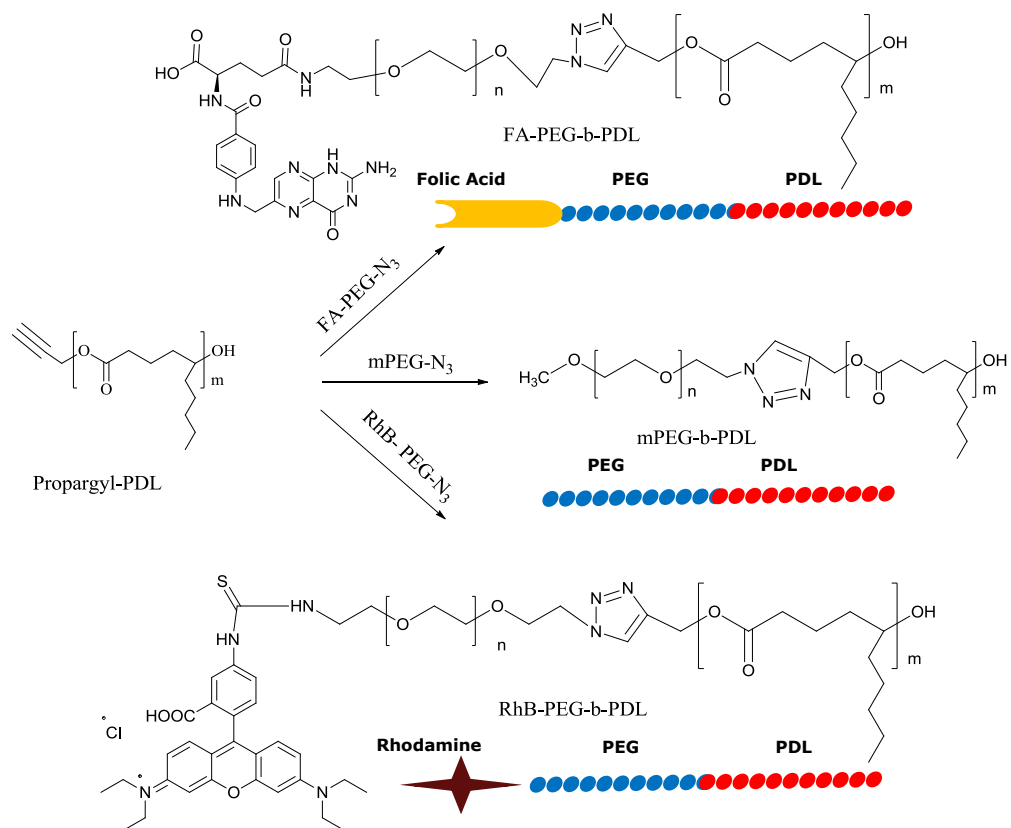


Figure 6-8 Picture of separated copper at bottom of eppendorf after centrifugation at 15000 rpm for 2 minutes. Copolymer (FA-PEG-b-PDL) solution was made in chloroform at a concentration of 100 mg/mL.



Scheme 6-2 Synthesis scheme of block copolymers of δ -decalactone via click chemistry

Purified block copolymers were characterised by FTIR (figure 6-9), NMR and by SEC to confirm synthesis and purity of products. Disappearance of peak in ^1H NMR at 3.3 ppm (corresponds to $\text{CH}_2\text{-N}_3$) and appearance of new peak at 7.8 (characteristic peak of triazole ring proton)³⁵, 5.2, 4.5 and 3.9 ppm suggested the successful conjugation of all azide terminated PEG to alkyne terminated PDL (figure 6-10 to 6-12). All other peak positions were matched with values reported in chapter 3.

Sample ID	M_n by ^1H NMR (KDa)	M_n by SEC (KDa)	PD by SEC
mPEG-b-PDL	12.2	21.0	1.06
FA-PEG-b-PDL	12.6	43.1	1.15
RhB-PEG-b-PDL	12.7	48.4	1.25

Table 6-1 M_n of synthesised copolymers determined by ^1H NMR and by SEC using chloroform as solvent and polystyrene polymer as reference (PD-polydispersity).

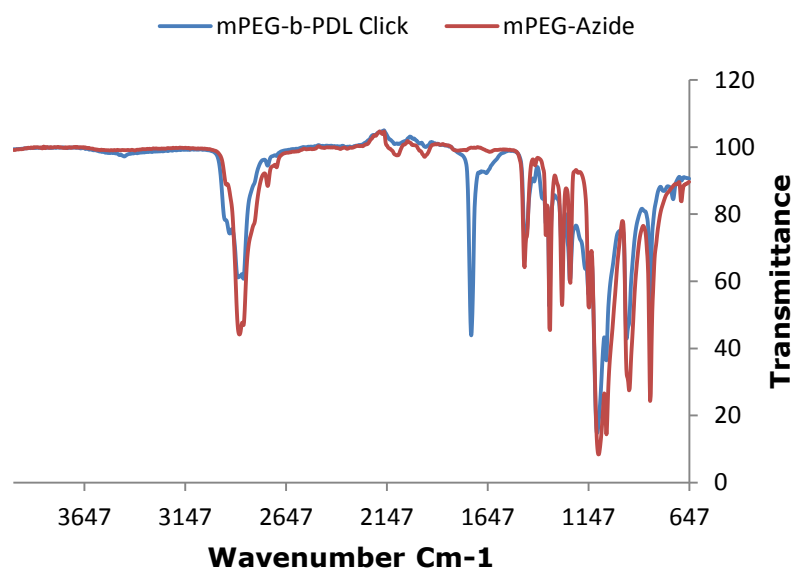


Figure 6-9 Overlapped FTIR spectra of mPEG-azide and mPEG-b-PDL synthesised by click reaction.

The ^1H NMR of copolymer FA-PEG-b-PDL and RhB-PEG-b-PDL were also acquired in DMSO to see the peaks of FA and RhB (figure 6-11 and 6-12). No change in peak positions of FA and RhB (conjugated with PEG) were observed after attachment of PEG onto PDL block. Molecular weight of copolymers were calculated through ^1H NMR by comparing the number of protons at 4.9 ppm (PDL chain, position 3) with respect to the proton resonance of PEG chain at 3.66 or 3.39 (for mPEG

only) ppm and the proton of the triazole ring at 7.8 ppm (table 6-1, figure 6-10 to 6-12).

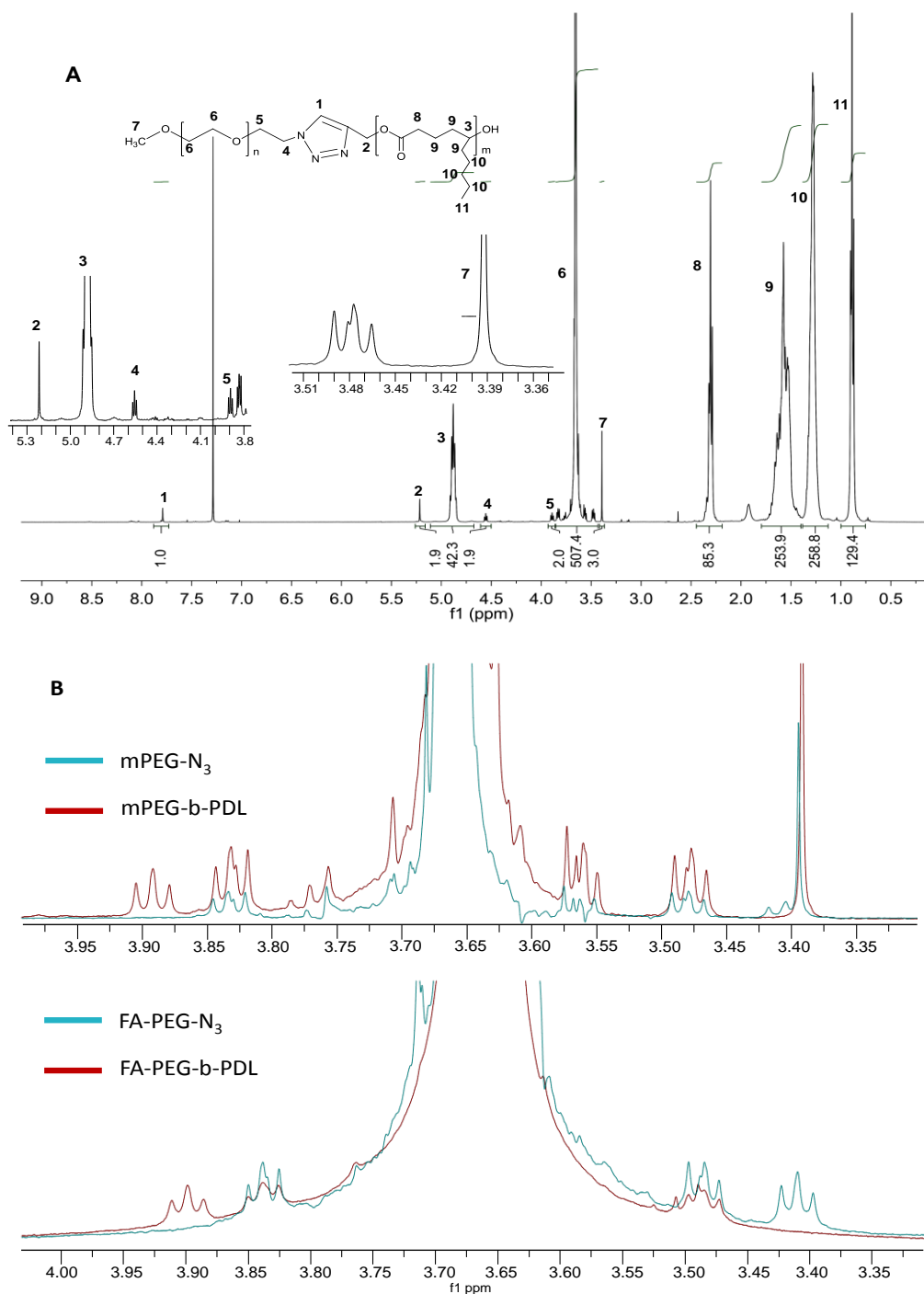


Figure 6-10 (A) ^1H NMR spectra of mPEG-b-PDL synthesised by click reaction and (B) overlapped ^1H NMR spectra of mPEG-N₃, mPEG-b-PDL, FA-PEG-N₃ and FA-PEG-b-PDL. Disappearance of peak at 3.42 ppm and appearance of peak at 3.90 ppm suggesting the conversion of azide in to triazole.

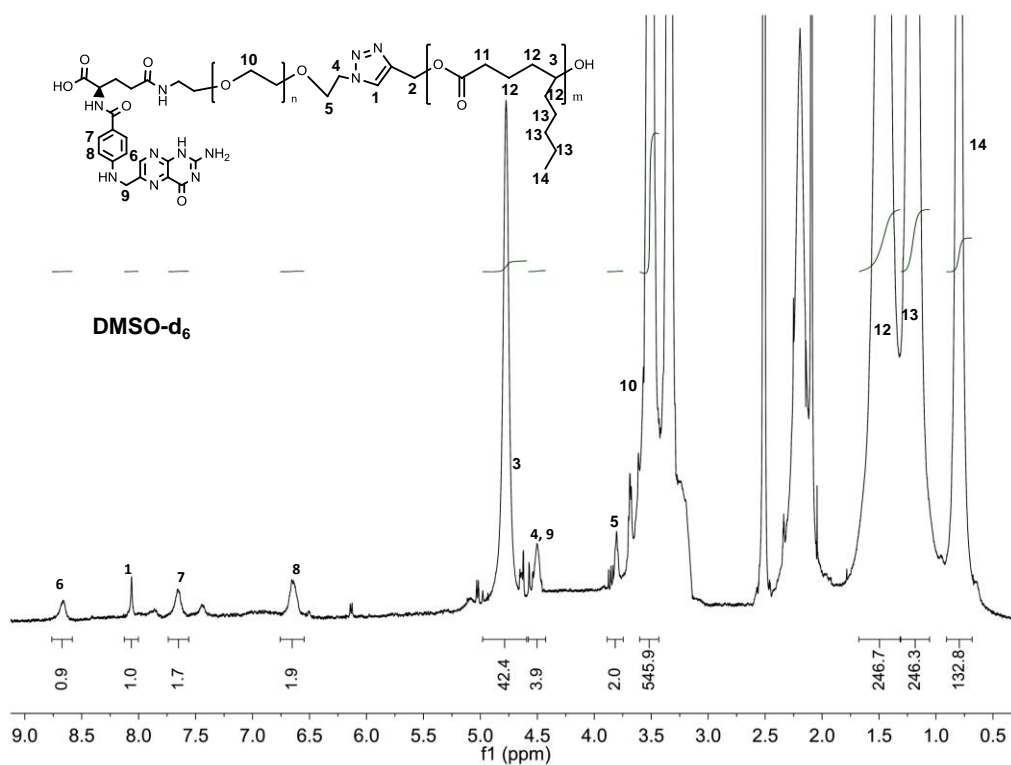
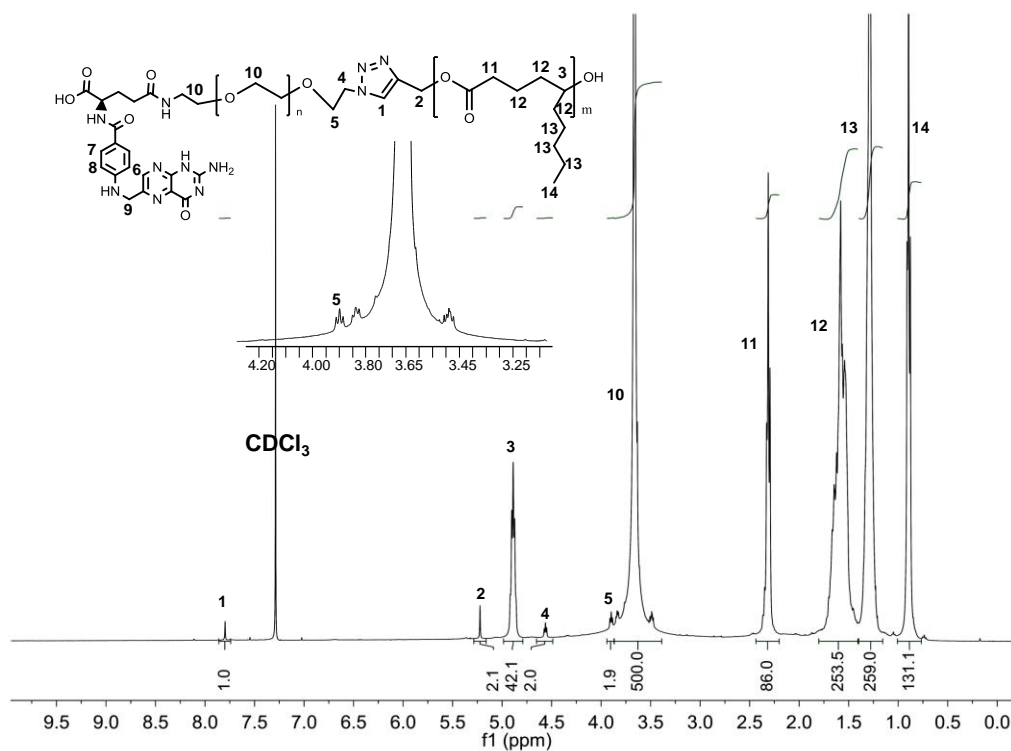


Figure 6-11 ¹H NMR spectra of FA-PEG-b-PDL acquired in chloroform-d and DMSO-d₆. Due to poor solubility of folic acid in chloroform-d, ¹H NMR spectra of FA-PEG-b-PDL was also acquired in DMSO-d₆ to visualise the folic acid peaks between 6.5-9.0 ppm.

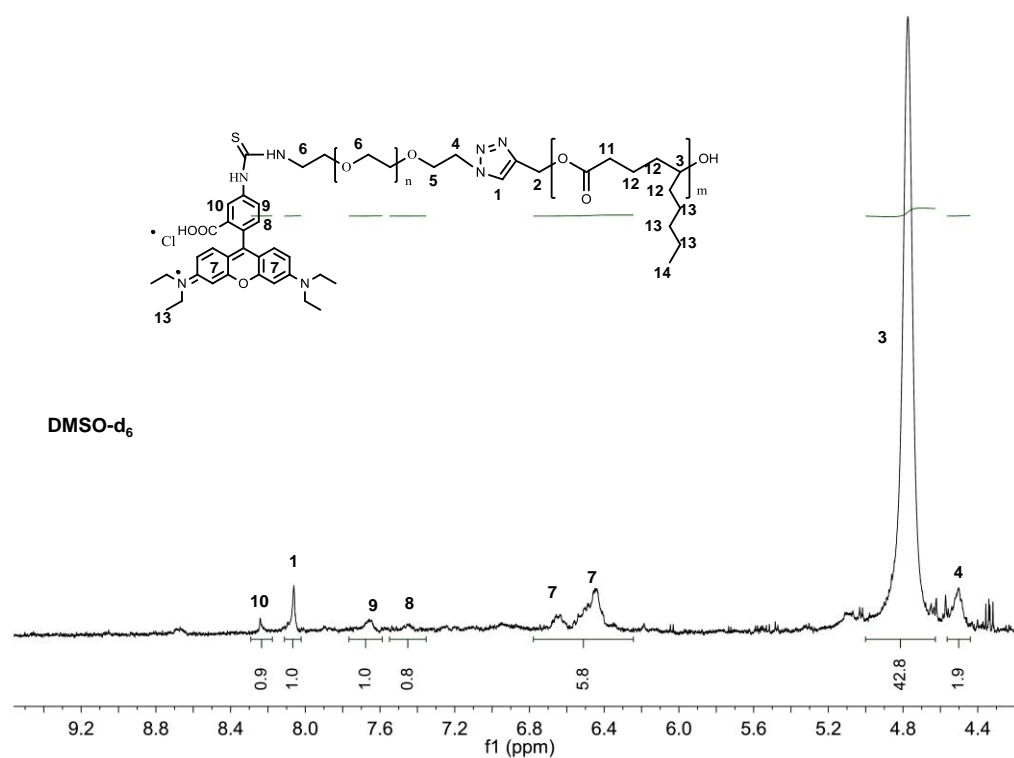
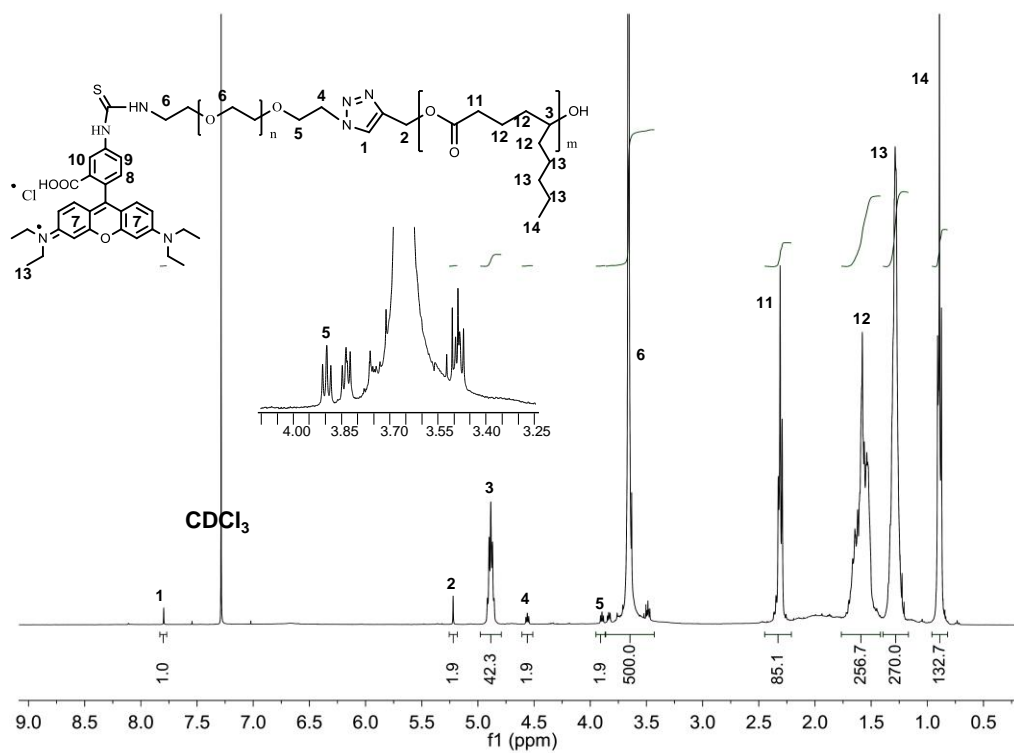


Figure 6-12 ¹H NMR spectra of RhB-PEG-b-PDL acquired in chloroform-d and DMSO-d₆. Due to poor solubility of rhodamine B in chloroform-d, ¹H NMR spectra of RhB-PEG-b-PDL was also acquired in DMSO-d₆ to visualise the rhodamine peaks between 6.0-8.5 ppm

Further samples were analysed on size exclusion chromatography. The SEC chromatogram was acquired using chloroform as eluent and M_n was obtained using polystyrene as internal standard (figure 6-13, table 6-1). The retention time observed for each sample confirmed the conjugation of the PDL block to the PEG block. However, additional peaks were also observed in the SEC traces, which suggested the presence of free PEG and PEG conjugates (FA-PEG and RhB-PEG) in the sample.

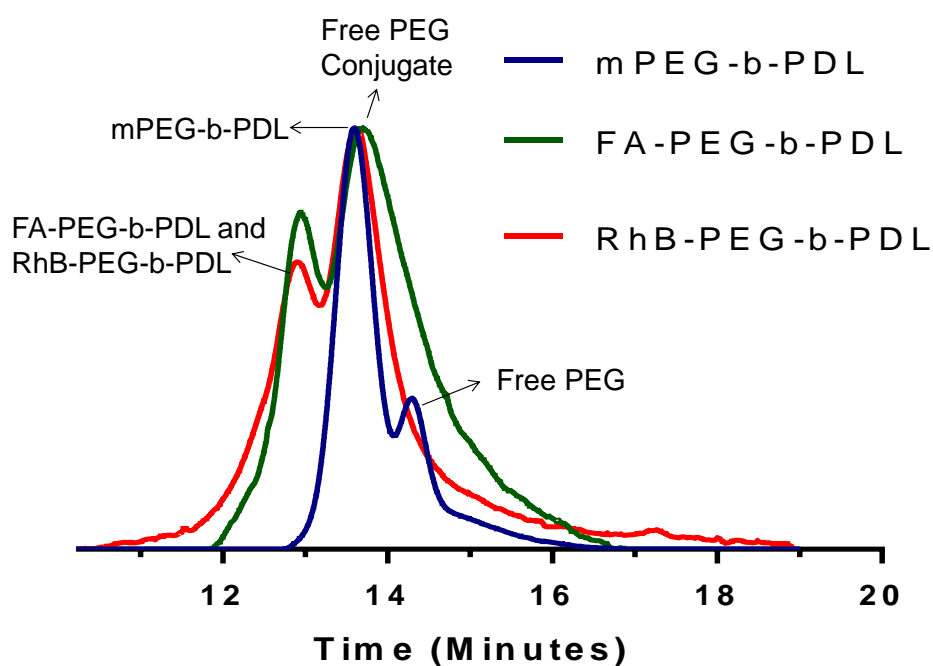


Figure 6-13 Overlapped SEC traces of various PEG-b-PDL copolymers. Chloroform was used as mobile phase and M_n was calculated against polystyrene polymer as reference.

6.3.2 Preparation and Characterisation of Block Copolymer Micelles

Micelles of synthesised block copolymers were prepared using an automated syringe pump *via* nanoprecipitation. The syringe pump was used to control the drop-rate of organic solvent in PBS, in order to obtain a consistent size in each batch. Due to the poor solubility of folic acid in water, PBS was used as a solvent during the fabrication of the micelles. The prepared micelle formulations is shown in figure 6-14.

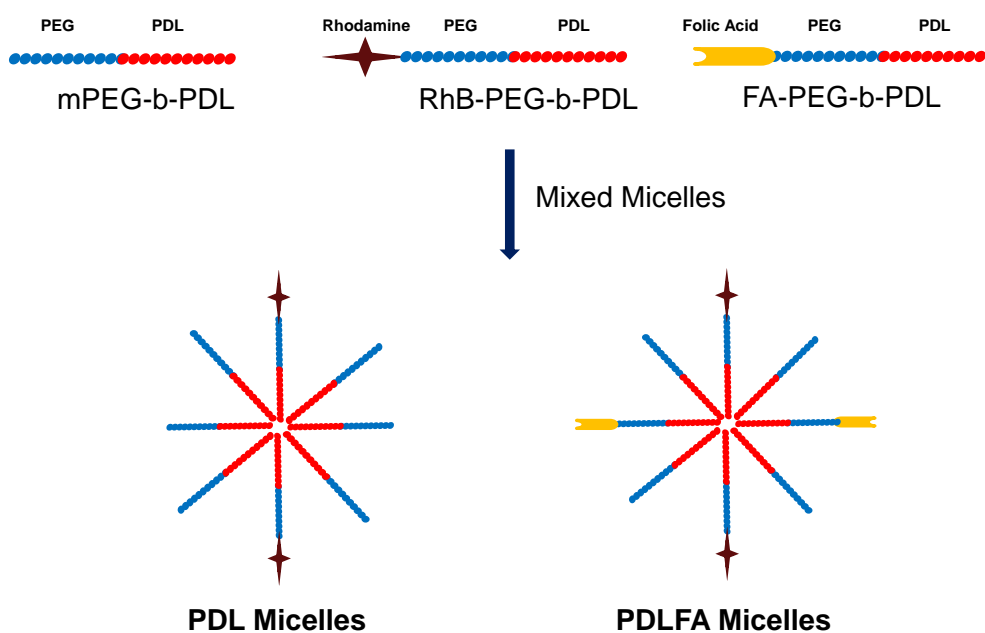


Figure 6-14 Pictorial presentation of different micelle formulations prepared in this study. PDL micelles were prepared by mixing mPEG-b-PDL (10 mg) and RhB-PEG-b-PDL (0.5 mg) block copolymers whereas PDLFA micelles were prepared by mixing mPEG-b-PDL (8 mg), FA-PEG-b-PDL (2 mg) and RhB-PEG-b-PDL (0.5 mg) block copolymers.

Both micelles preparations were characterised by DLS and the intensity and volume size distribution are shown in figure 6-15, while the mean sizes are reported in table 6-2. No significant difference in Z-average size was observed for the both micelle formulations. However, due to the broad size distribution of the obtained micelles, the obtained Z-average size was almost double to the size observed in previous studies (see chapter 4 & 5).

Sample	Size by intensity (d/nm) (\pm SD)	Size by volume (d/nm) (\pm SD)	Z-average Size (d/nm) (\pm SD)	PDI (\pm SD)	Zeta Potential (mv) (\pm SD)
PDL	133 \pm 5, 24 \pm 5	33 \pm 3	83 \pm 3	0.34 \pm 0.2	-2 \pm 1
PDLFA	118 \pm 5	32 \pm 3	76 \pm 4	0.30 \pm 0.1	-6 \pm 1

Table 6-2 Mean size and zeta potential of PDL and PDLFA micelles. Size was measured in PBS (10mM, pH-7.4) whereas zeta potential was measured in HEPES buffer (10mM, pH-7.4). The concentration of samples used for analysis was 70 μ g/mL. (SD - standard deviation, d/nm - diameter in nanometre, PDI- polydispersity index, mv- millivolt).

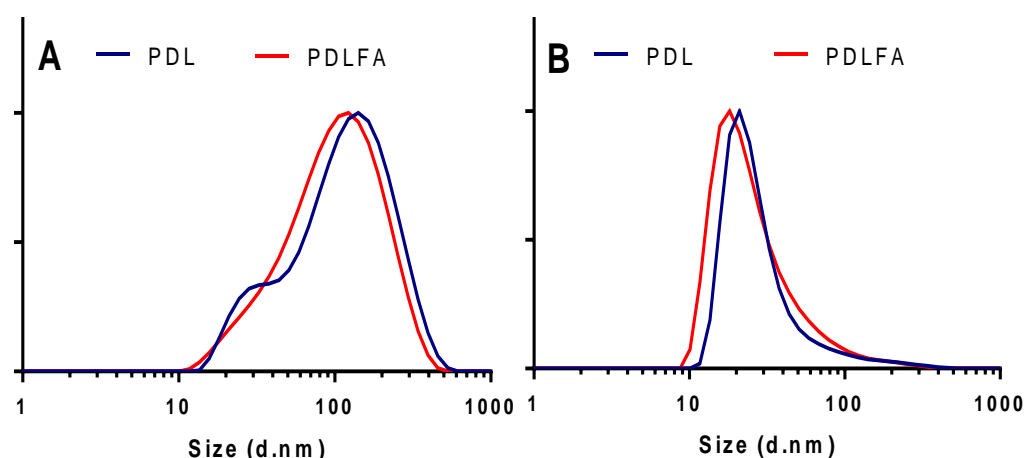


Figure 6-15 Size distribution by (A) Intensity and (B) volume of PDL and PDLFA micelles dispersed in PBS at room temperature. The concentration of samples used for analysis was 70 μ g/mL.

The size distribution of the micelles was also determined in RPMI-1640 (cell culture media used in uptake study) to understand the effect of solvent on size. Due to the presence of proteins, the major size distribution peak (by volume) observed in RPMI-1640 was at approximately at 8nm. Therefore, only size distribution by intensity was considered for the comparison (figure 6-16). The mean size observed in RPMI was 58 ± 3 nm for both samples. The size and size distribution detected for PDL and PDLFA micelles in RPMI-1640 were comparable and hence the effect of size during uptake studies for both formulations would be negligible³⁸.

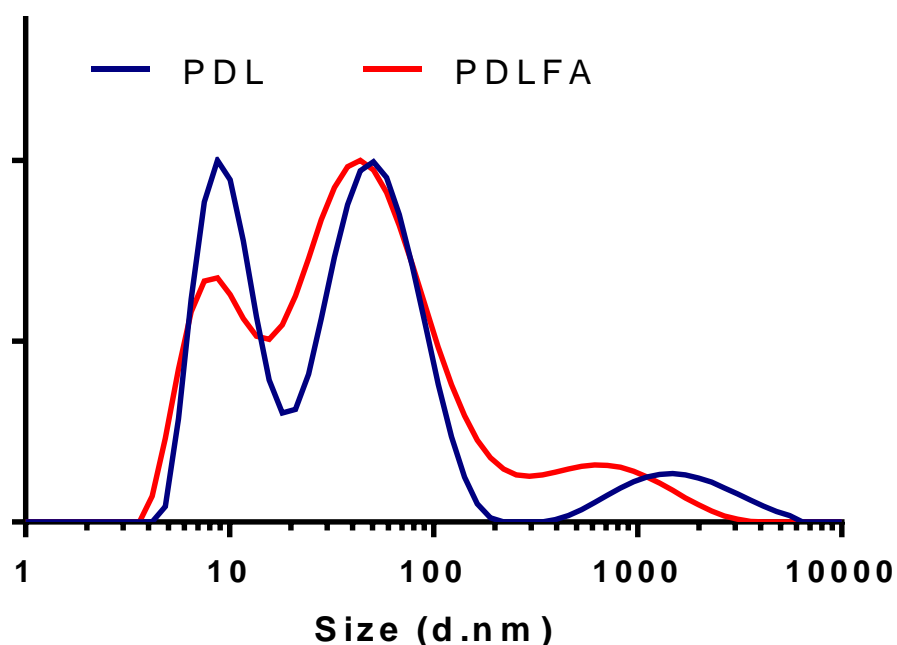


Figure 6-16 Size distribution by intensity of the micelles dispersed in RPMI media at room temperature. The concentration of samples used for analysis was 70 $\mu\text{g/mL}$.

The zeta potential observed for the PDL micelles was close to neutral. However, a slight negative charge was observed for PDLFA micelles when compared to PDL micelles due to the presence of folic acid on the micelles surface³⁹ (table 6-2, figure 6-17). Both samples were further imaged using TEM to check the morphology and to confirm the size. Images acquired from TEM suggested that both micelle formulations were approximately spherical in shape with smooth surfaces. The size determined from TEM images was in the range of 20 to 200nm, which spanned the size ranges detected by DLS (figure 6-18).

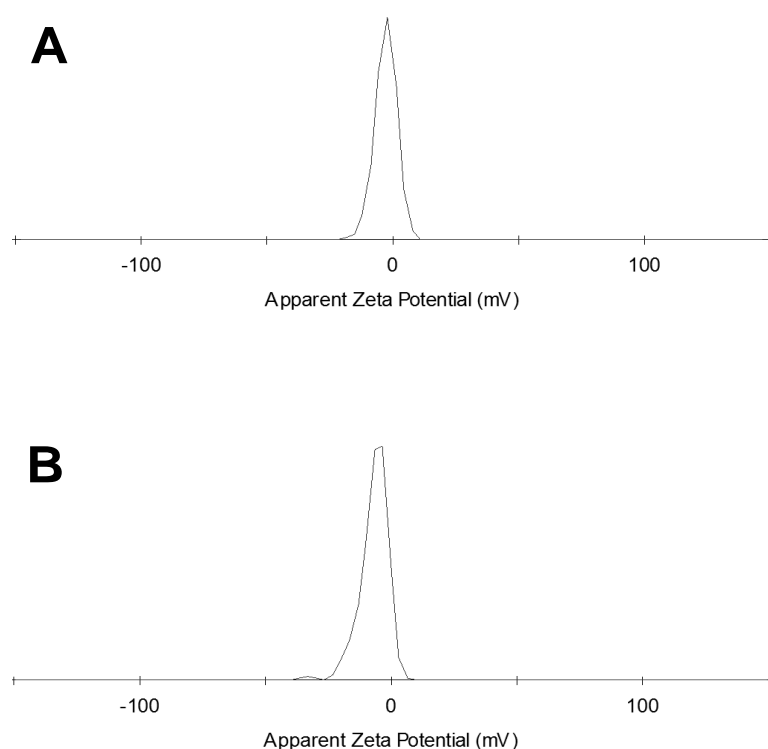


Figure 6-17 Zeta potential distribution of (A) PDL and (B) PDLFA micelles in HEPES buffer (10mM, pH-7.4). The concentration of samples used for analysis was 70 $\mu\text{g/mL}$.

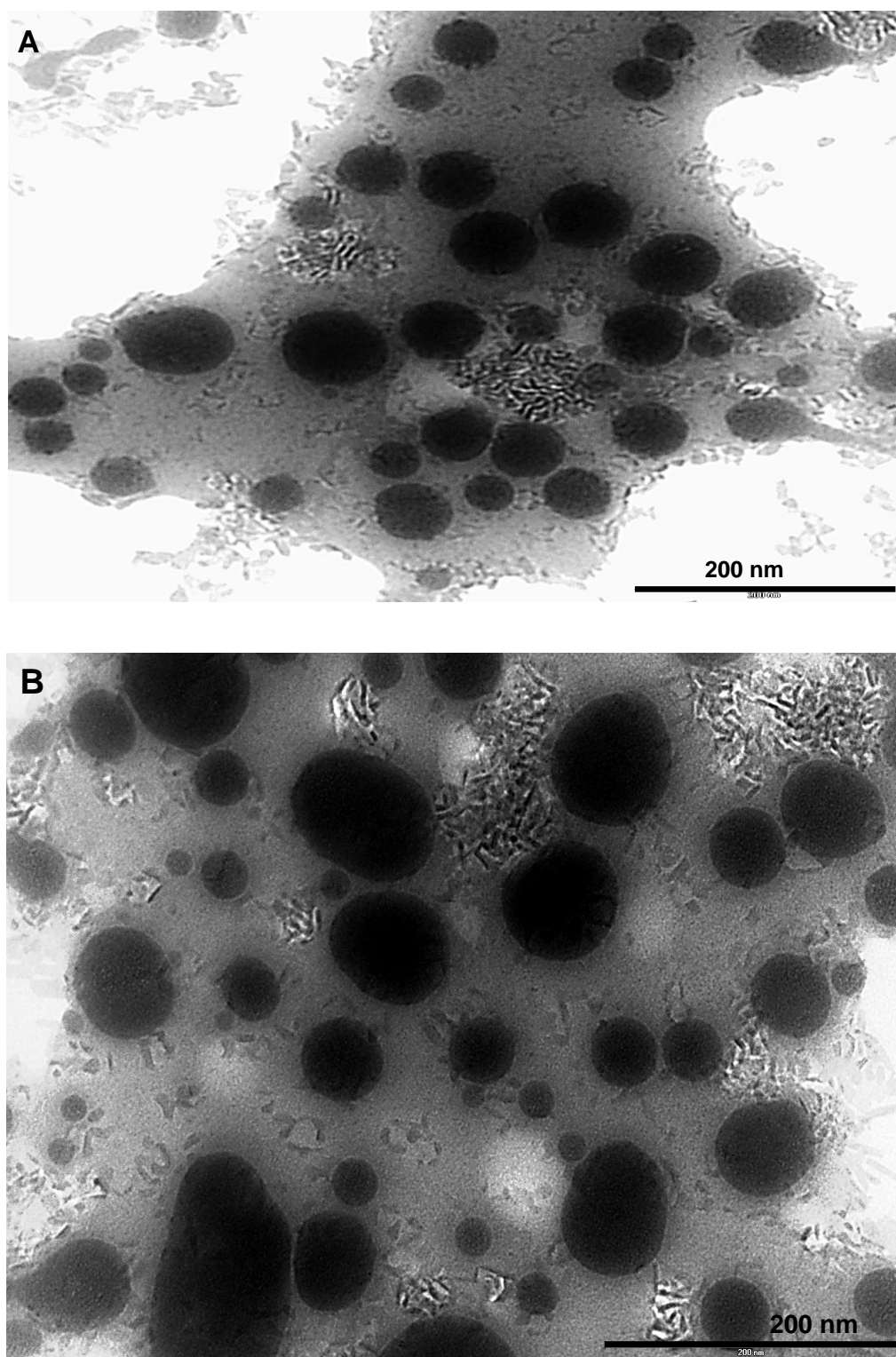


Figure 6-18 TEM image of (A) PDL and (B) PDLFA micelles. The samples were prepared in HPLC grade water with concentration of 70 $\mu\text{g}/\text{mL}$. Images were obtained without staining. Scale bar-200 nm.

The concentrations of rhodamine B and folic acid present in the final micelle formulations were determined by UV-vis spectroscopy. The overlaid UV-Vis spectrum of PDL and PDLFA micelles is presented in figure 6-19. The concentration of rhodamine B found in both micelle formulations was $13.4\mu\text{g/mL}$ whereas $39.4\mu\text{g/mL}$ of folic acid was present in PDLFA micelles.

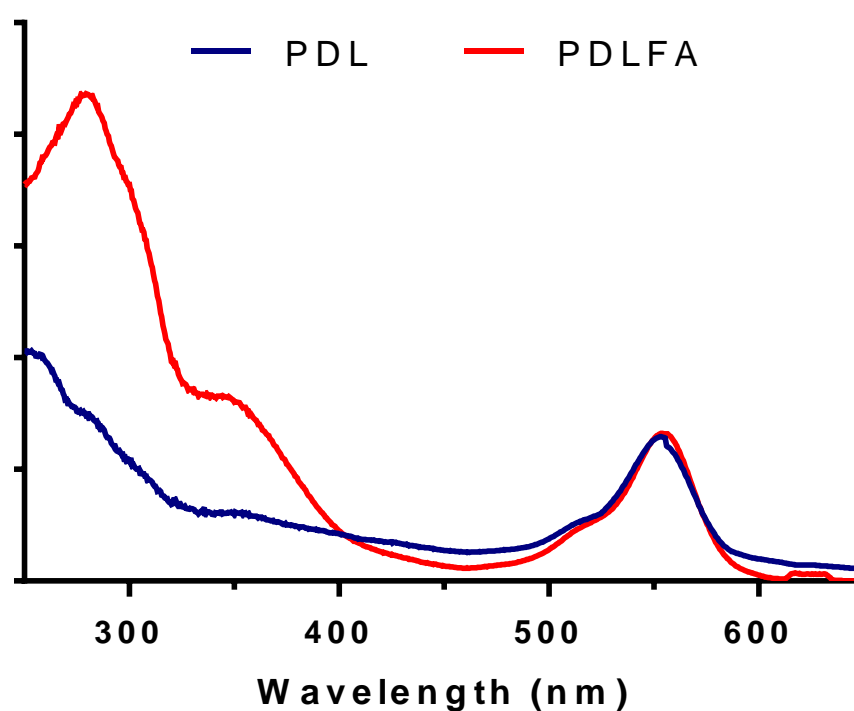


Figure 6-19 UV-Visible spectra of PDL and PDLFA micelles acquired using PBS as solvent. PDL and PDLFA micelles after purification were diluted by 10 times using PBS before scanning.

6.3.3 Cellular Uptake Study of Block Copolymer Micelles

Micelle formulations (PDL and PDLFA) were tested on two cell lines (*i.e.* A549 and MCF-7) to assess the effect of presence of folic acid on the micelles surface. The study was performed in the presence and absence of free folic acid in cell culture media to probe the folate receptor-mediated targeting (competitive assay). Interestingly, the uptake of both micellar formulations was observed in the tested cells regardless of the expected folate receptor expression level and presence/absence of free folic acid. As shown in figure 6-20 to 6-23, both formulations were taken up by the A549 (FR-ve) and MCF-7 (FR+ve) cell lines as evident by confocal microscopy images. No specific cellular uptake was observed, which was contrary to the expected results. The uptake of micelles was reduced significantly at 4°C, which suggested that the uptake process was energy-dependent (figure 6-24 and 6-25). These preliminary cell uptake studies thus suggested that the fabricated novel PEG-b-PDL copolymer micelles were taken up non-specifically by the human cancer cells (MCF-7 and A549) *via* endocytic pathways, which did not require folate-receptor recognition.

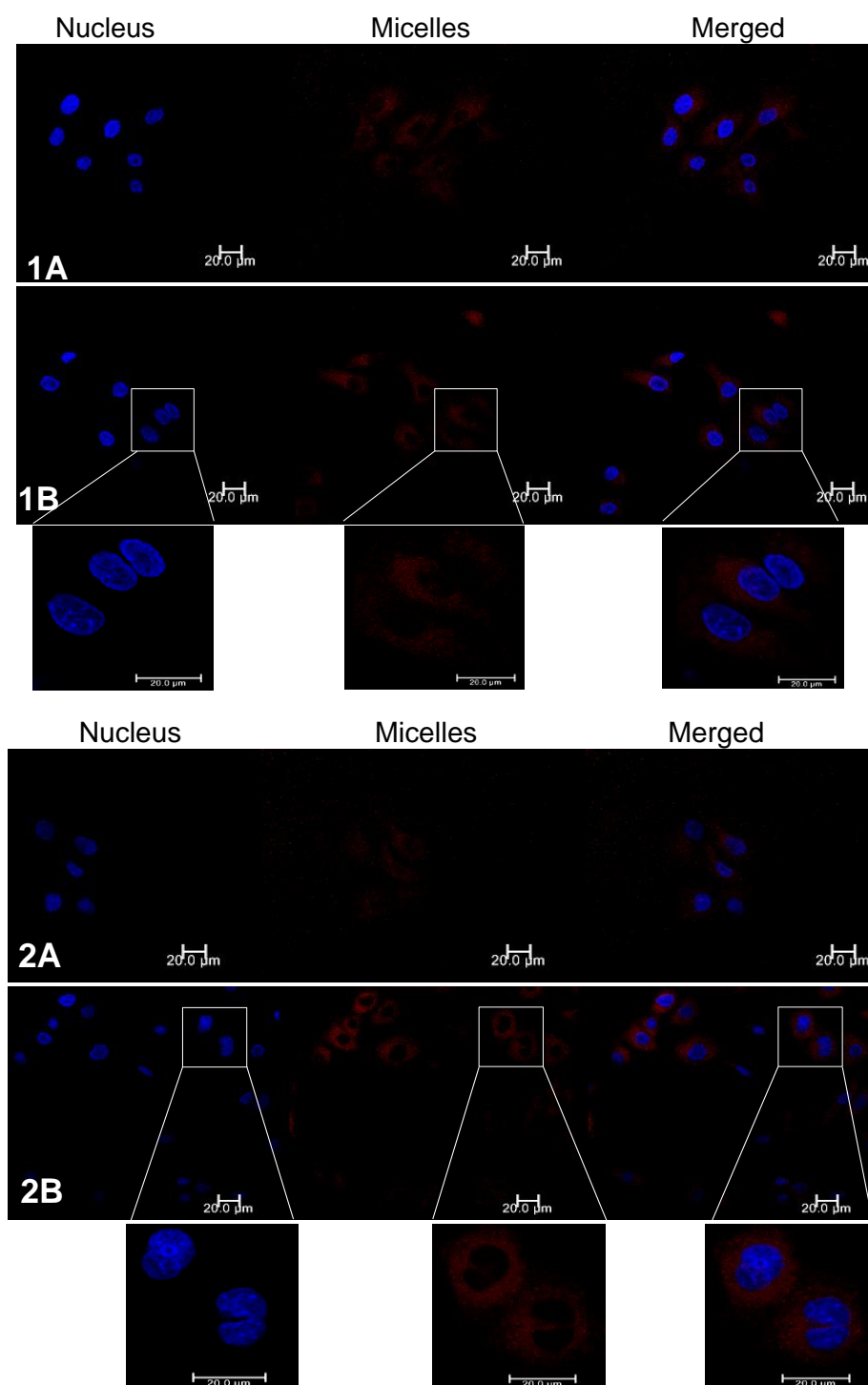


Figure 6-20 Confocal microscopy images of the A549 (FR-ve) cells treated with PDL micelles without (1A and 1B) and with added free folic acid (2A and 2B) present in the culture medium at 37°C for 2.5 hrs. Micelles were labeled with rhodamine (red) and nuclei of cells were stained with Hoechst (blue). The micelle concentration in the incubation medium was 100 μg/mL while the concentration of free folic acid used for the competitive assay was 500 μg/mL. PDL micelles were prepared by using mPEG-b-PDL (10 mg) and RhB-PEG-b-PDL (0.5 mg) block copolymer. Scale bars = 20μm.

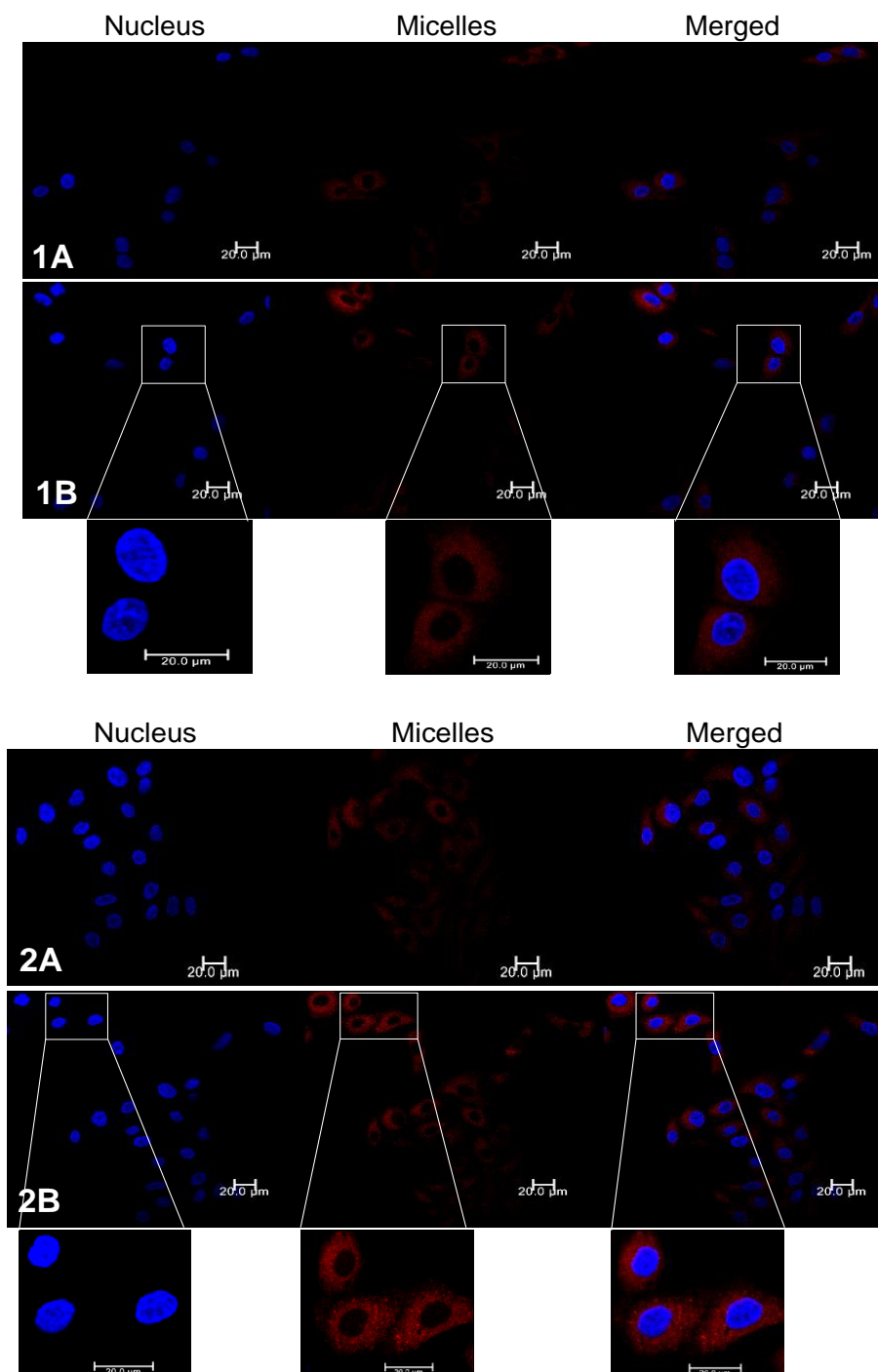


Figure 6-21 Confocal microscopy images of the A549 (FR-ve) cells treated with PDLFA micelles (folate conjugated) without (1A and 1B) and with added free folic acid (2A and 2B) present in the culture medium at 37°C for 2.5 hrs. Micelles were labeled with rhodamine (red) and nuclei of cells were stained with Hoechst (blue). The micelle concentration in the incubation medium was 100 $\mu\text{g}/\text{mL}$ while the concentration of free folic acid used for the competitive assay was 500 $\mu\text{g}/\text{mL}$. PDLFA micelles were prepared by using mPEG-b-PDL (8 mg), FA-PEG-b-PDL (2 mg) and RhB-PEG-b-PDL (0.5 mg) block copolymer. Scale bars = 20 μm .

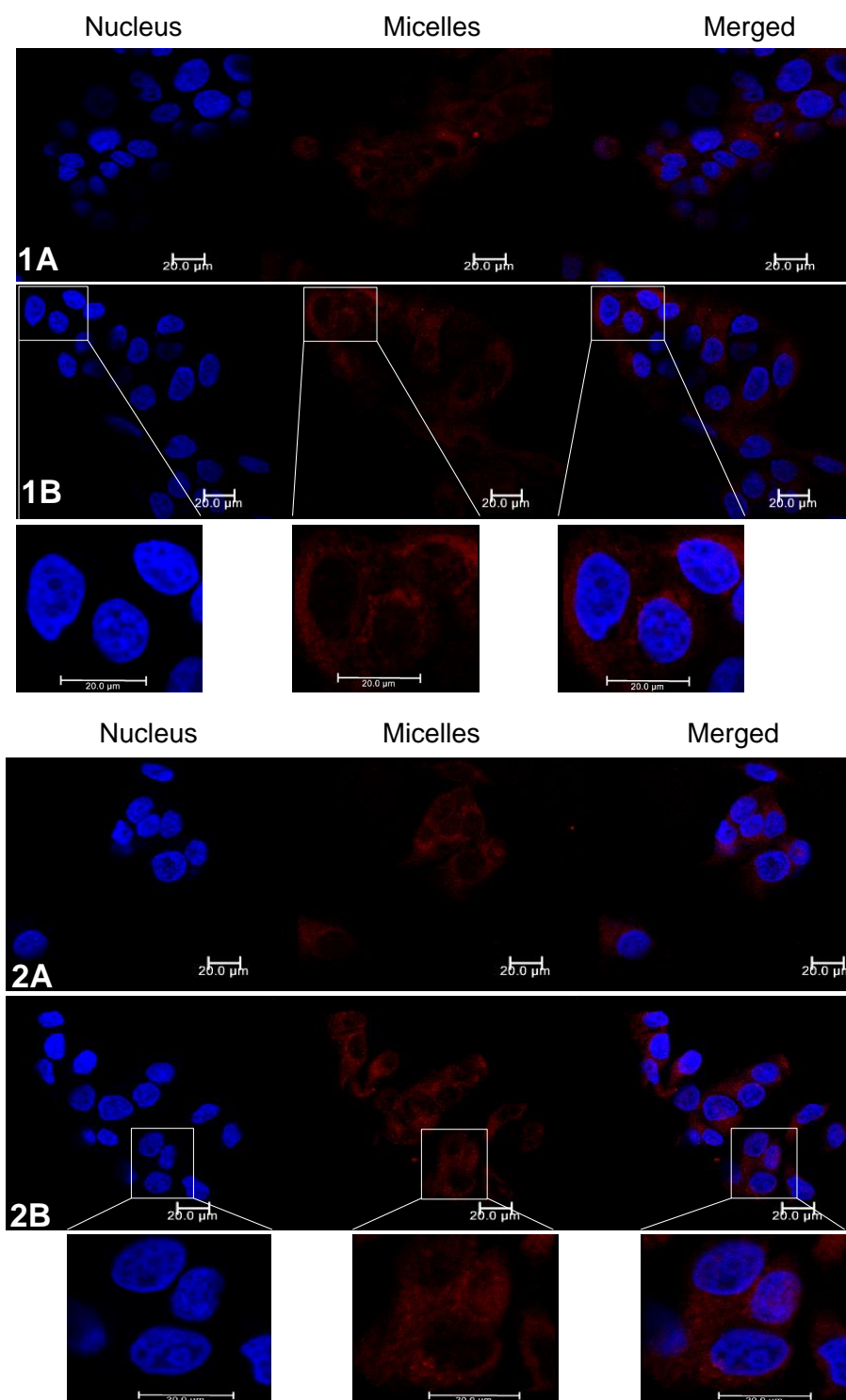


Figure 6-22 Confocal microscopy images of the MCF-7 (FR+ve) cells treated with PDL micelles without (1A and 1B) and with added free folic acid (2A and 2B) present in the culture medium at 37°C for 2.5 hrs. Micelles were labeled with rhodamine (red) and nuclei of cells were stained with Hoechst (blue). The micelle concentration in the incubation medium was 100 $\mu\text{g}/\text{mL}$ while the concentration of free folic acid used for the competitive assay was 500 $\mu\text{g}/\text{mL}$. PDL micelles were prepared by using mPEG-b-PDL (10 mg) and RhB-PEG-b-PDL (0.5 mg) block copolymer. Scale bars = 20 μm .

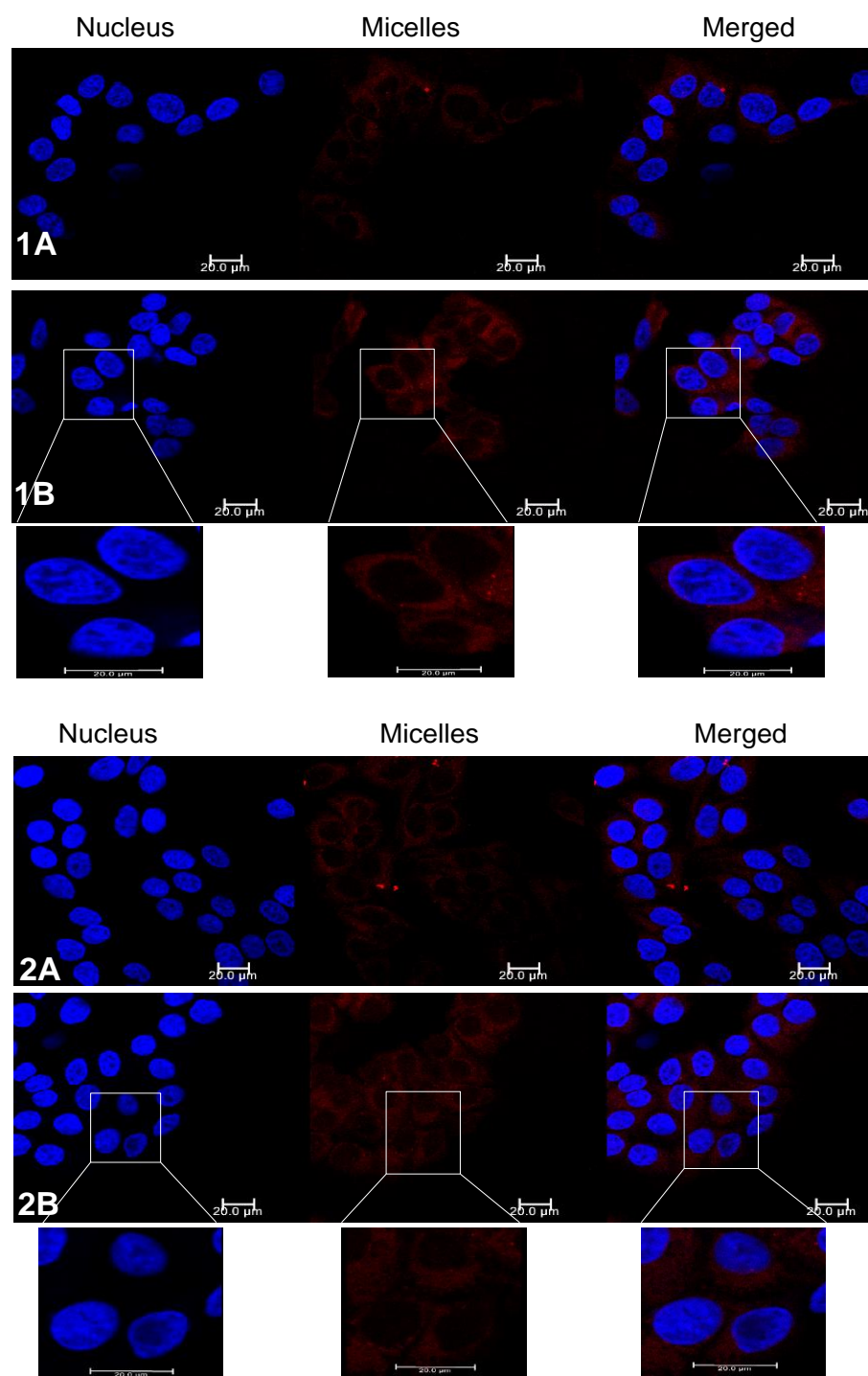


Figure 6-23 Confocal microscopy images of the MCF-7 (FR+ve) cells treated with PDLFA micelles (folate conjugated) without (1A and 1B) and with added free folic acid (2A and 2B) present in the culture medium at 37°C for 2.5 hrs. Micelles were labeled with rhodamine (red) and nuclei of cells were stained with Hoechst (blue). The micelle concentration in the incubation medium was 100 μg/mL while the concentration of free folic acid used for the competitive assay was 500 μg/mL. PDLFA micelles were prepared by using mPEG-b-PDL (8 mg), FA-PEG-b-PDL (2 mg) and RhB-PEG-b-PDL (0.5 mg) block copolymer. Scale bars = 20μm.

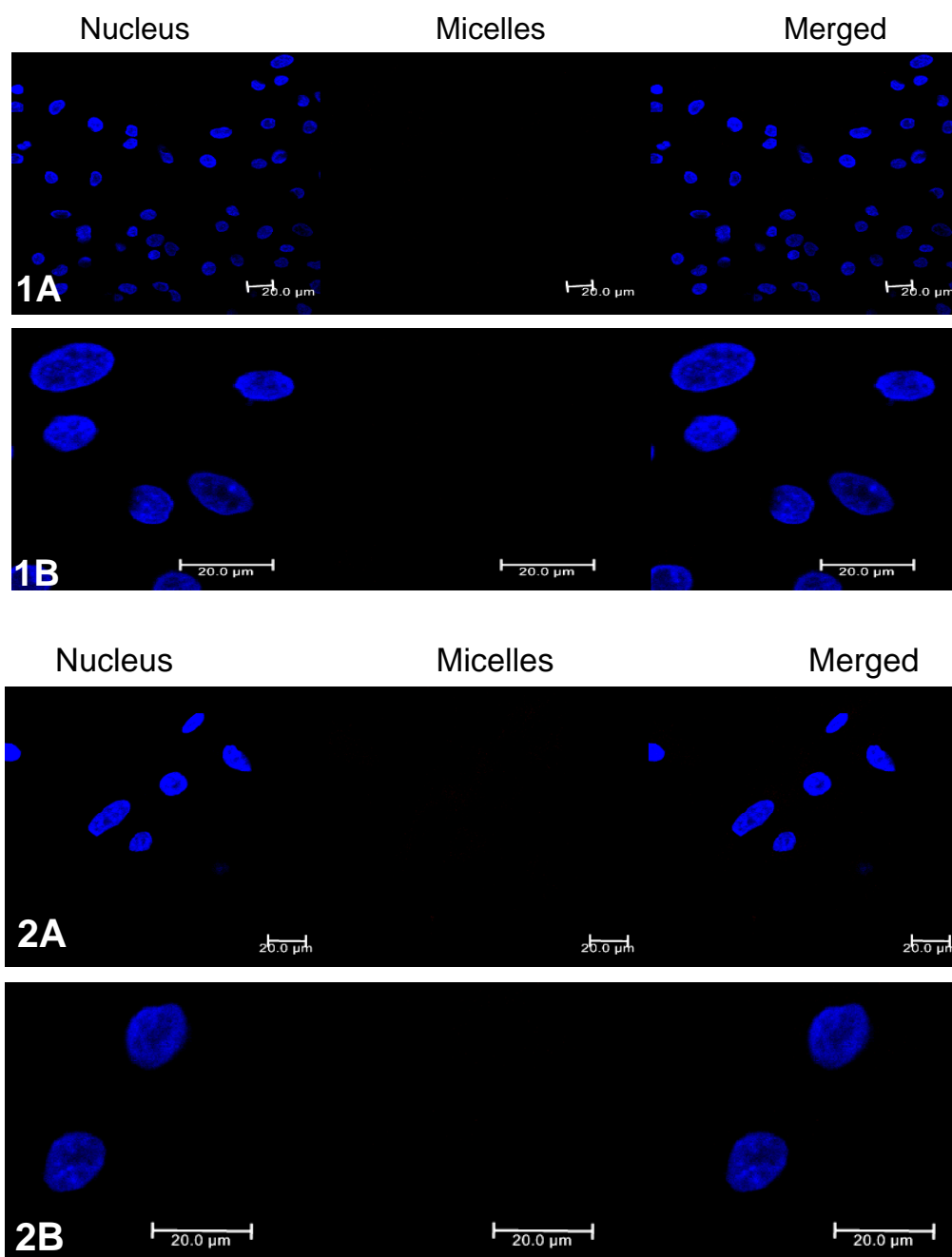


Figure 6-24 Confocal microscopy images of the A549 (FR-ve) cells treated with PDL (1A and 1B) and PDLFA (folate conjugated) (2A and 2B) micelles at 4°C for 2.5 hrs in the absence of folic acid in the culture medium. Micelles were labeled with rhodamine (red) and nuclei of cells were stained with Hoechst (blue). The micelle concentration in the incubation medium was 100 μg/mL. PDL micelles were prepared by using mPEG-b-PDL (10 mg) and RhB-PEG-b-PDL (0.5 mg) block copolymer. PDLFA micelles were prepared by using mPEG-b-PDL (8 mg), FA-PEG-b-PDL (2 mg) and RhB-PEG-b-PDL (0.5 mg) block copolymer. Scale bars = 20μm.

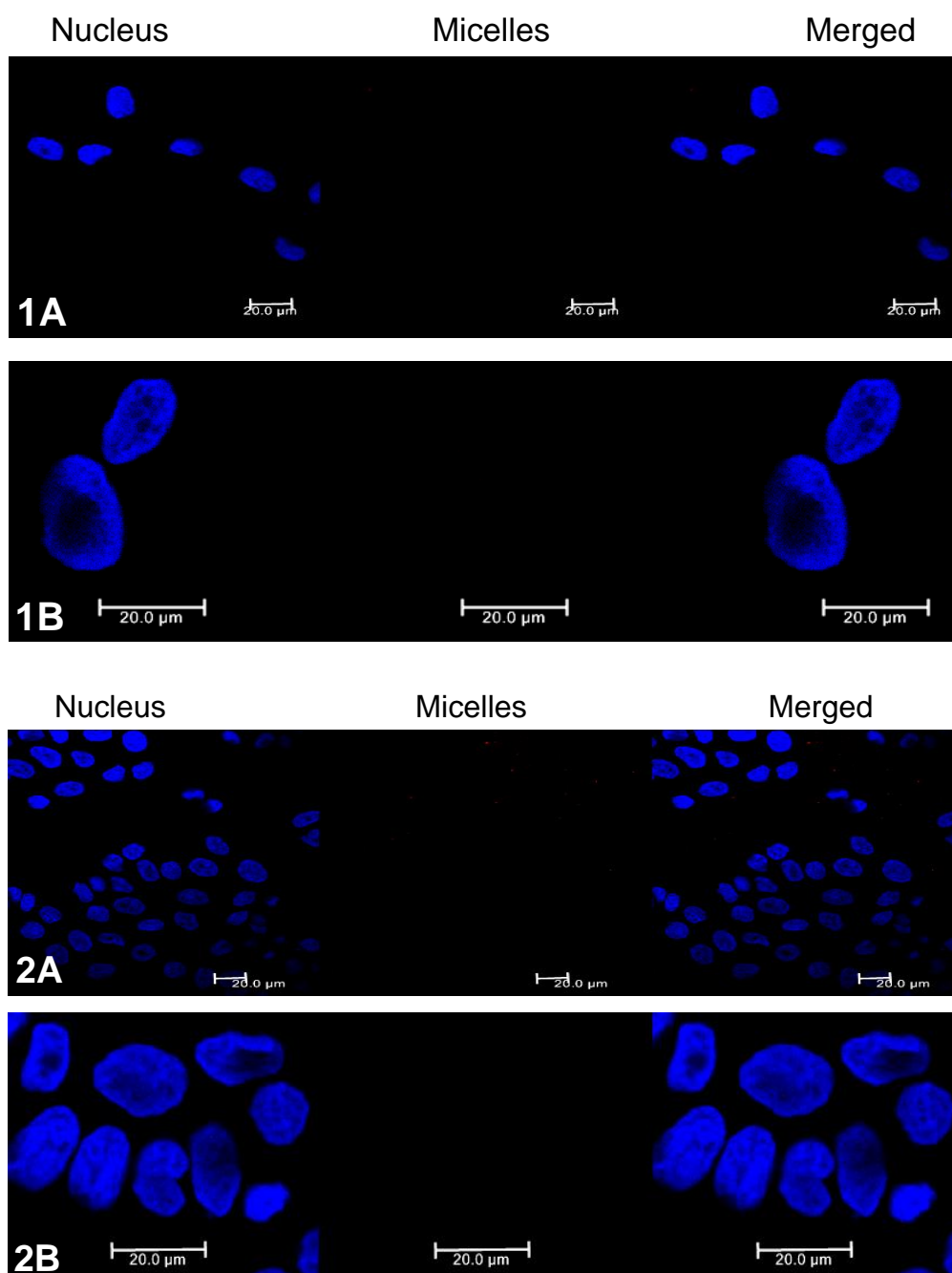


Figure 6-25 Confocal microscopy images of the MCF-7 (FR+ve) cells treated with PDL (1A and 1B) and PDLFA (folate conjugated) (2A and 2B) micelles at 4°C for 2.5 hrs in the absence of folic acid in the culture medium. Micelles were labeled with rhodamine (red) and nuclei of cells were stained with Hoechst (blue). The micelle concentration in the incubation medium was 100 μg/mL. PDL micelles were prepared by using mPEG-b-PDL (10 mg) and RhB-PEG-b-PDL (0.5 mg) block copolymer. PDLFA micelles were prepared by using mPEG-b-PDL (8 mg), FA-PEG-b-PDL (2 mg) and RhB-PEG-b-PDL (0.5 mg) block copolymer. Scale bars = 20μm.

6.4 Discussion

In chapter 3, the formation of undesired free homopolymer was noted during the ROP of δ -decalactone. Therefore, it was postulated that repetition of reactions to achieve the similar molecular weight polymer was not the best approach. Thus, to keep the same molecular weight of hydrophobic block (*i.e.* PDL) in all block copolymers, click chemistry was selected for the synthesis to generate amphiphilic block copolymers. The 1,3-dipolar cycloaddition of alkyne and azide often termed as "Click Chemistry" is a method of choice to couple a molecule containing an azide group with a molecule having alkyne groups, quickly and efficiently⁴⁰. Copper catalysed click chemistries usually promote efficient reactions at room temperature and are very robust processes to generate regioselective products⁴¹.

The azide-terminated methoxy-PEG was synthesised *via* a reported procedure with approximately 90 % of azide functionality present in the final product. The percent azide content observed with mPEG-N₃ synthesised in laboratory was almost identical to the commercialised PEG (NH₂-PEG-N₃), which was procured to synthesise the functionalised PEG-azide. Folic acid was conjugated to amine-terminated PEG *via* amide bond while rhodamine B was conjugated to the polymer

through a thiourea bond. The M_n observed by SEC for PEG conjugates (FA-PEG- N_3 and RhB-PEG- N_3) were higher than the expected values. This difference in the M_n detected by SEC was probably due to poor solubility of FA and RhB in chloroform (mobile phase used in SEC). Since the separation of product in SEC column is based on the solvo-dynamic radius and not on the molecular weight, the solubility of a given sample in the mobile phase markedly affects the measured molar mass. It is very likely that the PEG conjugates, due to the poor solubility of attached molecules (FA and RhB) could exist as aggregates in chloroform thus increasing the radius of polymeric species in solution. Any aggregates would have been eluted quickly, giving an apparent high M_n value compared to the polystyrene polymer standards used as calibrants. The poor solubility of folic acid and rhodamine in chloroform was clearly apparent in ^1H NMR spectra of FA-PEG- N_3 and RhB-PEG- N_3 . The proton peaks of FA and RhB were not visible in CDCl_3 (poor solvent for these compounds), probably due to the formation of micelle like structure of conjugates with PEG as corona and RhB or FA as core^{28, 42}.

The coupling of PEG-azide with alkyne PDL was evident by ^1H NMR in which a proton peak of a newly formed triazole ring

was clearly noticeable. The proton NMR spectra of FA-PEG-b-PDL and RhB-PEG-b-PDL were also acquired in DMSO- d_6 to observe the peaks of FA and RhB. The SEC traces obtained for the block copolymers suggested the presence of free mPEG and PEG conjugates (FA-PEG and RhB-PEG) in the final purified products. Although as per the $^1\text{HNMR}$, 100% of azide was converted into triazole but due to the presence of approximately 10% of non azide PEG, free mPEG and PEG conjugates (FA-PEG and RhB-PEG) were detected in SEC analysis. The amount of free PEG and/or PEG conjugates in final polymer was expected to be $\leq 10\%$ (based on azide functionalities). PEG itself is fully water soluble and it was reported that presence of PEG $_{5k}$ on the surface of nanoparticles reduced cellular uptake by minimizing protein adsorption⁴³. Hence, it is very unlikely that free PEGs would internalize in cells and therefore were not separated from block copolymers.

The Z-average size of the PDL and PDLFA micelles observed in PBS was almost double the size observed for mPEG-b-PDL micelles prepared in water. It should be noted that the presence of electrolytes in aqueous media during micelle fabrication does exert an effect on the aggregation number and ultimately size⁴⁴. It has been reported that the presence

of salts in the dispersion medium increase the aggregation number of micelles⁴⁵. A rise in aggregation number leads to an increased number of copolymers chains in the micellar structure which in turn gave large size micelles. This explains the difference in size, which was observed when micelles were prepared in PBS when compared with micelles fabricated in water.

The preliminary *in vitro* cellular uptake studies suggested the non-specific uptake of novel PEG-b-PDL micelles in MCF-7 and A549 cells lines. The PEG-b-PDL micelles might have been taken up by the cells *via* pinocytosis pathways based on their size and/or slightly negative charge^{46, 47}. Pinocytosis is a mechanism used by cells to internalise fluid surrounding them and it has been proposed that all substances present in the fluid phase are taken up simultaneously by cells⁴⁸. Recently, the uptake of pegylated liposomal doxorubicin formulation (DOXIL™) was reported via caveolae-mediated endocytosis in MDCK epithelial cancer cells⁴⁹. The diameter of tested DOXIL™ nanoparticles was 85.8 nm with a zeta potential of – 2.6 mV at pH 7.4, which was comparable to the PEG-b-PDL micelles⁴⁹. Hence, it has been hypothesised that the PEG-b-PDL micelles might be taken up by caveolae-mediated endocytosis (a class of clathrin independent endocytosis under pinocytosis). The

endocytosis of PEG-b-PDL micelles in cancer cells could be beneficial, after the accumulation of these micelles in a tumour *via* the EPR effect, in order to deliver the cytotoxic drugs within the cells without the use of any ligand. Recently, the uptake of mPEG-b-PLA micelles in the absence of any targeting ligand was also reported in A549⁵⁰ and MCF-7⁵¹ cells.

One reason that might explain the similar uptake (based on the observed fluorescence of rhodamine B) of PDL and PDLFA micelle formulations in both tested cell lines could be the amount of expressed folate receptors. It has been reported that MCF-7 expressed low, but measurable, levels of folate receptor⁵² while A549 cells were generally considered as folate deficient cell lines⁵³. Based on these reports, it was hypothesised that MCF-7 cells could behave as FR+ve cell lines whereas A549 cells might function as FR-ve cell lines (FR-ve). However, Yuan *et.al.* revealed that the A549 contains some level of folate receptor by demonstrating the higher uptake of folate decorated solid lipid nanoparticles in this cells⁵⁴. In another study, it has been suggested that A549 and MCF-7 cells have similar amounts of folate receptors by demonstrating the similar uptake of folic acid modified quantum dots in both cell lines⁵⁵. Considering these reports, it

was hypothesised that this might be because of very small differences in folate receptor expression in both cell lines, a difference in uptake would not be noticeable in folate-conjugated micelles compared to non-folate micelles. However, further experiments to evaluate the effect of parameters such as dose, incubation time, cell lines, amount of folic acid conjugated polymer used etc. are still needed before concluding the uptake mechanism of PEG-b-PDL micelles^{46, 48, 56}.

6.5 Conclusion

In this chapter, the syntheses of amphiphilic diblock copolymers of poly(decylactone) (PEG-b-PDL) *via* click chemistry has been reported. The azide derivative of PEG *i.e.* methoxy-PEG (mPEG-N₃), folic acid conjugated PEG (FA-PEG-N₃) and rhodamine B conjugated PEG (RhB-PEG-N₃) were used as hydrophilic blocks while propargyl-PDL was used as the hydrophobic block. The obtained co-polymers were characterised by ¹HNMR and SEC, which suggested the successful conjugation of both blocks via triazole ring formation. Two mixed micelle formulations of the copolymers were fabricated using a nanoprecipitation method in which one was targeted (FA-PEG-b-PDL + RhB-PEG-b-PDL) and another

was non-targeted (mPEG-b-PDL + RhB-PEG-b-PDL) formulation.

The size range observed for both micelle formulations was 20-200 nm with zeta potentials close to neutral. These micelle formulations were then tested for the folate-mediated targeted delivery to MCF-7 (FR+) and A549 (FR-) cell lines. The non-specific uptake of PEG-b-PDL micelles (targeted and non-targeted) in both cell lines was observed. This non-specific uptake was postulate to be taken place *via* an energy-dependent route but not specifically by the folate receptor pathway. It was proposed that the micelles were taken up by cells through caveolae-mediated endocytosis. However, extensive studies are still needed to characterise the endocytosis mechanism(s) for novel PEG-b-PDL micelles.

6.6 References

1. Brannon-Peppas, L.; Blanchette, J. O., *Advanced Drug Delivery Reviews* 2004, 56 (11), 1649-1659.
2. Ruoslahti, E.; Bhatia, S. N.; Sailor, M. J., *Journal of Cell Biology* 2010, 188 (6), 759-768.
3. Peer, D.; Karp, J. M.; Hong, S.; Farokhzad, O. C.; Margalit, R.; Langer, R., *Nature Nanotechnology* 2007, 2 (12), 751-760.
4. Maeda, H.; Wu, J.; Sawa, T.; Matsumura, Y.; Hori, K., *Journal of Controlled Release* 2000, 65 (1-2), 271-284.
5. Maeda, H.; Bharate, G. Y.; Daruwalla, J., *European Journal of Pharmaceutics and Biopharmaceutics* 2009, 71 (3), 409-419.
6. Bae, Y. H.; Park, K., *Journal of Controlled Release* 2011, 153 (3), 198-205.
7. Fang, J.; Nakamura, H.; Maeda, H., *Advanced Drug Delivery Reviews* 2011, 63 (3), 136-151.
8. Mastrotto, F.; Caliceti, P.; Amendola, V.; Bersani, S.; Magnusson, J. P.; Meneghetti, M.; Mantovani, G.; Alexander, C.; Salmaso, S., *Chemical Communications* 2011, 47 (35), 9846-9848; Noh, T.; Kook, Y. H.; Park, C.; Youn, H.; Kim, H.; Oh, E. T.; Choi, E. K.; Park, H. J.; Kim, C., *Journal of Polymer Science Part a-Polymer Chemistry* 2008, 46 (22), 7321-7331.
9. Park, J. W.; Kirpotin, D. B.; Hong, K.; Shalaby, R.; Shao, Y.; Nielsen, U. B.; Marks, J. D.; Papahadjopoulos, D.; Benz, C. C., *Journal of Controlled Release* 2001, 74 (1-3), 95-113.
10. Bertrand, N.; Wu, J.; Xu, X.; Kamaly, N.; Farokhzad, O. C., *Advanced Drug Delivery Reviews* 2014, 66, 2-25.
11. Danhier, F.; Feron, O.; Preat, V., *Journal of Controlled Release* 2010, 148 (2), 135-146.
12. Lu, Y. J.; Low, P. S., *Advanced Drug Delivery Reviews* 2002, 54 (5), 675-693; Lu, Y.; Low, P. S., *Advanced Drug Delivery Reviews* 2012, 64, 342-352.
13. Antony, A. C., *Annual Review of Nutrition* 1996, 16, 501-521.
14. Sudimack, J.; Lee, R. J., *Advanced Drug Delivery Reviews* 2000, 41 (2), 147-162.
15. Reddy, J. A.; Low, P. S., *Critical Reviews in Therapeutic Drug Carrier Systems* 1998, 15 (6), 587-627; Wang, S.; Low, P. S., *Journal of Controlled Release* 1998, 53 (1-3), 39-48.

16. Hilgenbrink, A. R.; Low, P. S., *Journal of Pharmaceutical Sciences* 2005, 94 (10), 2135-2146.
17. Xia, W.; Low, P. S., *Journal of Medicinal Chemistry* 2010, 53 (19), 6811-6824.
18. Teng, L.; Xie, J.; Teng, L.; Lee, R. J., *Expert Opinion on Drug Delivery* 2012, 9 (8), 901-908.
19. Torchilin, V. P., *Cellular and Molecular Life Sciences* 2004, 61 (19-20), 2549-2559; Torchilin, V. P., *Pharmaceutical Research* 2007, 24 (1), 1-16.
20. Kataoka, K.; Harada, A.; Nagasaki, Y., *Advanced Drug Delivery Reviews* 2001, 47 (1), 113-131.
21. Cabral, H.; Kataoka, K., *Journal of controlled release : official journal of the Controlled Release Society* 2014, 190, 465-76.
22. Murakami, M.; Cabral, H.; Matsumoto, Y.; Wu, S.; Kano, M. R.; Yamori, T.; Nishiyama, N.; Kataoka, K., *Science Translational Medicine* 2011, 3 (64).
23. Kim, D.; Lee, E. S.; Oh, K. T.; Gao, Z. G.; Bae, Y. H., *Small* 2008, 4 (11), 2043-2050.
24. Cho, K.; Wang, X.; Nie, S.; Chen, Z.; Shin, D. M., *Clinical Cancer Research* 2008, 14 (5), 1310-1316; Nishiyama, N.; Kataoka, K., *Pharmacology & Therapeutics* 2006, 112 (3), 630-648.
25. Oerlemans, C.; Bult, W.; Bos, M.; Storm, G.; Nijssen, J. F. W.; Hennink, W. E., *Pharmaceutical Research* 2010, 27 (12), 2569-2589.
26. Yoo, H. S.; Park, T. G., *Journal of Controlled Release* 2004, 96 (2), 273-283.
27. Park, E. K.; Kim, S. Y.; Lee, S. B.; Lee, Y. M., *Journal of Controlled Release* 2005, 109 (1-3), 158-168.
28. Yang, X.; Deng, W.; Fu, L.; Blanco, E.; Gao, J.; Quan, D.; Shuai, X., *Journal of Biomedical Materials Research Part A* 2008, 86A (1), 48-60.
29. Lee, E. S.; Na, K.; Bae, Y. H., *Journal of Controlled Release* 2003, 91 (1-2), 103-113; Han, X.; Liu, J.; Liu, M.; Xie, C.; Zhan, C.; Gu, B.; Liu, Y.; Feng, L.; Lu, W., *International Journal of Pharmaceutics* 2009, 372 (1-2), 125-131; Liu, S.-Q.; Wiradharma, N.; Gao, S.-J.; Tong, Y. W.; Yang, Y.-Y., *Biomaterials* 2007, 28 (7), 1423-1433.
30. Bae, Y.; Jang, W. D.; Nishiyama, N.; Fukushima, S.; Kataoka, K., *Molecular Biosystems* 2005, 1 (3), 242-250.
31. Kolb, H. C.; Finn, M. G.; Sharpless, K. B., *Angewandte Chemie-International Edition* 2001, 40 (11), 2004-+.

32. Opsteen, J. A.; van Hest, J. C. M., *Chemical Communications* 2005, (1), 57-59.
33. Matini, T.; Francini, N.; Battocchio, A.; Spain, S. G.; Mantovani, G.; Vicent, M. J.; Sanchis, J.; Gallon, E.; Mastrotto, F.; Salmaso, S.; Caliceti, P.; Alexander, C., *Polymer Chemistry* 2014, 5 (5), 1626-1636.
34. Azagarsamy, M. A.; Anseth, K. S., *Angewandte Chemie-International Edition* 2013, 52 (51), 13803-13807.
35. Ladmiral, V.; Mantovani, G.; Clarkson, G. J.; Cauet, S.; Irwin, J. L.; Haddleton, D. M., *Journal of the American Chemical Society* 2006, 128 (14), 4823-4830.
36. Pan, Z.; Yu, L.; Song, N.; Zhou, L.; Li, J.; Ding, M.; Tan, H.; Fu, Q., *Polymer Chemistry* 2014, 5 (8), 2901-2910; Yang, X.; Pilla, S.; Grailer, J. J.; Steeber, D. A.; Gong, S.; Chen, Y.; Chen, G., *Journal of Materials Chemistry* 2009, 19 (32), 5812-5817.
37. Ding, L.; Hayakawa, T.; Kakimoto, M.-a., *Polymer Journal* 2007, 39 (6), 551-557.
38. Win, K. Y.; Feng, S. S., *Biomaterials* 2005, 26 (15), 2713-2722; He, C.; Hu, Y.; Yin, L.; Tang, C.; Yin, C., *Biomaterials* 2010, 31 (13), 3657-3666.
39. Qiu, L.-Y.; Yan, L.; Zhang, L.; Jin, Y.-M.; Zhao, Q.-H., *International Journal of Pharmaceutics* 2013, 456 (2), 315-324.
40. Binder, W. H.; Sachsenhofer, R., *Macromolecular Rapid Communications* 2007, 28 (1), 15-54.
41. Rostovtsev, V. V.; Green, L. G.; Fokin, V. V.; Sharpless, K. B., *Angewandte Chemie-International Edition* 2002, 41 (14), 2596-+.
42. Glavas, L.; Olsen, P.; Odelius, K.; Albertsson, A.-C., *Biomacromolecules* 2013, 14 (11), 4150-4156.
43. Pozzi, D.; Colapicchioni, V.; Caracciolo, G.; Piovesana, S.; Capriotti, A. L.; Palchetti, S.; De Grossi, S.; Riccioli, A.; Amenitsch, H.; Lagana, A., *Nanoscale* 2014, 6 (5), 2782-2792; Charmainne, C.; B., C. D., *Journal of Nanomedicine Research* 2014, 1 (1), 6.
44. Muller, N.; Birkhahn, R. H., *Journal of Physical Chemistry* 1968, 72 (2), 583-&; Schick, M. J.; Eirich, F. R.; Atlas, S. M., *Journal of Physical Chemistry* 1962, 66 (7), 1326-&; Bahadur, P.; Pandya, K.; Almgren, M.; Li, P.; Stilbs, P., *Colloid and Polymer Science* 1993, 271 (7), 657-667.
45. Miyagishi, S.; Akasohu, W.; Hashimoto, T.; Asakawa, T., *Journal of Colloid and Interface Science* 1996, 184 (2), 527-534; Sammalkorpi, M.; Karttunen, M.; Haataja, M., *Journal of Physical Chemistry B* 2009, 113 (17), 5863-5870.

46. Sahay, G.; Alakhova, D. Y.; Kabanov, A. V., *Journal of Controlled Release* 2010, 145 (3), 182-195.
47. Kelf, T. A.; Sreenivasan, V. K. A.; Sun, J.; Kim, E. J.; Goldys, E. M.; Zvyagin, A. V., *Nanotechnology* 2010, 21 (28).
48. Iversen, T.-G.; Skotland, T.; Sandvig, K., *Nano Today* 2011, 6 (2), 176-185.
49. Sahay, G.; Kim, J. O.; Kabanov, A. V.; Bronich, T. K., *Biomaterials* 2010, 31 (5), 923-933.
50. Jiang, C.; Wang, H.; Zhang, X.; Sun, Z.; Wang, F.; Cheng, J.; Xie, H.; Yu, B.; Zhou, L., *International Journal of Pharmaceutics* 2014, 475 (1-2), 60-68.
51. Yi, Y. W.; Kim, J. H.; Kang, H. W.; Oh, H. S.; Kim, S. W.; Seo, M. H., *Pharmaceutical Research* 2005, 22 (2), 200-208.
52. Feng, D.; Song, Y.; Shi, W.; Li, X.; Ma, H., *Analytical Chemistry* 2013, 85 (13), 6530-6535; Zhang, Z.; Lee, S. H.; Feng, S.-S., *Biomaterials* 2007, 28 (10), 1889-1899.
53. Parker, N.; Turk, M. J.; Westrick, E.; Lewis, J. D.; Low, P. S.; Leamon, C. P., *Analytical Biochemistry* 2005, 338 (2), 284-293; Yoo, H. S.; Park, T. G., *Journal of Controlled Release* 2004, 100 (2), 247-256.
54. Yuan, H.; Miao, J.; Du, Y.-Z.; You, J.; Hu, F.-Q.; Zeng, S., *International Journal of Pharmaceutics* 2008, 348 (1-2), 137-145.
55. Bharali, D. J.; Lucey, D. W.; Jayakumar, H.; Pudavar, H. E.; Prasad, P. N., *Journal of the American Chemical Society* 2005, 127 (32), 11364-11371.
56. Vlashi, E.; Kelderhouse, L. E.; Sturgis, J. E.; Low, P. S., *Acs Nano* 2013, 7 (10), 8573-8582.

Chapter 7 Conclusions and Future Work

7.1 Conclusion

The work in the thesis is concluded below in two sections. The first section covers the work reported in chapter 3, 4 and 5. The second section synopsis the work reported in chapter 6, which was based on a possible targeted therapy in cancer.

7.1.1 Synthesis, Characterisation and Evaluation of Polymers and Block Copolymers generated from Renewable δ -Decalactone

The synthesis of homopolymers and novel block copolymers based on renewable monomers (δ -decalactone and ω -pentadecalactone) was carried out successfully *via* ROP using organic (TBD) and enzyme (novozymes-435) catalysts. Small molecule initiators such as propargyl alcohol, cis-1,3-O-benzylideneglycerol initiated the polymerisation of δ -decalactone at room temperature in the absence of solvents to obtain poly(decalactone) as an amorphous polymer. However, it was observed that polymers could also be obtained without an added alcohol initiator under certain circumstances. The reason for this unexpected polymerisation was not fully investigated owing to time constraints.

Block copolymers of δ -decalactone (*i.e.* mPEG-b-PDL and PDL-b-PEG-b-PDL) were synthesised using PEG as initiator at temperatures above the melting point of PEG to avoid the use

of solvents. Both block copolymers were successfully separated from homopolymer contamination by washing with ether. Characterisation data of the resultant polymers suggested the successful synthesis and purification of the desired products. Further, the synthesis of a triblock copolymer of ω -pentadecalactone was attempted using mPEG-b-PDL as initiator and TBD as catalyst but this approach did not produce the desired copolymer. Hence, Novozymes-435 was used for the ROP of ω -pentadecalactone, to generate an ABC type of triblock copolymer (*i.e.* mPEG-b-PDL-b-PPDL). It was observed that increases in the molecular weight of poly(pentadecalactone) block above 2 kDa decreased the solubility of the resultant block copolymer in acetone. Hence, poly(pentadecalactone) block of less than 2 kDa was targeted to generate an ABC type copolymer. The polydispersity index detected by SEC for all synthesised novel block copolymers was found to be less than 1.3. A diblock copolymer (*i.e.* mPEG-b-PCL) of poly(caprolactone) of similar molecular weight was also synthesised for comparative studies with mPEG-b-PDL.

The CMC values of these novel amphiphilic block copolymers in water were calculated using the pyrene fluorescence method, which were ranges between 1.07-1.77 $\mu\text{g/mL}$. The

CMC values detected for PDL block copolymers were approximately half the CMC value observed for mPEG-b-PCL. Micelles of amphiphilic block copolymers were prepared by nano-precipitation method and the Z-average sizes observed for these micelles was <200 nm. No significant difference in sizes of mPEG-b-PDL and mPEG-b-PCL micelles was observed. Micelles obtained from PDL-b-PEG-b-PDL copolymer gave a bimodal size distribution, in which the second peak was due to the formation of clusters, which was evident by TEM images. The size detected for mPEG-b-PDL-b-PPDL copolymer micelles was significantly higher when compared with mPEG-b-PDL micelles. The large size of these micelles was attributed to the change in solubility of mPEG-b-PDL-b-PPDL copolymer in acetone compared to mPEG-b-PDL, which in turn generates some big micelles and hence, enhance the Z-average size. Micelles fabricated from all block copolymers were roughly spherical in shape as evident by TEM images. The zeta potential obtained in HEPES buffer (10mM, pH-7.4) for block copolymer micelles was almost neutral except for PDL-b-PEG-b-PDL micelles, which was slightly negative due to the less dense PEG corona. It was hypothesised that due to the less dense corona, micelles obtained from PDL-b-PEG-b-PDL block copolymer were prone to make clusters.

All novel block copolymers of poly(decylactone) were successfully encapsulated Nile Red (NR) and Curcumin during a micelle fabrication process. A shift in UV-Vis absorbance maxima of NR suggested the self-assembly of block copolymer in water with PDL core. NR and curcumin loading did not significantly change the diameter of micelles except in case of PDL-b-PEG-b-PDL where reduction in clusters volume led to decrease in average diameter. No significant difference in curcumin loading content was observed for mPEG-b-PDL and mPEG-b-PDL-b-PPDL micelles when compared to the well-established mPEG-b-PCL copolymer micelles. In curcumin stability study, it was found that micelles of mPEG-b-PDL copolymer were able to reduce degradation of curcumin at physiological pH. *In vitro* release studies of curcumin loaded micelles suggested that micelles having the amorphous poly(decylactone) core gave a faster release compared to semicrystalline poly(caprolactone) and poly(pentadecylactone) cores.

In a subsequent study, effective loading of amphotericin B was demonstrated by utilising mPEG-b-PDL micelles *via* a nanoprecipitation method using methanol as an organic solvent. No significant difference in average size was observed for mPEG-b-PDL micelles prepared using methanol when

compared with the mPEG-b-PDL micelles fabricated using acetone. The loading results suggested that the mPEG-b-PDL micelles were able to encapsulate AmpB with high efficiency compared to their counterpart mPEG-b-PCL micelles. The *in vitro* release study suggested that mPEG-b-PDL micelles showed prolonged release of AmpB when compared with Tween 80 micelles. Additionally, with the help of an extra control (physically mixed copolymer) in release experiment, it was demonstrated that the partition coefficient of drug between carrier (micelles) and release phase is also a variable that influence the release rate determined by the dialysis method. Preliminary *in vitro* degradation study of mPEG-b-PDL micelles suggested that the ester bonds of PDL chain were susceptible to hydrolytic degradation. *In vitro* cell metabolic activity studies demonstrated that the novel mPEG-b-PDL and mPEG-b-PCL micelles were well tolerated by the studied HCT-116 human colon cancer cell line.

7.1.2 Synthesis, Characterisation and Evaluation of Ligand Mediated Targeting Efficiency of Amphiphilic Block Copolymers generated from Poly(decalactone)

In this study, the synthesis of amphiphilic diblock copolymers of poly(decalactone) (PEG-b-PDL) with different functionalities were reported *via* copper catalysed click chemistry. The azide

derivative of PEG *i.e.* methoxy-PEG (mPEG-N₃), folic acid conjugated PEG (FA-PEG-N₃) and rhodamine B conjugated PEG (RhB-PEG-N₃) were used as the hydrophilic blocks while propargyl-PDL was used as the hydrophobic block. Azide-alkyne click reaction between PDL and PEG blocks generate the desired amphiphilic block copolymer. The synthesised copolymers were characterised by ¹HNMR and SEC and was found that final purified copolymers contained some free PEG. Two mixed micelle formulations of the copolymers were fabricated using a nanoprecipitation method in which one was intended as a targeted (FA-PEG-b-PDL + RhB-PEG-b-PDL) formulation and another was non-targeted (mPEG-b-PDL + RhB-PEG-b-PDL) formulation. Copolymer RhB-PEG-b-PDL was used as a tracker to visualise the distribution of micelles in cells. The size range observed for both micelles formulation was 20-200 nm with a zeta potential close to neutral. These micelle formulations were then tested for the folate mediated targeted delivery to MCF-7 (folate receptor +ve) and A549 (folate receptor -ve) cell lines. A non-specific uptake of PEG-b-PDL micelles (targeted and non-targeted) in both cell lines was observed as evident by confocal images. . Based on the previously reported studies, it was proposed that the PEG-b-PDL micelles might be taken up by the cells through a caveolae-mediated endocytosis.

7.2 Future Work

A few of the studies reported in this thesis were in their preliminary stage. Therefore, the future studies related to the work presented in this thesis are as follows:

- The ROP of poly(decylactone) via TBD needs investigation to understand fully the reason for homopolymer formation.
- An extensive polymer degradation study is needed to establish the complete degradation profile of the synthesised novel block copolymer micelles.
- Comprehensive research needs to be done on a range of human cell lines to generate a polymer toxicity profile and to identify the uptake mechanism.
- Finally, *in vivo* studies are needed to establish the potential of novel poly(decylactone) block copolymer micelles as a drug delivery carriers.